

**COMPARATIVE STUDY OF STRUCTURE RESPONSE TO  
COAL MINE BLASTING**

**Prepared for**                      **Office of Surface Mining  
Reclamation and Enforcement  
Appalachian Regional Coordinating Center  
Pittsburgh, Pennsylvania**

**Contract No. CTO-12103**

**Prepared by**                      **C. T. Aimone-Martin  
Aimone-Martin Associates, LLC**

**M. A. Martell  
Aimone-Martin Associates, LLC**

**L. M. McKenna  
Northwestern University**

**D. E. Siskind  
DESA, Inc.**

**C. H. Dowding  
Northwestern University**

**Contracting Officer's Technical Representative**

**Kenneth K. Eltschlager**

**March 2003**

## TABLE OF CONTENTS

	Page
ABSTRACT	1
INTRODUCTION	3
ACKNOWLEDGEMENTS	4
PROJECT APPROACH	5
SITE AND STRUCTURE SELECTION	5
DESCRIPTION OF STRUCTURES	6
Pre-manufactured Trailer Structures	8
Mine Camp Structures	9
Log Structures	10
Masonry and Earth Structures	11
Wood-frame Structures	12
INSTRUMENTATION	12
Polarity Testing of Velocity Geophones	13
Sensor Locations within Structures	13
RESULTS	14
Mine Site Characteristics	15
Ground Vibrations and Airblast Measurements	15
<i>Ground Vibration Attenuation Plots</i>	15
<i>Airblast</i>	16
Frequency Content of Ground Motions	16
<i>Measuring Frequencies</i>	16
<i>Measured Vibration Amplitudes and Frequencies</i>	17

	Page
<i>Summary of Findings</i>	17
Structure Response	18
<i>Time History Comparisons: Structure Response Relative to Ground Motions and Air Overpressures</i>	19
Ground motion versus lower structure response	20
Lower structure response versus upper structure response	20
Ground and air pressure time histories relative to upper structure response	20
Mid-wall and upper structure response to air pressure	21
<i>Summary of Findings</i>	22
<i>Correlating Structure Response to Ground Motions and Air Pressures</i>	22
Structure response to ground vibrations	23
Structure response to airblast overpressures	24
<i>Summary of Findings</i>	25
Fundamental Frequency Analysis: Natural Frequencies and Structure Damping	25
<i>Natural Frequency of Structures</i>	25
<i>Structure Response Based on Ground Motion FFT Analysis</i>	26
<i>Verification of Spectral Analysis Ability of Seismic Data Analysis Software</i>	27
<i>Damping of Structure Motion</i>	28
<i>Summary of Findings</i>	29
Amplification Factors	29
<i>Summary of Findings</i>	30

	Page
Relative Displacements and Calculated Strains	30
<i>Summary of Findings</i>	33
Non-blasting Sources of Structure Vibrations	33
<i>Household Activities</i>	33
<i>Wind</i>	33
<i>Summary of Findings</i>	34
CONCLUSIONS	34
RECOMMENDATIONS	36
REFERENCES	36
TABLES	38
FIGURES	47
APPENDIX I	Structure Layouts and Photographs
APPENDIX II	Instrumentation Locations
APPENDIX III	Blast Data, Ground Vibrations, Airblast, and Structure Vibration Response Summaries by Site
APPENDIX IV	Typical Waveform Time Histories
APPENDIX V	FFT Frequency Correlation Plots
ADDENDUM I	Direct Measurement of Crack Response of Four OSM Study Structures
ADDENDUM II	Guidelines for Measuring and Evaluating Structure Response

## ABSTRACT

Whole structure and mid-wall responses of 25 structures to surface coal mine blasting were characterized. Eighty-nine blasts were conducted at 11 mine sites throughout the U.S. to measure blast-generated dynamic response of atypical structures found in the proximity of surface coal mining. Atypical structures selected for this study include log-type, manufactured (single wide and double wide trailers), “mine camp”-type, adobe, and stone. Traditional acoustic microphones, tri-axial (ground) and single component (structure) velocity transducers were used to record airblast, ground motions, and structure response time histories with a common time base. The relative responses of selected “atypical” structures to blast vibrations and non-blasting causes of structural stress, including natural forces, environmental effects, and human habitation, are compared.

Data analyses for blast-induced motions were conducted to:

- compare vibration time histories in terms of velocity and calculated displacement within structures relative to ground excitations,
- evaluate the influence of air overpressures on structure response,
- evaluate response frequencies to determine natural frequencies and damping characteristics,
- determine structure response amplification of ground motions, and
- compute differential displacements of construction components and corner motions to estimate global or gross structure strains.

Corner and mid-wall motions from blasting were compared to motions induced by normal household activities and external forces such as wind. In addition, wall crack deformation responses to environmental changes, human-induced vibrations and blasting were measured in four of the structures in a parallel study.

Amplitudes of ground vibrations measured at structures ranged from 0.02 to 1.25 inches per second (in/sec). Scaled distances ranged from 22.9 to 340.0 ft/lb<sup>1/2</sup>.

The amplifications of ground motions measured in upper structure corners varied by type of structure as well as for certain structures within each design type. Corner responses of log and wood-frame structures fell below values reported in U.S. Bureau of Mines RI 8507. For two structure designs (two-story log and two-story stone), amplifications greater than 4 were measured when excited by ground motions with predominant frequencies of 4 to 7 Hz.

Little difference in horizontal time histories between lower floor and ground motion responses were noted for all structure types with the exception of trailers without wood-frame add-ons. Single and double wide trailers produced wall base motions greater than exterior ground motions.

Trailer whole structure and mid-wall motions duplicated airblast time histories. Peak structure responses occurred within the airblast phase rather than within the ground motion phase, particularly when airblast exceeded 116 decibels. Mid-wall motions showed both high

frequency and low frequency characteristics for specific structures while trailer mid-walls tended to respond only at high frequencies. One-story camp and log structures and massive stone, concrete block and adobe structures did not respond to airblast.

Whole structure natural frequencies averaged 6.0 Hz. Mid-walls averaged 8.4 and 13.8 Hz in the transverse and radial walls, respectively. These values fell below those reported by the U.S. Bureau of Mines in RI 8507. Mid-wall motion frequencies duplicated low frequencies of the upper corner and also carried a high-frequency component. However, the range in data in this study corroborated U.S. Bureau of Mines findings.

Damping values fell well within the range reported in previous studies of 2 % to 10% of critical. Trailer transverse wall damping averaged 9.5% while log and trailer structures exhibited the highest whole structure (upper corner) radial damping of 9.7% and 9.6%, respectively. The least damped structure type was the two-story stone and measured 3.9% of critical.

Wall strains calculated from gross and mid-wall differential displacement were less than 20  $\mu$ -strains for wall bending. The maximum calculated in-plane tensile wall strain was 133.1  $\mu$ -strains and is well below cracking thresholds of 300 to 1000  $\mu$ -strains for plaster and wallboard.

Structure response to non-blasting events was measured. Human-induced whole structure responses up to 0.51 in/sec and mid-walls up to 2.14 in/sec were measured and are equivalent to ground vibration amplitudes of 0.28 in/sec for single wide trailers and 0.11 in/sec for double wide trailers and one-story adobe. Wind gusts generated air pressures that resulted in detectable levels of structure shaking and mid-wall responses in trailers up to 0.1 in/sec

Direct measurements of crack response were made for four structures. Addendum I is a report describing the measurement techniques and summarizing the long term (environmental) and transient (blast vibration) changes in crack width. Addendum II outlines protocols for implementing many of the measurement and analytical procedures described in this report.

## INTRODUCTION

Explosives are used to break rock overlying a coal seam. The rock can be broken in place (conventional blasting) or broken and partially displaced into the adjacent pit (cast blasting). In any blast, the majority of energy is spent breaking rock. The balance of energy emanates from the site into the environment as either seismic or airblast energy. Once blasted, all the rock is moved to expose the coal for mining.

Ground vibrations and airblast leaving the mine eventually arrive at adjacent properties. The energy is then transmitted into the buildings. In turn the buildings respond or shake. If ground vibrations and /or airblast are strong enough, the building may be damaged. The Office of Surface Mining (OSM) and other regulatory agencies limit the amount of energy received at the building regardless of how blasting is being conducted at the mine.

Based on the research conducted to date, damage to buildings has never been observed below ground vibrations of 0.5 in/sec or airblasts of 140 decibels. Federal regulations allow limits up to a maximum vibration of 1.0 in/sec (between 301 to 5000 feet) and 134 decibels, respectively. At these limits, no damage is expected but we acknowledge that hairline cracking of plaster is possible under certain site or building conditions. The intent of the regulatory scheme, as outlined in the preamble to the federal rules and the development of a blasting plan, is for the coal mine permittee and the regulatory authority to tailor the allowable limits based on the site specific need to prevent damage to occupied dwellings. The regulatory authority is responsible for lowering the limits if necessary to prevent damage

People inside buildings can feel the structure shake and hear bric-a-brac rattle at ground vibrations and airblast as low as 0.04 in/s and 100 decibels, respectively. Citizens often begin noticing normal house changes, such as cracks in walls, and blame the changes on the vibrations they feel. To some, any type of environmental vibration is intrusive and disturbing. Since low level blasts will annoy some people, complaints are common.

The part of any residential structure most susceptible to blast induced vibrations is the superstructure or portion above ground level. Research over the years has defined the structure response characteristics of "typical" one and two story residential structures. OSM has built their regulations around this research since the majority of structures near coal mines are residential.

Occasionally, structures are found near the mine that do not fall into the "typical" category or may not have been included in the body of data on which the rules were founded. Such structures may include pre-fabricated houses, trailers, log homes, sub-code homes and adobe structures. This study measures the response characteristics of these "untypical" structures to blast induced ground vibration and airblast and compares motion characteristics to those of "typical" structures studied by the U.S. Bureau of Mines (U.S.B.M) and others in establishing the widely adopted safe level blast vibration criteria in the U.S. As such, field measurements and analyses were made to duplicate those conducted by past researchers. U.S.B.M. research primarily considered traditional wood frame housing. Therefore, it was the goal of this research to extend the understanding of similarities and differences in dynamic response between traditional wood-frame constructions and non-traditional type structures.

The motivation for this study began because of blast-related complaints from residences living near surface coal mines, despite an industry-wide adherence to safe blasting criteria prescribed for the coal mining industry. Limited investigations of blast complaints conducted by government officials revealed that certain structure types may respond to blasting vibrations in unique and unusual ways. Currently there is no uniform approach or guidelines available to investigate the uniqueness in structure response. Therefore this study was initiated to address two issues. The first was to characterize the response to blasting in various types of structures that are unlike those types that have been previously studied. The second was to develop a methodology to investigate and evaluate structures by placing traditional vibration instrumentation within structures in a manner to address uniqueness.

An important objective was to compare the responses of this study data to the data previously obtained by the U.S. Bureau of Mines as a measure of uniqueness for all structures studied. Finally, this study provided the opportunity for government personnel (GP) to take part in structure instrumentation and analysis of response data. This on-site training process is valuable to enhance understanding and confidence that GP require when investigating blast-related complaints.

It is not the intent of this study to evaluate and compare the influence of blast design on ground motion and airblast excitations as a source of vibration response of structures. Furthermore, this study did not address wall cracking. No observations of crack extensions were made during structure response monitoring. Therefore, no conclusions have been made regarding the potential of specific ground motions and airblast excitations to induce cosmetic cracks in structures. Furthermore, there are no correlations of structure response with cracking potential.

## **ACKNOWLEDGMENTS**

This research project was sponsored and supported by the Department of Interior Office of Surface Mining (OSM) with the cooperation of state regulatory agency personnel. The Contracting Officer's Technical Representative was Kenneth K. Eltschlager. The authors acknowledge the generous assistance of Mr. Eltschlager.

The study was possible with the assistance and cooperation of many homeowners, mine operators, engineering consultants, and graduate students at Northwestern University and New Mexico Institute of Mining and Technology. Special thanks are due to the following state regulatory personnel for coordination of project activities in their respective states:

Alabama – John Cranor  
Indiana – Steve Weinzapfel  
Kentucky – Ralph King  
New Mexico – Mike Rosenthal  
Ohio – Mike Mann  
Pennsylvania – Bill Schuss  
Tennessee – Dennis Clark  
Virginia – Don Carter



## **PROJECT APPROACH**

Ground motion, airblast, and structural response data from surface coal mining blasting were collected at eleven mining sites. Structures instrumented in this study were selected to represent the range of structures found in the proximity of surface coal mining with focus on those not previously studied by the U.S. Bureau of Mines during structure response studies. These designs included pre-manufactured trailers, log, earth and stone, and mine “camp”. Time-correlated measured responses include those of whole structure, mid-wall, and selected structural components. Responses include those from human activities, environmental effects, and surface mine blasting.

A crack response study, supported by Northwestern University, was conducted in parallel to the structure response study within structures possessing a representative hairline drywall, plaster or concrete block crack. Transient displacements of the crack from blasting were compared to static crack movement produced from long-term changes in environmental climate conditions. Results of this crack study are found as an Addendum I to this report and titled “Direct Measurement of Crack Response Study of Four OSM Study Structures”. The monitoring of existing cracks within selected structures was neither part of the scope of work for this project nor was it required by the Office of Surface Mining. However, it was felt that a crack study, would provide another basis for understanding the manner in which structures respond to human habitation, environmental effects and blasting.

## **SITE AND STRUCTURE SELECTION**

Eleven coal mining sites were selected by OSM based on recommendations of state personnel. These states included Virginia, Kentucky (two sites), West Virginia (two sites), Tennessee, Alabama, Ohio, Pennsylvania, New Mexico (representing Native American Indian lands), and Indiana. State blasting specialists nominated coal mines, based on structure uniqueness.

Criteria for the selection of structures had to satisfy study objectives and facilitate project tasks within limited time constraints and resources. These criteria included structure uniqueness, the proximity of the structures to the mine blasting site(s), willingness of home owners to cooperate on the project, and availability of a significant number and intensity (e.g. amplitudes of ground vibrations and airblast) of planned mine blasts to ensure measurable structure response, and the cooperation and assistance of the mine operators.

Specific selection criteria for structures included the following:

- Structure uniqueness

A minimum of one “atypical” structure was needed at each mine. At some sites, traditional wood-frame structures were selected based on availability and satisfaction of all other criteria. Incorporation of a limited number of traditional wood-frame structures provided a basis of comparison responses with those of previous research and those of unique structures selected at the same mine site.

- Proximity to an active surface coal mining operation

To satisfy project objectives, sufficient blast-induced ground vibration and airblast energy was necessary to produce measurable vibrations and structure response. Therefore, the blast site distance to structures and the explosive charge weights (e.g. maximum charge weight detonated on one delay or within an eight millisecond, ms, delay interval) were important parameters to consider in site and structure selection. It was important that at least five blasts be detonated during the week monitoring to facilitate scheduling constraints and instrumentation requirements. Mine operations generating significant levels of ground vibrations (e.g., averaging 0.25 inches per second, or in/sec) and airblast (in excess of 115 dB) over a wide range of scaled distance factors were considered to be sufficient for the structure response study. Coordinating project logistics around five planned mine blasts one to two months ahead of site arrival provided challenges that were overcome by the cooperation of mine operators.

- Cooperation of the homeowner

Owners of structures that satisfied the criteria were provided written documentation describing the study. Home owners willing to participate were asked to sign a right of entry (required by OSM) and a release of claims (required by the contractor).

- Cooperation of the mine operator

Site scheduling was dependent on mine blasting activities near the homes. Mine operators were contacted by agency personnel and the contractor to coordinate study activities during specific weeks. Additionally, mine operators were requested to supply information on the location of blasts and proposed charge weights. In cases where five blasts were not possible during one week, an attempt was made to separate large blasts into smaller blasts or provide a few single hole detonations. In a few cases, less than five blasts were provided. However, redundancy in structure types among sites and greater numbers of blasts at other sites provided a sufficiently large data base to meet study objectives.

## **DESCRIPTION OF STRUCTURES**

Structures were characterized and construction details were documented in a number of ways. Photographs were taken of each structure exterior and interior as well as the foundation (for non-slab foundations and where access was available). Specific attention was given to the type of foundation support. Laser-level surveys were conducted to establish floor elevations for all structures and room dimensions were measured with a laser rangefinder. This information was used to assess the overall condition of structures that might be a function of foundation support, distribution of structure load, as well as unusual structure loads or other construction details.

Appendix 1 provides detailed documentation of each structure. Included are scaled room layouts and photographs of various features. Room measurements were necessary to compute gross strains within structure walls.

Table 1 presents general construction details of all structures in this study. Structures are identified by state and location in the order in which they appear in Appendix I.

Structure designs include the following categories:

- pre-manufactured trailers constructed as single wide, double wide, and wood-frame add-on support by concrete masonry units (CMU, or cinder blocks),
- log structures – one and two story traditional natural log and two story prefabricated, manufactured log structures with vaulted ceiling living areas
- mine “camp dwellings” constructed of wood frames with diagonally sheathed walls and foundations of perimeter CMUs and interior log poles
- masonry and earth - construction includes CMU’s, field stone and adobe, and traditional adobe
- traditional wood-frame structures - including one, two, and three story (cantilevered) designs

A brief description of each structure is given below. For clarity the following designations were used in identifying the structure category:

T – trailer	S – single-wide trailer
C – camp	SA – single-wide trailer with add-on
L – log	D – double wide trailer
E – masonry and earth	1S – one story
W – wood frame	2S – two story
	3S – three story

The designations following the structure category used to identify the states and mines (in alphabetical order) are:

AL - Alabama  
IN - Indiana  
KY1 – Kentucky site 1  
KY2 – Kentucky site 2  
NM – New Mexico  
OH - Ohio  
PA - Pennsylvania  
TN - Tennessee  
VA - Virginia  
WV1 – West Virginia site 1  
WV2 – West Virginia site 2

If two structures of the same category and design were selected, the following identifier was used:

- A – first structure of category and design
- B – second structure of same category and design

### **Pre-manufactured Trailer Structures**

Pre-manufactured trailers ranged from small, single wide units 64 ft. long by 14 ft. wide to large double wide trailers 74 feet long by 28 feet wide. Single wide trailers with wood frame add-ons were 54 to 46 ft. in length and 24 to 26 ft. wide. All trailer interior walls, with the exception of one double wide, were constructed of wood fiberboard coated with a thin layer of plaster compound. All walls were covered with wallpaper or wood paneling.

One double wide trailer possessed a recently constructed wood frame and drywall interior wall separating the dining area from the kitchen parallel to the “marriage” wall (e.g. long trailer axis). This was the only trailer founded on a full basement.

All other trailers rested on piers of unmortared concrete blocks that were leveled with wood wedge shims. Pier support geometries for single wide and double wide trailers are shown in Figure 1. Some trailers were fastened to the ground using perimeter hurricane strapping shown in Figure 2. Concrete blocks were stacked singly or in pairs and placed beneath steel beams as shown. Wood shims were placed between the pier and trailer beams in all cases. Piers for one trailer were supported on poured concrete pads. The remaining trailer piers were founded directly on the soil.

A number of piers were tilted from a vertical line and not aligned normal to the steel beams. Tilting piers are shown in Appendix I for all trailers with the exception of TD-TN (Note, TD-PA is founded on a full basement). Tilting results from eccentric loading about the pier support.

**TS-KY2** is a single wide trailer with interior paneled walls. The single CMUs were configured as shown in Figure 1 (a). No hurricane strapping was used.

**TS-IN** is a single wide trailer with a small room addition at the east end founded on a stack of single CMUs configured as shown in Figure 1 (a). Hurricane strapping was used and all interior walls were paneled.

**TS-AL** is a single wide trailer with hurricane strapping. Double concrete piers support beams as shown in Figure 1 (a). Interior walls were either paneled or papered.

**TS-OH** is a single wide trailer with loose hurricane strapping. The trailer was built into a hillside and supported by varying pier heights ranging from a single half-block to a double set of five blocks in the configuration shown in Figure 1 (a). Interior walls were either paneled with wood or covered with wallpaper.

**TSA-VA** is a single wide with a wood frame add-on along the entire back of the house. The original trailer section is supported with double CMU piers while the wood frame add-on is supported by a conventional CMU perimeter wall. A one by eight sill plate supports floor joints and does not support the trailer section cross members. All interior walls have wallpaper covering or were paneled. No hurricane strapping was used.

**TSA-KY2** is a single wide with a wood frame add-on along the entire front of the structure. A CMU wall exists around the entire perimeter. Beneath the trailer section, it serves as a skirt. Beneath the addition, it supports the frame. All interior piers were double concrete blocks. The wood-frame section is not supported with a perimeter wall and supported only with double concrete blocks. The support configuration is generalized in Figure 1 (b). No hurricane strapping was used.

**TD-WV2** is a two-year old double-wide trailer. The support configuration is generalized in Figure 1 (c) with one single width stack of CMUs placed along the “marriage” wall beam. The piers were founded on poured concrete pads. Standing water from a bathroom water leak was noted under the northwest corner of the trailer. No hurricane strapping was used and all walls were covered with vinyl wall covering.

**TD-TN** is a two-year old double wide trailer with hurricane strapping. Double CMU piers were used in the corners and along the “marriage” wall beam. Single CMU piers used for all other beams along the perimeter as shown in the configuration of Figure 1 (b). All interior walls have wallpaper covering.

**TD-PA** is a double wide trailer with a full basement constructed of CMUs. The center steel beam carrying the “marriage” wall was cut to accommodate the stairway into the basement from the laundry room. This main beam is supported by steel posts, spaced on 12-foot centers along the trailer long axis. CM walls support cross-beams. All interior walls were wallpapered. The newly constructed wood-frame wall between the kitchen and the dining area is completed with drywall.

## **Mine Camp Structures**

Mining camp houses ranged in age from 50 to 100 years old and construction widely varies. Exterior walls were constructed with two by fours placed at right angles to current wood frame construction practices. Shown in Figure 3, the four inch dimension of the studs is oriented parallel to the wall. Diagonal exterior boards complete the framing. Traditional camp houses in central Appalachia are supported on interior log poles, many of which are founded directly on bedrock. Others are supported on both logs and CMU piers. Floor joists rest on perimeter walls without sill plates and are randomly located rather than uniformly spaced. Other mine camp structures are supported on a mix of wood poles and concrete blocks or bricks. Perimeter foundations comprise a variety of fieldstone, CMUs, and poured concrete with rectangular wood post framing. A number of camp structures have been renovated by replacing stone foundations and adding modern wood-frame rooms.

**C1S-AL** is a one story mining camp structure approximately 55 years old. The frame construction rests on a CMU perimeter wall and interior piers of unmortared single concrete blocks or clay bricks. The interior walls of the house were paneled with a wood product. The living room has new sheet rock walls.

**C1S-VA** is a one-story structure built in 1945. The home is founded on bedrock using wood log posts. The exterior perimeter wall is constructed partly of field stones (front of the house) and cement block at the rear of the structure. Irregularly spaced floor joints do not form any particular pattern and rest directly on top of the perimeter concrete blocks with a sill plate formed of concrete. A number of log posts were found to be loose and not tied to the floor joists. All interior walls were paneled.

**C2S-KY1A** is a two-story camp home built in the early 1900's. Interior walls were plaster on lath covered with paneling throughout the house. Basement ceiling joists vary in spacing and were supported by log posts. Discontinuous two by eights were used to support the joists in many places. Basement walls were formed using field stone and mortar.

**C2S-KY1B** is a two-story camp home built in the 1950's with two additions. The rear addition forms the kitchen and a bathroom and a recent addition forms the living room. The older section of the structure is founded on a full basement while the additions are built upon a crawl space. The structure is supported with a perimeter concrete block wall and interior supports of many varieties. Interior supports include unmortared concrete block piers, wood posts, table legs, and a steel jack. Interior walls were newly constructed drywall or paneling.

## **Log Structures**

The five log homes in this study were constructed of horizontally laid logs fitted together by one of the three techniques: the saddle lock-notch, notched and scribed, and butt-jointed. Figure 4 shows the three types of log fittings used to construct the homes. Four of the structures combine corner notching, either the saddle lock-notch or notched and scribed, and the log weight is used to form stable structures. The remaining house was built using butt-joints throughout the structure. At the structure corners, log ends were nailed perpendicular to each other. The butt-joint combined with the log weight formed a stable structure.

The logs with a saddle lock-notch were stacked such that they do not rest against each other except at the notch leaving a crack or "chink" of one inch or more visible between the logs. Chinks allow for warping and expanding. The chinks were filled or caulked with a plaster or mud material. Scribing a log is the terminology used to describe fitting the entire length of the log to match the shape of one log to another. Scribed logs were notched at each end and a tongue or groove is cut from notch-to-notch the length of the log. The tongue and groove serves as a means of tightly fitting the logs together. The butt-joint technique does not require notching to stabilize the logs. Two logs were joined by placing one log perpendicular to one end of the other log and nailing the two together. The normal stabilization method for butt-jointed logs involves drilling vertically through the stacked logs of a wall and driving rebar down through the drilled hole to stabilize the wall.

**L1S-OH** is a one story log cabin with a full CMU block wall basement. The structure is 40 years old. Walls comprise hand-crafted milled logs, approximately nine inches in diameter, were notched and scribed.

**L1S-WV1** is a one-story primitive handcrafted log cabin constructed more than 100 years. The construction is called primitive because the bark was not removed from the logs. The original part of the structure was built from hand-hewn logs that were saddle lock-notched and horizontally stacked. The chink was caulked with a mud or plaster type material. The logs were approximately six inches in thickness with additional six inches of framing on the inside for a total wall thickness of 12 in. Interior walls have a plaster finish. The original cabin sits on concrete piers at the corners. A concrete block foundation was added under the front porch of the cabin and under an addition at the rear.

**L2S-TN** is a two-story handcrafted cabin built using a butt-joint technique for the wall construction and corners. The logs were railroad cross ties cut six inch by six inch square and joined end-to-end with length of a wall with a two by six board nailed along the top of the joined cross ties. The cabin walls stand only under the weight of the logs. No vertical structural supports or ties (e.g., rebar) were used to vertically tie logs together. The foundation comprises a CMU perimeter wall and interior block piers forming a two to three foot crawl space founded directly on bedrock.

**L2S-OH** is a modern mill-log custom home designed and built by the owner. It is approximately 2 years old with a full cinder block basement. The vaulted ceiling in the living and dining rooms were constructed with roof trusses and exposed beams and rafters. A partial second floor is designed over one-half of the structure.

**L2S-WV2** is constructed from a log home kit with modern mill-logs, a vaulted ceiling with exposed beams, rafters and trusses. A partial second floor is constructed over one-half of the structure. The structure is founded on a crawl space with a cinder block perimeter wall and interior piers of concrete block. A single post supports a balcony and the roof beam overlooking the living area.

## **Masonry and Earth Structures**

Masonry and earth structures include concrete block, stone, and adobe brick (stabilized from hardened soil blocks, baked in the sun) faced with stucco. Three structures falling in this category were located in New Mexico. Consistent with construction practices in the southwest, houses were founded on concrete slab or directly on the ground with stone perimeter beams supporting bearing walls.

**E1S-NMA** is a one-year old cinder block building founded on a reinforced eight-inch thick concrete slab.

**E2S-NM** is a two story stone (field rock with cement joint grout) structure built in 1880 with interior adobe walls. The stone exterior walls comprise two layers of sandstone block and mortar

without wood framing or a bond beam to tie the exterior stone walls together. The mansard roof rafters rest on two, two by eight inch headers lying on top of the stone walls. There are no nailed connections between the roof and the structure wall. Interior walls on the first floor are covered with structural plaster. Exterior stone and interior adobe walls rest on a rock wall foundation.

**E1S-NMB** is a 17-year old single story traditional adobe structure. Exterior walls were covered with stucco while interior walls comprise exposed adobe bricks. The house is founded on a four inch concrete slab.

### **Wood-frame Structures**

Wood-frame structures represent “typical” construction akin to structures previously selected by the U.S. Bureau of Mines. All wood-frame structures were founded on full basements.

**W1S-IN** is a one-story wood-frame structure with a full basement of CMU wall construction built in the 1950s.

**W1S-PA** is a newly constructed one-story wood-frame house with a full basement of CMUs.

**W2S-IN** is a house that was recently purchased by the mining company prior to mining through the property. It has a concrete block full basement and a partially completed attic. The structure age is unknown.

**W3S-WV1** is a three-story structure founded on a concrete slab. The first story, constructed of CMUs, serves as a shop. The second and third stories were of wood-frame construction of perimeter dimensions four feet wider than the first floor.

## **INSTRUMENTATION**

Whole structure and mid-wall responses were recorded with single axis velocity transducers attached to four-channel blasting seismographs manufactured by LARCOR, of Dallas, Texas. A connector interface box linked transducers to the seismograph, which allowed the air channel to be employed to record velocity. Three seismographs, one exterior (master) and two interior (slaves), were daisy-chained together to record ground and structure motions with a common time base. The master was set on trigger mode and the two slaves were set on manual mode. When triggered, the master unit sent a one-volt spike to the slave units to simultaneously start data recording. A tri-axial transducer buried in the ground and microphone recorded three components of ground motion and airblast at each structure exterior.

Interior transducer output was amplified by a factor of 2 (e.g., lowest detection level of 0.005 inches per second, in/sec All three seismographs were programmed to record 6 to 12 seconds of event time at a sample rate of 512 per second. The master unit was programmed to trigger at a ground particle velocity of 0.02 to 0.03 in/sec and the maximum range for all units varied from 2.5 to 10.0 in/sec depending on blast-to-structure distance and gain selected.



## **Polarity Testing of Velocity Geophones**

Polarity was checked for each geophone prior to deploying instruments in the field. When evaluating differential motions between the ground and structures, it is important to document the polarity of the geophones. For instance, polarity for a vertical sensor normally produces a positive phase first motion. If the polarity of a structure-mounted vertical sensor is such that the first motion is negative while a ground motion sensor vertical component produces a positive first motion, it is likely that the structure sensor polarity is reversed.

Polarity becomes critical when measuring and comparing relative motions between the ground and upper portions of structures, particularly when differential displacements are to be calculated in order to estimate gross structure strains and in-plane wall strains. If sensors are mismatched, differential displacements may be over two times greater than displacements for a common polarity.

## **Sensor Locations within Structures**

Typical instrumentation placements for many of the structures are shown in Figures 5 and 6. Horizontal sensor orientations for common polarity are found in Figure 7. The radial alignment of sensors placed in the ground and within structures was directed along the long axis of each structure. Efforts were made to place the ground R component in the same direction as positive (inward) wall and structure motions. Sometimes the position orientation of the radial ground sensor was placed in a direction opposite to that of the structure or mid-wall orientation. This opposite polarity was easily recognized and compensated during analysis.

Specific locations of exterior and interior geophones, and the seismograph unit serial number to which they were connected, are illustrated in the structure plans in Appendix II. Interior sensors S1 and S2 consisted of four single-component velocity transducers, three mounted to record horizontal motions and one mounted to record vertical motion. A sensor cluster (two horizontal and one vertical) was placed at the first floor structure corner base (S1) and a duplicate cluster (S2) was placed at the highest point of the same corner. Motions recorded at S1 and S2 were used to measure the whole structure response to blasting. Mid-wall response was measured using a third horizontal sensor, placed at or near the middle of each conjoined wall (shown as wall 1 and wall 2). At S1 and S2, the R sensor was aligned with the longest axis of the structure and T with the shortest axis, as shown in Figure 5 (b). The vertical, V, sensor was placed on either wall. Figure 6 shows a typical instrumentation set up for a one-story mining camp structure

Other instrumentation layouts, specific to a unique construction type, did not adhere to the typical layout shown in Figures 5 and 6. In most cases, the lower structure vertical response reflected the ground vertical vibrations. Therefore, in some structures the vertical component normally placed at the lower was placed on a ceiling or other more useful locations. Sometimes, motions between two or more construction components were monitored. Special layouts were used for double wide trailer TD-TN (where opposite sides of the “marriage” wall were

instrumented), single wide trailers TS-AL and TS-OH (measuring torsional motions at opposite ends of the trailer), and between two different construction types in TSA-VA. Motions were also measured in log structures along the “great” wall at the end of a vaulted ceiling room by placing single transducers at the roof peak, L2S-TN, L2S-OH, and between the roof beam, rafters and center post, L2S-WV2. In two structures, the vertical motions of the ceiling were measure (E2S-NM, TS-IN) rather than wall vertical motions.

## RESULTS

The focus of this study was to characterize the response of atypical structures to blasting vibrations and airblast generated from surface coal mines. The uniqueness of structure design was addressed by comparing vibration response characteristics with characteristics measured by the U.S. Bureau of Mines and others during previous studies using traditional design structures.

A total of 25 structures were selected for this study at 11 mine sites. Twenty-one structures represented non-traditional designs and four structures comprised traditional wood-frame construction. Ninety-nine mine blasts were conducted during response measurements and 2824 velocity time-histories were recorded and analyzed.

The results of this study are organized in two sections. The first section illustrates the characteristics in mine site blast vibration and airblast generation and attenuation. The second section provides the results of structure response, comparing the relative whole structure and mid-wall motions as well individual structure response relative to external ground vibrations and air overpressures. The response of structure motions relative to ground motions were evaluated in terms of amplification factor as defined by the U.S. Bureau of Mines (Siskind, et al, 1980a) and compared to amplification factors found for traditional structures. Fundamental (or natural) structure frequencies and damping characteristics were evaluated for structures only when significant ground motion and air overpressure intensities were generated. Maximum gross structure and wall strains were calculated based on whole structure differential displacements and mid-wall displacements integrated from velocity time histories. Lastly, the influence of airblast on certain airblast-sensitive structure designs was evaluated.

In each evaluation, data processing and analysis procedures are explained. Data are summarized in table format and selected data are plotted in figures for comparisons. All sensor records are available in electronic format

Summary tables for all sites are given in Appendix III. Data in these tables include the following:

- Blast date and time
- Maximum charge weight per delay and blast-to-structure distance
- Calculated scaled distance (square- and cube-root)
- Ground motion and airblast measurements
  - maximum velocity for each of the three components of ground motions  
(T, transverse, V, vertical and R, radial)

peak particle velocity (PPV, in in/sec), the highest of three components  
peak frequency (Hz) for three components (zero-crossing frequency)  
Fast Fourier Transform (FFT) predominant frequency (Hz) for three components  
airblast, in decibels (dB)

- Whole structure response, single components  
maximum velocity (in/sec), peak (zero crossing) frequency (Hz), and  
FFT frequency (Hz) for the R, V, and T components at either  
S1 (lower corner) and S2 (upper corner)  
S1 (lower corner) and S2 (upper peak or highest point in the structure)  
S1 (lower wall) and S2 (upper wall) for interior or exterior walls  
a variety of locations throughout the structure for conjoined components
- Mid-wall response, single components  
maximum velocity (in/sec), peak (zero crossing) frequency (Hz) and FFT  
frequency (Hz) for the radial (R) and transverse (T) walls

## **Mine Site Characteristics**

Table 2 summarizes the ranges in values for blast-to-structure distances, maximum charge weight per delay and square root scaled distance factors. The total number of mine blasts and number of structures instrumented per site are given. Scaled distance factors ranged from 23 ft/lbs<sup>1/2</sup> in New Mexico to 340 ft/lbs<sup>1/2</sup> at Kentucky site 2. Blast-to-structure distances ranged from 570 ft. in Ohio to 9219 ft. in Indiana. The maximum charge weight detonated per delay among all sites was 13,047 lbs. in New Mexico while the smallest of 126 lbs. was used in Indiana and West Virginia site 1.

## **Ground Vibrations and Airblast Measurements**

### *Ground Vibration Attenuation Plots*

Attenuation plots of peak particle velocity versus square root scaled distance (SRSD) are shown in Figure 8 for all blast data. Figures 9 and 10 are attenuation plots for surface coal mine sites by state. Best-fit lines (50-percentiles) through site data with a sufficient range in scaled distance and a statistically significant data set to allow trend analysis are shown in Figure 9. Included in Figures 9 through 10 is the best-fit line given in Report of Investigation (RI) 8507 by the U.S. Bureau of Mines (Siskind, et al. 1980a) for the maximum horizontal component of ground motion for all coal mine data. Equations and correlation coefficients ( $R^2$ ) for these lines are found in Table 3. The equations were fit to the PPV. Data for sites included in Figure 10 were not correlated. This is because either data represented a narrow range in blast-to-structure distances and charge weights, the data was highly scattered, or a limited number of blasts were conducted to produce a significant data set for correlation purposes.

Central Appalachia data in Figure 10 show a clustered set of similar scaled distances in Virginia and in West Virginia at site 2. Blasting at the remaining sites was conducted at various scaled distances in a number of different compass directions from structures. As such, data trends are not apparent and a narrow spread in ground motion values was recorded below 0.1 in/sec (98.5% of the data fell below 0.1 in/sec).

Interestingly, the New Mexico site generated data for both unconfined (casting) and highly confined (pre-split) as shown in Figure 9. The data fell with two distinct groups and the effects of greater confinement provided by pre-splitting blasting techniques resulted in far higher ground motion amplitudes compared to those produced from casting blast at a given scaled distance. Charge weights per delay for pre-splitting averaged 300 lbs/delay and for casting blasts, charge weights averaged 13,000 lbs/delay.

Equations describing the attenuation of ground motions, shown in Table 3, are compared with those provided by the U.S. Bureau of Mines for surface coal mines (Siskind, et al., 1980a). Site-specific data presented in the current study show a good degree of data correlation for the Alabama, Indiana, and New Mexico sites and scaled distance slope exponents (-b) ranging from -1.34 in Indiana to -2.22 in Alabama. The intercept or source term, 'a', varies from 64 in Indiana for highwall blasts with high relief (e.g. long delay periods along the face) to 5448 in New Mexico for highly confined pre-split blasts. The source term is a good indicator of explosive energy coupling at the blast site. Average values for data parameters 'a' and 'b' are slightly higher than values reported for coal mine data by the U.S. Bureau of Mines summarized in RI 8507, where 'b' is -1.52 and 'a' equal to 119 for all components of ground motion. This difference may indicate the presence of higher attenuating geologies at the current study sites in comparison with the U.S.B.M. sites.

### *Airblast*

Airblast overpressure attenuation is given in Figure 11 for cube root scaled distance (CRSD) showing 50-percentile best-fit lines. Table 4 summarizes the best-fit equations in comparison with equations given by the U.S. Bureau of Mines (Siskind, et al, 1980b). The U.S. Bureau of Mines equation for highwalls shows a source term 'a' of 0.146 and 'b' equal to -0.823,  $R^2$  of 0.77. The data for all sites compare favorably with past U.S. Bureau of Mines data.

## **Frequency Content of Ground Motions**

### *Measuring Frequencies*

Previous research has produced frequency-based velocity data without a clear definition of frequency or methods used to calculate frequencies. Frequency components of a vibration are equally important as the particle velocities. When the intent is to evaluate damage potential, the entire time history, or all frequency component, is an important factor to consider.

Frequency is most reliably computed by applying the Fourier frequency function, or FFT (Fast Fourier Transform), to transform the ground motion time histories (time domain) into the frequency domain. In this manner, the distribution of frequency content can be compared based on relative intensities of ground motion at specific frequencies, and predominant frequencies can be easily identified.

In contrast, the “zero-crossing” method has been widely adopted by industry for determining and reporting a single frequency value at the peak velocity of ground motions

measured in three directions (R, T, and V), or the PPV. Current industry practices employ this “zero-crossing” frequency at the PPV to determine compliance with frequency-based limits (referred to henceforth as the peak frequency). A problem arises when the peak frequency occurs in a complex vibration time history containing a variety of frequencies and amplitudes. If the peak velocity occurs early in the time history within the high frequency components (e.g. above 20 to 30 Hz), the zero-crossing method may result in a frequency well above the natural frequency range of residential structures, even if the entire time history contains a strong low-frequency component. This peak frequency may not represent the frequency at which the maximum vibration energy is transferred into the structure. Most seismograph analysis software provides a means to plot the “zero-crossing” frequency for every peak contained within the time history. In this respect, the vibration energy contained over all frequencies can be evaluated with respect to potential structure response.

### *Measured Vibration Amplitudes and Frequencies*

Peak particle velocity (PPV) data versus frequency are plotted in Figures 12 and 13. The upper bounds are shown for safe level blasting criteria recommendations reported in U.S. Bureau of Mines RI 8507 (Siskind, et al, 1980a) and Office of Surface Mining (1983). Frequency in Figure 12 is the peak frequency at the PPV while in Figure 13, it is the predominant frequency calculated from the power spectrum of the Fast Fourier Transform (FFT).

Table 5 summarizes site-specific differences in frequency ranges calculated by the “zero-crossing” (Z.C.) and FFT methods. In all cases, with the exception of Tennessee, Z.C. frequencies at the PPV are higher at the upper end of the range compared with the FFT method. The change in the highest frequency within the range is most dramatic at five sites (Kentucky 1, New Mexico, Alabama, Kentucky-2, and Indiana) with upper Z.C. frequencies from 18 to 34 Hz and upper FFT frequencies less than 20 Hz. The remaining sites did not show such a large difference. The Tennessee site FFT frequencies actually increased over the Z.C. frequency. This increase is probably because the structure foundations rests directly on bedrock and measured ground motions were recorded within the thin, overlying soil layer where high frequencies were preserved.

Since the FFT method accounts for the entire wave train, it is preferred for structure response analysis. FFT is closely related to response spectra of ground motions and are employed to calculate structural natural frequencies and damping from structure motions.

### *Summary of Findings*

These observations serve to illustrate a number of important points as follows:

- Different site characteristics, particularly structure site geology and blast-to-structure distance, produced different frequency content. Structure distances ranged from 570 ft. to 6280 ft. from the blasting. Certain structures such as those in Tennessee were founded directly on bedrock while others (in New Mexico) were founded on thick soils. Sites with different foundation materials produced a spread in ground motion frequencies while

sites with similar geology produced a concentration of data within a narrow frequency range.

- At all but one mine site, FFT frequencies fell below “zero-crossing” frequencies and within the natural frequencies of structures for walls (12 to 20 Hz) and superstructures (5 to 10 Hz) reported by Dowding (1996).
- The Z.C. method employed to calculate frequencies were generally above those computed using the FFT method when only the peak velocities were analyzed.
- Frequencies calculated using the FFT method is preferred since they involve the full wave form and are a more conservative estimate of the dominant excitation frequency.
- Airblast attenuation was similar to that observed by the U.S. Bureau of Mines.
- Peak particle velocities for Appalachian coal mines were consistently below mean values predicated using scaled distance by the U.S. Bureau of Mines in RI 8507 for all coal mines with the exception of Pennsylvania. This is because mining in Appalachia is conducted at elevations higher than those of structures and well behind slope berms. As a result, PPV values are highly attenuated.
- Pre-split blasting consistently shows PPV values well above the mean for coal mining in RI 8507.

## **Structure Response**

The measured response of structures to blasting vibrations and airblast are important to assess damage potential to individual components of the building. The amount of structure shaking is a function of the amplitude and frequency content of external ground velocity and airblast overpressure and the natural frequency and damping characteristics of the structure. Horizontal components of ground velocities are often amplified in structures while the highest structure velocities are measured when the ground frequency occurs at or within the structure's natural frequencies. The amplification of structure response relative to external ground vibrations is an important factor when assessing blast damage potential.

Two modes of structure vibrations occur during blasting and are referred to as mid-wall and whole structure responses. Mid-wall response is the motion of individual components such as wall, floors and ceilings, where motions are perpendicular to the plane of the building component. Mid-walls generally respond at high frequencies and tend to rattle windows and loose objects attached to walls. Resulting bending strains tend to be the greatest when the walls respond at their natural frequencies.

Whole structure response is vibration of the entire structure frame, measured at an outside corner, resulting in distortions, or racking, in walls. At low frequencies and high amplitudes of ground motions, whole structure deflections produce wall shear strains that, in turn, may be

potentially damaging. Structure deflections are measured in terms of differential displacements between the upper and low (ground) corners in structures.

*Time History Comparisons: Structure Response Relative to Ground Motions and Air Overpressures*

Structural response (SR) to ground velocity and air pressure (airblast) are shown for (S2) upper structure corner locations or wall peaks, in rooms with vaulted ceilings and (S1) lower structure corners, at the base of the first floor wall, and mid-walls in Appendix IV. Ground velocities (GV) and air pressure (AP) are shown for comparisons. Peak values for velocities and airblast are provided. Superimposing excitation and structure response waveforms provides a visual means of evaluating the energy transferred into the structures over time. It further allows visual evaluation of structure or mid-wall free response after passage of the ground and air pressure pulses. Horizontal components of velocity were selected for comparisons. The maximum structure velocity in either the radial or transverse component is shown in Appendix IV figures, depending on the peak occurring within the structure.

Vertical components were only evaluated for manufactured (trailers) structures where structure response vertical motions were amplified. For all other structure designs, negligible differences among the lower and upper structure responses relative to ground vertical motions could be detected. Vertical structure motions within most structures duplicated ground vertical components in frequency, amplitude, and phase.

All vibrations are plotted in terms of velocity, in inches per second (in/sec). Vertical scales are not given and may vary between figures. However, among waveforms being compared in any one figure, constant vertical scales are used. Air pressure (AP) vertical scales are consistent among all plots.

Waveform time histories are expanded in time to illustrate similarities or differences in amplitudes, frequencies, and phases. Phase refers to the positive and negative pulse shapes forming the sinusoidal characteristics of a waveform. Vibrations of structures that are well-coupled to the ground may show good time history in-phase match with ground motions. However, when ground motion exhibit frequencies close to the natural frequency of the structure, structure vibrations are amplified and exhibit a near 90-degrees phase shift from the forcing or excitation motions.

Structure designs used for comparisons include manufactured (trailers), log, camp, earth, stone, and masonry. Responses of standard wood-frame structures are not shown as responses do not show uniqueness beyond what other structure studies show.

Figure IV-1 compares ground motions with those at the structure base (S1). Figure IV-2 shows comparisons between S1 and S2, the upper structure response. In Figures IV-3 through IV-6, ground and S2 motions are compared relative to air pressure time histories. Air pressure time histories are plotted with mid-wall and S2 structure responses in Figures IV-7 through IV-10 to show the airblast effects of whole structure and wall responses.

**Ground motion versus lower structure response:** Lower structure horizontal responses (S1) are generally equal to or lower in amplitude than the same component of ground motion for all structure design with the exception of trailers. Trailer structure base motions for single wide and double wide trailers shown in Figure IV-1(a) can exceed those of the ground except in the case of trailers with wood-frame add-ons (TSA-KY2). This is observed also for camp structures to a less extent in Figure IV-1(d). One-story traditional log structure base response given in Figure IV-1(b) and earth, stone, and masonry structures shown in Figure IV-1(c) often fell well below motions in the ground.

Vertical components of ground and S1 velocities are superimposed in Figure IV-1(e) to show the amplification of vertical motions in single and double wide trailers. Vertical trailer responses are amplified because trailers are not coupled to the ground and are free to bounce. Furthermore, the tendency of trailers to rotate around the long axis (radial direction) in the transverse directions can often translate a portion of this response in the vertical direction, resulting in higher vertical response than would be predicted by ground motions. This type of structure response is unique to trailers and was not measured in other structure designs.

**Lower structure response versus upper structure response:** Differential horizontal motions, or the difference between upper structure response, S2, and lower structure response, S1, induce whole structure strains in walls from racking distortions. Computing differential displacements, by first integrating the velocity time histories and subtracting S1 from S2 over time, allows the best estimation of strains.

A visual comparison of relative horizontal motions between the upper (S2) and lower (S1) walls of structures is shown in Figure IV-2. A good agreement of velocity time histories for most structure designs exists with the exception of log structures, shown in Figure IV-2 (b), and the two-story camp structure (C2S-KY1A) in Figure IV-2(d). All trailer motions showed good phase agreement (e.g. time history peaks and troughs matched in frequency). Motions in adobe (E1S-NMB) and concrete block (E1S-NMA) structures given in Figure IV-2 (c) show good phase agreement and amplification of S1 motions in the upper structure (at S2). The two-story stone structure (E2S-NM) did not show good phase matching.

Log structures, regardless of design, do not show similar upper and lower structure responses. Motions do not match in peaks while two-story designs show amplification of the upper response that is absent in one-story designs. This is to be expected because log structures are not constructed with a frame and the upper and lower horizontal log members move independently.

**Ground and air pressure time histories relative to upper structure response:** Upper structure (S2) response relative to ground motions and air pressure (or the pressure equivalent of airblast) are shown in Figures IV-3 through IV-6. Structures used to illustrate air pressure effects were subjected to airblast levels at or above 116 decibels (dB) (with the exception of camp structure C2S-KY1A). Single wide trailer responses (Figure IV-3) are less sensitive to ground vibrations than to airblast pressures. The airblast phase of structure response shows higher S2 amplitudes than for the ground motions phase for trailers TS-KY2, TS-IN, and TSA-KY2 with a wood-frame add-on. Airblast influence is not as apparent in double wide trailer TD-WV2 because the



instruments used to measure whole structure response were placed along the interior center (marriage) wall. Note that the ground and S2 responses are approximately 90-degrees out of phase (where structure peaks lag behind peak in the ground motion) indicating that the deformation response of the structure is at a maximum.

Airblast excitation of whole structure response is apparent in the two-story log structures shown in Figure IV-4 (L2S-WV2 and L2S-TN) and is not as noticeable in one-story log, camp, earth, and masonry structures. The two-story stone structure E2S-NM, shown in Figure IV-5, was responding at the natural frequency by the time that the air pressure arrived and shows not additional response. This is evidence again by the phase shift in S2 response relative to the ground motion.

**Mid-wall and upper structure response to air pressure:** Mid-wall and upper structure (S2) motions shown in Figures IV-7 through IV-10 are compared with airblast arrival. Mid-wall motions show both high frequency and low frequency characteristics for log, camp, earth, stone, and masonry structures while trailer mid-walls responded only at high frequencies. Of the log structures for which mid-walls were measured, only L2S-OH mid-wall duplicated the low frequency peak S2 response. This is because the wall measured was the “great wall” in the living room with a vaulted ceiling containing a massive stone chimney. Therefore, the mid-wall and upper peaks tended to move as one unit. This response was also observed in the two-story stone structure E2S-NM in Figure IV-9. The absence of high frequency components in the upper story mid-wall shows the strong influence of the whole structure motions on the massive stone mid-wall, indicating that the mid-wall moved in concert with the structure and not independently.

The one-story log structure L1S-WV1 did not show detectable mid-wall response to airblast (Figure IV-8). Similarly, the influence of air pressures is not significant for earth, stone and masonry mid-walls given in Figure IV-9. One-story adobe and concrete block structures also showed a correspondence in motions between upper structure and mid-walls. However E1S-NMB responded with both high and low frequencies.

Trailer mid-wall response is similar to the low frequency whole structure response with high frequencies superimposed. The large difference in exterior wall mid-wall response from S2 response for TD-WV2 given in Figure IV-7 is because S2 was measured on an interior wall and mid-wall response is shown for an exterior wall.

The mid-wall response of the one-story camp structure in Figure IV-10 is typical of motions for loose surface covering such as wood paneling in a thin-walled structure. In this case the mid-wall shows a large amplification over the upper structure response because of the loosely nailed paneling on this exterior wall to which the motion sensor was attached. The mid-wall response therefore is not necessarily true mid-wall response but rather the response of the material covering the wall. It is indicative, however, of rattling of objects on or adjacent to walls.

### *Summary of findings*

- Lower corner horizontal responses for single wide and double wide trailers and camp structures exceeded ground velocities for similar components. Single wide trailer with wood frame add-ons do not show this behavior.
- The lower horizontal corner response in log, earth, and masonry structures are equal or less than external ground motions.
- Trailers exhibited amplification of vertical ground velocities. Vertical structure response was less than external vertical vibration for all other structure designs.
- Upper (S2) and lower (S1) corners move in phase for trailers and one story camp, earth, stone, and masonry construction. Log structure corner motions are highly random and out of phase because they lack the frame support provided in other structure designs. Two story stone and camp structures show similar characteristics to log designs.
- The influence of airblast on whole structure response, for airblast of 116 dB and above, is clearly measured for trailers and two-story log structures. Earth, masonry and camp designs do not clearly show structure response to airblast.
- Mid-walls respond at high frequencies relative to whole structure responses. However, for log, camp, earth, stone, and masonry structures, mid-walls carried additional low frequencies associated with whole structure responses. Mid-walls did not respond to airblast in one-story log, earth, masonry, and two-story stone structures. Airblast effects are readily measured in mid-wall of all trailers, with both high and low frequency (whole structure) components, and camp structures.
- Loosely attached construction components and wall covering, such as paneling, can create high mid-wall motions that are not associated with structure response.

### *Correlating Structure Response to Ground Motions and Air Pressures*

Whole structure (S2) and mid-wall responses were plotted against PPV and maximum airblast overpressure to compare the relative influences on structure response. Depending on structure design, the maximum structure responses will fall within the ground motion phase or airblast phase of structure response. For instance, trailer are sensitive to airblast and many of the peak velocities contained within the mid-wall time histories occur simultaneously with the airblast arrival (airblast phase) rather than during the passage of the ground motion wave (ground phase). Other structures show a greater sensitivity to ground motions and relatively little response to air pressures.

Maximum velocities within the upper structure (corner or peak measured at S2) and mid-wall time histories were plotted against the respective excitation driving the peak (e.g. peak air

pressure or peak ground motion). Only horizontal components in the transverse, T, or radial, R, directions are considered.

Best-fit equations of structure response versus PPV for each structure design are presented in Table 6 to be consistent with RI 8507. Earlier discussions showed the importance of the entire excitation wave train. Thus these equations should not be used to predict structure response motion.

All equations were forced through the origin with a y-intercept value of '0'. A positive y-intercept at  $x = 0$  is meaningless as it is not possible to measure a structure response without a positive driving force. A negative y-intercept is feasible in the case where a threshold force is necessary to measure a response. Although comparing this threshold among structures may be of interest, it was not a necessary component of response and therefore not measured. For comparisons with U.S. Bureau of Mines structure response equations given in RI 8507, positive y-intercepts were necessary to compute in some cases, but are not shown in Table 6.

**Structure response to ground vibrations:** Ground motion-induced peak structure responses are compared in Figures 14 and 15 for whole structures and mid-walls. Upper corner peak motions in Figure 14 show that only two structure designs (one-story log and earth, stone, and masonry) were subjected to peak ground motions greater than 0.40 in/sec. By comparing the data in Figure 14 with Figure 35 in RI 8507, it is apparent that atypical structure responses fall with the range of U.S. Bureau of Mines data.

However, the response of the two-story stone structure within a narrow range of ground motions from 0.21 to 0.45 in/sec shows amplifications above those exhibited by other structures within the same PPV range. The stone structure response can be explained by two factors. The unusual construction does not include an upper bond beam along the top of the walls. As such, the stone structure is free to respond without typical wall constraints. The second factor is that the ground frequency matched the natural frequency of the structure (about 4 Hz).

Mid-wall responses are shown for all structures in Figure 15. The mid-wall response of the stone structure is well above other structure designs. This is because the mid-walls did not move independently of the whole structure and amplified the 4 Hz ground vibrations. Mid-wall horizontal motions fall within the range of mid-wall responses reported in RI 8507 Figure 33.

Trailers are unique in that they have large ratios of transverse to radial wall dimensions. Figure 16 shows that the mid-wall responses in all trailers fall within two trends. Trailers tend to "rock" along the long axis and whole structure responses are far larger in the transverse direction than in the radial direction. As stated previously, mid-walls carry the same motion carried by the whole structure. Hence, transverse mid-walls in trailers respond to this higher transverse motion.

Best-fit lines for one and two-story whole structure horizontal corner responses are given in Figure 17. Equations in Table 6 for these lines (given for all structures) show a large difference in slopes averaged for all structures. The one-story slope coefficient of 0.63 agrees with U.S. Bureau of Mines data fit for one-story wood frame structures (0.56 slope). Although the two-story slope of 1.43 falls above the 0.55 slope reported in RI 8507 for coal mine data,

two-story whole structure responses fall within U.S. Bureau of Mines measurements when quarry and iron mine data are included.

**Structure response to airblast overpressures:** Airblast induced whole structure and mid-wall responses are shown in Figures 18 and 19. Earth, stone, and masonry structures did not respond to airblast over the ranges measured. All peak structure responses occurred strictly in the ground motion phase. Log structures exhibited little whole structure responses and no air-blast induced mid-wall responses.

The greatest airblast sensitivity existed in trailers for both mid-wall and whole structure responses. The large population of airblast-induced data for trailers indicates that the majority of the peak structure responses tended to fall within the airblast phase as opposed to the ground motion phase. Wood-frame and camp structures exhibited some sensitivity to airblast relative to ground motion. A comparison of mid-wall motions shows approximately 1.3, 1.8 and 2.9 times greater air-induced motions relative to ground-induced motions among trailers, wood-frame, and camp structure, respectively.

The unusual trailer and wood frame response to airblast (shown grouped within the ellipse in Figure 18) were recorded during an 11.6 Hz airblast pulse. The airblast frequency precisely matched the detonation time equal to the 67 ms front row delays plus the arrival time between holes spaced 21 feet apart, adding a 19 ms inter-hole travel time (21 ft. divided by the speed of sound in air around 1100 ft.). The inverse of 0.086 ms pulse beat is a strong 11.6 Hz that matched the power spectrum peak. This unusual airblast frequency is shown in Figure IV-7 for structure TS-IN and the response of the mid-walls and, to some degree, the whole structure, is evident.

Whole structure (racking) airblast responses in this study were very close to previous U.S. Bureau of Mines studies and recent measurements by Siskind (2002). The envelope of maximum response shown in Figure 18 is 77 in/sec/psi for well-confined blasts and 155 in/sec/psi for unusually high frequency airblasts. Historical U.S. Bureau of Mines and values provided by Siskind (2002) for equivalent type airblasts were 42 and 135 in/sec/psi, respectively. With the high variability of airblast characteristics and hence responses, these results can be considered equivalent and normal.

Airblast and vibration guidelines can be compared. The racking response maximum value of 155 in/sec/psi and regulatory limits of 132 dB for a 2-Hertz system (0.0129 psi), gives a maximum structure response of 2.06 in/sec.

In contrast to whole structure response, mid-wall responses to airblast shown in Figure 19 are higher than historical values, specifically for the trailer type structures. This study's worst case envelope for mid-wall responses was 442 in/sec/psi. The historical U.S. Bureau of Mines value was about 319 in/sec/psi, but did not include trailers. This study's results, exclusive of trailers, found a maximum of 266 in/sec/psi that is fairly close to the U.S. Bureau of Mine's value.

### *Summary of findings*

- Whole structure and mid-wall peak responses induced by ground motions for all structures fell within data provided in U.S. Bureau of Mines RI 8507.
- Ground motion-induced whole structure response for one-story structures agrees with U.S. Bureau of Mines data fit for one-story wood frame structures. Two-story structure response falls above structure response reported in RI 8507 for coal mine data and within U.S. Bureau of Mines measurements when quarry and iron mine data are included.
- Earth, stone, and masonry structures did not response to airblast pressures while log structures produced measurable mid-wall responses and low whole structure responses.
- Trailers showed the highest whole structure and mid-wall responses to airblast with envelopes of 155 in/sec/psi and 442 in/sec/psi., respectively. Envelopes for other structures are 77 in/sec/psi and 266 in/sec/psi. These envelopes agree with historical U.S. Bureau of Mines data for non-trailer structures and are within normal ranges.

### **Fundamental Frequency Analysis: Natural Frequencies and Structure Damping**

The natural frequency of each structure design was estimated using three methods. The first two methods were used to compute the natural frequencies during free response, when ground motions arrested, and during ground motion activity, when structure response peaks were 90-degrees out of phase with the ground motion peaks. The third method employed FFT analysis to calculate the predominant frequency of motion in structures when there was no free response. Calculating predominant frequencies using FFT analysis to estimate structure frequency response is desirable because blasting seismograph software easily accommodates this analysis. Isolating and computing natural frequencies over the response portion of structures that truly represents free response is often time consuming and requires experience. Therefore, a comparison of free response natural frequencies to FFT predominant frequencies is given herein to determine if using FFT analysis provides a good measure of structure free response.

#### *Natural Frequency of Structures*

Natural frequencies in structures can be observed either during free vibrations, when ground motions have ended, or during ground motions, producing a near-perfect sinusoid response, symmetrical about the time history x-axis and containing one single frequency. In the later case, structure vibration peaks will show a 90-degree phase angle shift from the ground motion (excitation) peaks, as described by Crum (1997) and predicted by theory (Harris, 2001). Examples of waveform time histories showing natural frequencies produced in the second floor upper corner and mid-wall during ground motions are given in Figures 20 (a) and (b). The ground motions are 90-degrees out of phase within the mid-wall and upper structure motions beyond the time marked by the vertical dashed lines. Just beyond this time the natural frequency can be measured. It should be pointed out that only two structures, TD-WV2 and E2S-NM, exhibited natural frequency response during ground motion activity.

Figure 20 (c) illustrates free response of an upper corner once ground motions have arrested and before arrival of the airblast. The structure response in this region, between 3.5 sec. and 6 sec., is 4.0 Hz. True free response measurements are often difficult to detect and analyze in the absence of ground motions and before the arrival of the airblast pulse. If the airblast arrives before ground motions arrest, free response may not be detected. The majority of structures exhibited this form of free response for natural frequency measurements. However, a sufficient number of structure responses in which ground motions could be isolated from airblast influence to obtain reliable free response measurements.

Table 7 shows the natural frequencies computed during the response phase shift from ground motions for E2S-NM (two-story stone structure) and TD-WV2 (double wide trailer). The 4.0 Hz stone structure radial and transverse mid-wall sensors were located on the first and second floors, respectively. The transverse S2 sensor placed in the 7.0 Hz double wide trailer was located along the marriage (center) wall and the radial sensor was placed on the outside wall, center at the structure peak. Both mid-walls were placed on outside walls. Within each structure, the frequency responses in mid-walls and the whole structure were identical, indicating that mid-walls do not respond independently but rather with the upper structure. Table 8 summarizes structure free response frequencies, calculated using the FFT of the time history after the ground motion has arrested. Data from structure response given in Table 3 from U.S.B.M RI 8507 for wood-frame structures are provide for comparison. Whole structure free response data for all structure and all sites compare well with U.S.B.M. data. Mid-wall response data may not compare because the U.S.B.M placed mid-wall sensors on the wall facing the blasts to capture air pressure effects. Therefore orientations could not be verified and mid-wall response data are averaged for both T and R directions.

#### *Structure Response Based on Ground Motion FFT Analysis*

Appendix V contains plots of relative amplitude from FFT analysis for S2 and MW as well as predominant frequencies of structure response compared to the dominant FFT frequencies of ground motions. Data are grouped by responses for radial, R, and transverse, T, walls to demonstrate that R and T frequencies are different for most structures.

Plotting structure response FFT frequencies based on relative amplitude from spectral analysis is a good means of identifying specific structures that respond at a unique and consistent frequency, regardless of ground motion amplitude and airblast levels. This further serves to illustrate how structures may amplify ground motions if the predominant ground frequency is close to the natural frequencies of the whole structure or mid-walls.

Figure V-1 through V-4 show relative amplitudes plotted against FFT predominant frequency at the upper structure (S2) and mid-walls (MW) for T and R walls. These peaks do not necessarily correlate with the averages given in Table 8 for all structures within each category as they represent the strong, dominating frequency for a single structure within the design category. For instance, in Figure V-1 (a), the single, strong peak at 3.8 Hz represents the predominant upper structure motion in TS-OH while all other single-wide trailers responded at higher frequencies. Whole structure double-wide trailer responses (TD-WV2 and TD-PA) shown

in Figure V-1 (b) are centered at 7.2 Hz. Trailers with wood-frame add-ons responded at 4.4 Hz and 7.7 Hz.

Other dominating T frequencies are observed for all log structures, between 6.1 and 6.4 Hz, for designs with vaulted ceilings at 8.3 Hz, and earth, stone, and masonry structures, centered at 4.0 Hz. Camp and wood-frame structures show various amplitudes at a variety of frequencies that are not centered on one value.

Radial structure and wall motions show some predominance at 6.6 Hz for single-wide trailer TS-OH. Earth, stone, and masonry and log structures show central R frequencies similar to those in the T direction while camp and wood-frame structure show some focus between 6 to 7 Hz.

In Figures V-5 through V-8, T and R upper structure frequency responses are plotted against ground motions in terms of peak FFT frequencies. Data in Figure V-5 and V-7 indicate that single-wide and double-wide trailer structure frequencies do not correlate with ground motion frequencies for the same component. Response frequencies vary for whole structure and mid-walls. Wood-frame add-on trailers and log structures show a uniform behavior in response frequencies over a wide range of ground motion frequencies. Mid-walls tend to respond at frequencies higher than the upper structure. This is also observed for T walls for wood-frames structures in Figure V-6 (d).

Therefore, regardless of ground motions frequencies, structure frequencies were low and structures tended to respond at their natural frequencies. Trailers are an exception where structure frequencies highly varied.

#### *Verification of Spectral Analysis Ability of Seismic Data Analysis Software*

When using FFT methods to calculate frequency content, a question always arises regarding the computation schemes used in computing the power spectrum. The ability of computations to resolve the peak or predominant frequency in a spectral plot is a function of the number of data in the time history (record length) and sample rate (number of data points). The longer the record length, the more data are contained in the time history, and the frequency intervals become smaller. When only a small segment of the waveform (e.g. containing the natural frequency) is used in the FFT analysis, frequency intervals may become large, on the order of 0.5 to 1 Hz. Resolving the dominant frequency within  $\pm 0.2$  Hz may not be possible and the true peak may be missed.

Spectral plots using two software are compared in Figure 21 for the upper corner transverse response for TS-OH given in (a). Spectral plots using Seismograph Data Analysis 2000 v. 6.2.3 from White Industrial Seismology, Inc., and NUVIB (Huang, 1994) for various record length segments shown in Figure 21 (a) are given in Figures 21 (b) through 21 (d). Although the frequency intervals are not the same for each record length selected, the predominant frequencies calculated by each methods are in good agreement as follows:

	Predominant frequency in Hz	
	White software	NUVIB
Entire waveform	3.75	3.72
Segment 1	4.00	4.00
Segment 2	3.75	3.72

### *Damping of Structure Motion*

Structure damping near the natural frequency or during free responses was computed. Damping is the structure's resistance to movement and causes the structure to return to its resting position in a harmonic sinusoid. The harmonic vibration peaks decay in a well-defined exponential function from a maximum value,  $P_1$ , according to the following:

$$\beta = \frac{1}{2\pi m} \ln \frac{P_1}{P_{m+1}} \quad (100\%) \quad (1)$$

where  $\beta$  is the damping coefficient,  $P_1$  and  $P_{m+1}$  are the successively peak amplitudes where  $P_1 > P_{m+1}$  and  $P_1$  is usually taken as the peak “free” response after the ground vibration has ceased.  $P_{m+1}$  is any peak following  $P_1$ , “m” cycles later in time. The damping coefficient is defined as the percentage of critical damping, where perfect damping is 100%. A perfectly damped system (such as a well-coupled geophone) is one that responds exactly the same as the driving force. On the other hand, at 0% damping, a structure would resonate and never stop vibrating. Values for successive damped peaks in the time history used to calculate  $\beta$  are illustrated in Figure 20 as  $P_1$  and  $P_2$ .

Damping in structures is low as it takes many oscillations for a structure to complete moving. Dowding (1985) reports damping for residential structures in the range of 2 % to 10% of critical.

Damping terms were computed for structures that exhibited response peaks out of phase from ground motions, shown in Table 7, and for structures that exhibited free response after ground motions arrested, summarized in Table 9. Based on the data in Table 9, trailer transverse mid-walls showed the greatest damping (9.5% of critical). Log and trailer structures exhibited high damping in the radial structure peaks (9.7% and 9.6%, respectively). The least damped structure type was the earth, stone, and masonry structures with a 3.9% average damping term (the CMU block structure, E1S-NMA, did not show free response and therefore damping could not be computed). High damping in trailer and log structures can be explained by the unconstrained nature of construction components that do not effectively transmit frequencies. CMU piers supporting trailers are not mortared while logs are not nailed together to form a solid, supporting mass. Structure response amplitude may be high in such structures, but they quickly dampen due to the lack of structure bonding.



### *Summary of Findings*

- Whole structure and mid-wall natural frequencies were determined for free response motions. Whole structures averaged 6.0 Hz and mid-wall averaged ranged from 8.4 to 13.8 Hz. U.S. Bureau of Mines whole structure natural frequencies range 7.1 to 7.8 Hz and mid-walls averaged 16.4 Hz.
- Average damping for all structure was 7.8% for whole structure vibrations and ranged between 7.3 % to 6.2 % for mid-walls. Average damping values found by the U.S. Bureau of Mines ranged 4.4 % to 5% for whole structures and 1.8 % to 2.3 % for mid-walls.
- FFT methods are preferred to predict dominant frequencies because it takes into account the entire time history.
- Structures tended to respond at their natural frequencies with the exception of trailers. Structure response frequencies in trailers are highly varied and often are higher than the natural frequency.
- Log and trailer structures are more highly damped because of their lack of structure bonding.

### **Amplification Factors**

Time-correlated amplifications of ground motions within structures were computed in terms of an amplification factor (AF) defined by Siskind et al. (1980a) and explained by Crum (1997). AF is defined as

$$AF = \frac{S2_{peak}}{V} \quad (2)$$

where  $S2_{peak}$  is the maximum velocity of the upper structure and  $V$  is the velocity of the ground motion for the same component at the corresponding moment of time or immediately preceding the time at the peak  $S2$  motion. AF values were also computed using peak mid-wall responses relative to  $V$  in the ground.

Whole structure and mid-wall amplifications were determined from superimposed velocity time histories as shown in Figure 22 for the upper structure relative to ground velocity.

Plots of AF for whole structure responses are plotted for predominant FFT ground motion frequencies in Figures 23 through 27. For ground motion FFT frequencies greater than 7.1 Hz, the mean AF is 1.7 with a maximum of 3.3. At 7.1 Hz and below, the mean AF is 2.2 with a maximum of 5.0. Amplification factors greater than 3 were associated with ground motion frequencies between 4.0 and 7.1 Hz.

In U.S.B.M RI 8507, typical whole structure amplification factors are reported to be 1.5 with 4.0 being the highest value. The greatest values occurred at ground motion frequencies between 5 and 12 Hz. The U.S.B.M. study did not include sites with ground motion frequencies less than 5 Hz and included ground motions up to 85 Hz. In the current study, the average site ground motion frequency was 9.6 Hz with 28% of the sites exhibiting ground motion dominant frequencies of 5 Hz or less. It is reasonable to conclude that the U.S.B.M. data did not include AF greater than 4 because ground motion frequencies did not fall within the lower ranges of structure natural frequencies included in the current study.

Amplification plots by structure show that the two-story stone and two-story camp structures show the highest average amplification factors because structure natural frequencies matched those of the ground. The 4-Hz stone structure (E2S-NM) was subjected to six blasts with an average ground motion frequency of 4 Hz. One single two-story camp structure, with a natural frequency response of 6.1 Hz, was subjected to five blasts with ground motions averaging 6.4 Hz.

#### *Summary of Findings*

- Time correlated amplification factors (AF) ranged from 0.4 to 5. The U.S. Bureau of Mines calculated AF from 1.5 and 4.0.
- The highest AF values were observed for the two-story stone (4.6) and two-story camp structures (5.0) where the ground vibration frequencies matched the natural frequency of the structures. Log and one-story earth and masonry structures exhibited the lowest values of AF. Amplification factors in trailer were 4.0 and less.
- The highest amplification factors occurred when ground motion predominant frequencies matched structure natural frequencies.

#### **Relative Displacements and Calculated Strains**

Previous studies involving crack observations during blasting have shown that a strong correlation exists between peak particle velocity and blast-induced threshold wall damage (Nicholls, et al., 1971; Siskind, et al., 1980a; Stagg, et al., 1984). Studies that included dynamic strain gage instruments mounted on walls have produced limited insight to threshold strains that cause wall cracking. This is because changes in crack lengths and widths for blasting events are similar for time periods when no blasting took place. Furthermore, it is not possible to anticipate the wall locations that cracking will take place such that strain gages can be strategically placed.

Only two studies are notable. Wiss and Nicholls (1974) measured failure strains in gypsum wallboard during blasting and found new cracks formed during a maximum dynamic wall strain of 1010  $\mu$ -strains. Critical tensile failure strains in gypsum wallboard are given in RI 8507 by Siskind, et al., 1980a. Openings along butt joints and new cracks appeared during blasting events at failure strains in excess of 300 to 400  $\mu$ -strains. Strains associated with mortar

joint cracking during blasting were measured in excess of 300  $\mu$ -strains (Edwards and Northwood, 1960; Northwood, et al., 1963).

Differential structure displacement time histories were computed by integrating velocity traces and used to compute the maximum differential whole structure strains. Peak or maximum differential displacements,  $\Delta\delta_{\max}$ , between the upper and lower structure motions were used to determine global wall shear strains,  $\gamma$ , and maximum wall bending strains,  $\varepsilon$ . A schematic showing displacement and global shear strain is given in Figure 28. Note that the sensors mounted on the radial walls (the wall of the shortest overall structure lateral dimensions) measure gross structure motions in the transverse direction. Similarly, the transverse sensors measure motions in the radial walls.

Maximum differential displacements were computed by subtracting time-correlated displacement time histories measured at S1 (lower structure corner) from S2 time histories (upper structure corner). Since the polarity of the transducers was known, the resultant displacements were automatically accounted. Thus the relative displacement was obtained by simple subtraction. However only the absolute values are reported.

The maximum global structure shear strain of the wall,  $\gamma$ , is computed using the peak or maximum differential displacement divided by the wall height as follows:

$$\gamma = \frac{\Delta\delta_{\max}}{L} \quad (3)$$

where L is the wall height in inches and  $\Delta\delta_{\max}$  is in inches. Therefore  $\gamma$  is given as  $\mu$ -in./in. or  $\mu$ -strains.

The in-plane tensile wall strain,  $\varepsilon_L$ , is related to the gross structure shear strain for the same wall being affected by the motions. The maximum in-plane strain,  $\varepsilon_{L(\max)}$ , is aligned along a 45 degree diagonal as shown in Figure 28, where  $\theta = 45^\circ$  is the direction of the maximum strain. The solution for in-plane tensile strains can be found in basic mechanics textbooks and  $\varepsilon_{L(\max)}$  is given as

$$\varepsilon_{L(\max)} = \gamma_{\max} \sin \theta \cos \theta \quad (4)$$

which reduces to

$$\varepsilon_{L(\max)} = (0.5) \gamma_{\max}$$

when  $\theta = 45^\circ$  for square walls and  $\varepsilon_{L(\max)}$  is one-half of the gross structure strain,  $\gamma$ . Global or overall in-plane tensile strains are critical to threshold wall cracking potential.

Calculations of wall bending strains with midwall motions is more challenging because it is necessary to estimate the bending mode shape. Dowding (1985) discusses this issue when relative upper corner superstructure displacements are known. The degree of fixity of the wall

top and bottom controls the mode shape and thus the calculation of bending strains. Two of the possible mode shapes, fixed-free, and fixed-fixed, lead to following equations for maximum wall bending strain:

$$\varepsilon = \frac{6d\Delta\delta'_{\max}}{L^2} \quad (\text{fixed-fixed}) \quad (5)$$

$$\varepsilon = \frac{3d\Delta\delta'_{\max}}{L^2} \quad (\text{fixed-free}) \quad (6)$$

where  $d$  is the wall thickness divided by two, in inches, and  $\varepsilon$  is given as  $\mu\text{-in./in.}$  or  $\mu\text{-strains}$ . Even though the mode shapes and thus the coefficients to the strain equations can vary considerably as a result of the mode shape, a coefficient of 6 was employed in this study along with the maximum wall height for  $L$ .

The relative nature of the midwall displacements that are employed to calculate strains is also important. Where the midwall displacements,  $MW$ , are greater than those at either  $S1$  or  $S2$ , it is difficult to know the relative midwall displacement with respect to displacements at the upper and lower corners. In this study, the average of the  $S1$  and  $S2$  was employed and the maximum wall displacement,  $\Delta\delta'_{\max}$ , assumed to be located at the mid-wall, is calculated as

$$\Delta\delta'_{\max} = S_{mw} - \left( \frac{S_2 + S_1}{2} \right) \quad (7)$$

where  $S_{mw}$  is the peak mid-wall displacement and  $S2$  and  $S1$  are the time-correlated upper and lower corner displacements.

Calculated in-plane tensile strains and wall bending strains are summarized by structure design in Table 11. Average and maximum values are reported. Figures 29 (a) and (b) show examples of differential displacements (in terms of absolute values) calculations for the E2S-NM two-story stone structure in the radial and transverse directions, respectively. These displacements, given in inches, represent the average measurements for this structure during the study. Velocity time histories at the upper ( $S2$ ) and lower ( $S1$ ) structure corners were integrated and the resulting displacement time histories are subtracted ( $S2 - S1$ ) to obtain the differential wall shear displacements. The absolute value of  $S2 - S1$  is shown to readily display the maximum value of  $\Delta\delta_{\max}$ .

Maximum calculated in-plane tensile strains and maximum calculated wall bending strains are shown in Figures 30 and 31 plotted against maximum ground motion for the same component. The largest in-plane tensile strains shown in Figure 30 were calculated from time-correlated differential displacements in the second story of the stone structure (E2S-NM). Motions in the radial direction resulted in a maximum calculated in-plane tensile strain of 113.1  $\mu\text{-strain}$  in the transverse wall. The second story transverse wall produced a maximum calculated bending strain of 46.6  $\mu\text{-strain}$ , assuming a fixed-free model of bending and is shown in Figure 31 at a PPV of 0.46 in/sec. The fixed-free model for structure E2S-NM is justified based on the

absence of a top plate or beams affixed to the stone exterior walls to render the upper structure rigid. Calculated strains in the stone structure are below levels measured during previous research on mortar joint cracking during blasting.

One- and two-story log structures carry large strains due to their natural flexibility supplied by the individual wood members. Radial motions produced transverse wall peak strains of 95.5 and 66.6  $\mu$ -strain for one- and two-story log structures, respectively. Mid-wall strains were relative small for two-story structures and among the highest for one-story designs. Depending on the quality of wood, failure strains for logs can range from 7000 to 20,000  $\mu$ -strain (USDA, 1999). Therefore, calculated strains produced by blasting during this study are far below those strain levels that could possibly cause cracks in log walls.

Calculated strains produced in trailers, camp, wood-frame, concrete block, and adobe structures were as high as 12.5  $\mu$ -strains for gross structure shear (for which the highest was computed for wood frame types) and less than 9.2  $\mu$ -strains for all bending wall strains. Strains calculated for the one-story cinder block structure for radial and transverse in-plane strains fell below those calculated for wood frame structures. Cinder block wall strains are well below critical failure strains.

#### *Summary of Findings*

- Peak in-plane tensile strains calculated from whole structure differential displacements were 113.1  $\mu$ -strain in the two story stone structure. A value of 95.5  $\mu$ -strain was computed for a one-story log structure. For all other structures, whole structure wall strains were less than 40  $\mu$ -strain.
- Peak calculated mid-wall bending strains were the greatest in the two-story stone structure with a value of 46.4  $\mu$ -strains. Bending strains for all other structures were less than 26  $\mu$ -strain.
- In some structures, ground velocities may compare to structure response at S1. Therefore, ground velocities may be used to evaluate response in structures expect in the case of trailers where S1 does not match ground velocities.

### **Non-blasting Sources of Structure Vibrations**

#### *Household Activities*

Structure responses to non-blasting events are shown in Table 12 for seven structures. A comparison of non-blasting event responses are shown in Table 13 compared with the maximum whole (upper) structure and mid-wall velocities recorded during blasting. It was not difficult to generate structure motions during normal household activities within trailers and wood frame structures. Structure responses from household activities were equal to those produced during blasting in the single wide trailer, TS-IN.

The more massive masonry and earth structures did not significantly respond during non-blasting influences. Therefore, responses shown in Table 12 are very low in amplitudes. Log and camp structures were not included in these tests.

### *Wind*

Table 14 summarizes whole structure and mid-wall maximum velocities and strains for three trailers that responded to significant wind gusts traveling between 12 and 32 miles/hour. The maximum upper structure (S2) velocity and calculated whole structure strains ( $\gamma_{\max}$ ) are given for the T and R components or walls. Note that the upper structure response for the given component drives the shear strains in the opposing wall as previously described. For instance, the 0.055 in/sec maximum velocity recorded at S2 in the T direction produced an estimated 3.5  $\mu$ -strains of shear in the radial wall.

Upper structure transverse (S2) and mid-wall responses (both T and R walls) for air pressures (AP) from blasting and wind gusts are compared in Figure 32 for single wide trailer TS-KY2. Wind gusts are not efficient driving forces compared with blasting to excite significant structure responses. However wind gusts can generate air pressures that result in detectable levels of structure shaking and mid-wall responses up to 0.1 in/sec.

### *Summary of Findings*

- Whole structure trailers motions from household activities were measured equal to motions induced from blasting. Mid-wall responses were general equal to or less than the responses from blasting. Structure responses from household activities in earth, stone and masonry structures were far lower and in some cases barely detectable in comparison with blasting responses.
- Trailer structure responses to wind gusts produced whole structure motions that were generally one-half of the motions generated during blasting.

## **CONCLUSIONS**

1. Predominant frequencies of the ground motion time histories, as estimated from the Fast Fourier Transform power spectrum tended to be smaller than those computed using the zero-crossing method computed at the PPV. The frequency range with zero-crossing at the PPV was 16 to 32 Hz compared to a 7 to 20 Hz from the power spectrum. In all cases except one site, FFT frequencies fell below zero-crossing frequencies. The exception was the Tennessee site in which structure were founded directly on bedrock.

2. Fourier transforms and response spectra are preferable in structure response analysis to determine predominant excitation frequencies as the entire waveform is involved in the process.

3. Structure response relative to ground motions and airblast was evaluated by comparing horizontal time histories for the ground, lower structure (S1), upper structure (S2), and the mid-

walls. Differences between lower floor response and ground motions were small for all structure types with the exception of trailers in the vertical direction. Single and double wide trailers sustained wall base motions greater than exterior ground motions. In the case of trailers, wall base motions should to be instrumented in order to compute differential wall displacements. Although S1 measurements are preferred exterior ground motions may be used to estimate lower structure horizontal responses when foundations are coupled to the ground.

4. Whole structure motions, as indicated by the best-fit slope of upper structure response versus PPV, were the highest in the one two story stone (3.22) and camp (2.70) structures. Trailers, one-story wood frame, and log structures responded similarly with slopes of 1.29, 1.30, and 1.54, respectively. Other one story structures (log, earth and masonry) exhibited structure responses less than ground motions.

5. The greatest mid-wall responses, as indicated by the best-fit slope of mid-wall response versus PPV, were measured in log structures possessing “great walls” (2.98) and camp structures (2.58). Responses were similar for trailers (2.09) and wood frame (2.09) mid-walls

6. The influence of airblast over 116 decibels on the upper structure (S2) and mid-wall responses was observed for trailers. Whole structure and mid-wall motions duplicated airblast time histories and peak structure responses occurred within the airblast phase rather than within the ground motion phase. Mid-wall motions show both high frequency and low frequency characteristics for specific structures while trailer mid-walls tended to respond only at high frequencies. Upper (second story) mid-walls and upper structure corners move as one unit in most two story structures studied. In a number of cases, mid-wall responses duplicate airblast waveform signatures. Structure types that clearly did not show a response after the air pressure pulse arrival include one-story camp, log structures, and massive stone, concrete block and adobe structures.

7. Average values were determined for natural frequencies of mid-walls (8.4 Hz and 13.8 Hz) and whole structures (6.0 Hz) in both the radial and transverse directions. U.S. Bureau of Mines in RI 8507 reported average values of 16.4 Hz for mid-walls (no specific component) and 7.1 to 7.8 Hz for the whole structure. Dowding (1996) reported mid-wall frequencies between 12 to 20 Hz. Whole structure natural frequencies ranged 5 to 10 Hz. Data in this study corroborate these whole structure findings.

8. Damping characteristics during free response were evaluated for all structures. The greatest damping in mid-walls was found for the transverse direction in trailers equal to 9.5% of critical. Log and trailer structures exhibited the highest whole structure radial damping of 9.7% and 9.6%, respectively. The least damped structure type was the two-story stone that responded with an average damping of 3.9%. Values for damping fall well within those reported in the range of 2 % to 10% of critical by Dowding (1985).

9. Amplification factors varied by type of structure as well as for certain structures within each design type. These observations may be compared with those from U.S. Bureau of Mines RI 8507 where the maximum was 4 for structure corners. Corner responses of log and wood-frame structures fell below RI 8507 values. Out of this study of 25 atypical structures chosen for their

unusual character, only two structure designs displayed amplifications greater than 4. These included the two story stone and two story camp structures with upper structure motions amplified by 5.0 and 4.6, respectively. These values can be attributed to the fact that these structures were vibrated at or near their natural frequencies of 4 to 7 Hz.

10. In-plane tensile wall strains calculated from gross structure differential displacements were below cracking thresholds of 300 to 1000  $\mu$ -strains for plaster and wallboard. Calculated wall bending strains were less than 20  $\mu$ -strains.

11. Peak structure velocities induced in these atypical structures by occupant-induced motions were found to vary by structure type and distance between the source and measuring transducer. Habitation excitations that generated structure responses were primarily door and window closings. Those structures with low-mass walls (e.g., trailers) responded more than did structures with more massive walls to similar activities.

## **RECOMMENDATIONS**

1. Time histories collected during this study of 25 atypical structures should be electronically archived for future access and analysis. They represent an unusually rich source of data that included ground motions as well as structural and crack responses.

2. The crack measurements presented in Addendum I to this study involved monitoring crack displacements, demonstrating that inexpensive techniques can be used to measure both long-term (environmental or weather-induced) and transient (blast induced) changes in crack widths, when conditions allow, to supplement traditional structure response techniques.

3. For atypical structures, time-correlated ground motion and structure velocity responses could be measured with systems similar to those employed in this study if conducted as outlined in Addendum II. Whole structure response motions should be measured at the top and bottom wall corners of uniform construction. Mid-wall response as well as crack deformations can be measured as additional options.

## **REFERENCES**

Crum, S.V., 1997, House Responses from Blast-Induced Low Frequency Ground Vibrations and Inspections for Related Interior Cracking, U.S. Department of Interior, Office of Surface Mining Report, Contract No. 143868-PO96-12616.

Dowding, C.H., 1996, *Construction Vibrations*, Prentice Hall.

Edwards, A. T., T. D. Northwood, 1960, Experimental Studies of the Effects of Blasting on Structures, *The Engineer*, v. 210.



- Huang, F., 1994, NUVIB (Northwestern University Vibration Analysis Software), V. 1.01, Department of Civil Engineering, Northwestern University, Evanston, IL.
- Nicholls, H.R., C.F. Johnson, and W. I. Duvall, 1971, Blasting Vibrations and Their Effects on Structure, U.S. Bureau of Mines Bull. 656.
- Harris, C. M., 2001, Harris' Shock and Vibration Handbook, McGraw-Hill.
- Martell, M.A., 2002, Log Structure Response to Coal Mine Blasting, M.S. Thesis, New Mexico Institute of Mining and Technology, Socorro, NM.
- Northwood, T. D., R. Crawford, and A. T. Edwards, 1963, Blasting Vibration and Building Damage, *The Engineer*, v. 15, No. 5601.
- Siskind, D.E, 2002, personal communication.
- Siskind, D.E., M. S. Stagg, J. W. Kopp, and C. H. Dowding, 1980a, Structure Response and Damage Produced by Ground Vibration From Surface Mine Blasting, U.S. Bureau of Mines RI 8507.
- Siskind, D.E., V. J. Statura, M. S. Stagg, and J. W. Kopp, 1980b, Structure Response and Damage Produced by Airblast from Surface Mining, U.S. Bureau of Mines RI 8485.
- Stagg, M.S., D.E. Siskind, M. G. Stevens, and C. H. Dowding, 1984, Effects of Repeated Blasting on a Wood-Frame House, U.S. Bureau of Mines RI 8896.
- U.S. Department of Agriculture, 1999, Wood Handbook – Wood as an Engineering Material. General Tech. Rep FLP-GTR-113. Madison, WI. U.S.D.A. Forest Service, Forest Products Laboratory.
- Wiss, J.F. and H.R. Nicholls, 1974, A Study of Damage to a Residential Structure from Blast Vibrations, ASCE, New York.

Table 1 Summary of construction types

Category	Structure type	Site	Designation	Structure	Wall height	Wall thickness	Overall house dimensions	Maximum differential elevation
					(in)	(in)	(ft x ft)	(in)
pre-manufactured trailers	single wide	KY2	TS-KY2	no strapping	94	4	65 x 14	3.9
		IN	TS-IN	strapping	90	4	64 x 14	3.8
		AL	TS-AL	strapping	94	6	72 x 16	2.8
		OH	TS-OH	strapping	94	6	73 x 15	3.5
	single wide add-on	VA	TSA-VA	add-on	94	5	54 x 14	3.3
				original trailer	82	4	54 x 12	
		KY2	TSA-KY2	add-on	94	4	56 x 12	8.2
				original trailer	94	4	56 x 12	
	double wide	VW2	TD-WV2	center wall	94	6	64 x 28	2.4
		TN	TD-TN	center wall	104	4	74 x 28	1.8
		PA	TD-PA	basement	117	8	48 x 24	3.8
				first floor	84	4		
mine camp	single-story	AL	C1S-AL	first floor	86	8	50 x 27	4.0
		VA	C1S-VA	first floor	82	2	34 x 28	7.4
	two-story	KY1	C2S-KY1A	first floor	92	4	28 x 28	5.1
				second floor	92	4		
		KY1	C2S-KY1B	first floor	94	5.5	48 x 29	3.3
				second floor	94	5.5	29 x 16	
log	one-story	OH	L1S-OH	basement	91.6	9	38 x 23.5	3.7
				first floor	90.4	9		
		VW1	L1S-WV1	historic log cabin	78	12	24 x 26	5.9
	two-story	TN	L2S-TN	first floor	111.5	6.75	29 x 25	3.5
				second floor loft	93.5	6.75		
		OH	L2S-OH	first floor	great-wall 282 in. mid-wall at 144 in. from base	7	37 x 25	2.0
				second floor	82	7		
				west wall	94	8		
		WV2	L2S-WV2	center post	286	8	46 x 30	2.7
				second floor loft	82	8		
earth, stone, and masonry	one story cinder block	NM	E1S-NMA	ground floor	120	8	60 x 40	1.7
	two-story historic stone	NM	E2S-NM	first floor	108	24	37 x 30	5.0
				second floor	90	15		
	one-story adobe	NM	E1S-NMB	first floor	114	10	70 x 32	3.1
wood-frame	one-story	IN	W1S-IN	basement	92.4	8	40 x 22	3.7
				first floor	96	6		
		PA	W1S-PA	first floor	102	6	66.5 x 35	3.2
	two-story	IN	W2S-IN	basement	90	8	35 x 30	Nm
				first floor	96	6		
	three-story cantilever	WV1	W3S-VW1	garage	101	8	42 x 16	1.9
				first floor	94	5	42 x 20	
				second floor	52	5	42 x 20	

Nm – not measured

Table 2 Site information

Site	Number of Structures	Number of Blasts	Blast-to-Structure Distance (ft)	Charge Weight per Delay (lbs)	Square-Root Scaled Distance Factor (ft/lbs <sup>1/2</sup> )
Alabama	2	4	852-1520	280-550	36-86
Indiana	3	16	816-9219	126-1712	44-223
Kentucky – 1	2	7	1830-5140	404-1044	60-184
Kentucky – 2	2	7	1510-4600	183-808	68-340
New Mexico	3	6	2095-5565	300-13047	23-278
Ohio	3	23	570-6280	284-4130	25-268
Pennsylvania	2	4	1390-1510	612-486	58-68
Tennessee	2	3	1225-6110	885-2809	34-149
Virginia	2	6	1212-1390	313-361	64-77
West Virginia – 1	2	5	4640-2240	126-2076	78-215
West Virginia – 2	2	8	1610-2670	415-973	76-118

Table 3 Ground motion attenuation equations from Figure 9

Site	Equation	Correlation Coefficient (R <sup>2</sup> )
	$[a (D/W^{1/2})^{-b}]$	
Alabama	$958 (D/W^{1/2})^{-2.22}$	0.97
Indiana	$64 (D/W^{1/2})^{-1.34}$	0.91
Ohio	$231 (D/W^{1/2})^{-1.67}$	0.75
New Mexico – casting	$256 (D/W^{1/2})^{-1.93}$	0.98
New Mexico – pre-split	$5448 (D/W^{1/2})^{-2.03}$	0.90
U.S. Bureau of Mines coal mine data*	$133 (D/W^{1/2})^{-1.50}$ (maximum horizontal) $119 (D/W^{1/2})^{-1.52}$ (all components)	

\* U.S. Bureau of Mines RI 8507 (Siskind, et al, 1980a)

Table 4 Airblast overpressure attenuation equations

Site	Equation $[a (D/W^{1/3})^{-b}]$	Correlation Coefficient ( $R^2$ )
All sites	$0.35 (D/W^{1/3})^{-0.95}$	0.45
Coal mine data for highwalls *	$0.146 (D/W^{1/3})^{-0.823}$	0.77
Coal mine data for coal parting *	$49.6 (D/W^{1/3})^{-1.62}$	0.50

\* U.S. Bureau of Mines RI 8485 (Siskind, et al, 1980b)

Table 5 Comparisons of two methods used to determine frequencies: zero-crossing and FFT methods

Site	Range of Frequencies (Hz)	
	Measured at the PPV using zero-crossing method	Calculated using FFT method
<b>Sites with the great change in frequency between the two methods</b>		
Kentucky – 1	9 – 22	6 – 7
New Mexico	4 – 18	4 – 8
Alabama	10 - 34	8 – 17
Kentucky – 2	18 - 30	15 – 19
Indiana	3 - 28	2 – 19
<b>Sites with little change in frequency between the two methods</b>		
Ohio	4 - 24	3 – 18
Pennsylvania	8 - 22	7 – 20
Virginia	7 - 23	6 – 20
West Virginia – 1	11 - 16	11 – 14
West Virginia – 2	7 - 19	6 – 16
Tennessee	10 - 32	12 – 35

Table 6 Best fit equations relating structure response in terms of whole structure and mid-wall motions to ground motions and air overpressures for different structure designs

Driving force	Response	Structure design	Stories or component	Best fit equation slope (a)	Correlation Coefficient ( $R^2$ )
peak particle velocity ground motion PPV	whole structure $WSR = a * PPV$	trailers	1	0.66	0.64
		log	1	0.45	0.91
			2	1.54	0.84
		earth, stone, and masonry	1	0.91	0.76
			2	3.22	0.42
		wood-frame and camp	1	1.30	0.88
			2	2.70	0.73
		all structures	1	0.63	0.45
			2	1.43 <sup>(1)</sup>	0.75
	mid-wall $MWR = a * PPV$	trailers	R	1.32	0.86
			T	2.09	0.73
		log	R	1.90	0.80
			T	2.98	0.94
		camp	R	2.58	0.87
			T	2.25	0.98
		wood-frame	R	1.83	0.92
			T	2.08	0.67
		earth, stone, and masonry	R	1.52	0.90
			T	1.24 <sup>(1)</sup>	0.83
airblast overpressure AP	whole structure $WSR = a * AP$	trailers	1	28.9	0.51
	mid-wall $MWR = a * AP$	trailers	R	206.1	0.52
			T	155.4	0.55
		camp	R	120.0	0.67
			T	131.0	0.95
		wood-frame	R	175.0	0.74
			T	213.6	0.70

(1) excluding the historic stone structure response

Table 7 Natural frequencies and damping coefficients calculated when ground motions occur at a 90 degrees phase shift from structure response

Structure	Shot Date (time)	PPV	Airblast	Transverse				Radial			
				whole structure		mid-wall		whole structure		mid-wall	
				natural frequency	damping coefficient	natural frequency	damping coefficient	natural frequency	damping coefficient	natural frequency	damping coefficient
		(in/sec)	(dB)	(Hz)	(%)	(Hz)	(%)	(Hz)	(%)	(Hz)	(%)
E2S-NM	6/22/01 (14:16)	0.258	131	4	6.31	4	4.88	4	2.33	4	3.55
	7/17/01 (12:52)	0.46	119	na	na	4	4.91	na	na	4	6.93
	7/23/01 (11:23)	0.23	110	4	3.09	4	5.89	na	na	4	4.58
	7/26/01 (11:05)	0.253	106	4	7.73	4	7.28	4	5.36	4	2.90
	7/26/01 (14:55)	0.21	122	4	4.58	4	3.55	4	3.55	4	6.45
	<b>Average</b>			<b>4</b>	<b>5.43</b>	<b>4</b>	<b>5.30</b>	<b>4</b>	<b>3.75</b>	<b>4</b>	<b>4.88</b>
TD-WV2	12/04/01 (12:22)	0.095	112	7	3.64	7	3.00	7	3.55	Na	Na
	12/05/01 (16:54)	0.060	116	7	4.89	7	3.55	7	6.45		
	12/06/01 (16:52)	0.085	117	7	1.8	7	5.43	7	11.06		
	<b>average</b>			<b>7</b>	<b>3.44</b>	<b>7</b>	<b>3.99</b>	<b>7</b>	<b>7.02</b>		

Na – not applicable as response is not detected

Table 8 Average and range (minimum to maximum) of natural frequencies computed during free response after ground motions have arrested

Design	Transverse (Hz)		Radial (Hz)	
	whole structure	mid-wall	whole structure	mid-wall
Trailer	6.9 (3.5 – 13.5)	9.5 (4.3 – 29.3)	6.3 (4.3 – 6.8)	19.9 (6 – 29)
Log	6.5 (6 – 8)	15.8 (8 – 24)	6.4 (5 – 7.5)	13.8 (6 – 27.5)
Earth, stone, and masonry	4.4 (4 – 4.8)	4.3 (3.8 – 4.8)	4.3 (4 – 4.5)	4.3 (3.8 – 4.5)
Camp	5.3 (3 – 7.5)	3.4 (3 – 3.8)	6.9 (6.5 – 7.5)	6.9 (6.5 – 7.5)
Wood-frame	7.6 (3 – 13)	8.9 (4 – 13.5)	Nd	23.9 (22 – 25.5)
Average for all structures	6.1	8.4	6.0	13.8
U.S.B.M. RI 8507 (Table 3)	7.1 (4 – 10)		7.8 (4 – 11)	16.4 (8.3 – 36) <sup>(1)</sup>

(1) The U.S.B.M. instrumented only the mid-wall facing the blast to measure air pressure effects

Table 9 Average damping coefficients for free response computed in Table 7

Design	Transverse (% of critical)		Radial (% of critical)	
	whole structure	mid-wall	whole structure	mid-wall
Trailer	8.9	9.5	9.6	8.7
Log	8.5	8.5	9.7	6.8
Earth, stone, and masonry <sup>(1)</sup>	3.9	6.4	6.6	8.7
Camp	9.2	6.2	5.5	8.2
Wood-frame	8.2	5.8	Nd	8.5
Average for all sites	7.7	7.3	7.9	8.2
U.S.B.M. RI 8507 (Table 3)	5.0	2.3	4.4	1.8

Nd – not detected

(1) excluding CMU block structure

Table 10 Amplification factors

Design	Description	Time-correlated Amplification Factors	
		average	minimum-maximum
Trailers	Single-wide	1.0	1.0 – 3.6
	Double-wide	2.4	1.1 – 4.0
	Add-on	1.9	0.4 – 3.3
Log	One story	1.4	0.4 – 3.0
	Two story	2.1	0.9 – 3.0
Earth, stone, and masonry	One story	1.1	0.6 – 1.6
	Two story	3.5	1.7 – 5.0
Camp	One story	2.1	1.5 – 3.5
	Two story	3.3	1.5 – 4.6
Wood-frame	One story	1.7	1.0 – 2.5
	Two story	1.3	1.1 – 1.5
	Three story	1.6	1.3 – 1.9

Table 11 Blast-induced strains for the radial, R, and transverse, T, walls

Design		In-plane tensile strains <sup>(1)</sup> ( $\mu$ -strains)		Wall bending strains ( $\mu$ -strains)	
		Average (maximum)		Average (maximum)	
		R	T	R	T
Trailer	single wide	5.0 (23.5)	6.7 (38.3)	1.5 (11.5)	2.9 (25.7)
	double wide	3.5 (33.2)	8.9 (23.4)	9.2 (18.9)	1.8 (16.0)
	add-on	8.0 (30.0)	4.9 (10.1)	0.9 (3.9)	6.0 (11.1)
Log	one-story	2.7 (41.7)	4.8 (95.5)	10.5 (13.3)	8.9 (15.5)
	two-story	3.0 (24.5)	4.1 (66.6)	0.2 (1.6)	Na
Earth, stone, and masonry	cinder block	7.4 (10.4)	11.6 (13.4)	Na	3.6 (11.7)
	adobe	4.2 (4.9)	3.9 (7.3)	8.8 (12.1)	5.1 (9.0)
	2-story stone	49.0 (98.9)	55.1 (113.1)	5.2 (18.3) <sup>(2)</sup>	18.9 (46.6) <sup>(3)</sup>
Camp	one-story	11.6 (27.4)	9.5 (18.7)	4.5 (8.0)	5.4 (9.2)
	two-story	2.9 (6.6)	1.7 (13.2)	0.03 (1.4)	0.1 (0.3)
Wood- frame	one-story	11.0 (39.4)	12.5 (33.7)	5.2 (13.0)	3.1 (9.6)
	two-story	2.0 (15.2)	2.7 (13.7)	Na	7.5 (13.0) <sup>(3)</sup>

<sup>(1)</sup> Note that the wall being strained is 90-degrees from the motion sensor recording velocity (e.g., the radial sensor records motion of the transverse walls while the transverse sensor records motion of the radial wall)

<sup>(2)</sup> first floor

<sup>(3)</sup> second floor

Na – no sensor used in this location



Table 12 Structure responses to non-blasting activities

Structure Design	Designation	Activity	Maximum velocity (in/sec)			
			upper structure response		mid-wall response	
			R	T	R	T
single wide trailer	TS-IN	shut north bedroom door	0.10	0.06	0.98	0.29
		child running	0.04	0.02	0.07	0.13
		close north window	0.51	0.40	1.08	0.42
		shut room closet door	0.10	0.50	0.78	0.74
		children playing in family room	0.07	0.04	0.14	0.10
		shut family room outside door	0.05	0.07	0.70	0.22
Double wide trailer	TD-PA	shut west bedroom door	0.05	0.03	0.17	0.34
		slam west bedroom door	0.16	0.10	0.49	1.46
		shut west bathroom door	0.20	0.30	0.50	2.14
		shut exterior kitchen door	0.06	0.12	0.23	0.34
		close west bedroom window	0.15	0.15	0.16	0.74
		jump in bedroom	0.02	0.05	0.16	0.42
		chair fall back in dining room	0.05	0.04	0.06	0.09
one-story wood frame	W1S-IN	shut front door	0.065	0.10	1.58	0.14
		walk in living room	0.02	0.01	0.38	0.17
		child bouncing a ball in living room	0.03	0.05	0.38	0.10
two-story wood frame	W2S-IN	jump in living room	0.03	0.06	Na	Na
		running down stairs	0.04	0.03		
		drop sofa end in living room	0.03	0.05		
		close kitchen window	0.01	0.06		
one-story earth, stone, and masonry	E1S-NMA	shut garage door	0.01	0.02	Na	0.03
	E1S-NMB	shut patio door	0.05	0.12	0.08	0.07
		bump wall with shoulder	0.02	0.04	0.02	0.15
		bump wall with a broom	0.01	0.02	0.01	0.14
two-story earth, stone, and masonry	E2S-NM	Backhoe dropping flagstone near house	0.05	0.04	Na	0.03
			0.03	0.04		0.06
			0.02	0.02		0.03
			0.02	0.02		0.03

Na – no mid-wall sensors mounted

Table 13 Comparison of structure responses for household activities with blasting

Structure designation	Structure response velocity (in/sec)							
	Maximum from household activities				Maximum from blasting activities			
	whole structure		mid-walls		whole structure		mid-walls	
	R	T	R	T	R	T	R	T
TS-IN	0.51	0.40	1.08	0.42	0.52	0.41	1.24	0.64
TD-PA	0.20	0.30	0.50	2.14	0.19	0.20	1.08	0.535
W1S-IN	0.065	0.10	1.58	0.14	0.82	0.55	0.16	0.15
W2S-IN	0.03	0.06	Na	Na	0.24	0.25	Na	Na
E1S-NMA	0.01	0.02	Na	0.03	0.66	0.31	Na	0.78
E1S-NMB	0.05	0.12	0.08	0.07	0.15	0.22	0.27	0.305
E2S-NM	0.05	0.04	Na	0.03	1.52	1.24	0.63	2.64

Na – sensor not mounted in location

Table 14 Velocities and calculated strains in trailers produced by wind for wind speeds ranging from 12 to 32 miles/hour

Structure Design	Designation	Component or wall	Maximum upper structure response	Whole structure transverse shear strain	Maximum mid-wall response	Mid-wall bending strains
			(in/sec)	(μ-strains)	(in/sec)	(μ-strains)
Single wide trailer	TS-KY2	T	0.055	1.5	0.090	1.1
		R	0.035	3.5	0.055	1.2
		T	0.040	1.2	0.060	0.7
		R	0.025	3.4	0.060	0.8
	TS-AL	R	0.010	Na	0.030	1.8
		T	0.030	Na	Na	1.6
Double wide trailer	TD-PA	R	0.005	1.1	0.010	0.6
		T	0.010	1.0	0.025	0.3

Na – strain could not be computed as sensors were not placed in lower corners or not on radial mid-walls

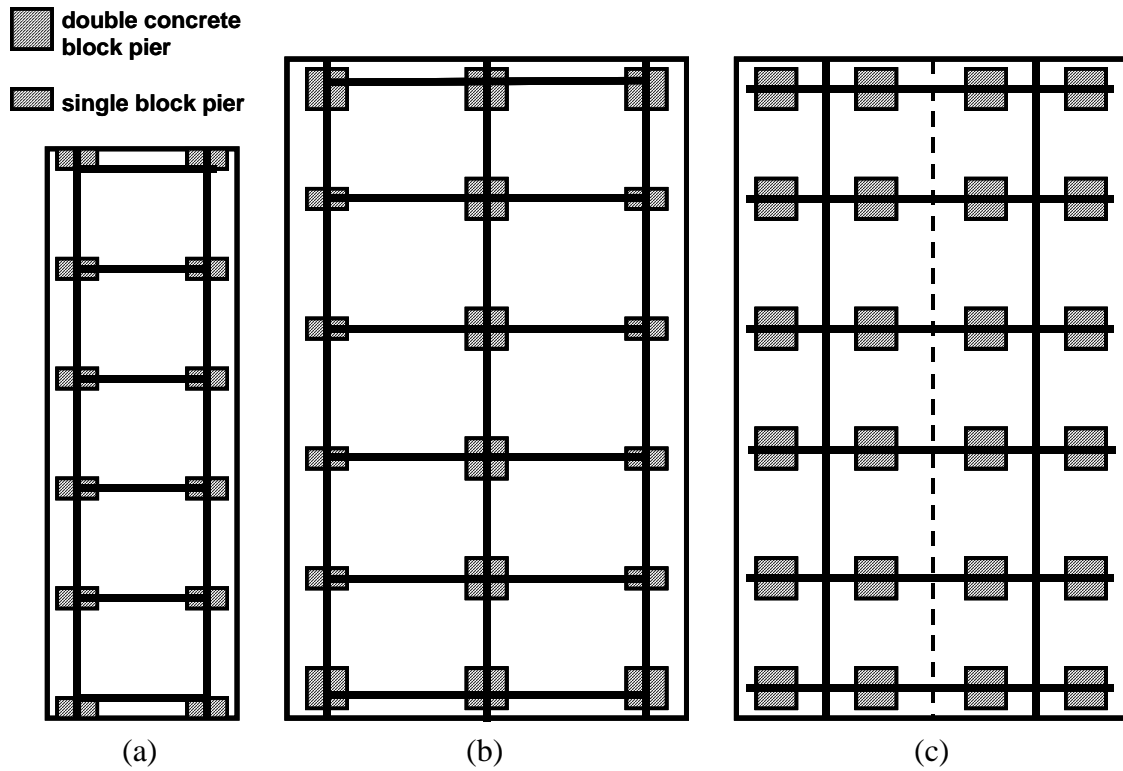


Figure 1 Three generalized trailer pier support system layouts (a) for single wide trailers using single stacked CMUs, and double wide trailer supports (b) using single and double CMUs beneath three axis beams (c) four rows of double CMUs



Figure 2 Hurricane straps required by building code in states in which trailer were selected for the study in Ohio, Tennessee, Alabama, and Indiana

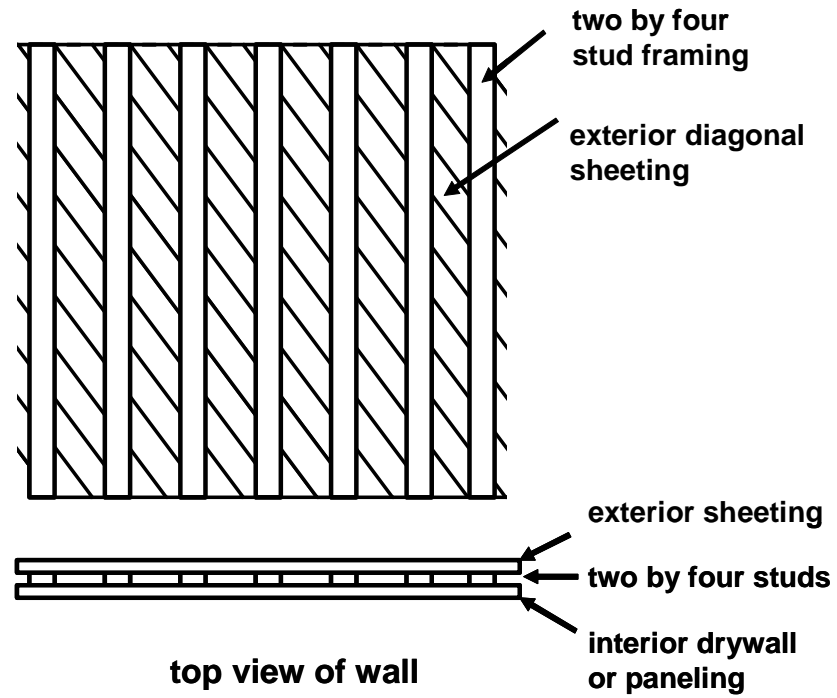


Figure 3 Details of mining camp wall structure

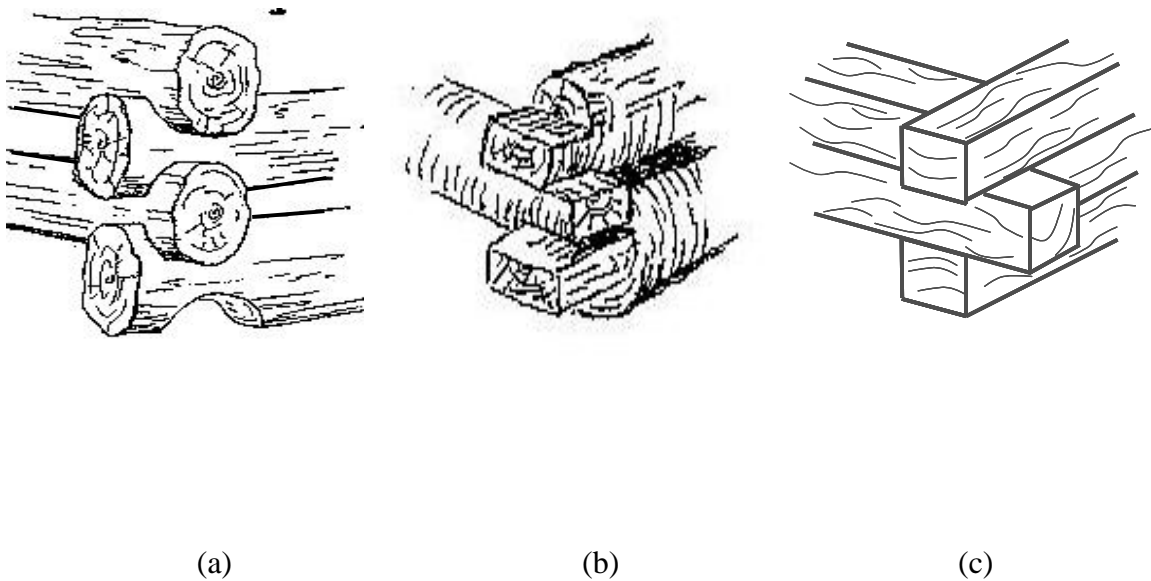
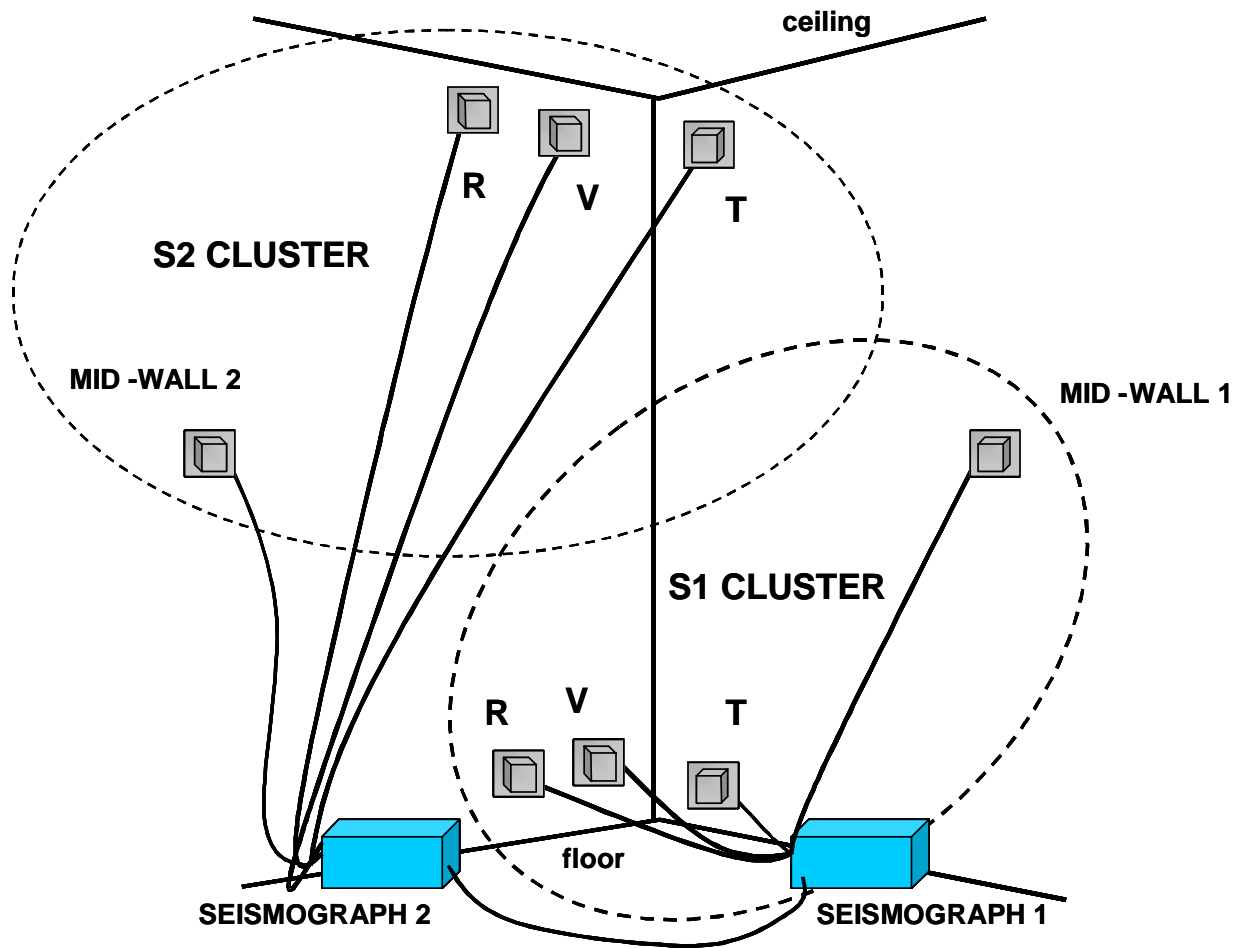
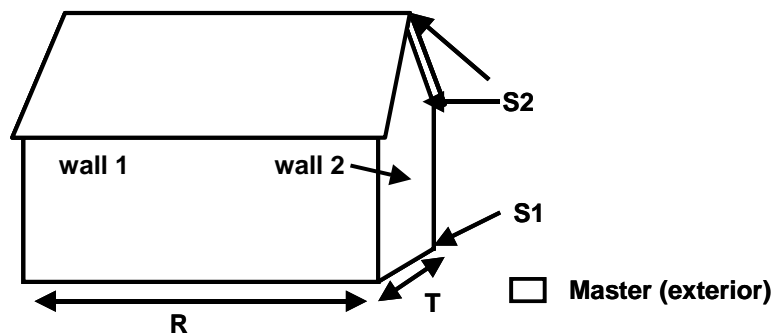


Figure 4 Three types of log fitting (a) saddle lock-notched with spacing between the logs for chinking, (b) notched and scribed, and (c) butt-jointed (After Martell, 2002)

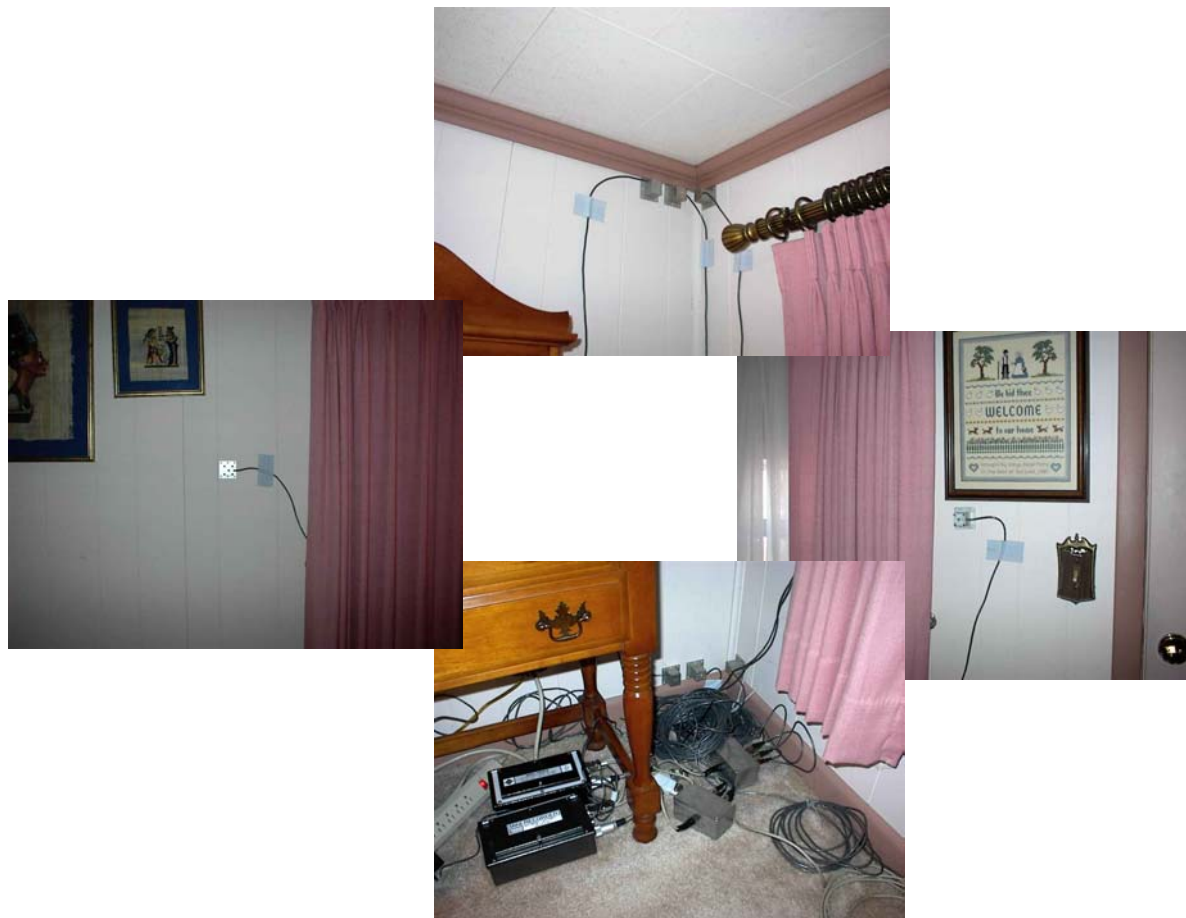


(a)

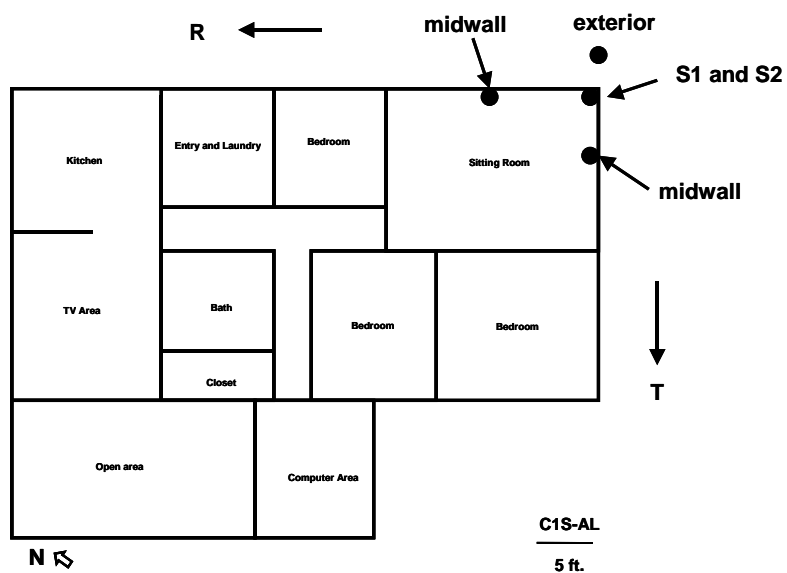


(b)

Figure 5 Typical instrument layout showing (a) S1 and S2 interior velocity sensors used to measure whole structure and mid-wall vibrations (b) location of exterior master seismograph showing orientations of the radial (R) and transverse (T) components



(a)



(b)

Figure 6 Instrumentation layout for mining camp structure C1S-AL

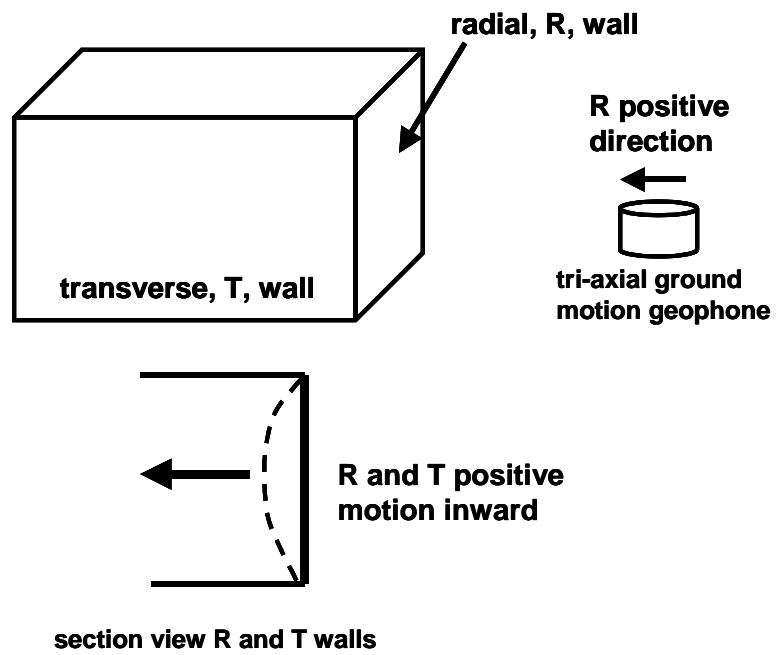


Figure 7 Convention used for radial, R, and transverse, T, geophone orientations

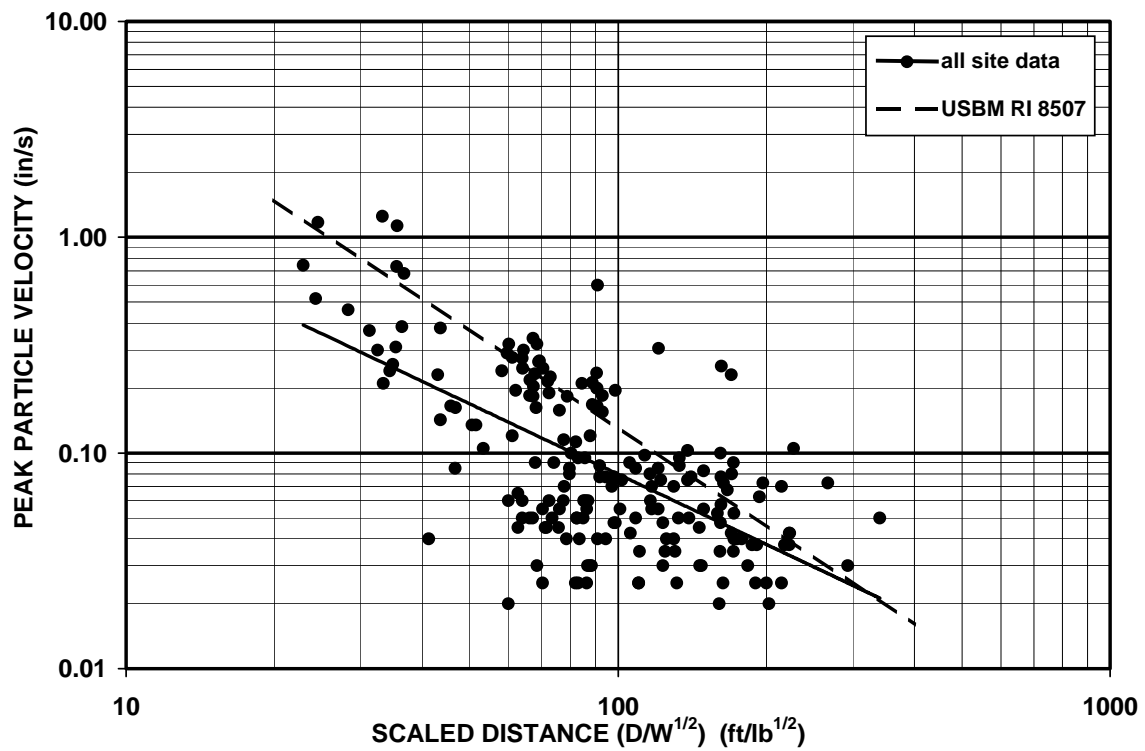


Figure 8 Attenuation plot of maximum ground vibrations for all data

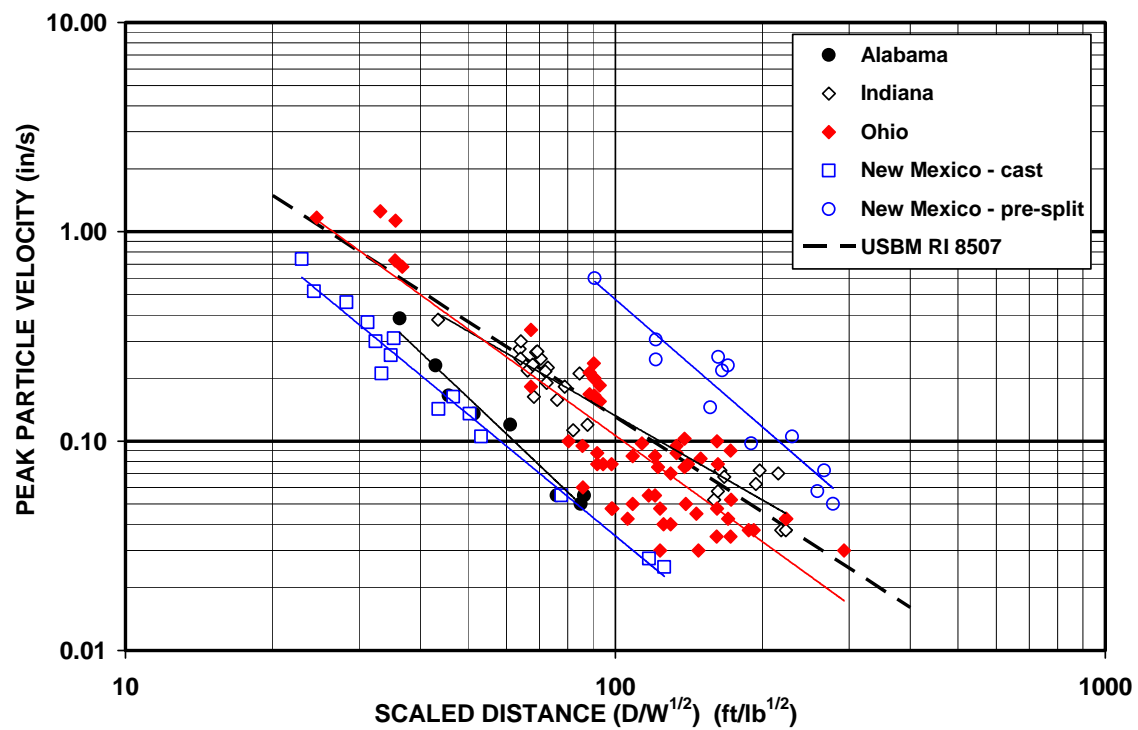


Figure 9 Attenuation plots of maximum ground vibrations separated by site (regression equations shown in Table 3)



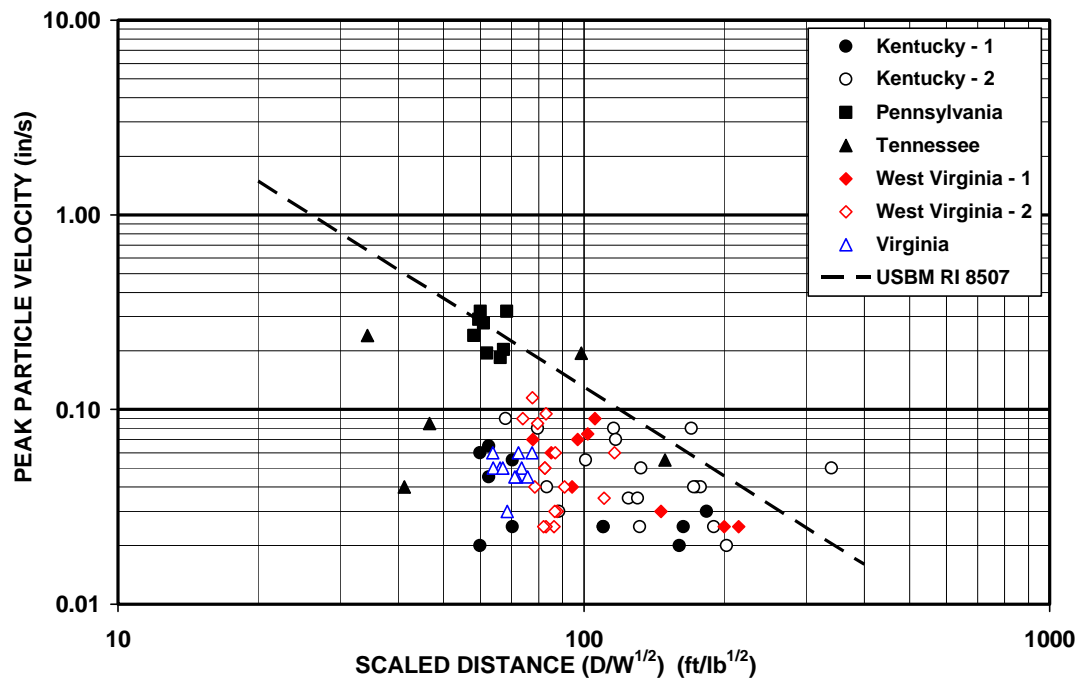


Figure 10 Maximum ground vibrations for clustered and uncorrelated data

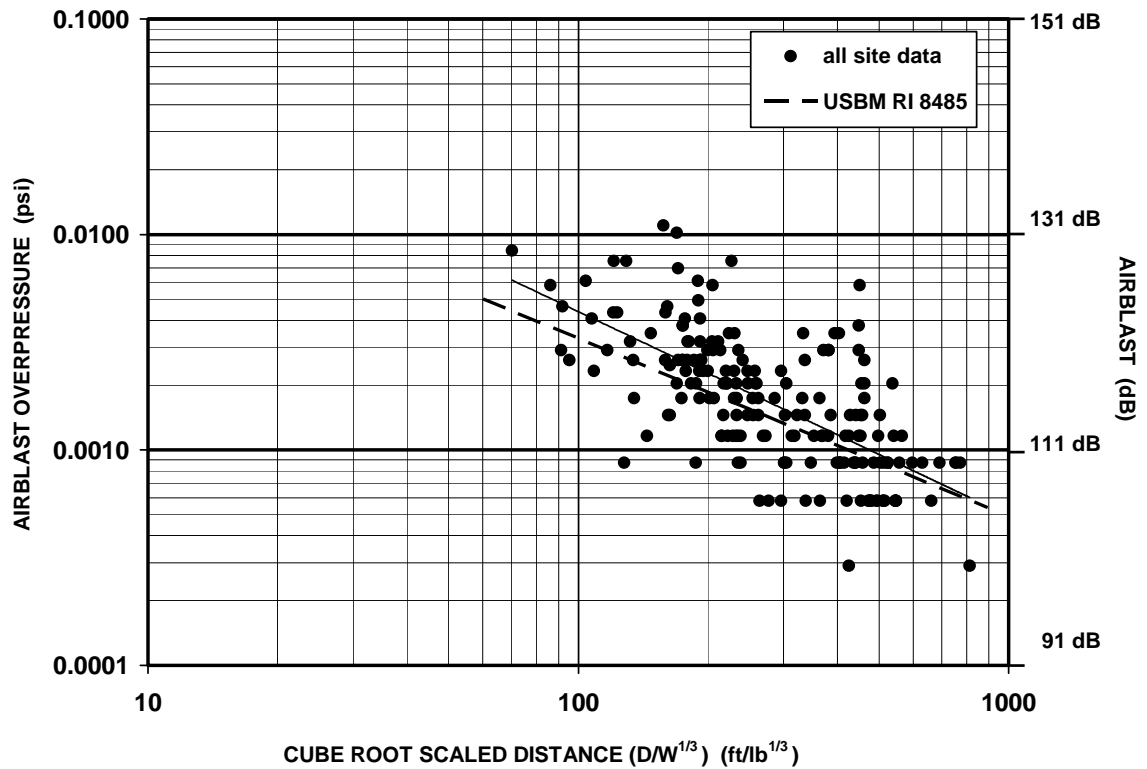


Figure 11 Airblast overpressure attenuation for all data (airblast in dB = 20 log [overpressure in psi] + 170.8)

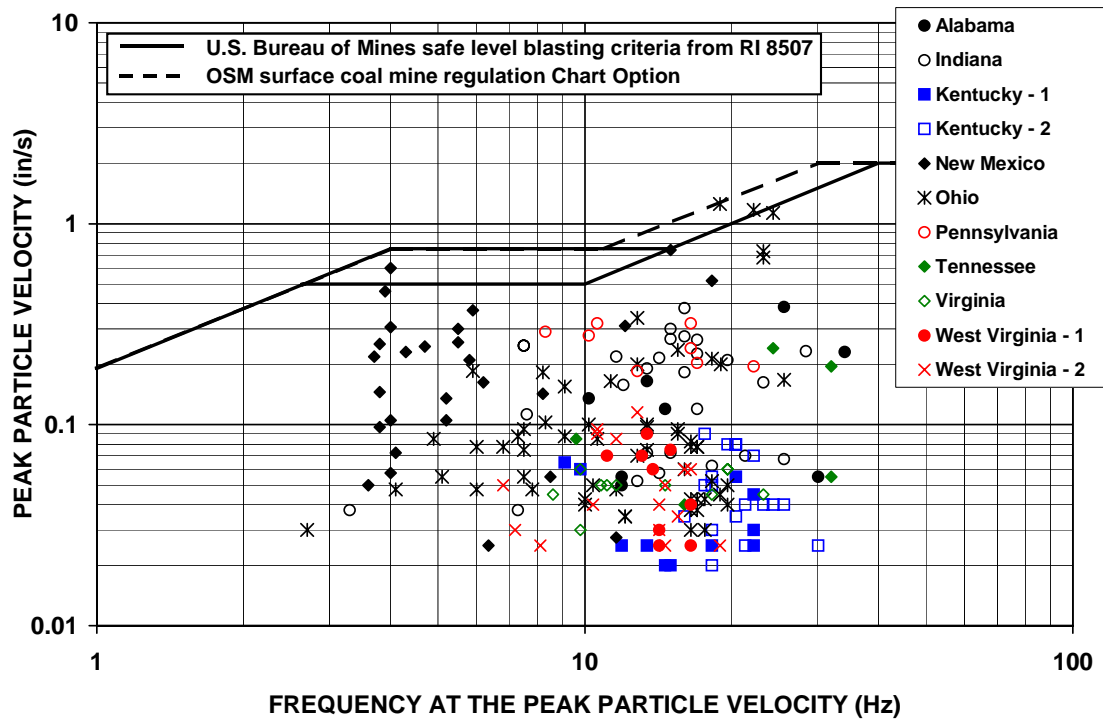


Figure 12 Peak particle velocity (PPV) versus frequency at the PPV

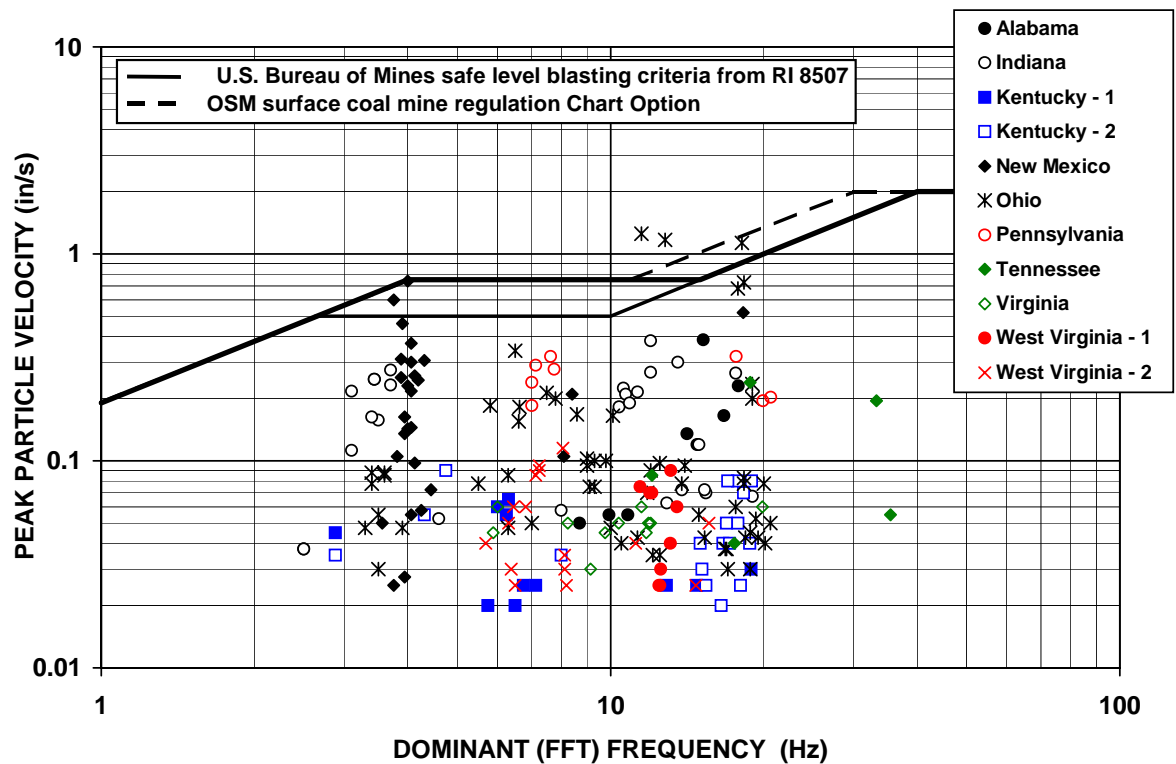


Figure 13 Peak particle velocity (PPV) versus predominant frequency using FFT methods

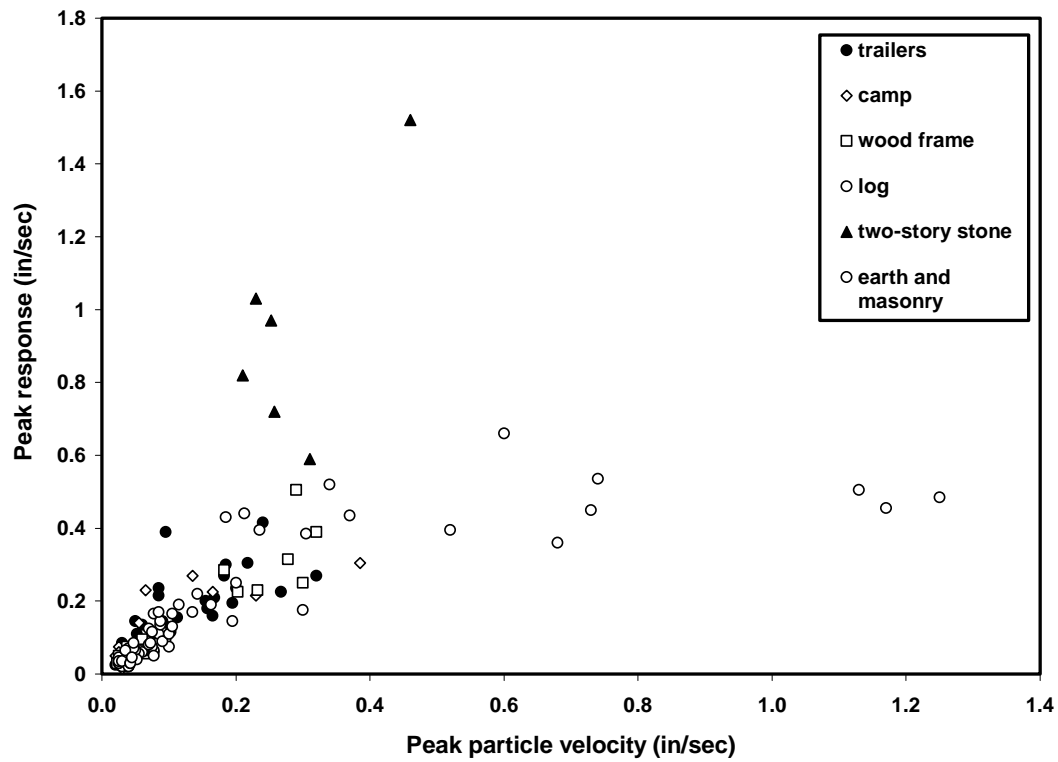


Figure 14 Ground motion-induced whole structure response

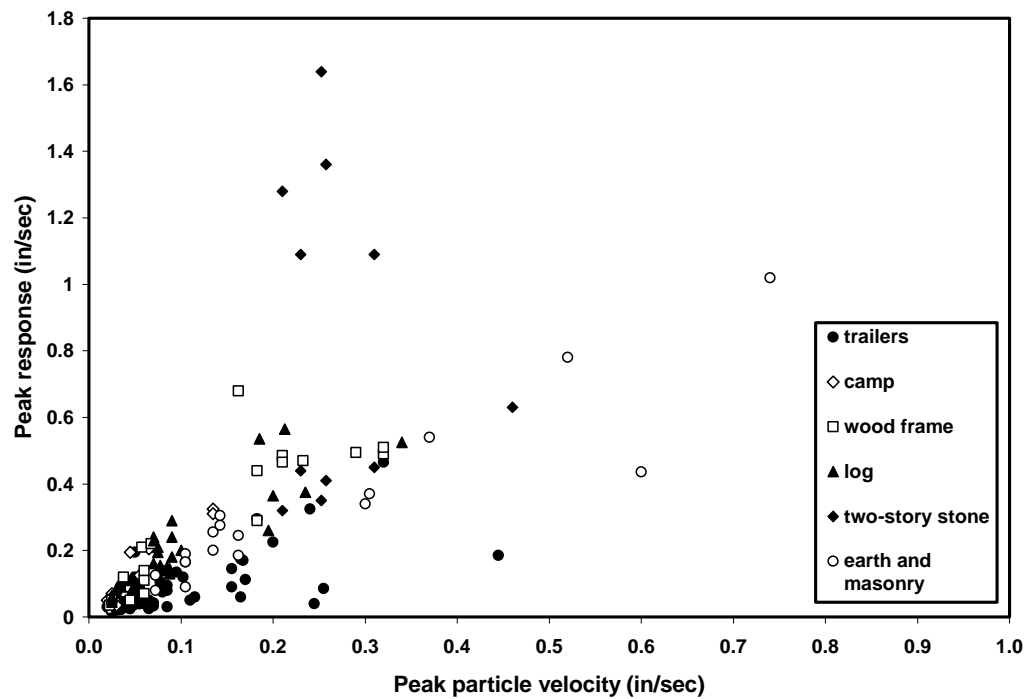


Figure 15 Ground motion-induced mid-wall response

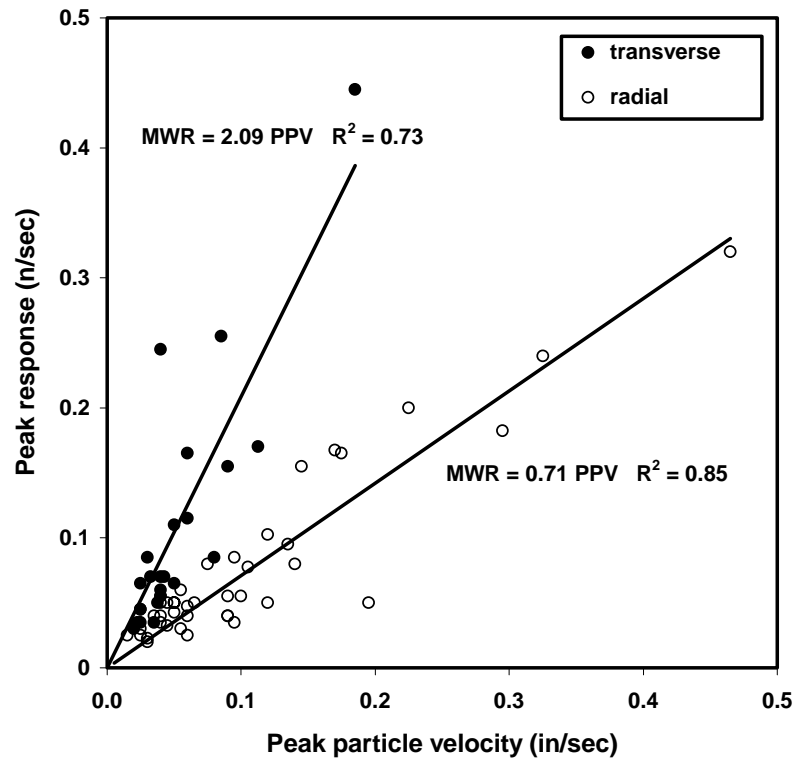


Figure 16 Ground motion-induced mid-wall responses for trailers

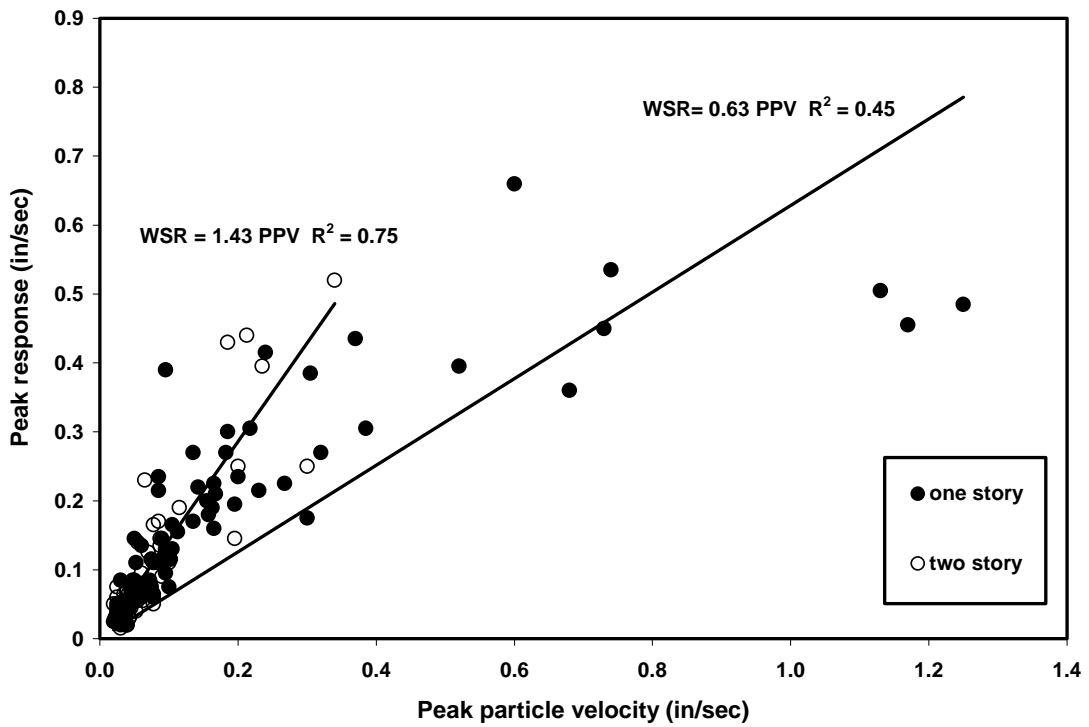


Figure 17 Ground motion-induced whole structure response for one and two story structures

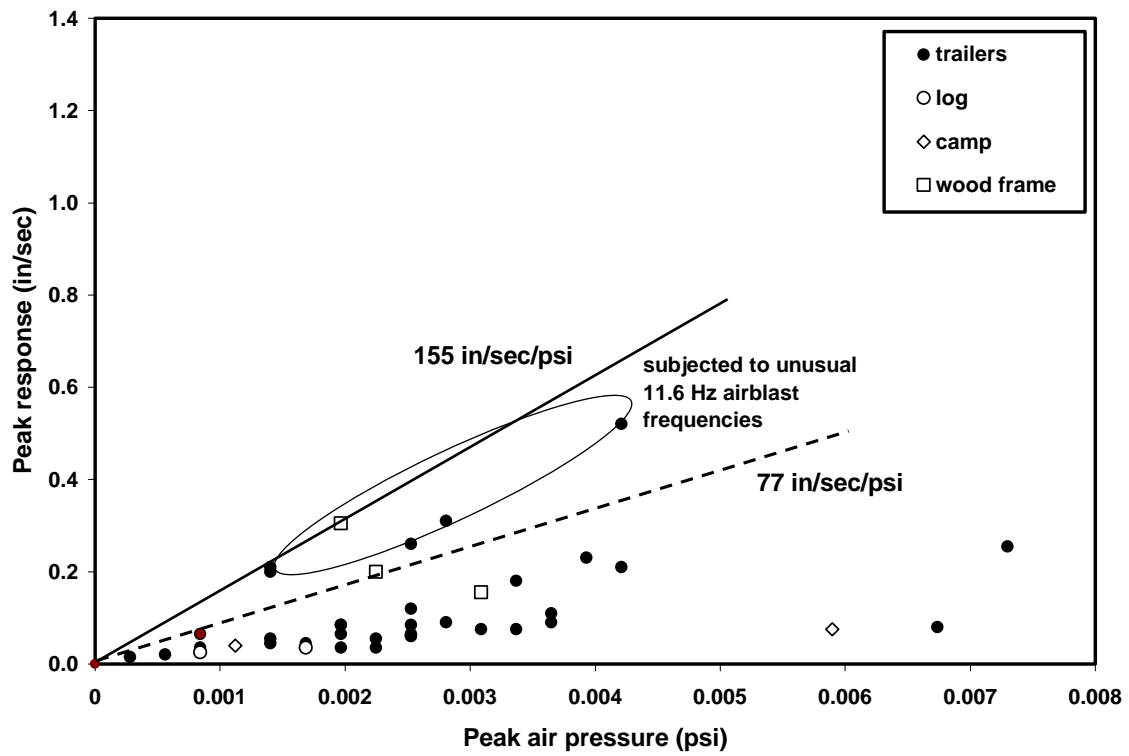


Figure 18 Airblast-induced whole structure response

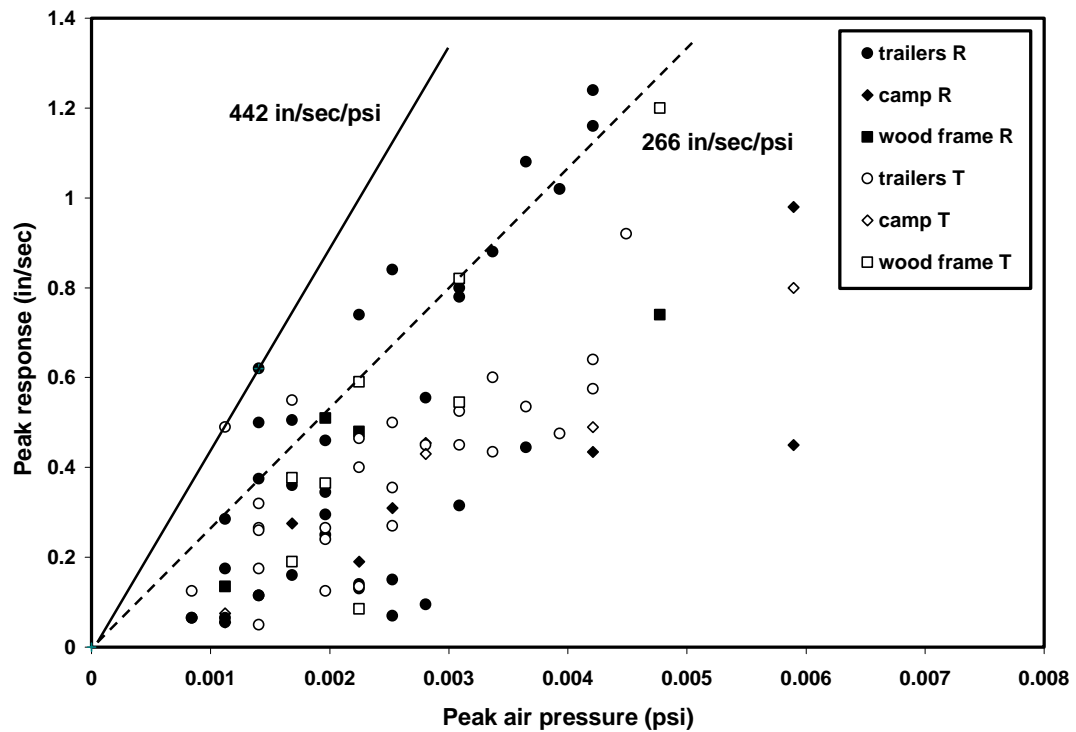


Figure 19 Airblast-induced mid-wall response

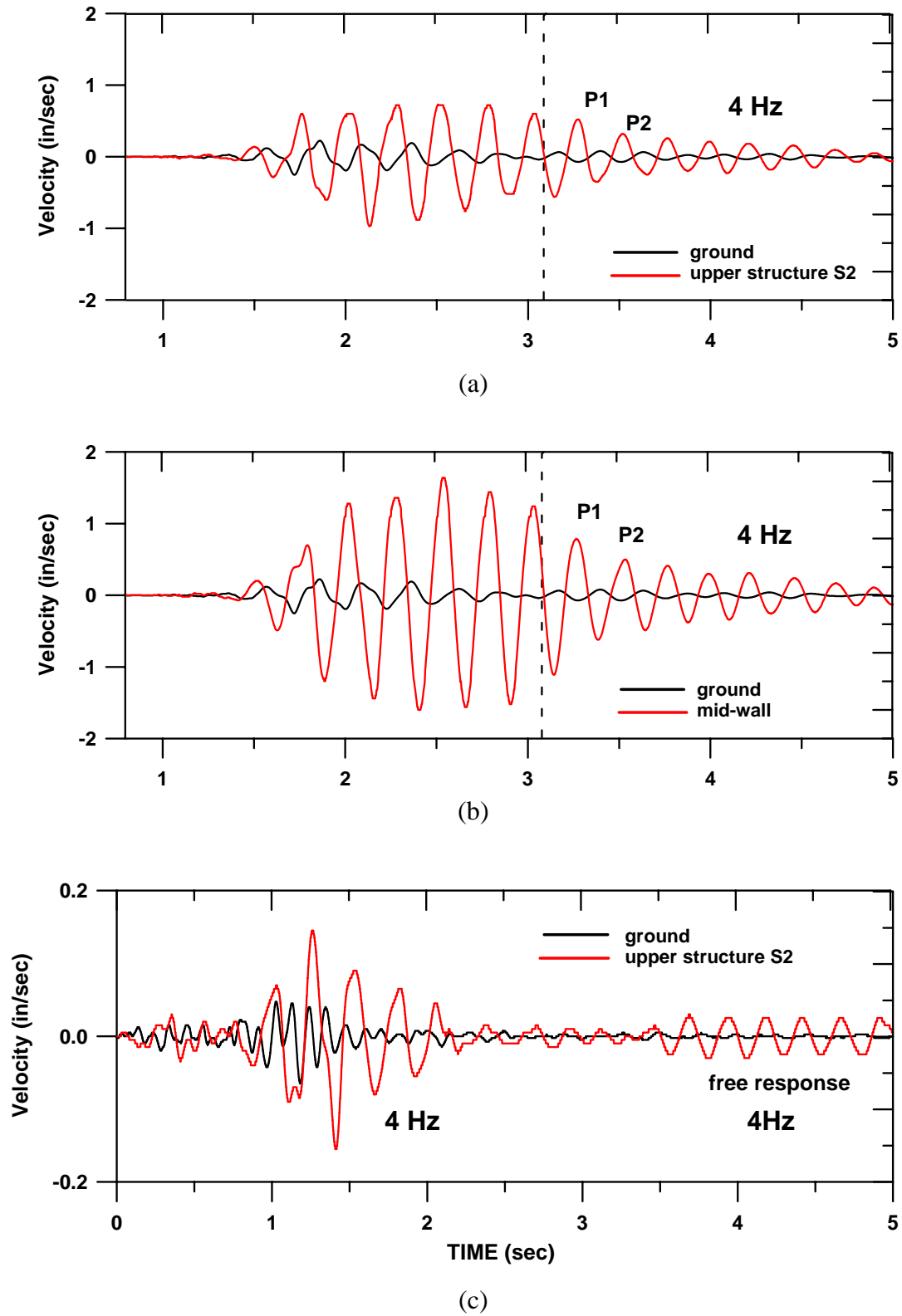


Figure 20 Natural frequency response for stone structure E2S-NM (a) whole structure and (b) mid-wall horizontal structure response compared with ground motions; (c) whole structure free response in trailer structure TS-OH prior to airblast arrival at 4.7 seconds.

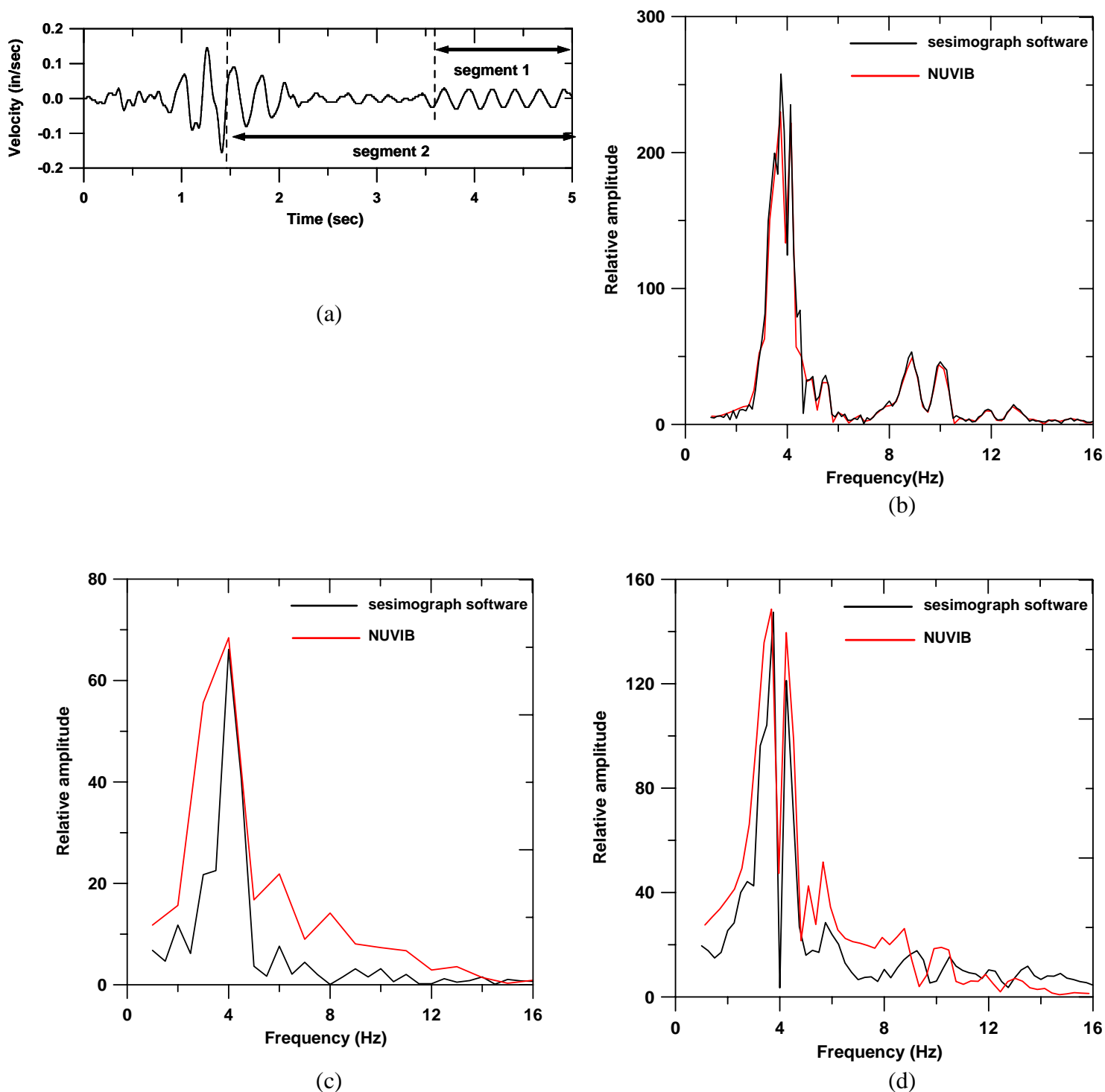


Figure 21 Upper corner transverse response FFT plots for trailer TS-OH response shown in (a), comparing the FFT power spectrum using two different software for (b) the entire time history, (c) segment 1 free response only, and (d) segment 2

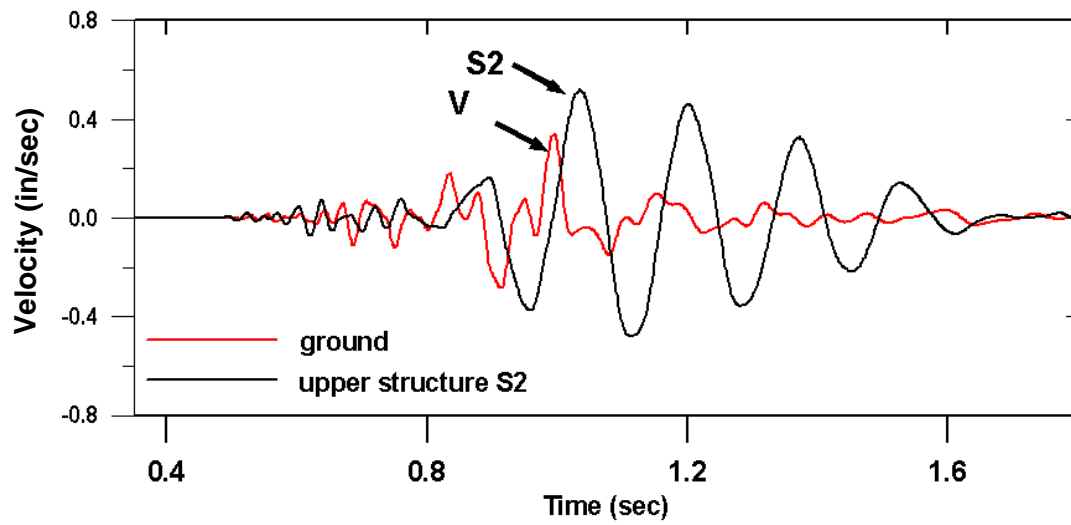


Figure 22 Selection of peaks S2 and V for calculating amplification factors AF

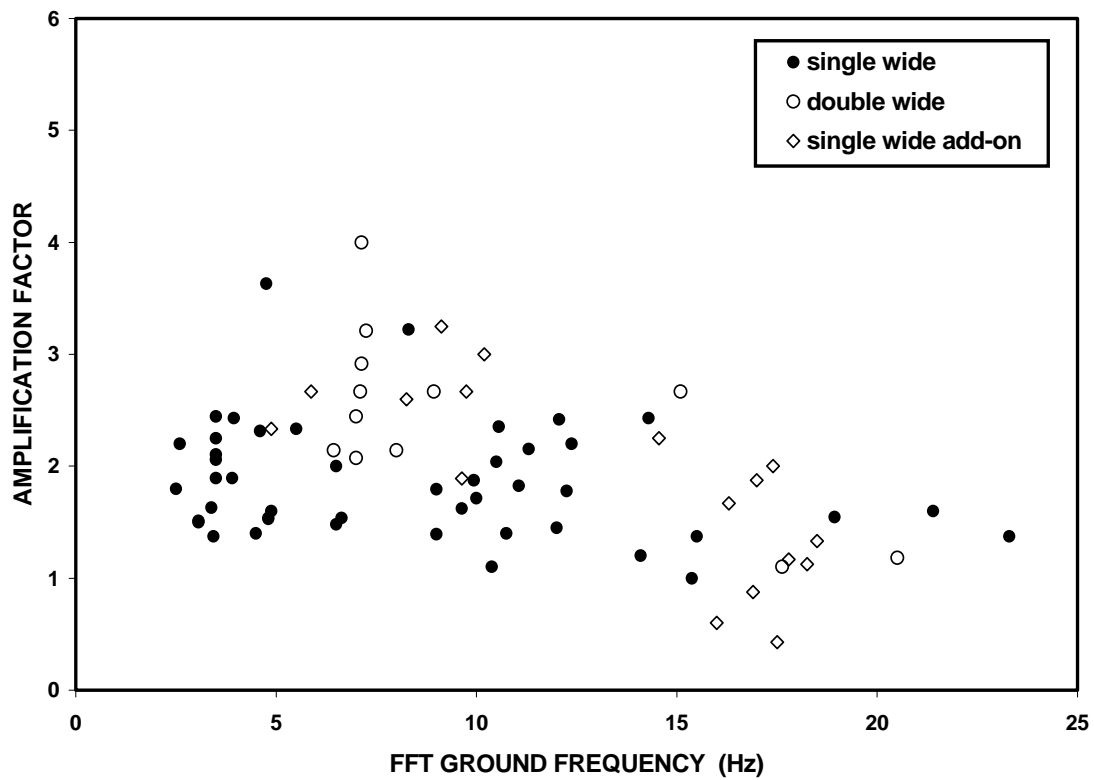


Figure 23 Amplification factor versus FFT ground frequency for all trailers



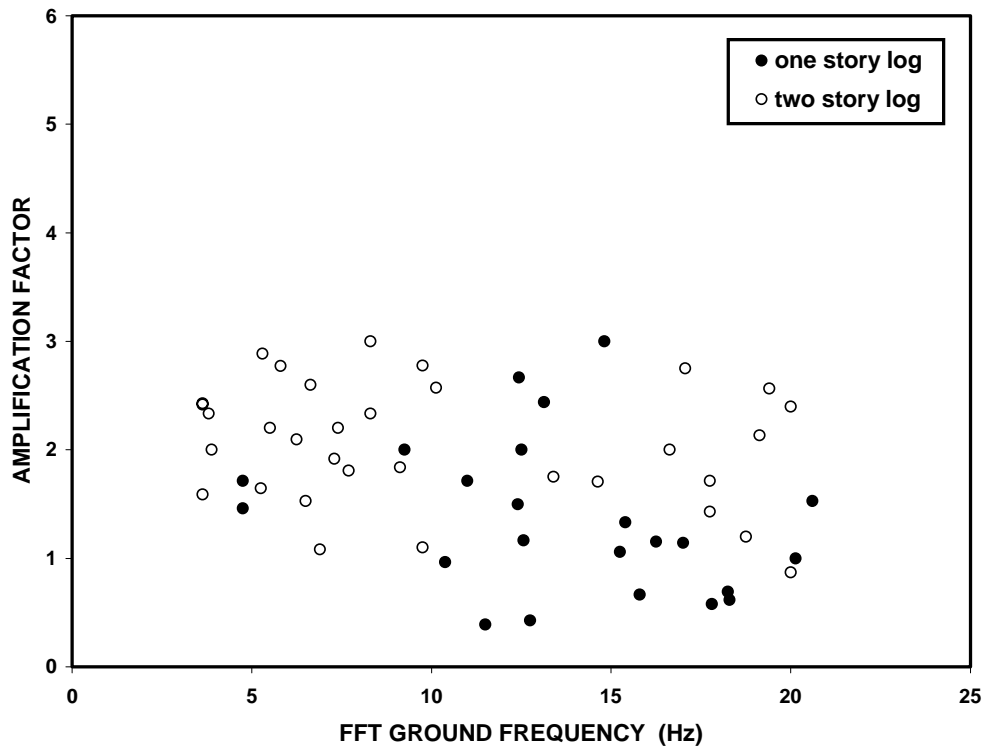


Figure 24 Amplification factor versus FFT ground frequency for all log structures

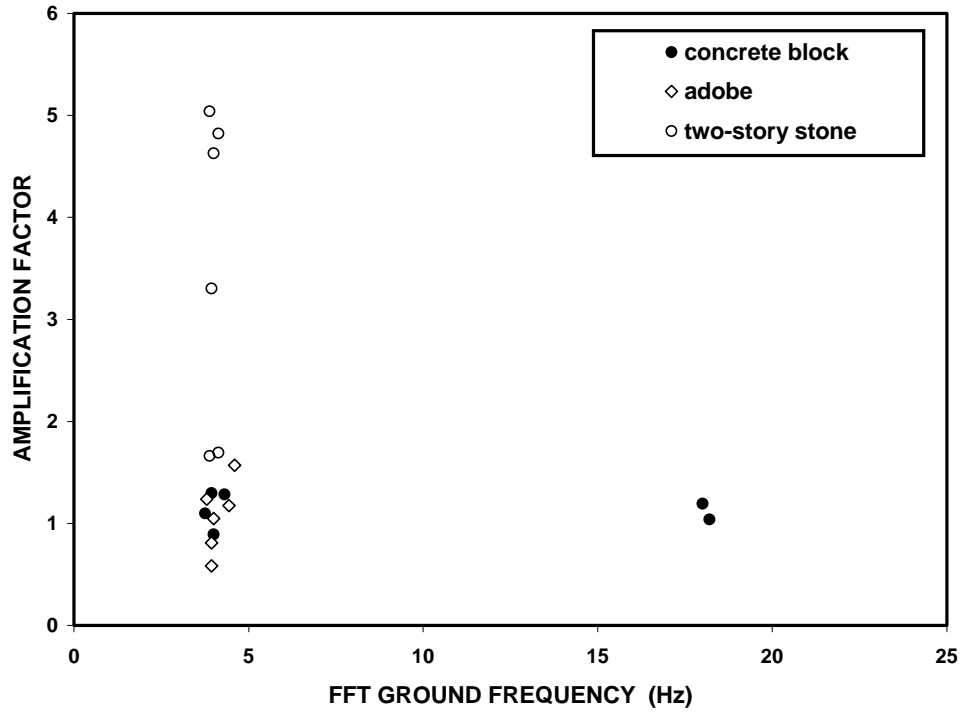


Figure 25 Amplification factor versus FFT ground frequency for all earth and masonry structures

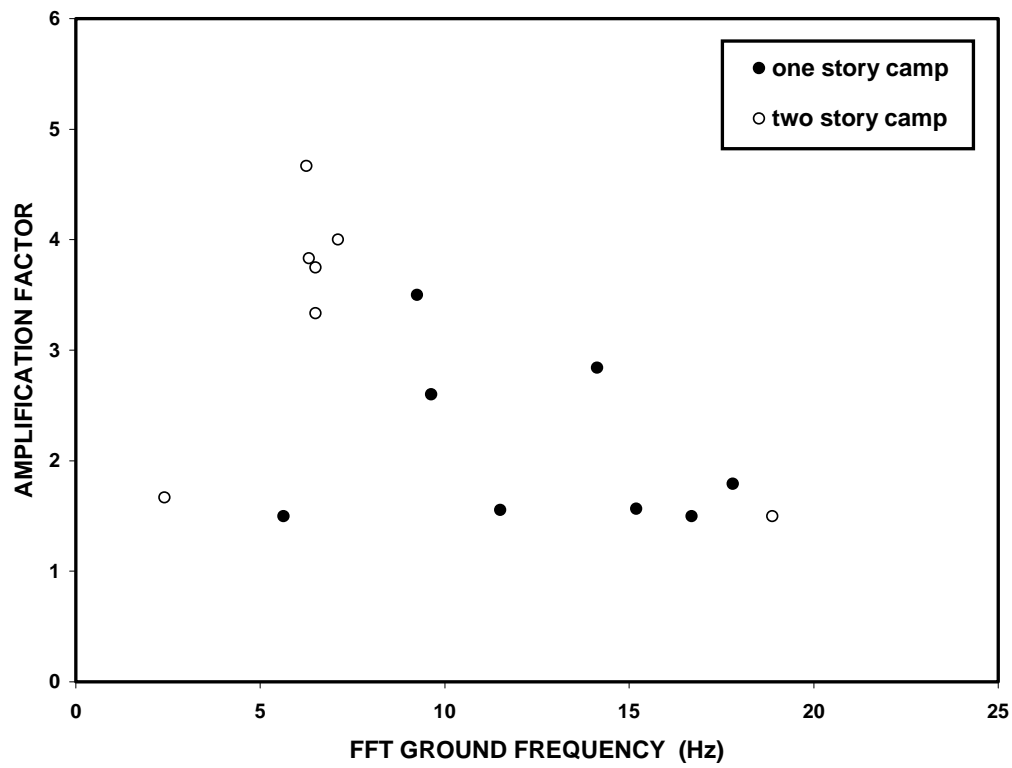


Figure 26 Amplification factor versus FFT ground frequency for all camp structures

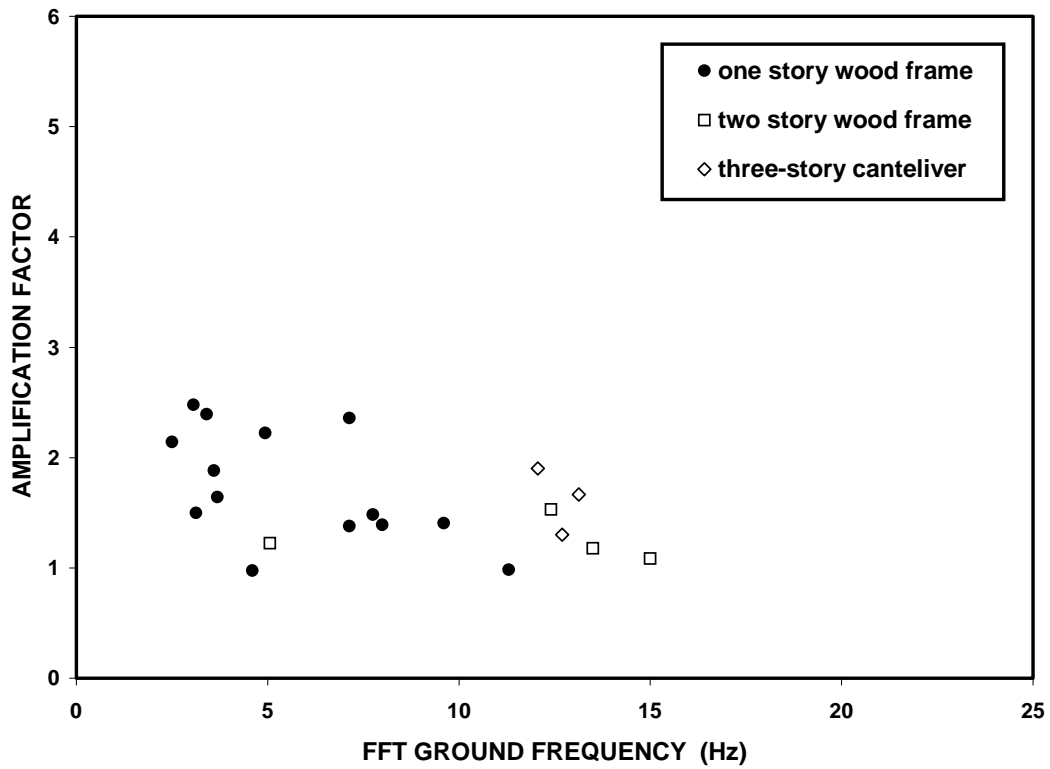
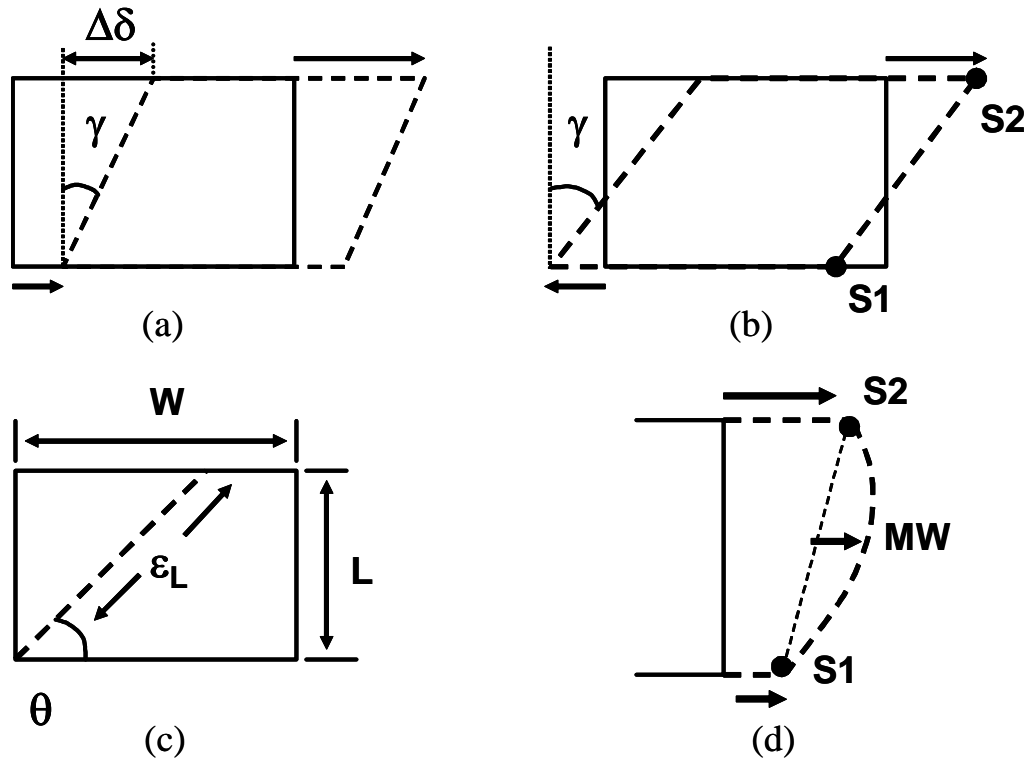


Figure 27 Amplification factor versus FFT ground frequency for all wood-frame structures

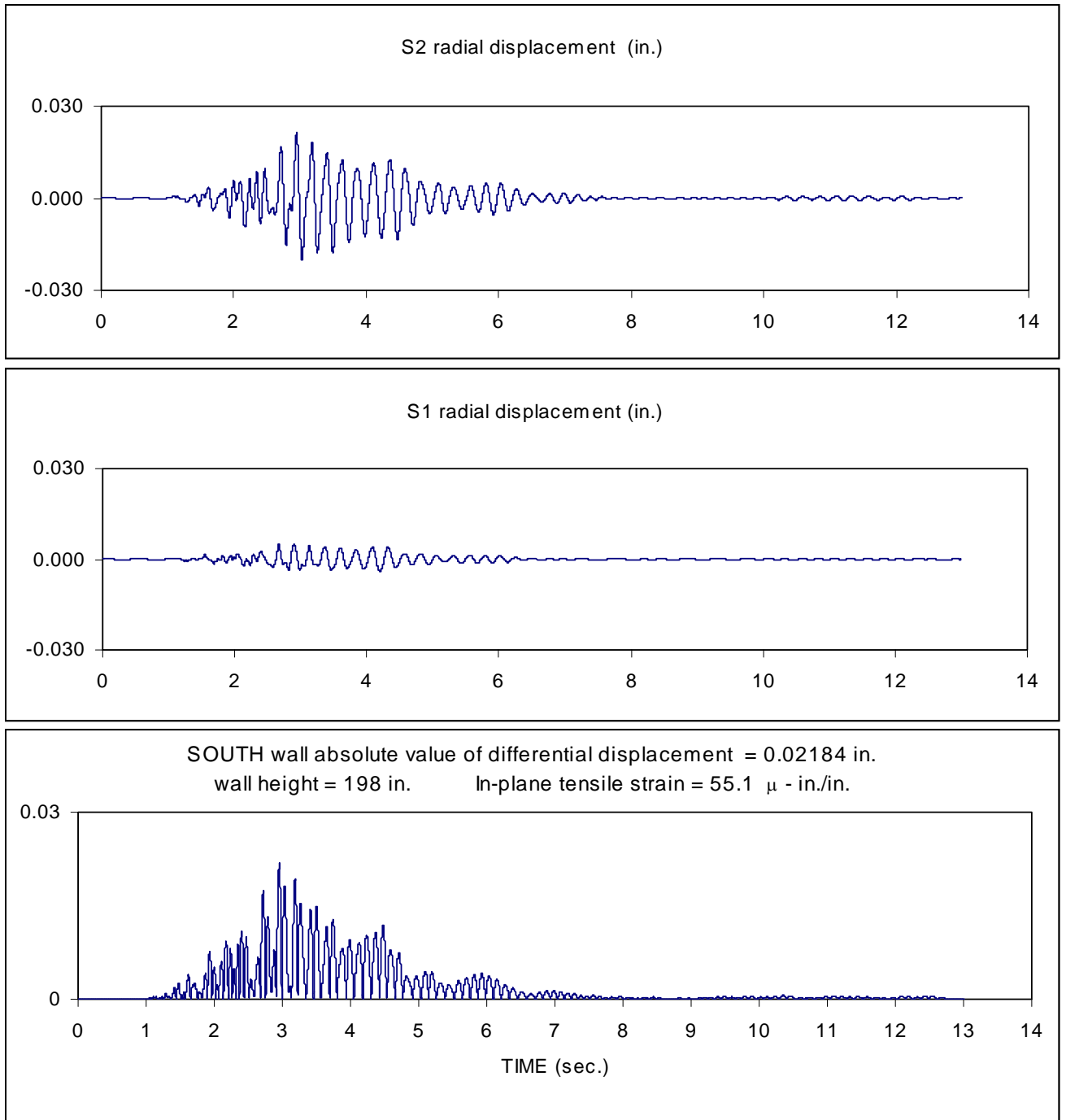


$\gamma$  = angle between S1 and S2

$\epsilon_L$  = sum of all strain components along the wall diagonal

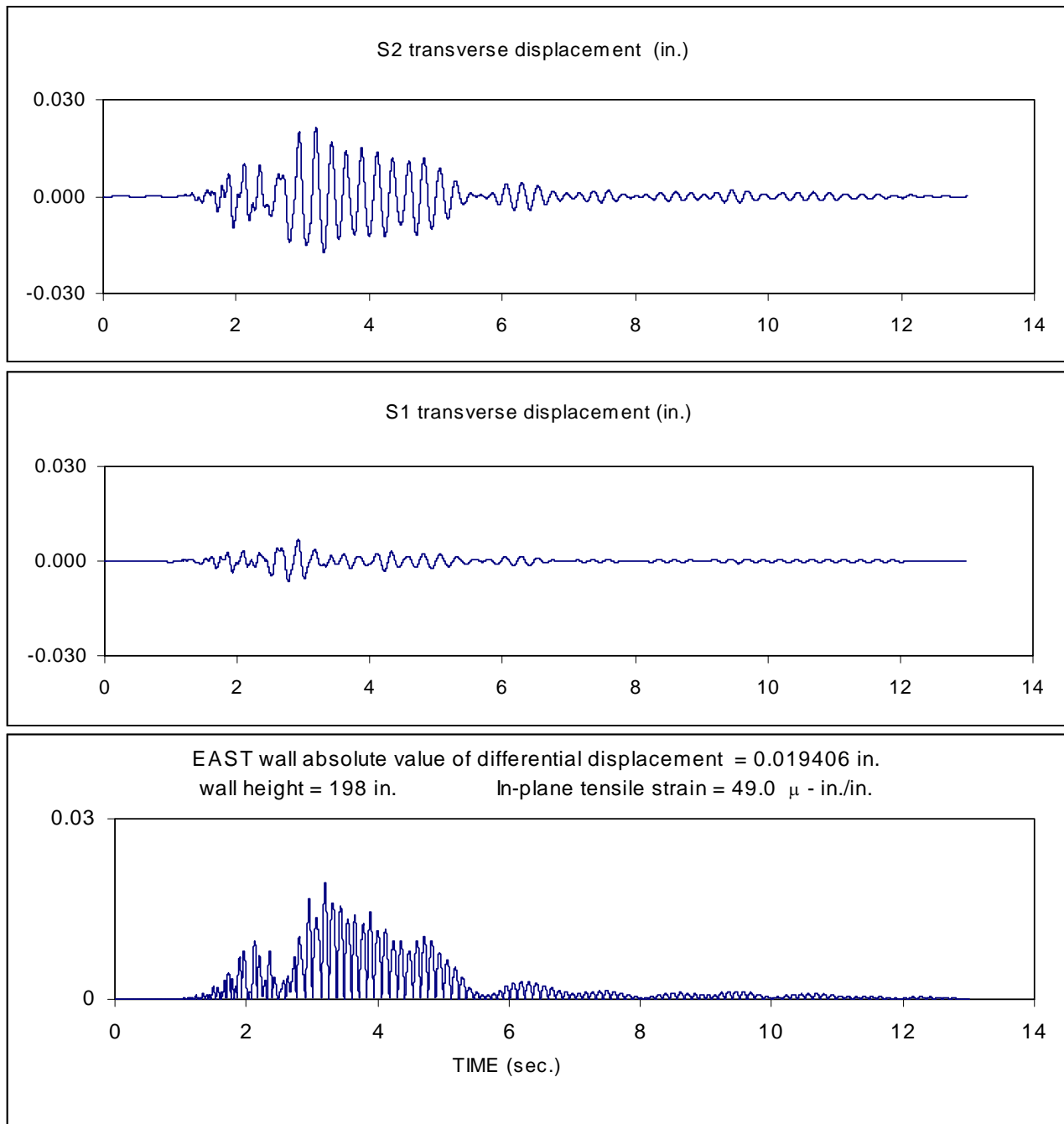
$\Delta\delta$  = differential displacement

Figure 28 Global structure strains for (a) in-phase and (b) out-of-phase structure motions; in-plane tensile wall strains are defined in (c), and wall bending strains are shown in (d)



(a)

Figure 29 (a) Example calculations for whole structure differential displacement (absolute values) time history for the radial direction (transverse wall) of structure E2S-NM



(b)

Figure 29 (b) Example calculations for whole structure differential displacement (absolute values) time history for the transverse direction (radial wall) of structure E2S-NM

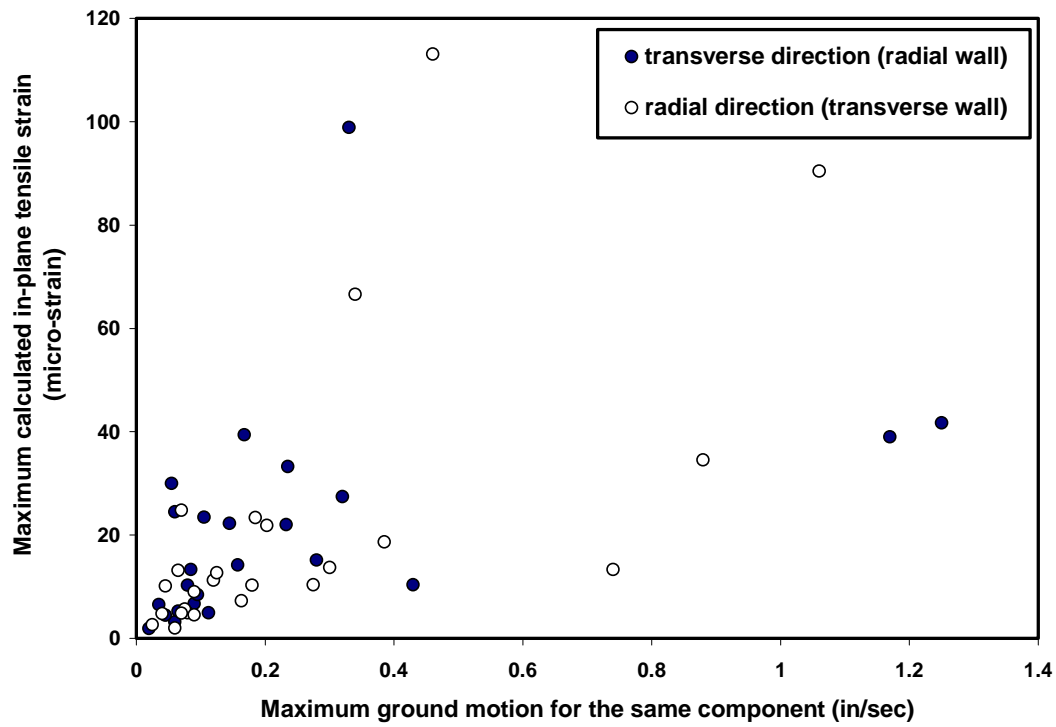


Figure 30 Calculated in-plane tensile strains versus peak particle velocity

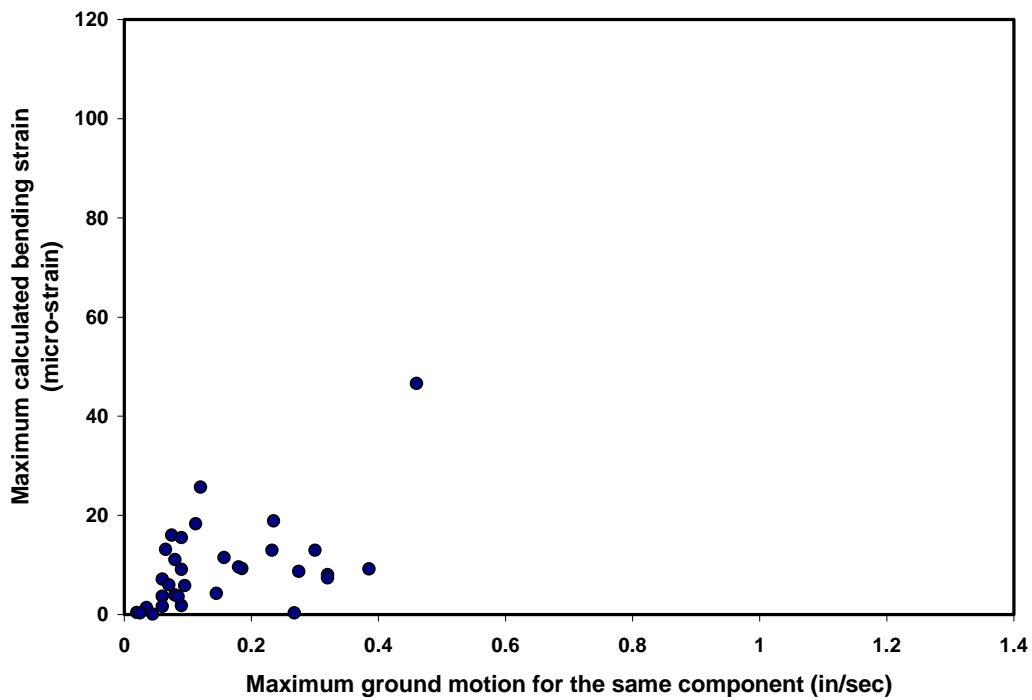
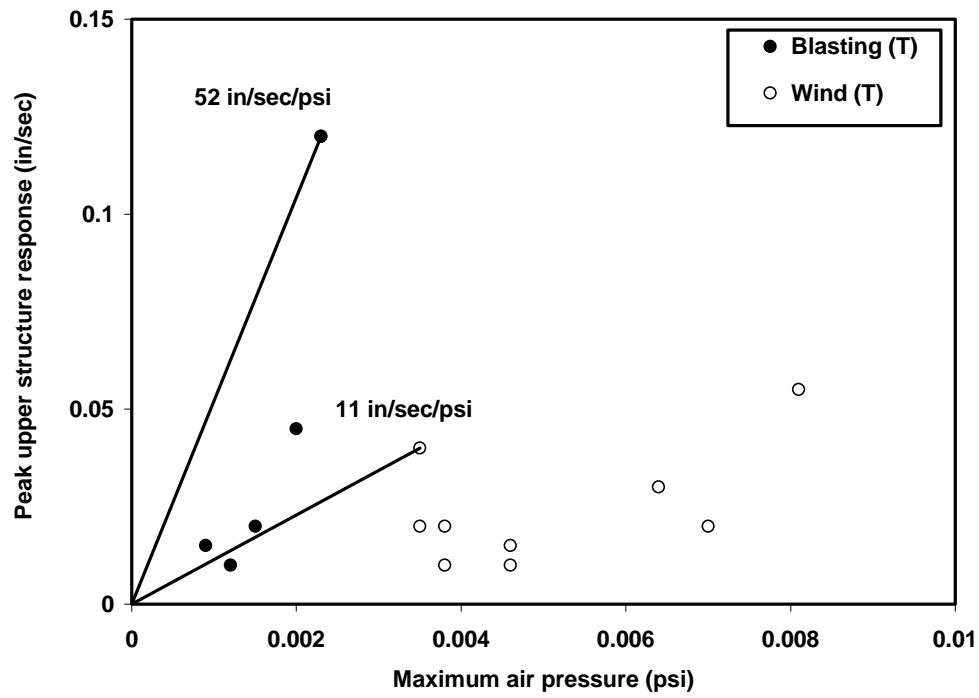
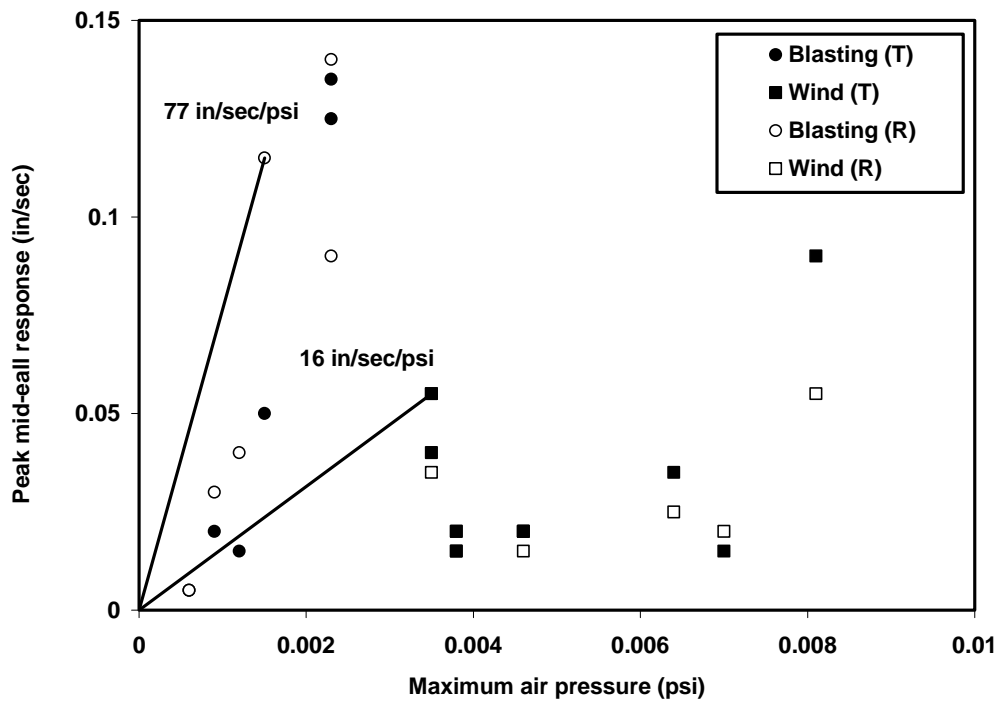


Figure 31 Calculated wall bending strains versus the corresponding peak particle velocity for all horizontal components



(a)



(b)

Figure 32 Structure response versus maximum air pressure measured during blasting and wind gusts for single wide trailer TS-KY2 (a) upper structure (S2) and (b) mid-wall responses

## APPENDIX I

### Structure Layouts and Photographs



		Entry	-0.35	1.2	1.95	2.15	5.35	3.05	
-0.35	0.0						Bedroom	5.05	6.45
Master Bedroom		-0.85	Kitchen			TV Room	6.1		Bedroom
		Bath					3.6		
1.75	0.65		-0.35	-0.05	-0.05	1.95	2.45	2.75	3.05



**TS-KY2**

**10 ft.**



TS-KY2



TS-IN

10 ft.



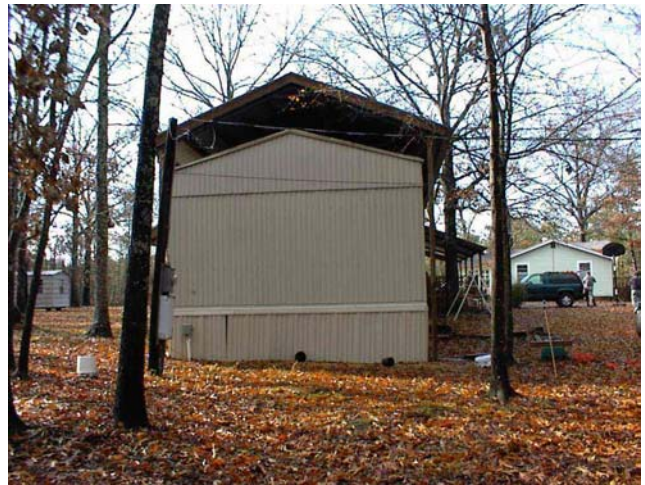
TS-IN single wide trailer





**TS-AL**

**10 ft.**



TS-AL single wide trailer

	2.0	1.2		0.2	0.1	0.0	0.0	-0.7		0.0	0.4
	Master Bedroom			Kitchen		Living Room		Bedroom	Bath	Bedroom	
Bath	2.1	1.9		-1.7	-1.8	0.8	-0.1			-1.4	-1.4

N



TS-OH

10 ft.



TS-OH single wide trailer





2.4	-2.1				-0.7	-2	-3.4
Bedroom				0.8	Kitchen		
		Bath				Bedroom	
-2	-1.9	-0.1	-0.2	0.2	-0.6	0.2	0.4
1.8	0.4	Living Room				4.9	3.4
Bedroom							
						Bedroom	
2.7	1.4	4.8			-1.3	0.0	0.5



N

TSA-KY2

---

10 ft.



TSA-KY2 single wide add-on



0.55	0.75	1.05	-0.1	0.15	-0.05	0.15	0.25	0.15	0.65
Master Bedroom		Main Entry Room		Bedroom		Bath		Bedroom	
0.65	-0.15	-0.1	-0.45	-0.05	-0.05	0.25	0.55	0.35	1.15
-0.05	0.05	Closet		0.0	1.13	-0.1	0.05	Closet	
Bath		Entry		Kitchen		Dining Area		Living room	
0.65	0.35	0.0	0.0	-0.1	0.0	0.45	1.65	1.9	

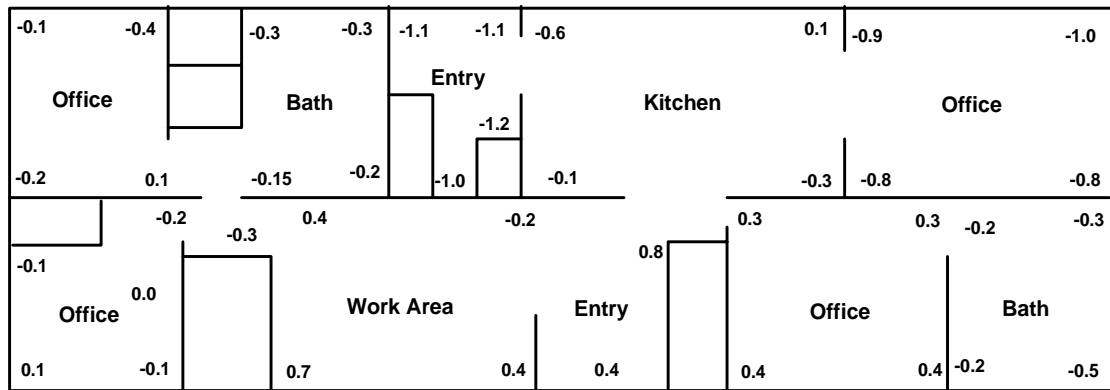


TD-WV2

10 ft.



TD-WV2 double wide trailer



N

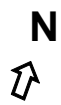
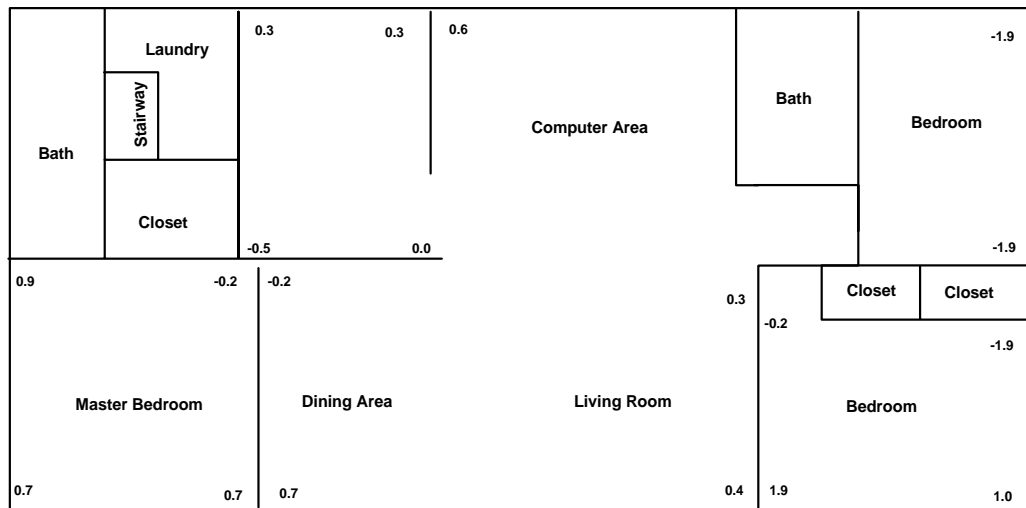
TD-TN

10 ft.



TD-TN double wide trailer



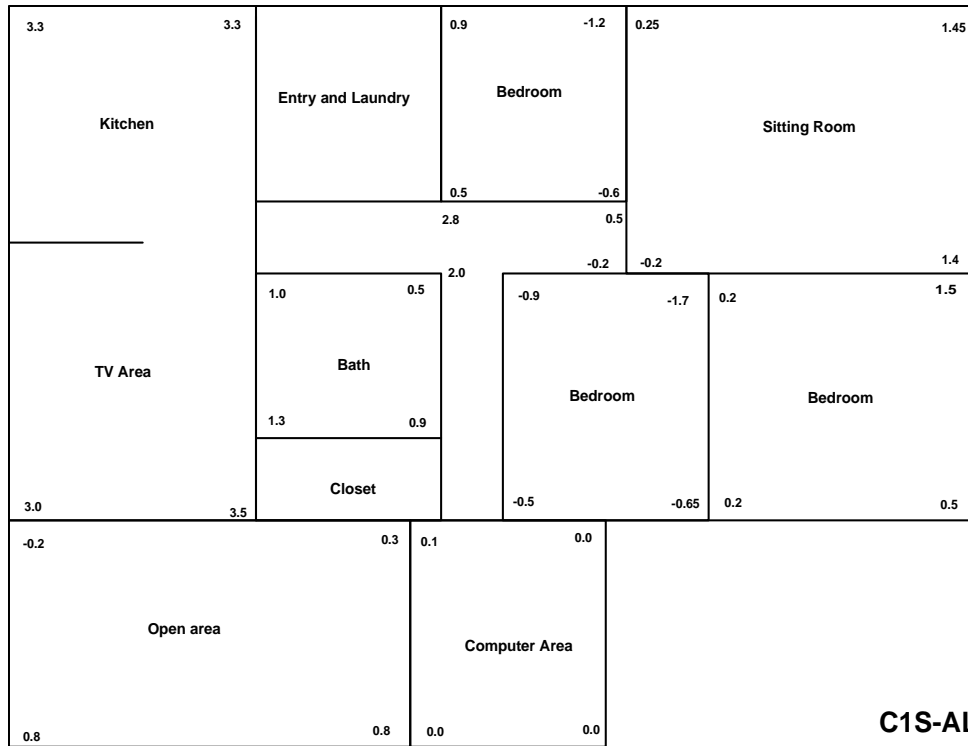


**TD-PA**

5 ft.



PD-PA double wide trailer with full basement



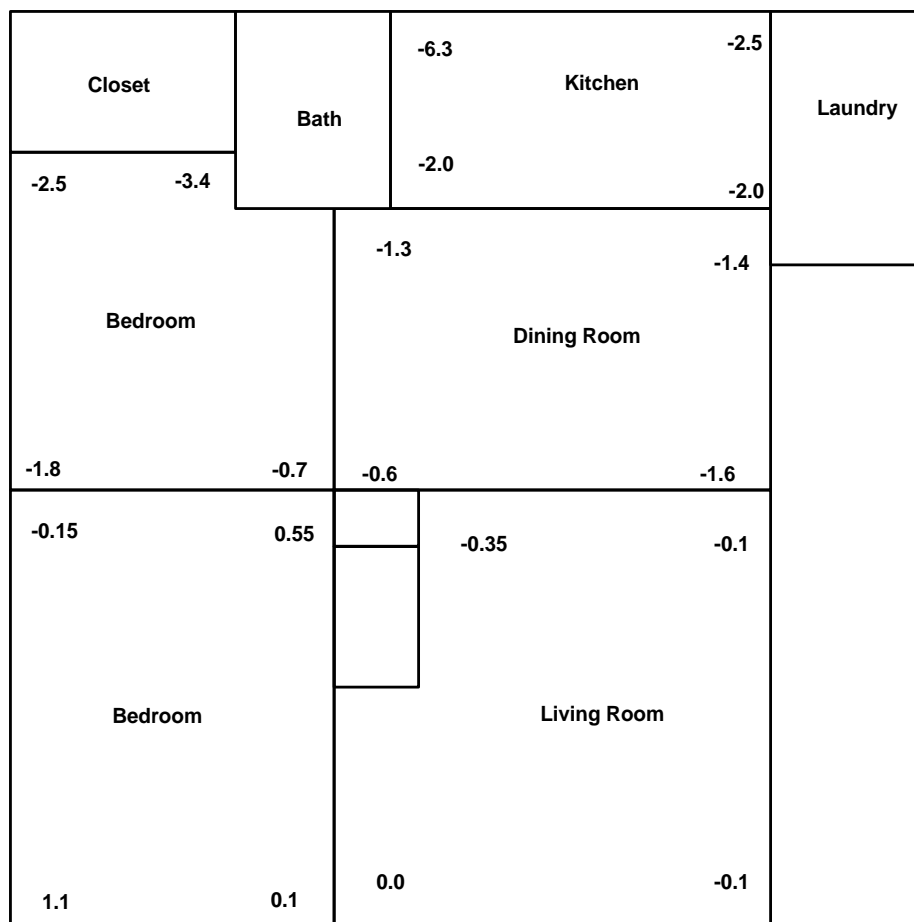
**C1S-AL**

**N** ↖

**5 ft.**



C1S-AL camp house



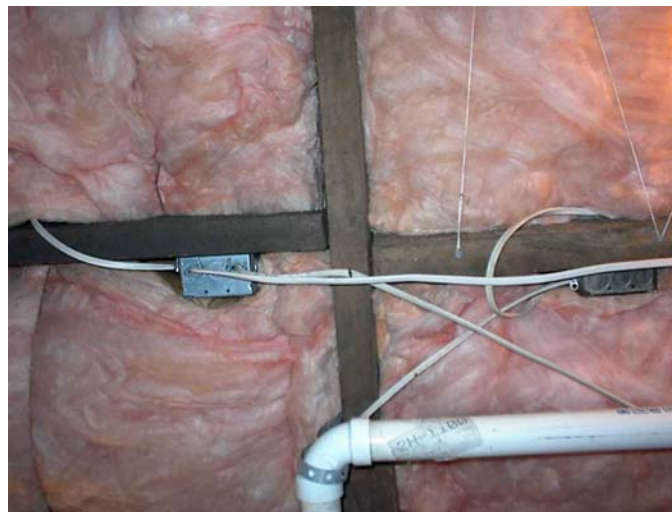
N ↙

C1S-VA  
5 ft

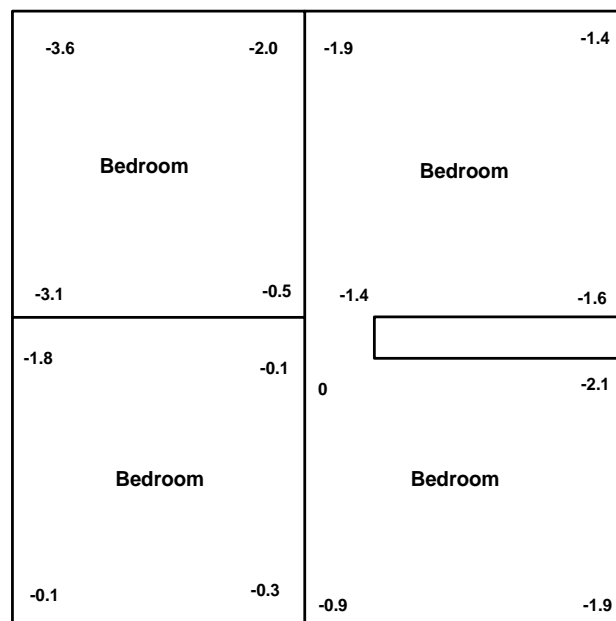
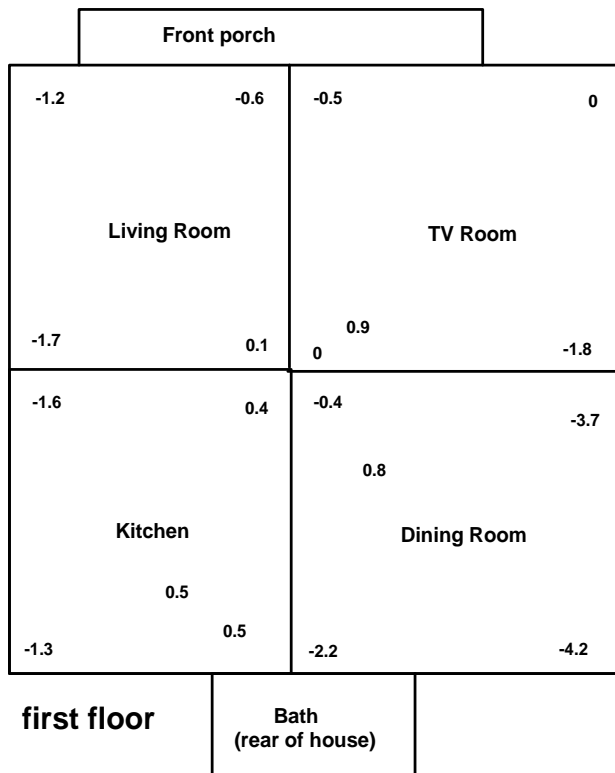


C1S-VA camp house





C1S-VA (cont.) camp house



second floor

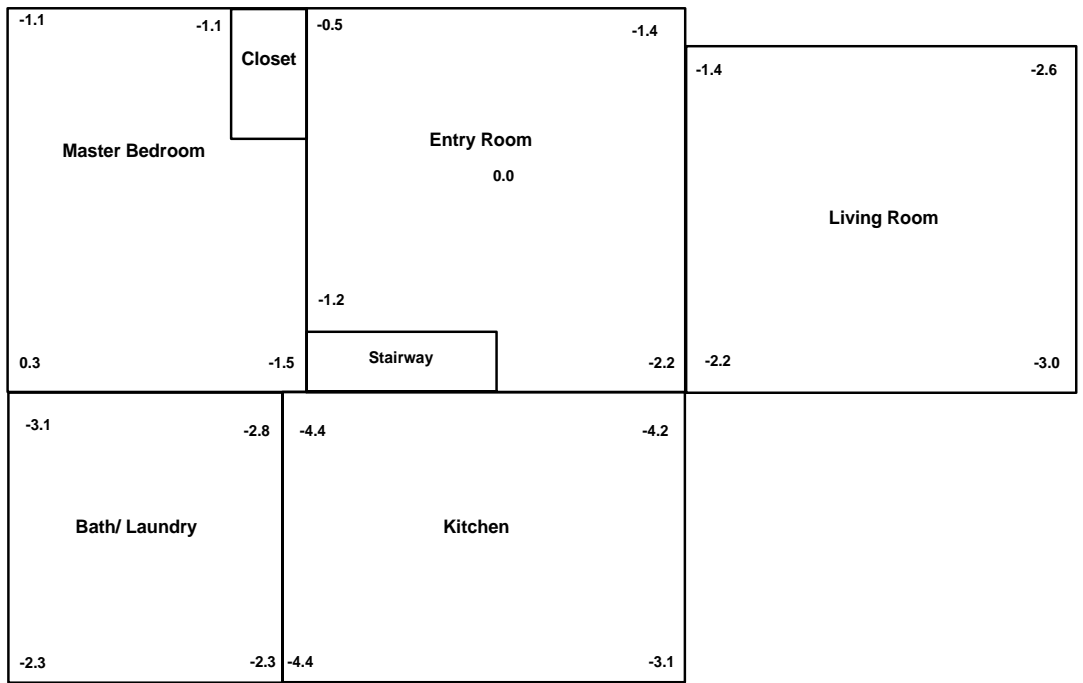
**C2S-KY1a**

5 ft.



C2S-KYA Two story camp house





**N**



**first floor**

**C2S-KY1b**

**5 ft.**



**N**



**second floor**

**C2S-KY1b**

**5 ft.**

C2S-KY1B Two story camp house





C2S-KY1B Two story camp house



**N**

**L1S-OH**

**5 ft.**



**N**

**basement**

**L1S-OH**

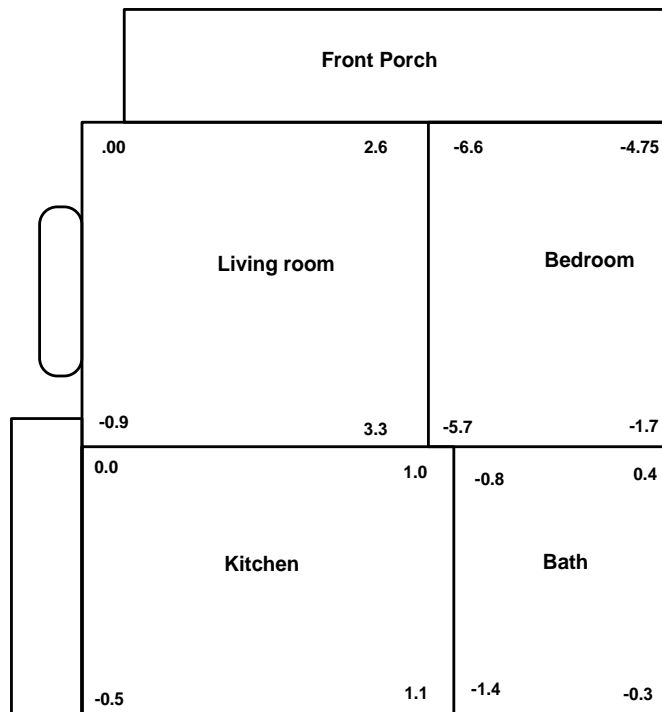
**5 ft.**

L1S-OH Traditional log house





L1S-OH (cont.) Traditional log house

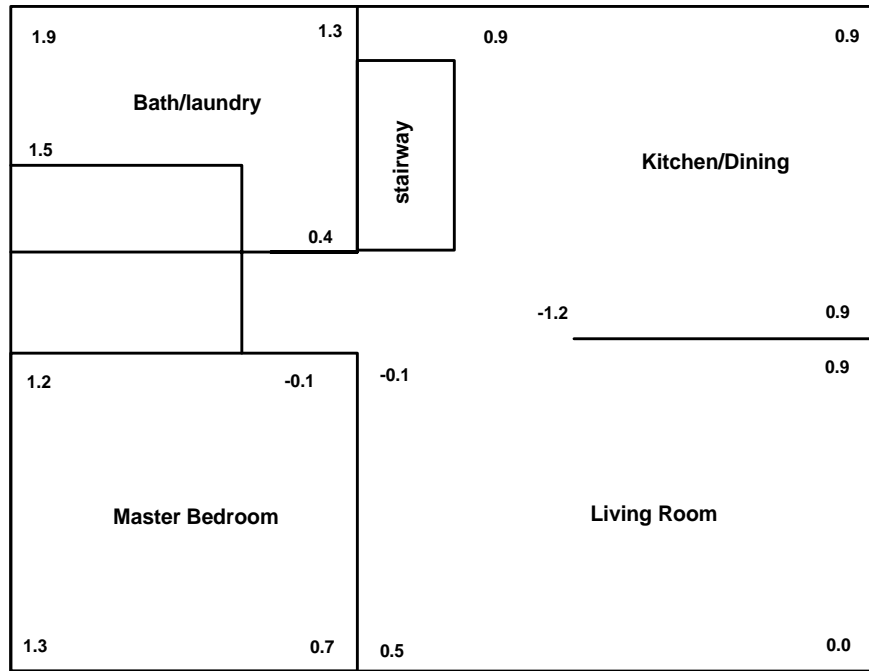


↓  
N

L1S-WV1  
5 ft.



L1S-WV1 Historic log structure

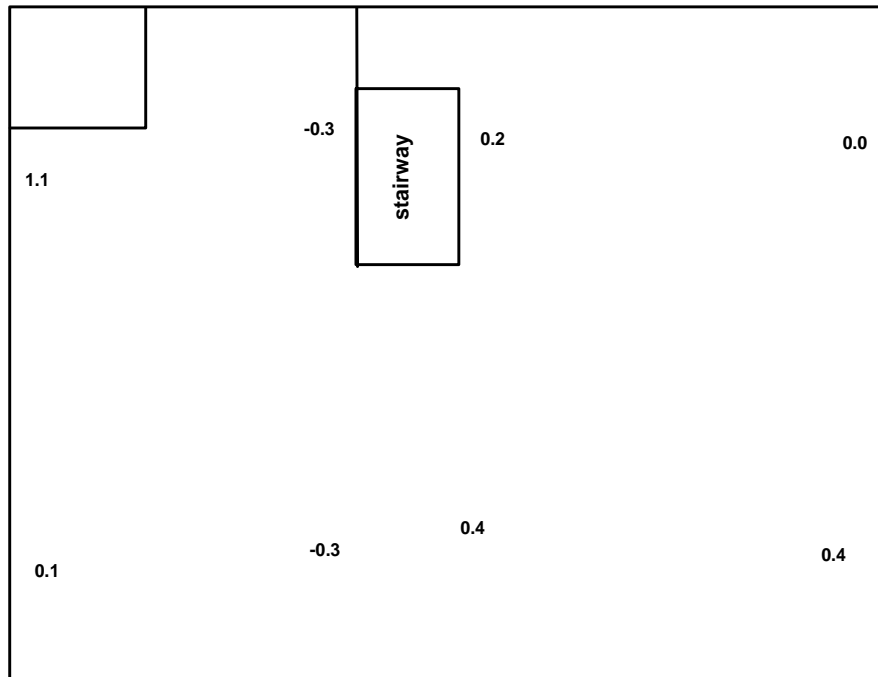


**N**

**first floor**

**L2S-TN**

**10 ft.**



**N**

**second floor**

**L2S-TN**

**10 ft.**

L2S-TN Two-story log house

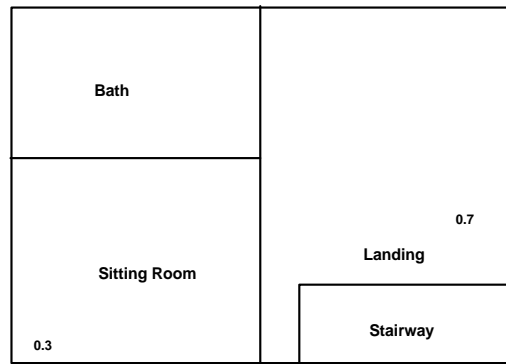




L2S-TN (cont.) Two-story log house



first floor



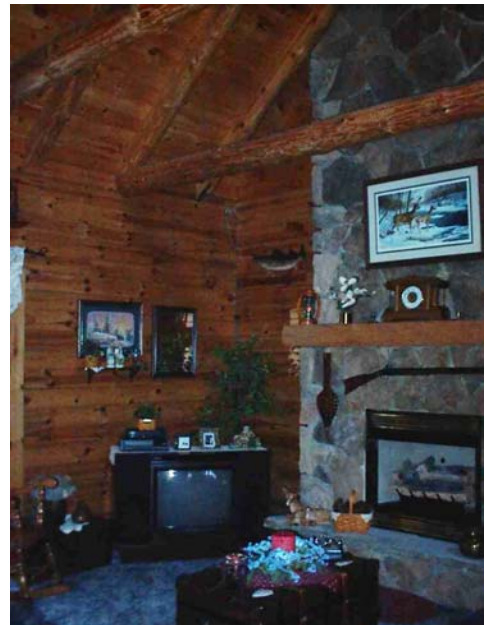
second floor



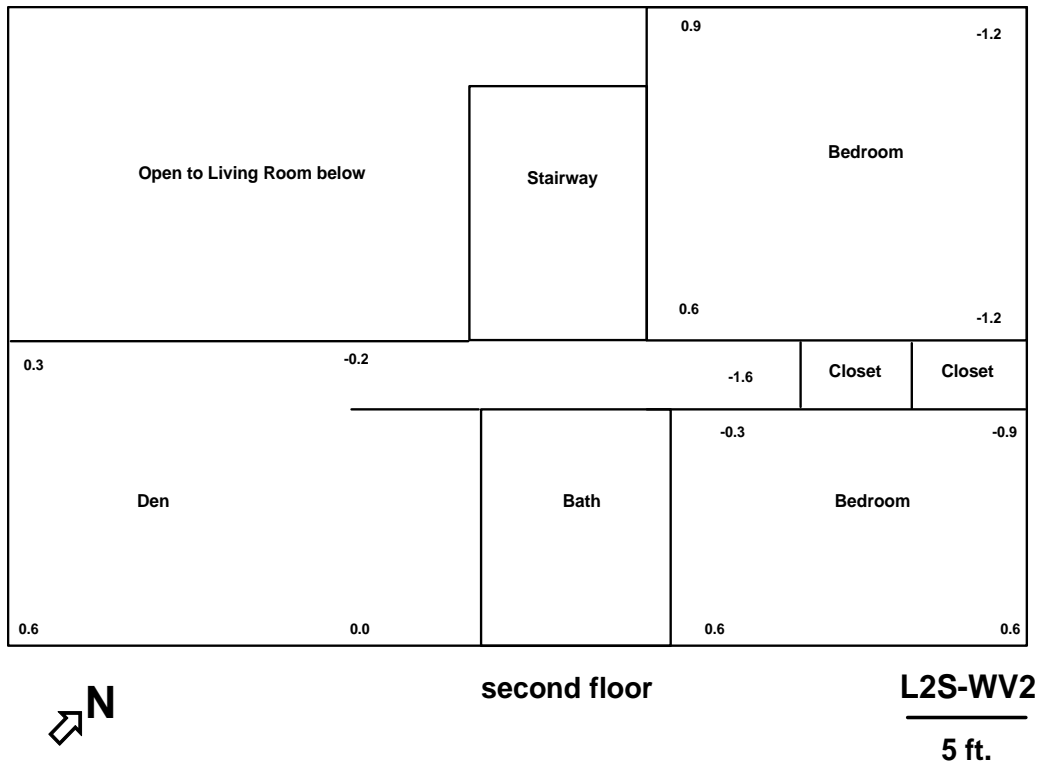
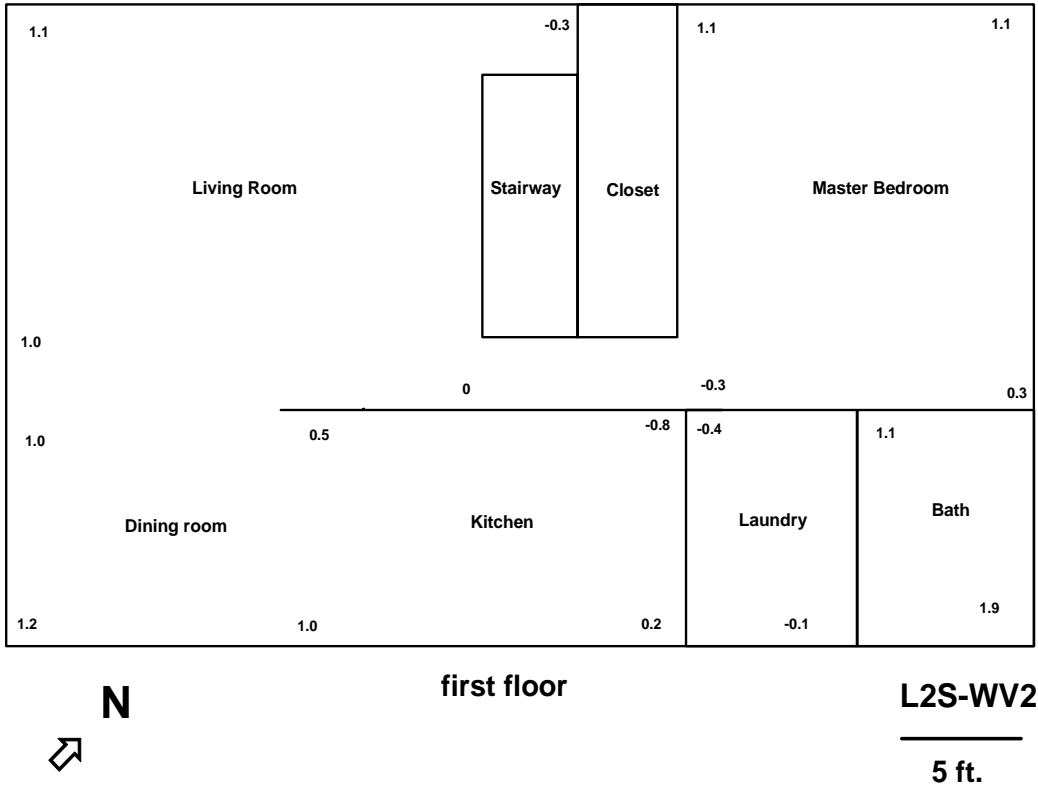
N

L2S-0H

5 ft.

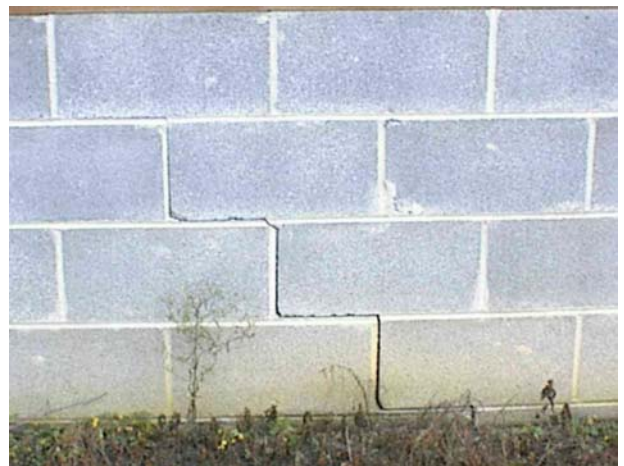
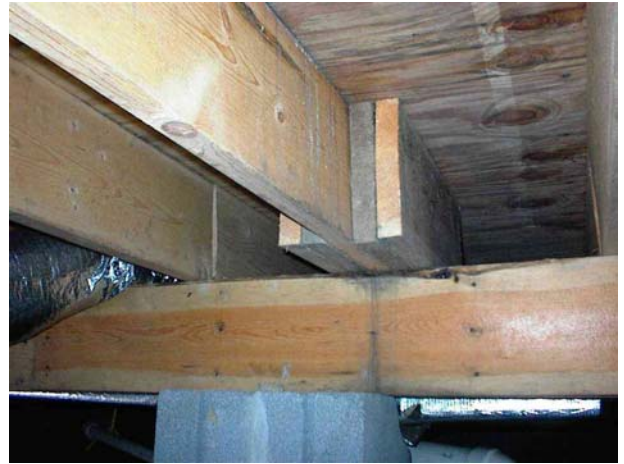


L2S-0H Two-story log house

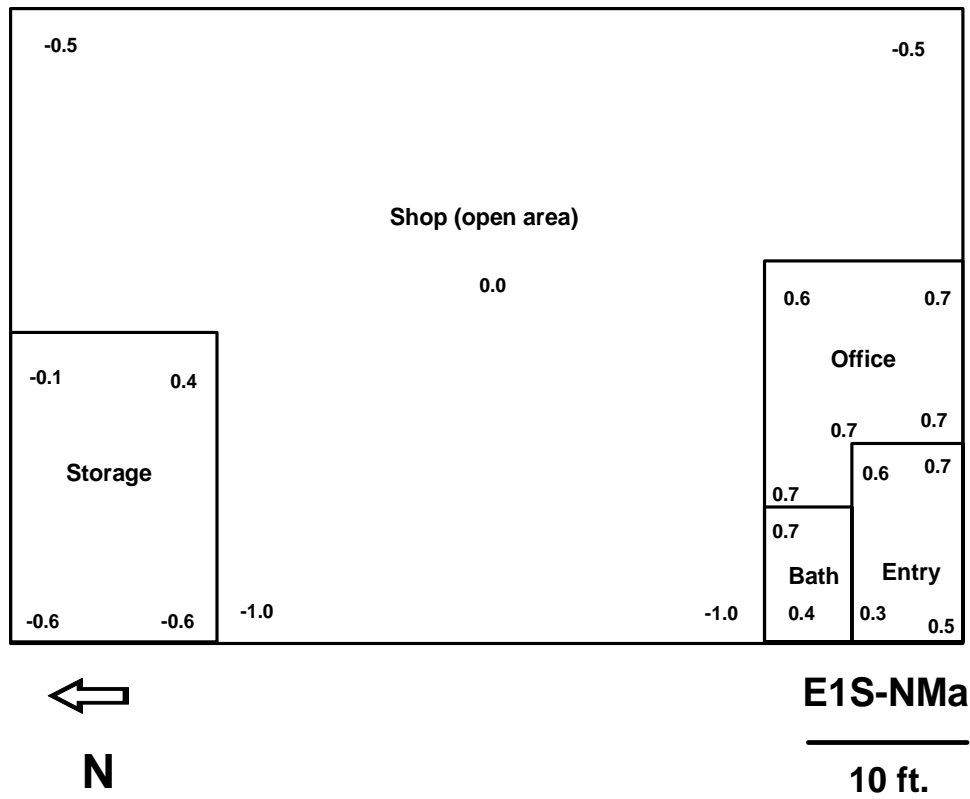


L2S-WV2 Two-story log house



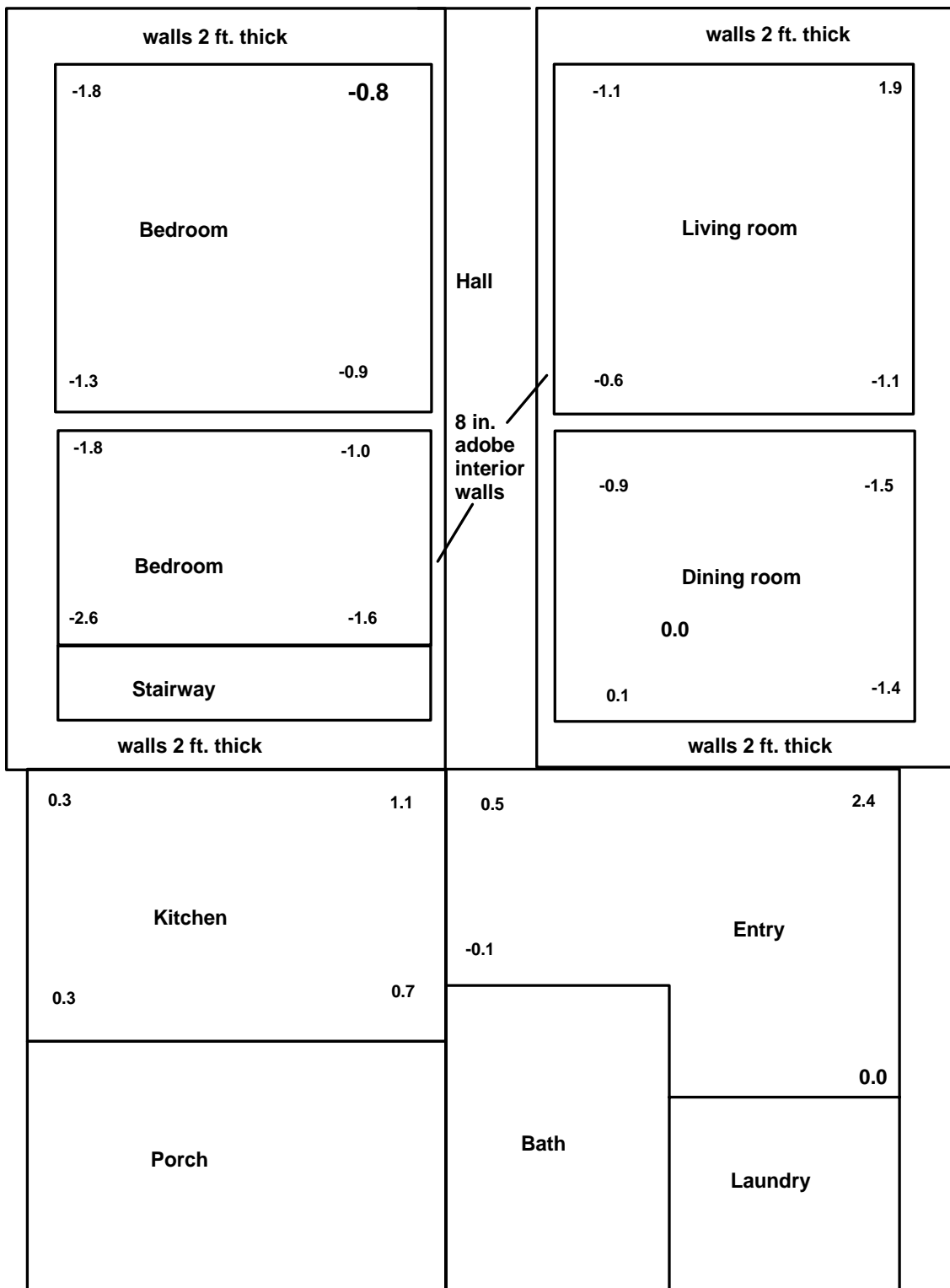


L2S-WV2 Two-story log house



E1S-NMA Concrete block structure





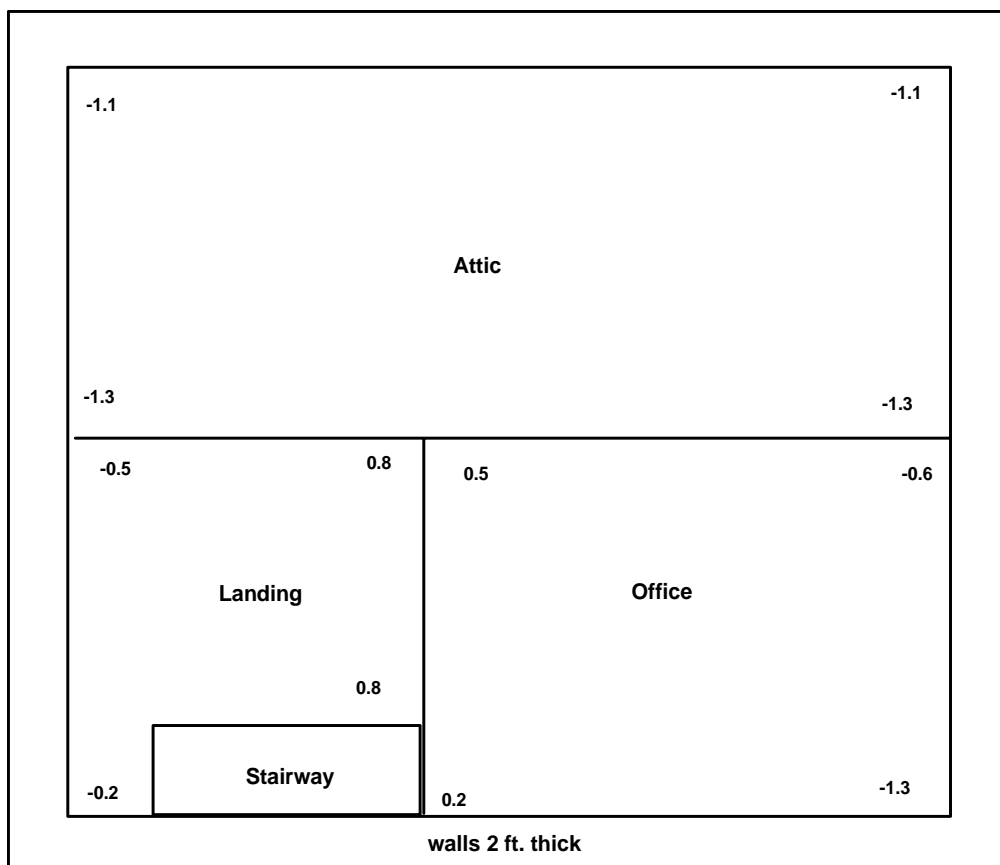
**N**

**first floor**

**E2S-NM**

**5 ft.**

E2S-NM Two-story stone house



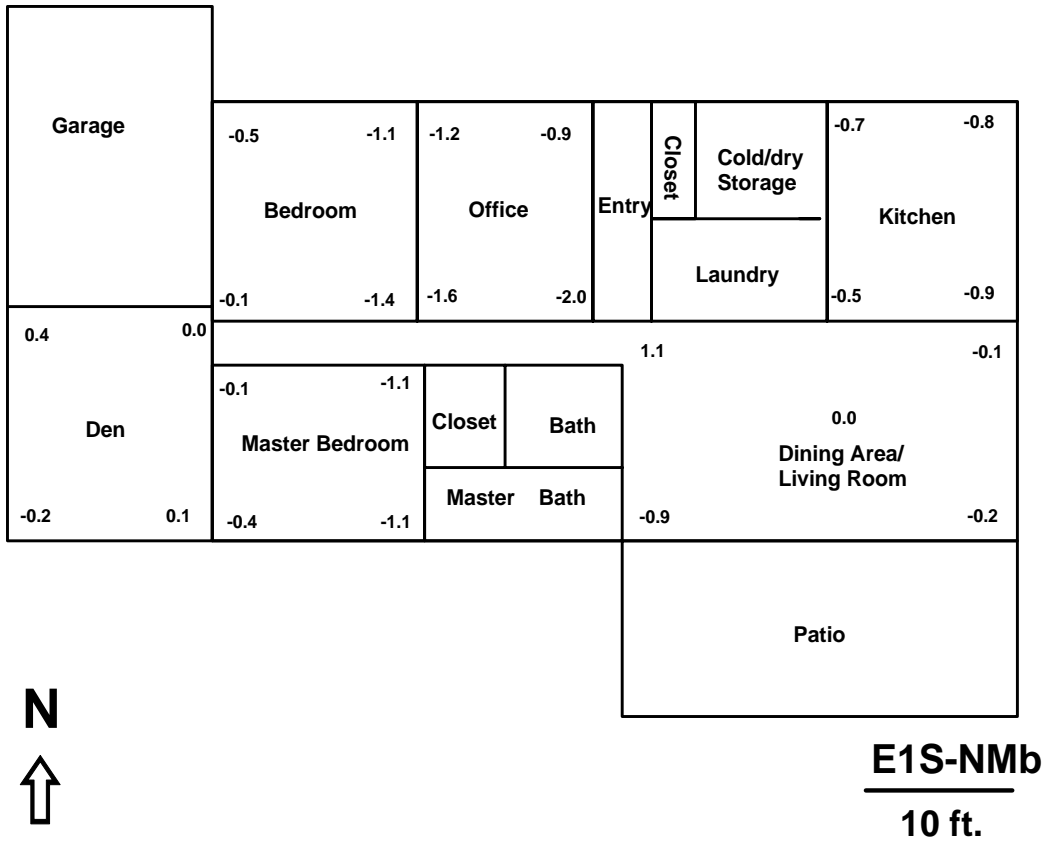
second floor

**E2S-NM**

**5 ft.**



E2S-NM (cont.) Two-story stone house



E1S-NMB Traditional adobe house

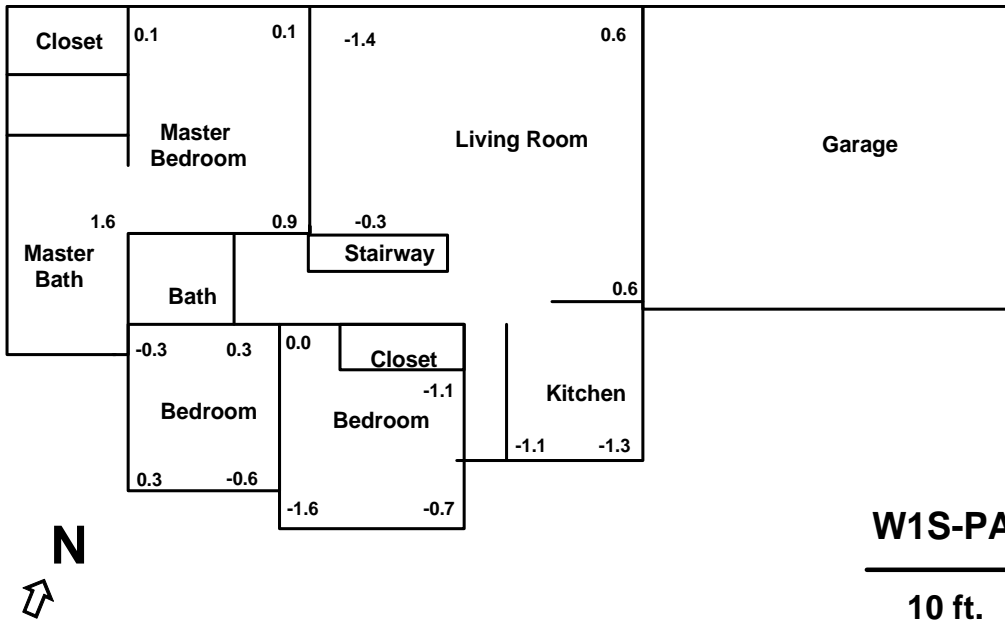


**W1S-IN**

**5 ft.**

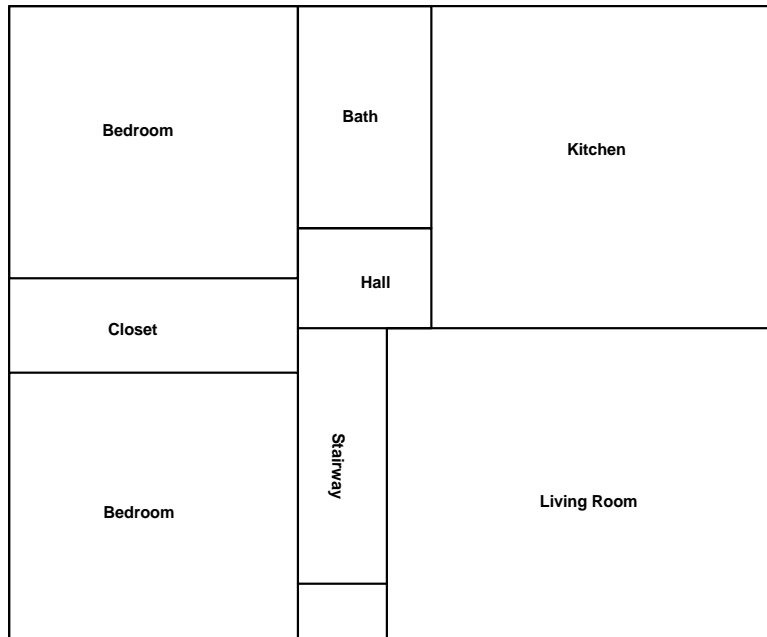


W1S-IN Wood-frame house



W1S-PA Wood-frame house under construction

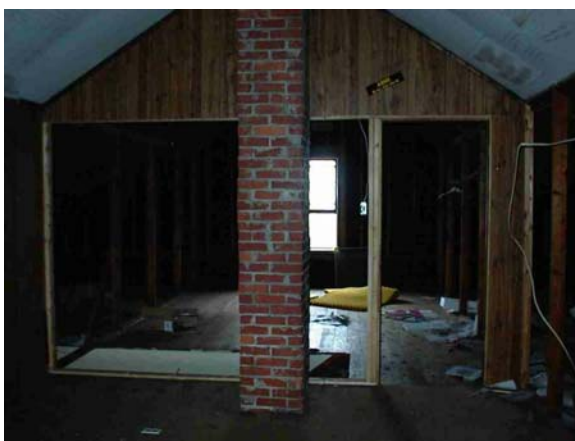




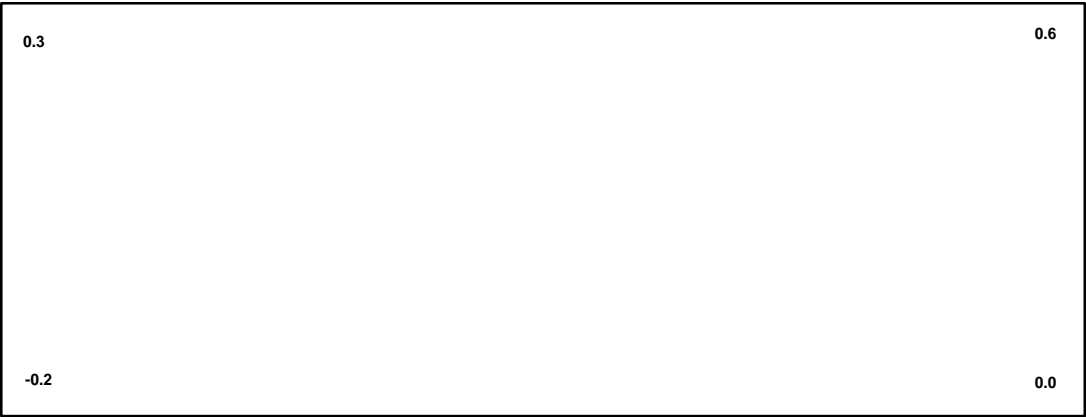
N ←

W2S-IN

5 ft.



W2S-IN Wood-frame house



**N**

**first floor**

**W3S-WV1**

**5 ft.**

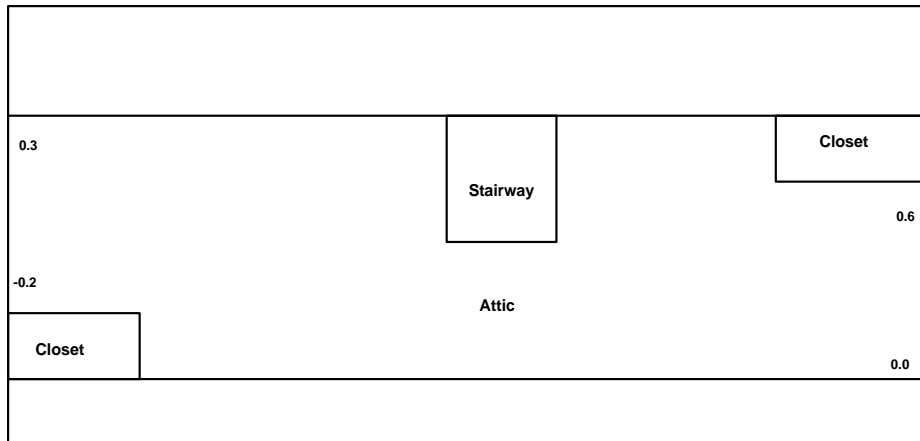


**N**

**second floor**

**W3S-WV1**

**5 ft.**



**N**

**third floor**

**W3S-VW1**

**5 ft.**

W3S-WV1 Three-story cantilever house



W3S-WV1 (cont.) Three-story cantilever house

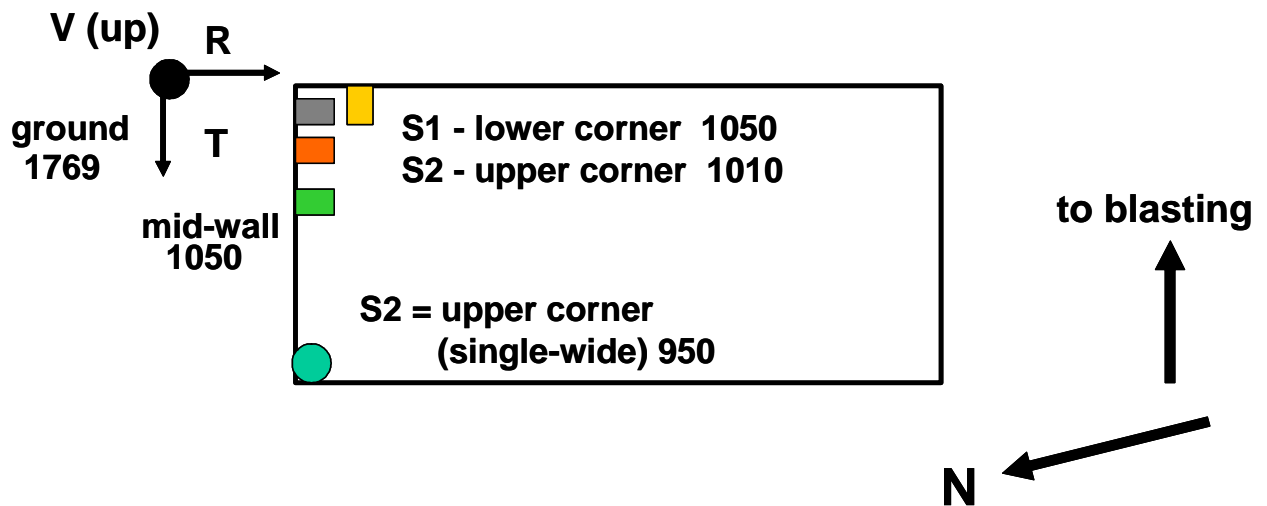


## APPENDIX II

### Instrumentation Locations

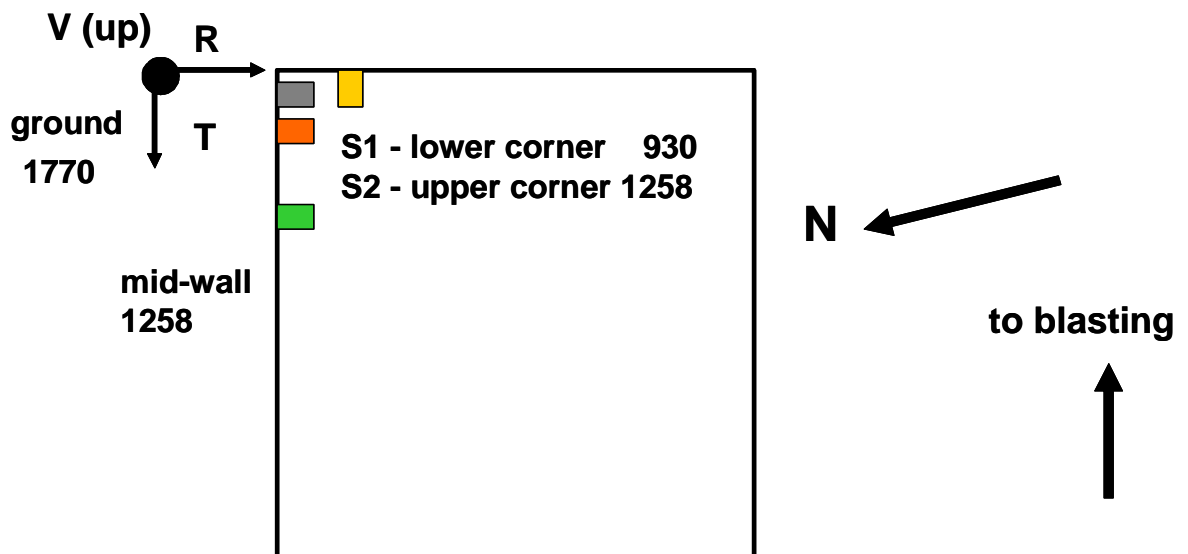
- Radial
- Transverse
- Vertical
- Mid-wall (R)

## TSA-VA single-wide and wood-frame add-on



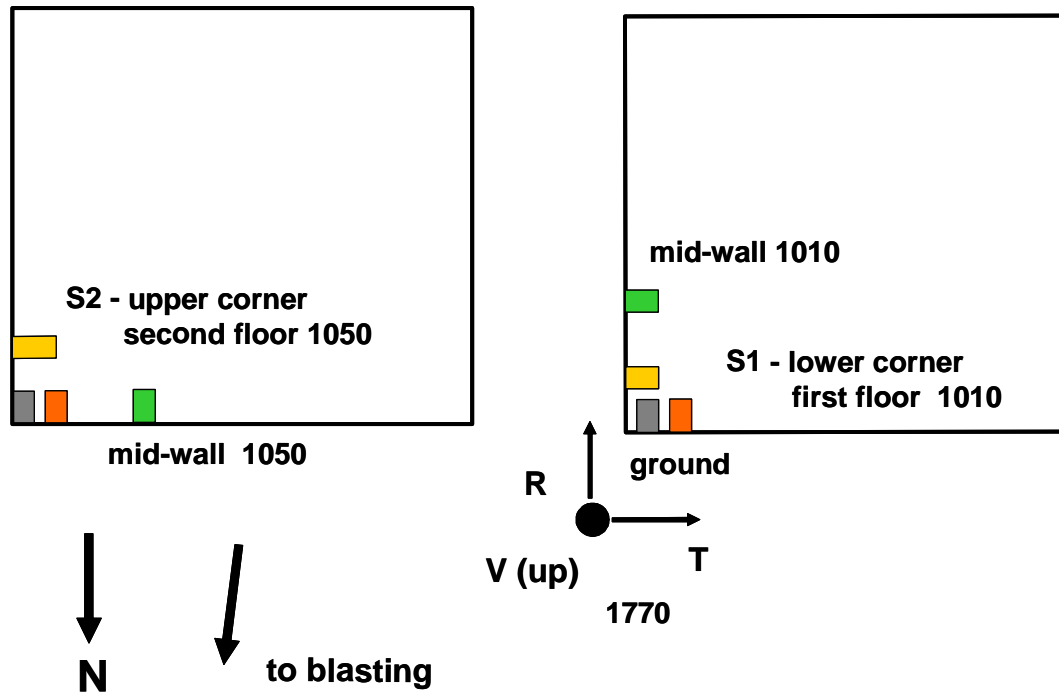
- Radial
- Transverse
- Vertical
- Mid-wall (R)

## C1S-VA single-story wood-post camp house



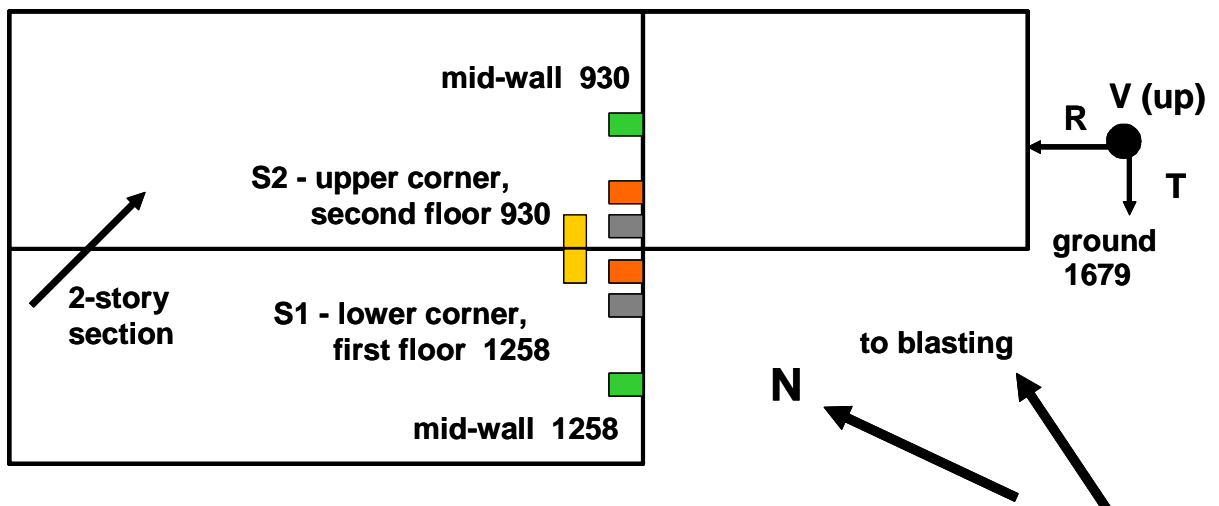
- Radial
- Transverse
- Vertical
- Mid-wall (R or T)

**C2S-KY1A**  
2-story, wood post  
camp house



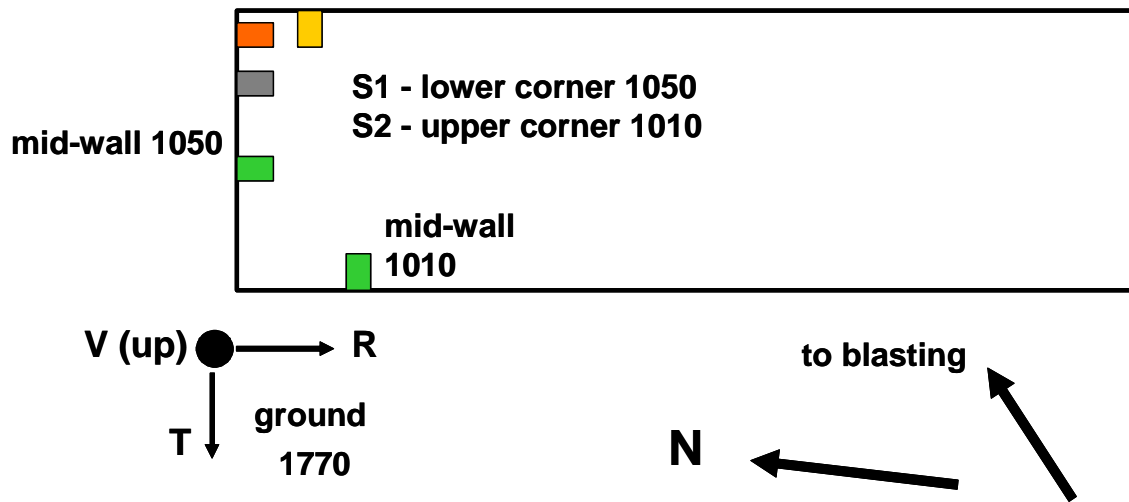
- Radial
- Transverse
- Vertical
- Mid-wall (R)

**C2S-KY1B**  
2-story, wood frame  
wood-post and CMU support



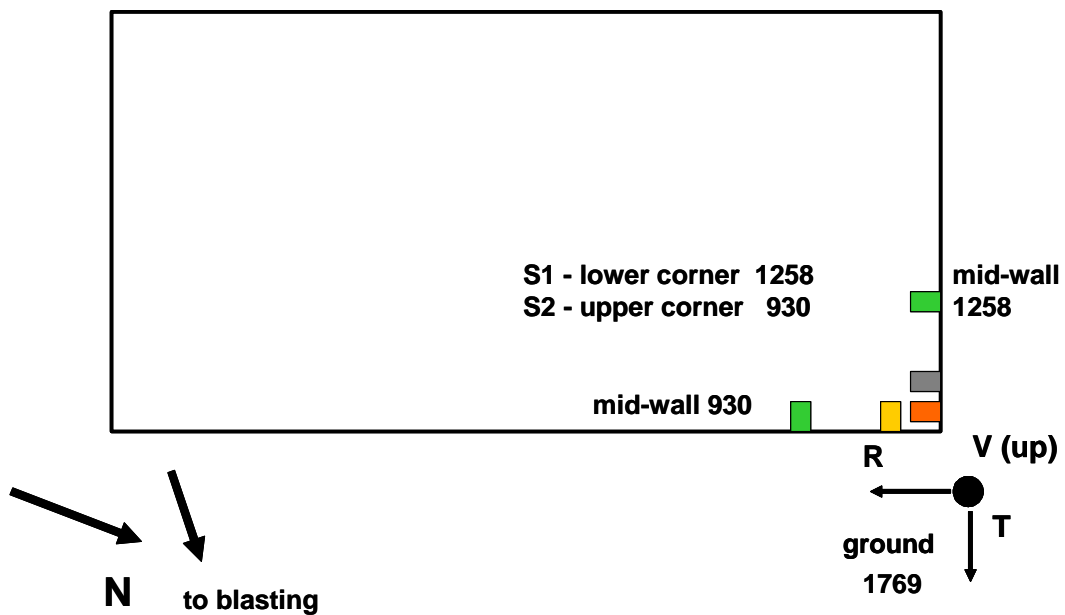
- Radial
- Transverse
- Vertical
- Mid-wall (R or T)

**TS-KY2**  
single-wide,  
CMU support



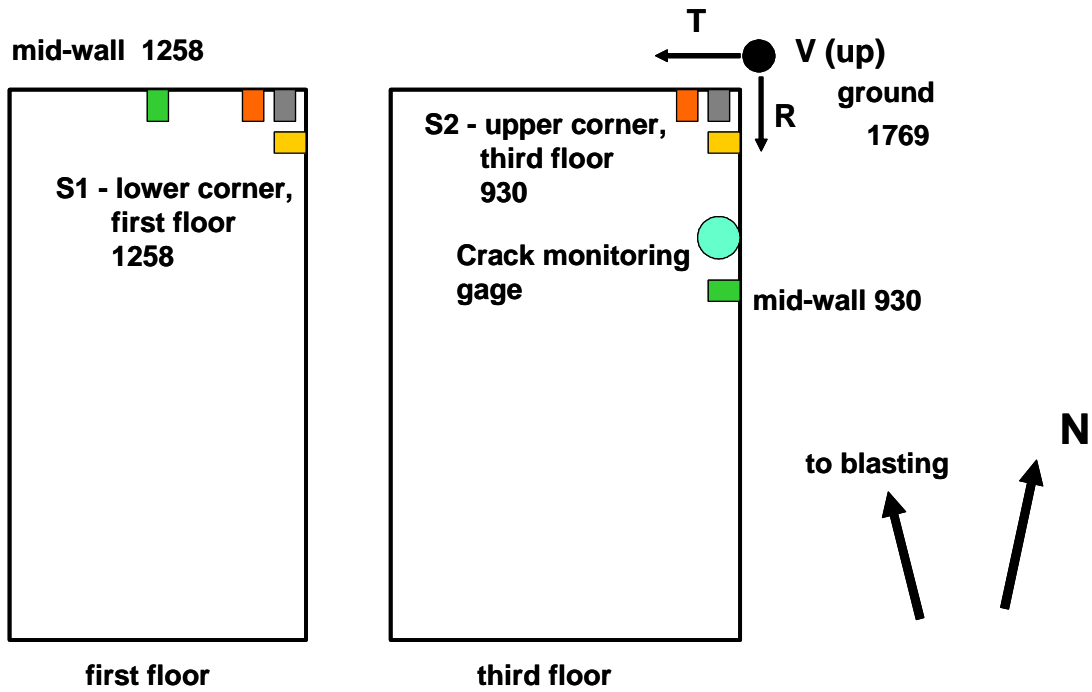
- Radial
- Transverse
- Vertical
- Mid-wall (R or T)

**TSA-KY2**  
single-wide, add-on  
wood frame, CMU support



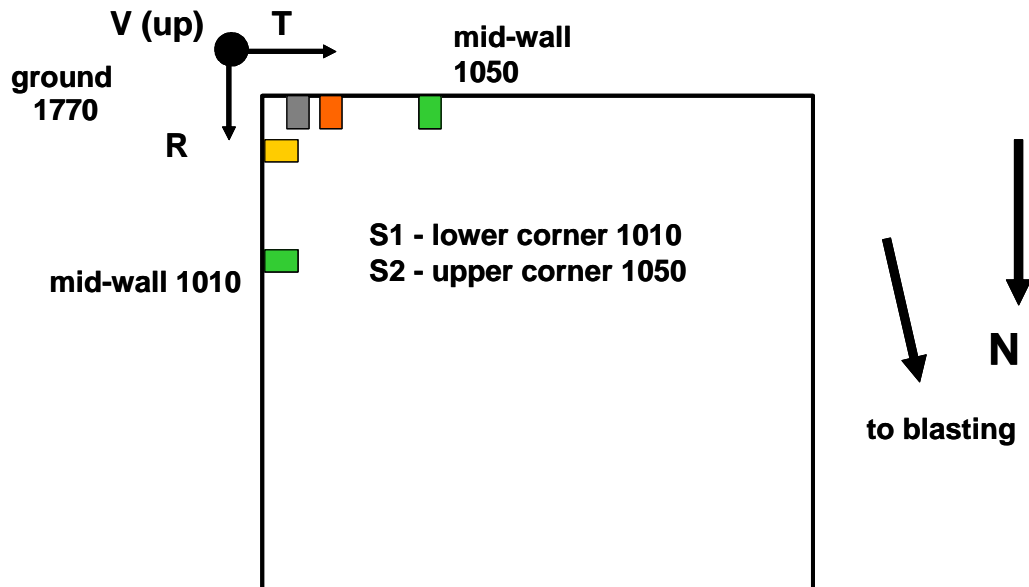
- Radial
- Transverse
- Vertical
- Mid-wall (R or T)

**W3S-WV1**  
3-story, slab floor, wood frame, upper floors cantilevered



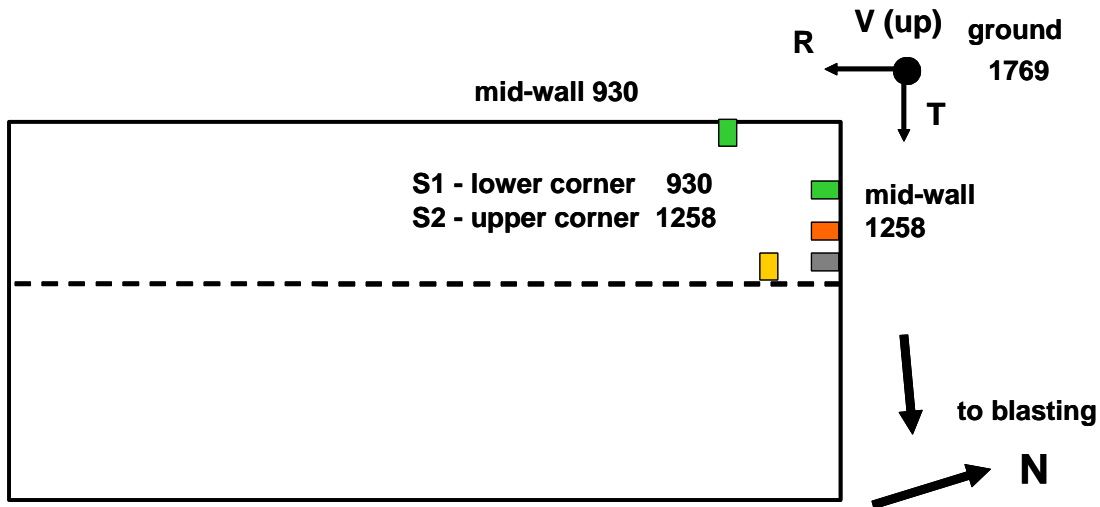
- Radial
- Transverse
- Vertical
- Mid-wall (R or T)

**L1S-WV1**  
one-story log cabin wood post



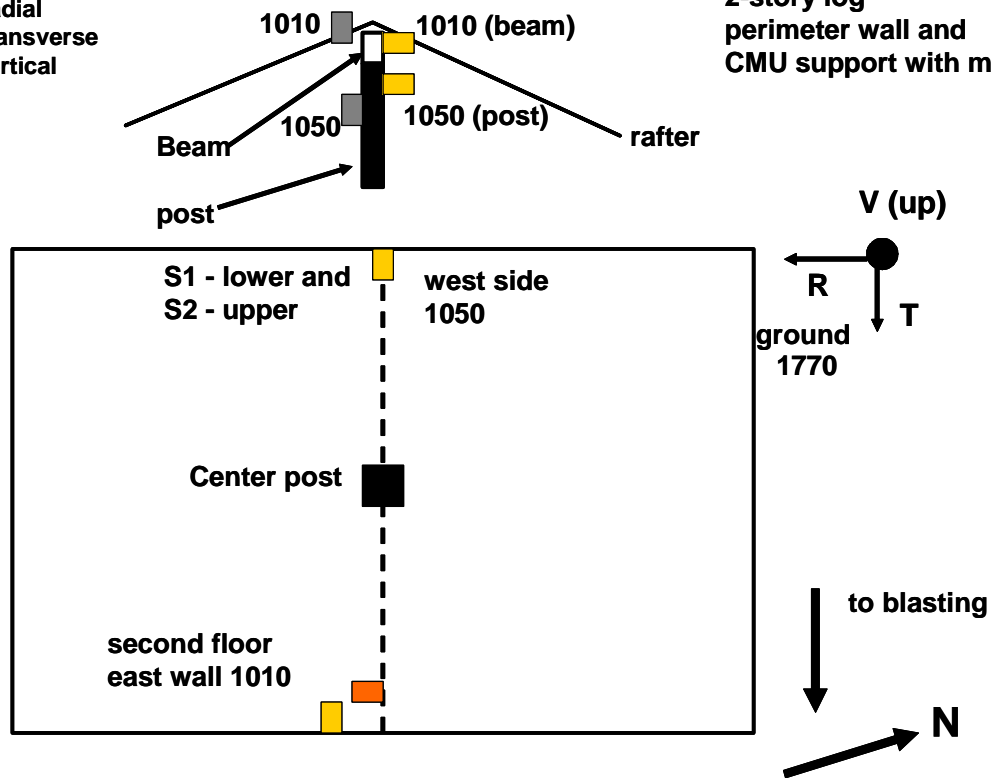
- Radial
- Transverse
- Vertical
- Mid-wall (R or T)

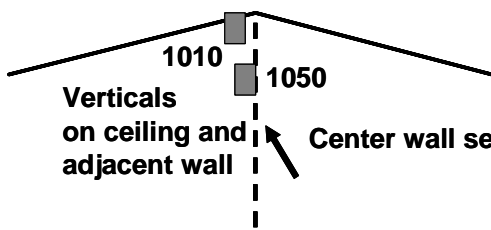
TD-WV2  
double-wide  
CMU support



- Radial
- Transverse
- Vertical

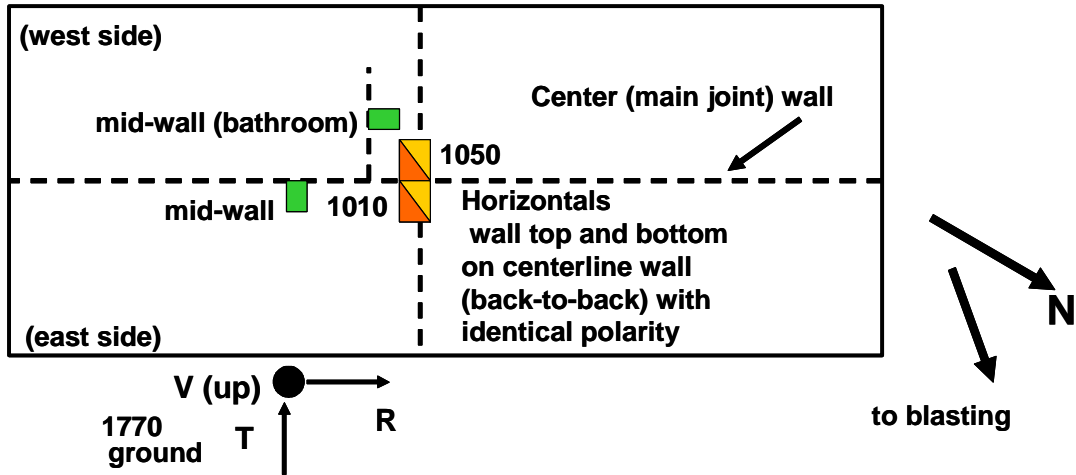
L2S-WV2  
2-story log  
perimeter wall and  
CMU support with mortar





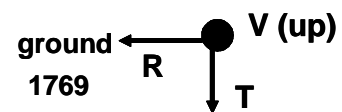
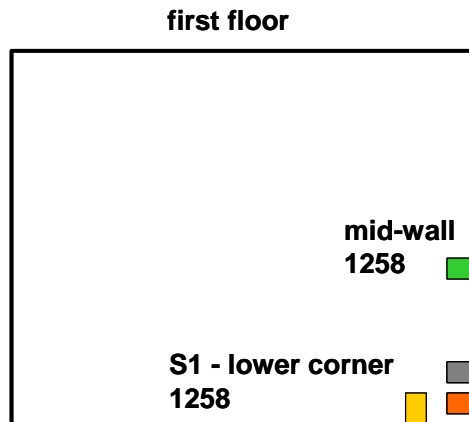
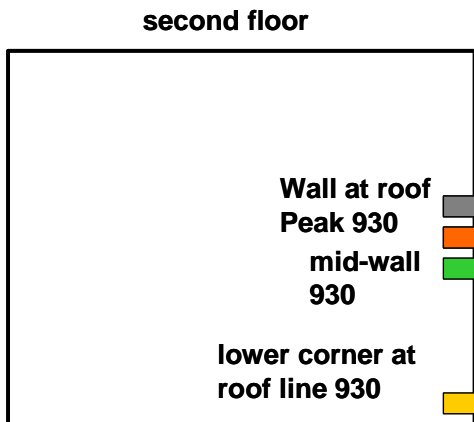
TD-TN  
double-wide  
CMU support  
with strapping

- Radial
- Transverse
- Vertical
- Mid-wall (R or T)



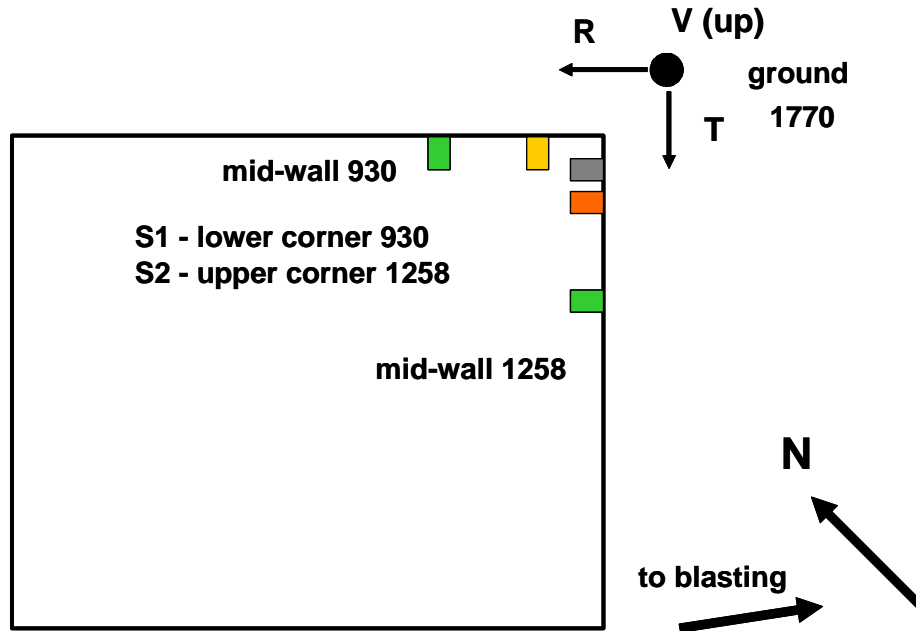
- Radial
- Transverse
- Vertical
- Mid-wall (R)

L2S-TN  
log structure  
CMU support



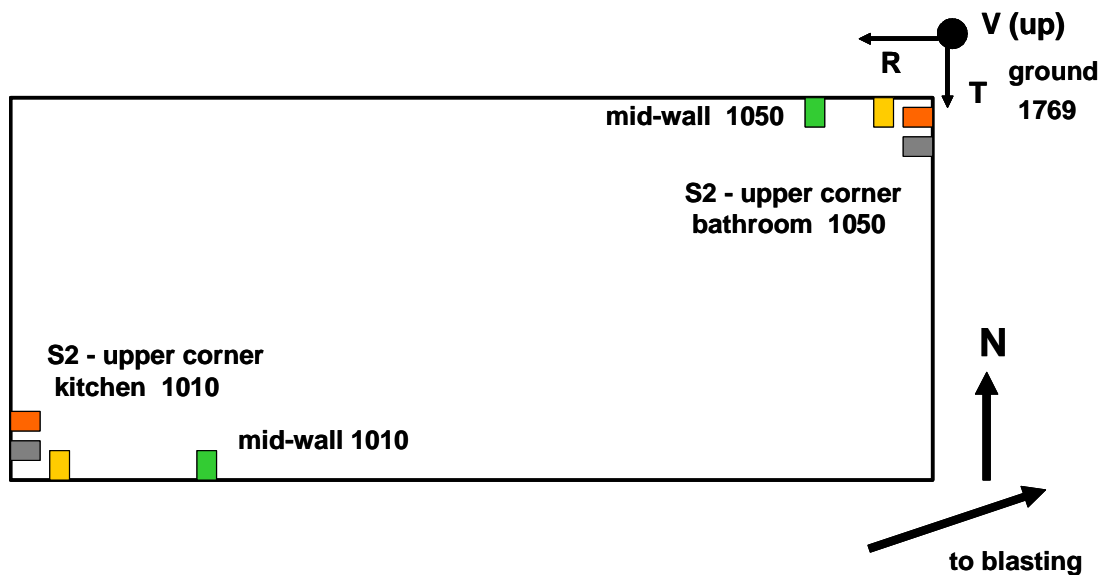
- Radial
- Transverse
- Vertical
- Mid-wall (R or T)

**C1S-AL**  
camp house  
CMU interior and  
exterior; slab add-on



- Radial
- Transverse
- Vertical
- Mid-wall (T)

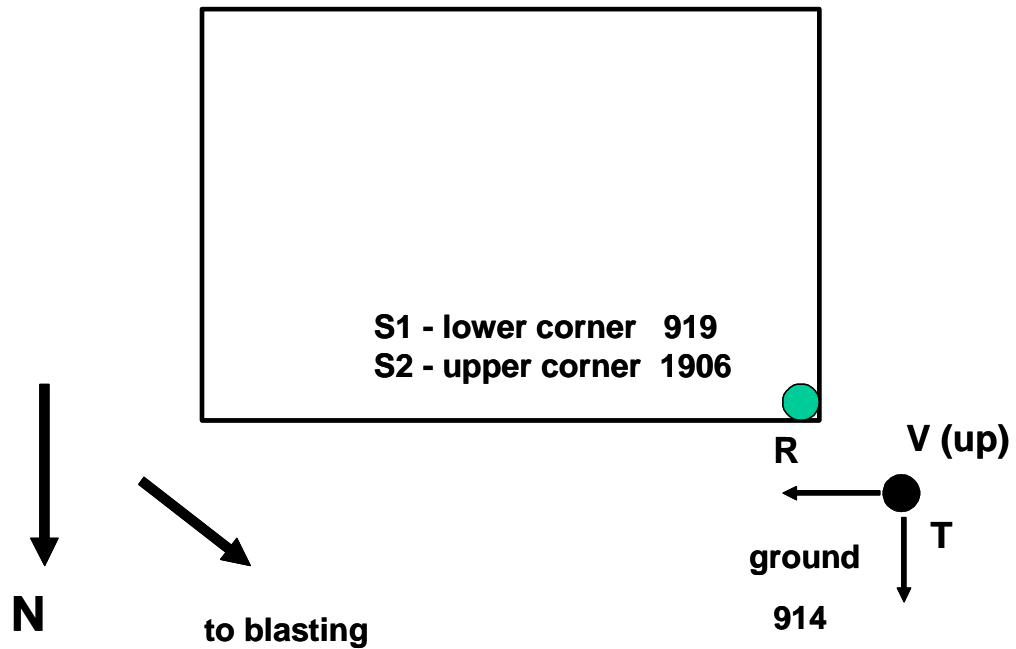
**TS-AL**  
single-wide  
CMU support with  
exterior straps





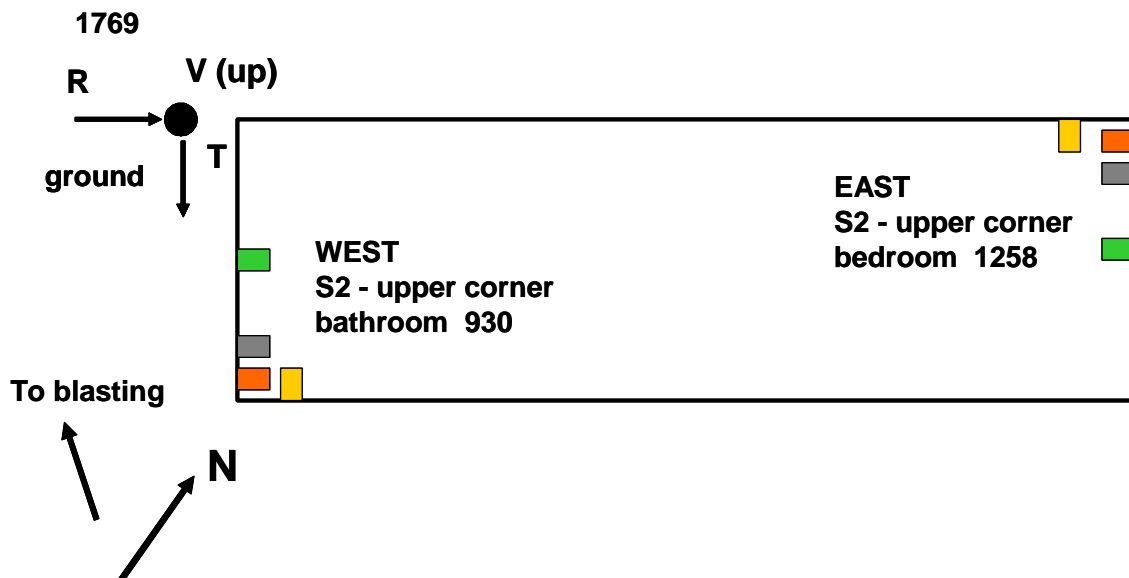
● 3-component transducer

**L1S-OH**  
log structure,  
poured concrete  
basement floor/walls

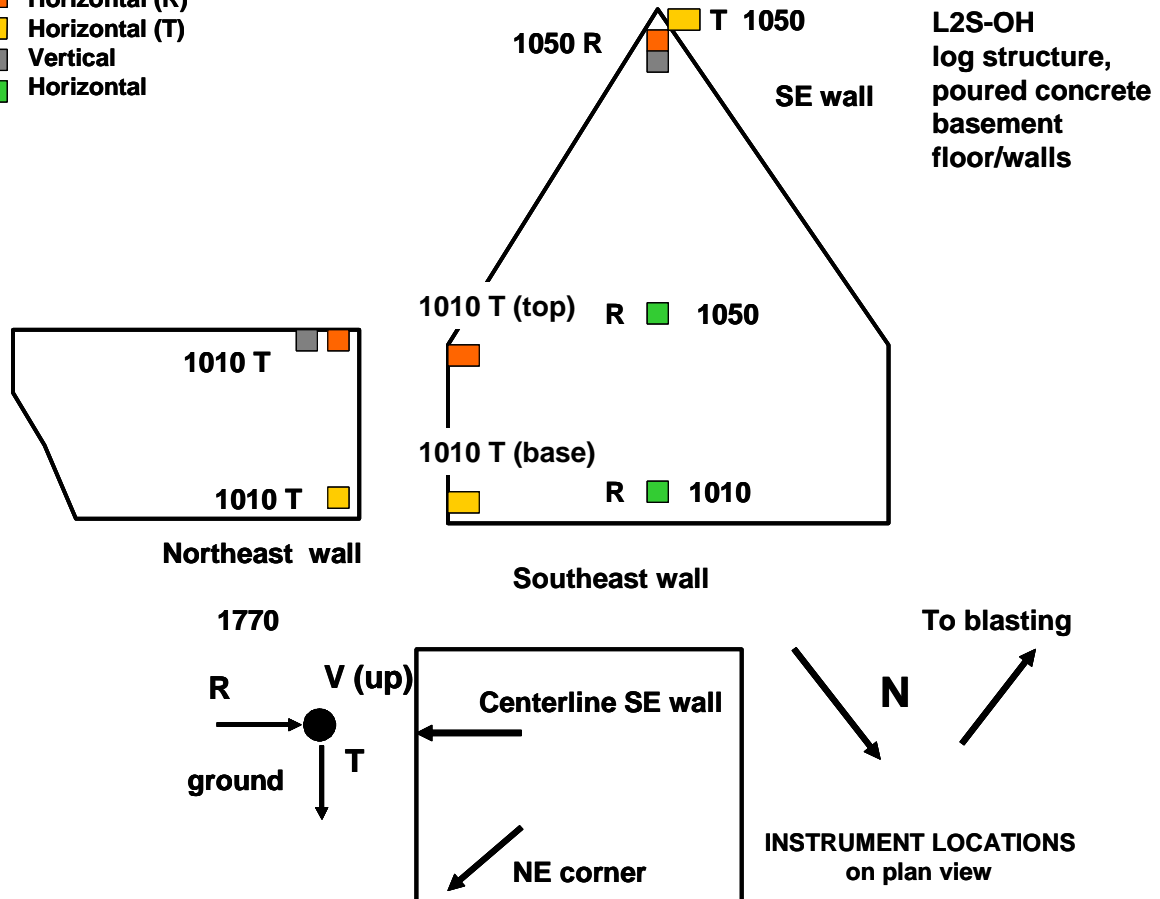


■ Radial  
 ■ Transverse  
 ■ Vertical  
 ■ Mid-wall (R)

**TS-OH**  
single-wide trailer  
CMU piers with  
exterior straps

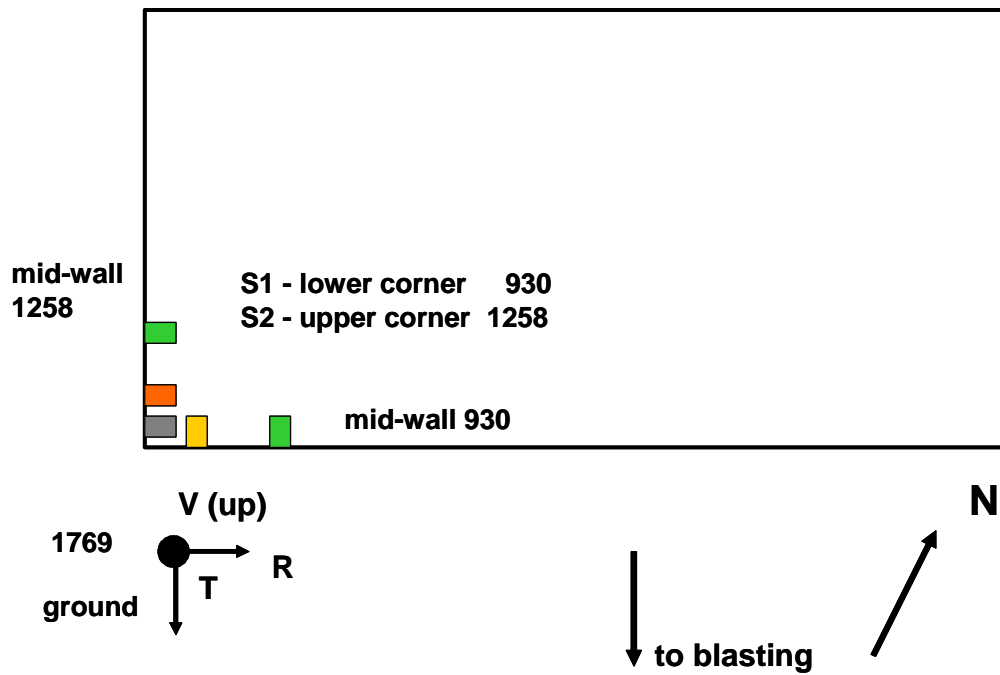


- Horizontal (R)
- Horizontal (T)
- Vertical
- Horizontal



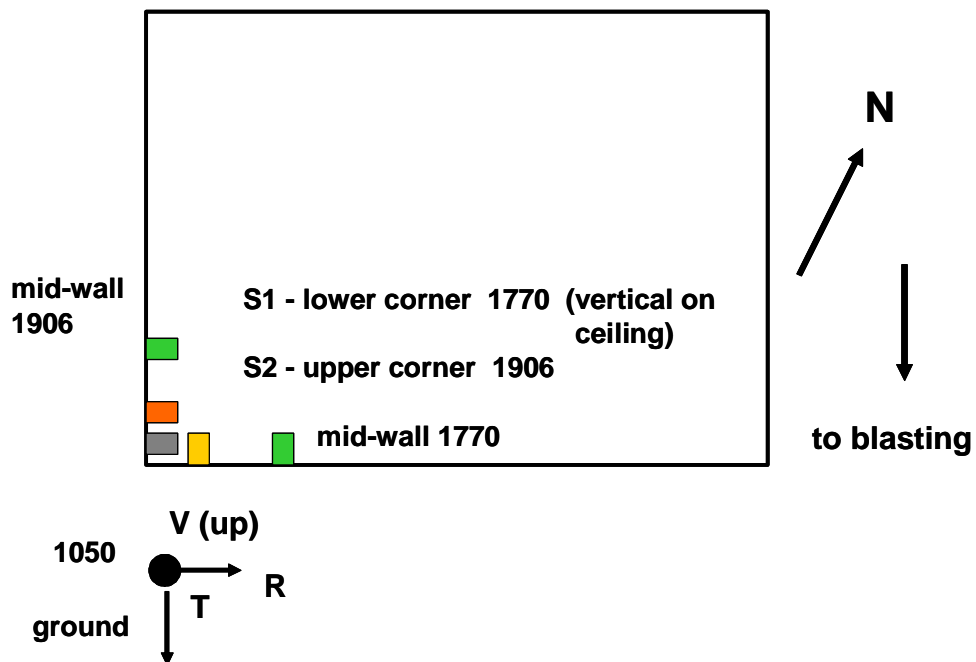
- Radial
- Transverse
- Vertical
- Mid-wall (R or T)

**TD-PA**  
double-wide  
concrete block basement



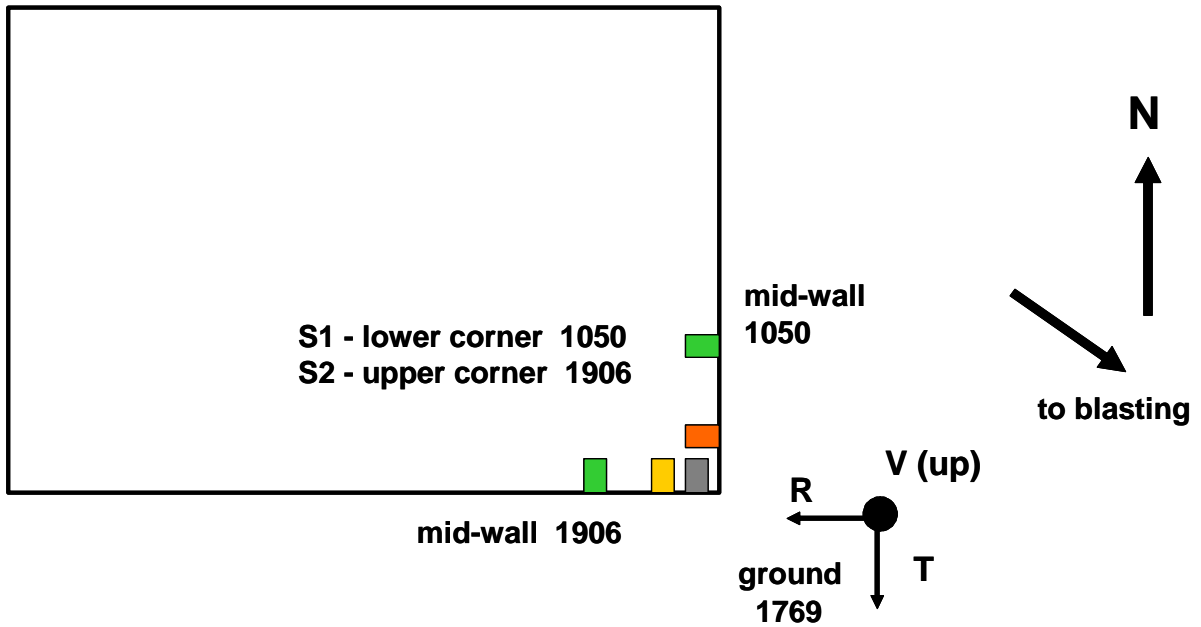
- Radial
- Transverse
- Vertical
- Mid-wall (R or T)

**W1S-PA**  
Wood-frame  
Concrete block basement



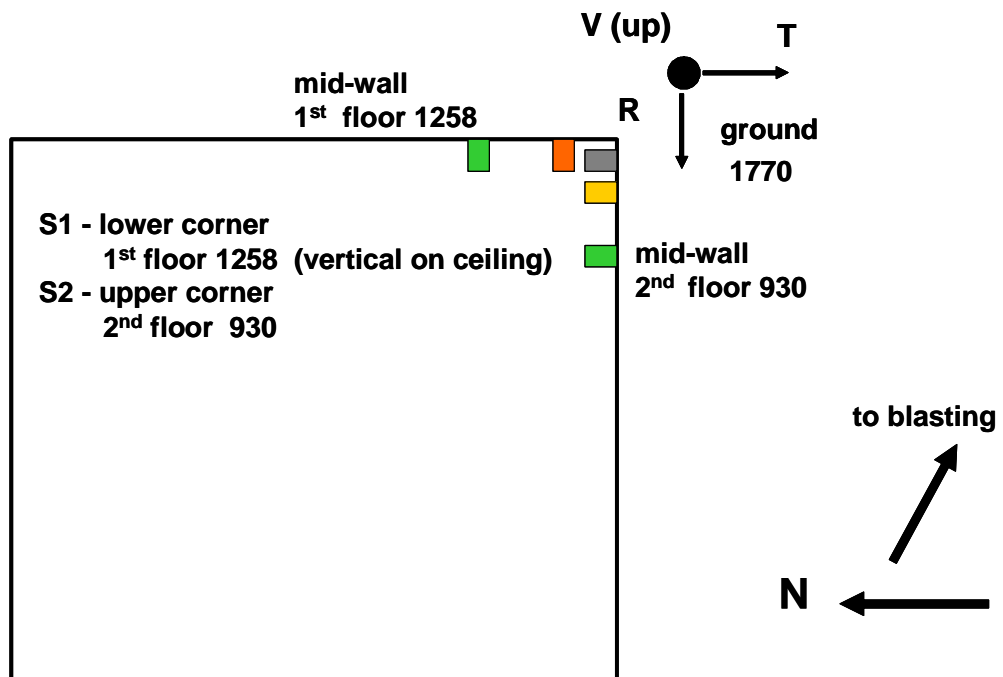
- Radial
- Transverse
- Vertical
- Mid-wall (R or T)

**E1S-NMB**  
Adobe



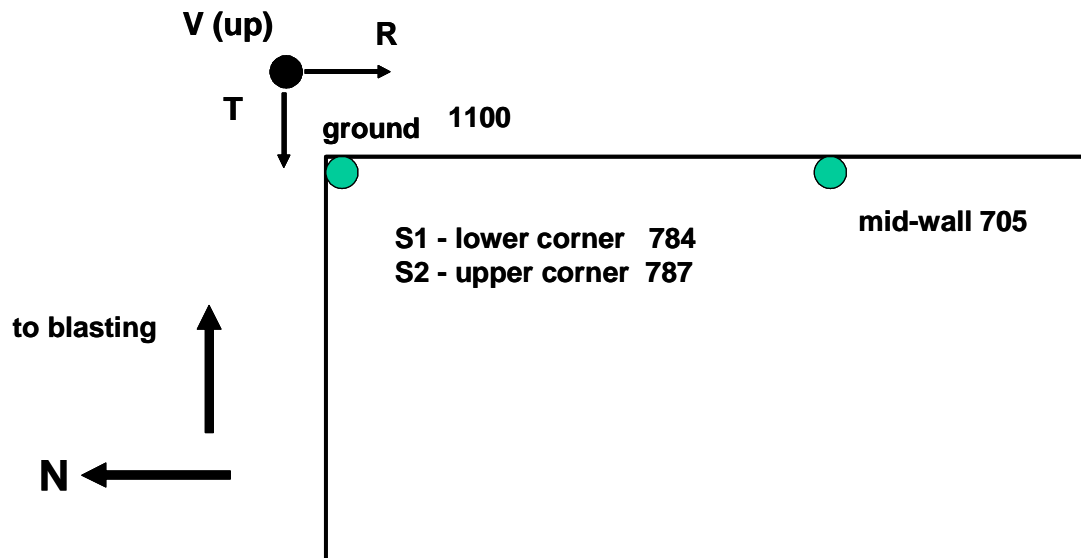
- Radial
- Transverse
- Vertical
- Mid-wall (R or T)

**E2S-NM**  
Two-story stone  
adobe interior  
walls on flagstone  
wall footings



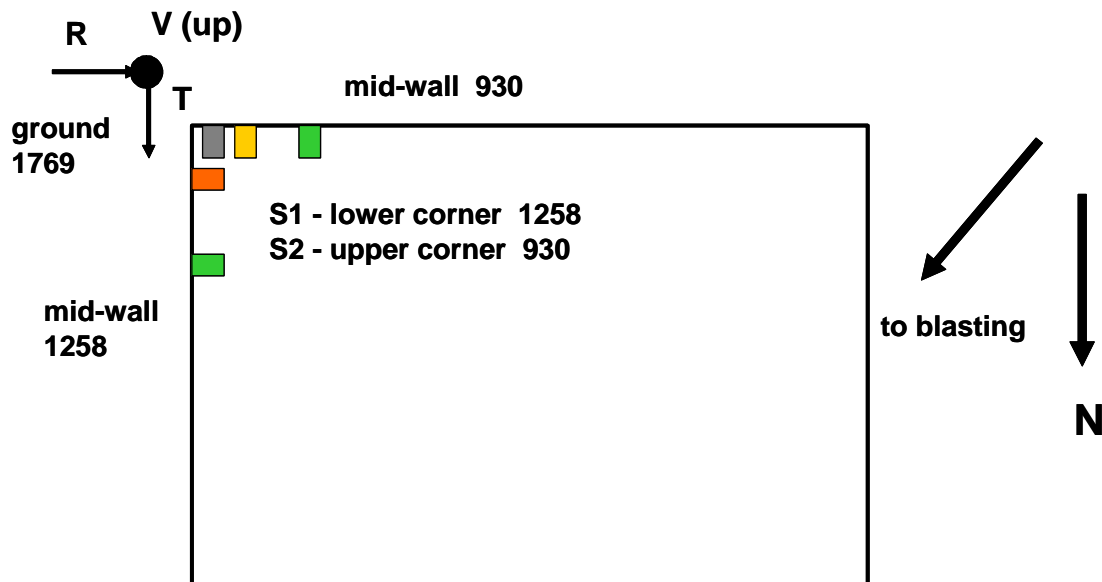
● 3-component transducer

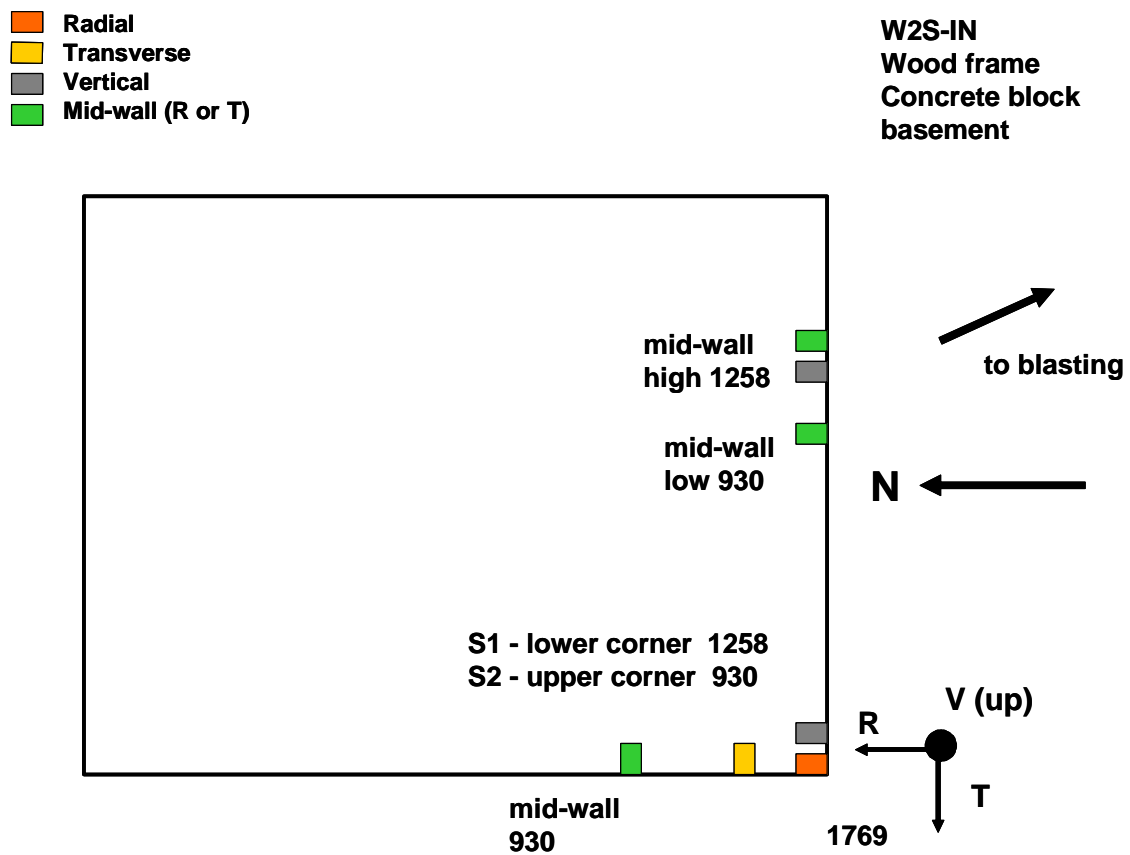
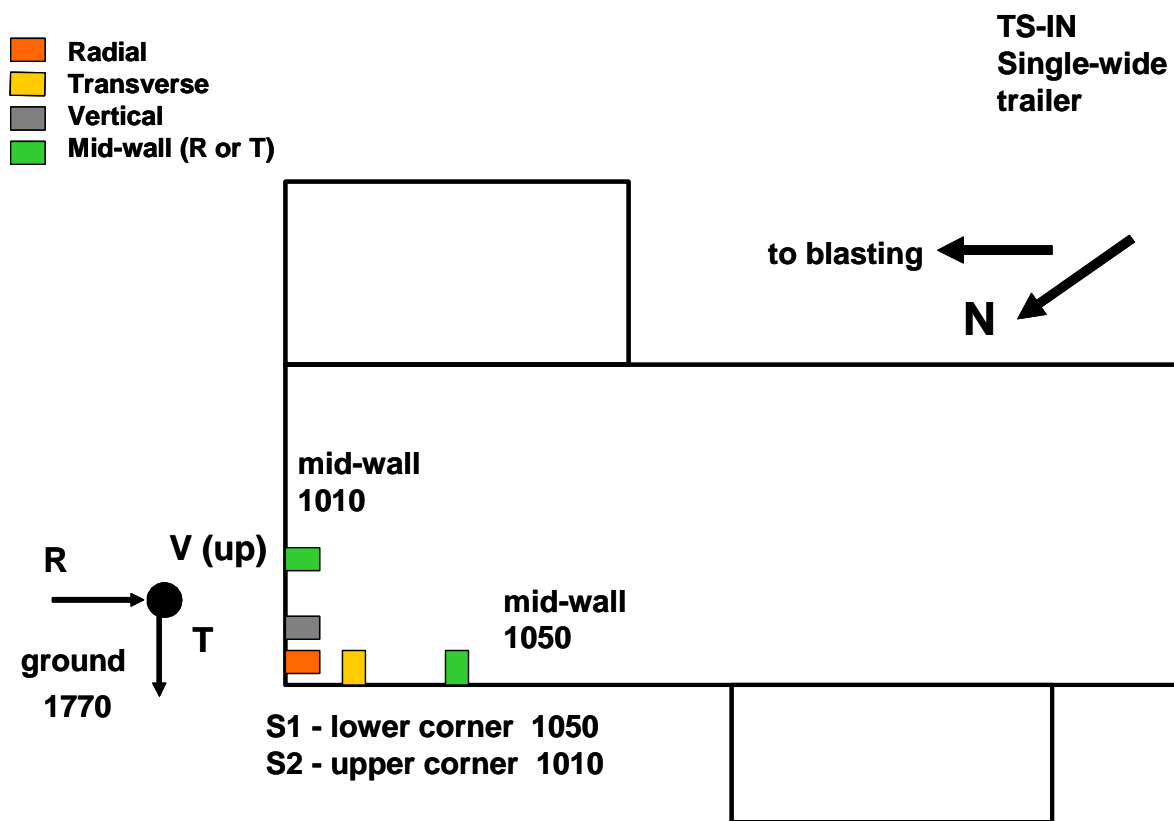
E1S-NMA  
Concrete Block  
on 6 in. slab



Radial  
Transverse  
Vertical  
Mid-wall (R or T)

W1S-IN  
Wood-frame  
Concrete block basement





### APPENDIX III

Blast Data, Ground Vibrations, Airblast, and  
Structure Vibration Response Summaries by Site

Structure	Shot Date and Time	Unit	Structure Location	Placement of Transducer(s)	Distance (ft)	Charge Weight/Delay (lb)	Scaled Distance (ft/lb <sup>1/3</sup> )	Scaled Distance (ft/lb <sup>1/3</sup> )	Peak Particle Velocity (in/sec)	T (in/s)	Peak Frequency (Hz)	FFT Frequency (Hz)	V (in/s)	Peak Frequency (Hz)	FFT Frequency (Hz)	R (in/s)	Peak Frequency (Hz)	FFT Frequency (Hz)	Airblast (dB)
TS-AL	12/19/00	1769	NE corner	ground	1430	550	61.0	174.9	0.12	0.105	26.9	15.5	0.115	32	42.6	0.12	14.6	14.8	122
	14:32	1010	SW top	kitchen top corner						0.305	17.6	13.4	0.18	18.2	13.9	0.115	15.5	15.1	
		1010	S wall	mid-wall						0.16	10	5.6	0.2	14.6	15.2	0.445	18.9	15.8	
		1050	NE top	bathroom top corner												1.68	20.4	21.3	
		1050	N wall	mid-wall												0.72	12.1	7.8	
	12/20/00	1769	NE corner	ground	1445	280	86.4	221.3	0.055	0.055	30.1	10.8	0.045	34.1	11.63	0.05	19.6	14.3	117
	15:29	1010	SW top	kitchen top corner					0.245	0.245	11.9	11.9	0.16	12.8	11.56	0.085	10.8	10.8	
		1010	S wall	mid-wall												0.250	12.1	11.9	
		1050	NE top	bathroom top corner						105	8.1	5.6	0.1	18.9	11.31	0.075	10	10.9	
		1050	N wall	mid-wall												0.45	18.9	5.6	
	12/22/00	1769	NE corner	ground	1480	380	75.9	204.7	0.055	0.055	11.9	9.9	0.055	13.8	15.44	0.035	15.5	16.8	121
	11:00	1010	SW top	kitchen top corner					0.25	0.25	11.3	12.0	0.14	14.6	12	0.1	12.8	8.9	
		1010	S wall	mid-wall												0.315	14.6	11.9	
		1050	NE top	bathroom top corner					0.075	0.075	8.2	5.9	0.1	16.5	15.4	0.075	11.6	8.9	
		1050	N wall	mid-wall												0.78	18.2	18.6	
	12/22/00	1769	NE corner	ground	1520	320	85.0	222.7	0.05	0.05	11.9	8.7	0.045	11.3	8.31	0.05	11.1	8.3	112
	14:50	1010	SW top	kitchen top corner					0.115	0.115	9.1	8.4	0.08	16.5	8.56	0.145	8.3	8.5	
		1010	S wall	mid-wall												0.195	10.2	16.4	
		1050	NE top	bathroom top corner					0.075	0.075	8.3	5.6	0.12	11.9	8.63	0.16	8.2	8.4	
		1050	N wall	mid-wall												0.44	20.4	23.9	
C1S-AL	12/19/00	1770	NE corner	ground	852	550	36.3	104.2	0.385	0.32	14.6	14.4	0.315	30.1	20.44	0.385	25.6	15.2	126
	14:32	930	NE corner base	S1					0.36	0.36	15.5	14.4	0.28	34.1	20.8	0.485	46.5	8.9	
		930	N wall	mid-wall					0.8	0.8	20.4	17.4							
		1258	NE corner top	S2					0.265	0.265	12.4	8.3	0.28	32	20.8	0.305	11.6	9.1	
		1258	E wall	mid-wall												0.98	21.3	14.9	
	12/20/00	1770	NE corner	ground	860	280	51.4	131.7	0.23	0.19	22.2	17.8	0.175	39.3	42.38	0.23	34.1	17.8	120
	15:29	930	NE corner base	S1					0.17	0.17	39.3	14.8	0.14	16.5	11.1	0.17	36.5	17.9	
		930	N wall	mid-wall					0.43	0.43	12.4	10.9							
		1258	NE corner top	S2					0.205	0.205	12.1	10.9	0.14	21.3	10.94	0.215	16	10.7	
		1258	E wall	mid-wall												0.455	13.4	14.4	
	12/22/00	1770	NE corner	ground	890	380	45.7	123.1	0.165	0.14	30.1	14.8	0.16	18.9	15.4	0.165	13.4	16.7	124
	11:00	930	NE corner base	S1					0.145	0.145	36.5	14.9	0.16	32	15.6	0.19	26.9	9.9	
		930	N wall	mid-wall					0.49	0.49	25.6	16.8							
		1258	NE corner top	S2					0.145	0.145	16.5	8.8	0.16	13.4	15.9	0.225	11.3	10.0	
		1258	E wall	mid-wall												0.435	23.2	15.5	
	12/22/00	1770	NE corner	ground	920	320	51.4	134.8	0.135	0.105	11.6	13.8	0.1	14.6	8.44	0.135	10.2	14.1	116
	14:50	930	NE corner base	S1					0.115	0.115	10.6	13.6	0.120	16.5	8.5	0.145	10	8.3	
		930	N wall	mid-wall					0.31	0.31	11.3	8.9							
		1258	NE corner top	S2					0.175	0.175	8.5	9.0	0.12	12.4	8.63	0.27	9.8	9.3	
		1258	E wall	mid-wall												0.325	10.6	14.4	



Structure	Shot Date and Time	Unit	Structure Location	Placement of Transducer(s)	Distance (ft)	Charge Weight/Delay (lb)	Scaled Distance (ft/lb <sup>1/3</sup> )	Scaled Distance (ft/lb <sup>1/3</sup> )	Peak Particle Velocity (in/sec)	T (in/s)	Peak Frequency (Hz)	FFT Frequency (Hz)	V (in/s)	Peak Frequency (Hz)	FFT Frequency (Hz)	R (in/s)	Peak Frequency (Hz)	FFT Frequency (Hz)	Airblast (dB)
Indiana	08/18/01 12:55	1770	E side	ground	1968	781	70.4	214.2	0.2475	0.295	7.5	3.4	0.2025	18.2	3.5	0.2025	6.7	3.6	120
	08/18/01 12:55	1050	N corner	S1(V-ceiling)					0.2475	0.295	4	3.9	0.36	25.6	17	0.275	8.2	3.6	
	08/18/01 12:55	1010	N corner	mid-wall					0.2475	0.295	4	3.9	0.36	25.6	17	0.275	7.1	3.6	
	08/18/01 12:55	1010	N corner	S2					0.2475	0.295	4	3.9	0.36	25.6	17	0.275	7.1	3.6	
	08/18/01 12:55	1010	N corner	mid-wall					0.2475	0.295	4	3.9	0.36	25.6	17	0.275	7.1	3.6	
	08/18/01 12:55	1010	N corner	mid-wall					0.2475	0.295	4	3.9	0.36	25.6	17	0.275	7.1	3.6	
	08/18/01 12:55	1010	N corner	mid-wall					0.2475	0.295	4	3.9	0.36	25.6	17	0.275	7.1	3.6	
	08/18/01 12:55	1010	N corner	mid-wall					0.2475	0.295	4	3.9	0.36	25.6	17	0.275	7.1	3.6	
	08/18/01 12:55	1010	N corner	mid-wall					0.2475	0.295	4	3.9	0.36	25.6	17	0.275	7.1	3.6	
	08/18/01 12:55	1010	N corner	mid-wall					0.2475	0.295	4	3.9	0.36	25.6	17	0.275	7.1	3.6	
Indiana	08/19/01 17:33	1770	E side	ground	1365	451	63.8	177.1	0.275	0.165	11.6	6.7	0.14	25.6	15.6	0.275	16	3.7	123
	08/19/01 17:33	1050	N corner	S1(V-ceiling)					0.275	0.165	11.6	6.7	0.14	25.6	15.6	0.275	16	3.7	
	08/19/01 17:33	1010	N corner	mid-wall					0.275	0.165	11.6	6.7	0.14	25.6	15.6	0.275	16	3.7	
	08/19/01 17:33	1010	N corner	S2					0.275	0.165	11.6	6.7	0.14	25.6	15.6	0.275	16	3.7	
	08/19/01 17:33	1010	N corner	mid-wall					0.275	0.165	11.6	6.7	0.14	25.6	15.6	0.275	16	3.7	
	08/19/01 17:33	1010	N corner	mid-wall					0.275	0.165	11.6	6.7	0.14	25.6	15.6	0.275	16	3.7	
	08/19/01 17:33	1010	N corner	mid-wall					0.275	0.165	11.6	6.7	0.14	25.6	15.6	0.275	16	3.7	
	08/19/01 17:33	1010	N corner	mid-wall					0.275	0.165	11.6	6.7	0.14	25.6	15.6	0.275	16	3.7	
	08/19/01 17:33	1010	N corner	mid-wall					0.275	0.165	11.6	6.7	0.14	25.6	15.6	0.275	16	3.7	
	08/19/01 17:33	1010	N corner	mid-wall					0.275	0.165	11.6	6.7	0.14	25.6	15.6	0.275	16	3.7	
Indiana	08/19/01 13:27	1770	E side	ground	1837	584	76.0	220.2	0.1575	0.23	8	3.1	0.083	15	9	0.1575	12	3.5	118
	08/19/01 13:27	1050	N corner	S1(V-ceiling)					0.1575	0.23	8	3.1	0.083	15	9	0.1575	12	3.5	
	08/19/01 13:27	1010	N corner	mid-wall					0.1575	0.23	8	3.1	0.083	15	9	0.1575	12	3.5	
	08/19/01 13:27	1010	N corner	S2					0.1575	0.23	8	3.1	0.083	15	9	0.1575	12	3.5	
	08/19/01 13:27	1010	N corner	mid-wall					0.1575	0.23	8	3.1	0.083	15	9	0.1575	12	3.5	
	08/19/01 13:27	1010	N corner	mid-wall					0.1575	0.23	8	3.1	0.083	15	9	0.1575	12	3.5	
	08/19/01 13:27	1010	N corner	mid-wall					0.1575	0.23	8	3.1	0.083	15	9	0.1575	12	3.5	
	08/19/01 13:27	1010	N corner	mid-wall					0.1575	0.23	8	3.1	0.083	15	9	0.1575	12	3.5	
	08/19/01 13:27	1010	N corner	mid-wall					0.1575	0.23	8	3.1	0.083	15	9	0.1575	12	3.5	
	08/19/01 13:27	1010	N corner	mid-wall					0.1575	0.23	8	3.1	0.083	15	9	0.1575	12	3.5	
Indiana	08/19/01 16:23	1770	E side	ground	3379	451	159.1	441.5	0.0525	0.06	12.8	13.2	0.05	21.3	21.3	0.0525	12.8	4.6	114
	08/19/01 16:23	1050	N corner	S1(V-ceiling)					0.0525	0.06	15	8.8	0.09	11.1	13.44	0.075	11.1	4.6	
	08/19/01 16:23	1010	N corner	mid-wall					0.0525	0.06	15	8.8	0.09	11.1	13.44	0.075	11.1	4.6	
	08/19/01 16:23	1010	N corner	S2					0.0525	0.06	15	8.8	0.09	11.1	13.44	0.075	11.1	4.6	
	08/19/01 16:23	1010	N corner	mid-wall					0.0525	0.06	15	8.8	0.09	11.1	13.44	0.075	11.1	4.6	
	08/19/01 16:23	1010	N corner	mid-wall					0.0525	0.06	15	8.8	0.09	11.1	13.44	0.075	11.1	4.6	
	08/19/01 16:23	1010	N corner	mid-wall					0.0525	0.06	15	8.8	0.09	11.1	13.44	0.075	11.1	4.6	
	08/19/01 16:23	1010	N corner	mid-wall					0.0525	0.06	15	8.8	0.09	11.1	13.44	0.075	11.1	4.6	
	08/19/01 16:23	1010	N corner	mid-wall					0.0525	0.06	15	8.8	0.09	11.1	13.44	0.075	11.1	4.6	
	08/19/01 16:23	1010	N corner	mid-wall					0.0525	0.06	15	8.8	0.09	11.1	13.44	0.075	11.1	4.6	
Indiana	08/19/01 17:27	1770	E side	ground	9025	1712	218.1	756.3	0.0375	0.04	7.5	4.3	0.025	18.2	14	0.035	4.5	4.3	110
	08/19/01 17:27	1050	N corner	S1(V-ceiling)					0.0375	0.04	7.5	4.3	0.025	18.2	14	0.035	4.5	4.3	
	08/19/01 17:27	1010	N corner	mid-wall					0.0375	0.04	7.5	4.3	0.025	18.2	14	0.035	4.5	4.3	
	08/19/01 17:27	1010	N corner	S2					0.0375	0.04	7.5	4.3	0.025	18.2	14	0.035	4.5	4.3	
	08/19/01 17:27	1010	N corner	mid-wall					0.0375	0.04	7.5	4.3	0.025	18.2	14	0.035	4.5	4.3	
	08/19/01 17:27	1010	N corner	mid-wall					0.0375	0.04	7.5	4.3	0.025	18.2	14	0.035	4.5	4.3	
	08/19/01 17:27	1010	N corner	mid-wall					0.0375	0.04	7.5	4.3	0.025	18.2	14	0.035	4.5	4.3	
	08/19/01 17:27	1010	N corner	mid-wall					0.0375	0.04	7.5	4.3	0.025	18.2	14	0.035	4.5	4.3	
	08/19/01 17:27	1010	N corner	mid-wall					0.0375	0.04	7.5	4.3	0.025	18.2	14	0.035	4.5	4.3	
	08/19/01 17:27	1010	N corner	mid-wall					0.0375	0.04	7.5	4.3	0.025	18.2	14	0.035	4.5	4.3	
Indiana	08/20/01 9:30	1770	E side	ground	unknown	unknown			0.0225	0.045	3.2	4.2	0.01	41	3.2	0.02	4.1	2.9	<100
	08/20/01 9:30	1050	N corner	S1(V-ceiling)					0.0225	0.045	3.2	4.2	0.01	41	3.2	0.02	4.1	2.9	
	08/20/01 9:30	1010	N corner	mid-wall					0.0225	0.045	3.2	4.2	0.01	41	3.2	0.02	4.1	2.9	
	08/20/01 9:30	1010	N corner	S2					0.0225	0.045	3.2	4.2	0.01	41	3.2	0.02	4.1	2.9	
	08/20/01 9:30	1010	N corner	mid-wall					0.0225	0.045	3.2	4.2	0.01	41	3.2	0.02	4.1	2.9	
	08/20/01 9:30	1010	N corner	mid-wall					0.0225	0.045	3.2	4.2	0.01	41	3.2	0.02	4.1	2.9	
	08/20/01 9:30	1010	N corner	mid-wall					0.0225	0.045	3.2	4.2	0.01	41	3.2	0.02	4.1	2.9	
	08/20/01 9:30	1010	N corner	mid-wall					0.0225	0.045	3.2	4.2	0.01	41	3.2	0.02	4.1	2.9	
	08/20/01 9:30	1010	N corner	mid-wall					0.0225	0.045	3.2	4.2	0.01	41	3.2	0.02	4.1	2.9	
	08/20/01 9:30	1010	N corner	mid-wall					0.0225	0.045	3.2	4.2	0.01	41	3.2	0.02	4.1	2.9	
Indiana	08/20/01 16:05	1770	E side	ground	844	150	68.9	159.1	0.265	0.165	10.2	10.5	0.246	36.5	32.9	0.265	17	17.6	119
	08/20/01 16:05	1050	N corner	S1					0.265	0.165	10.2	10.5	0.246	36.5	32.9	0.265	17	17.6	
	08/20/01 16:05	1010	N corner	mid-wall					0.265	0.165	10.2	10.5	0.246	36.5	32.9	0.265	17	17.6	
	08/20/01 16:05	1010	N corner	S2					0.265	0.165	10.2	10.5	0.246	36.5	32.9	0.2			

Indiana (cont.)																			
W1S-IN	08/18/01 17:33	1769 1258 1258 930	SE corner SE corner E wall SE corner	ground S2 lower corner S2 mid-wall	1439	451	67.8	188.0	0.2325	0.2325	28.4	3.7	0.16	36.5	6.63	0.18	28.4	3.8	117
	08/19/01 13:27	1769 1258 1258 930	SE corner SE corner E wall SE corner	ground S2 lower corner mid-wall S2	1906	584	78.9	228.5	0.1825	0.1825	16	10.4	0.09	32	10.2	0.1325	6.9	3.1	112
	08/19/01 16:43	1769 1258 1258 930	SE corner SE corner E wall SE corner	ground S2 lower corner mid-wall S2	3438	451	161.9	449.2	0.0575	0.0575	25.6	4.3	0.0325	25.6	13.9	0.0575	14.2	8	
	08/19/01 17:27	1769 1258 1258 930	SE corner SE corner E wall SE corner	ground S2 lower corner mid-wall S2	9219	1712	222.8	772.6	0.0375	0.0375	3.3	2.5	0.015	8.5	2.31	0.02	15	4.1	110
	08/20/01 9:30	1769 1258 1258 930	SE corner SE corner E wall SE corner	ground S2 lower corner mid-wall S2	unknown	unknown			0.0225	0.0225	4.4	3.1	0.01	5.2	5.7	0.0075	5.2	2.9	<100
	08/20/01 12:41	1769 1258 1258 930	SE corner SE corner E wall SE corner	ground S2 lower corner mid-wall S2	unknown	unknown			0.025	0.025	5	4.9	0.01	6	5.2	0.0075	5.3	4.8	100
	08/20/01 distant mine	1769 1258 1258 930	SE corner SE corner E wall SE corner	ground S2 lower corner mid-wall S2	unknown	unknown			0.025	0.025	5	4.9	0.01	6	5.2	0.0075	5.3	4.8	100
	08/20/01 12:33	1769 1258 1258 930	SE corner SE corner E wall SE corner	ground S2 lower corner mid-wall S2	3540	451	166.7	462.6	0.0675	0.0675	25.6	19.0	0.035	15	13.8	0.05	13.4	23.5	116
	08/20/01 16:02	1769 1258 1258 930	SE corner SE corner E wall SE corner	ground S2 lower corner mid-wall S2	1035	150	84.5	195.1	0.21	0.21	25.6	11.4	0.12	16	7.8	0.21	19.6	10.7	118
	08/21/01 9:48	1769 1258 1258 930	SE corner SE corner E wall SE corner	ground S2 lower corner mid-wall S2	1122	240	72.4	180.9	0.19	0.19	13.4	10.9	0.125	42.6	10.1	0.175	21.3	11.3	121
W2S-IN	08/21/01 17:33	1769 1258 1258 930	SW corner SW corner E wall SW corner	ground S1(V-crack) mid-wall S2	2209	1051	68.1	217.8	0.1625	0.1625	23.2	3.4	0.105	6.2	9.8	0.1425	12.1	3.8	117
	08/23/01 13:00	1769 1258 1258 930	SW corner SW corner E wall SW corner	ground S1(V-crack) mid-wall S2	3730	301	215.0	557.6	0.07	0.07	14.2	12.4	0.0425	32	28	0.07	21.3	15.4	110
	08/23/01 17:30	1769 1258 1258 930	SW corner SW corner E wall SW corner	ground S1(V-crack) mid-wall S2	4163	447	196.9	545.6	0.0725	0.0725	15	15.0	0.045	28.4	25.8	0.0725	15	15.3	106
	08/24/01 12:10	1769 1258 1258 930	SW corner SW corner E wall SW corner	ground S1(V-crack) mid-wall S2	3358	300.5	193.7	502.3	0.0625	0.0625	23.2	5.1	0.045	36.5	29.2	0.0625	18.2	12.9	114
	08/24/01 12:10	1769 1258 1258 930	SW corner SW corner E wall SW corner	ground S1(V-crack) mid-wall S2	3358	300.5	193.7	502.3	0.0625	0.0625	23.2	5.1	0.045	36.5	29.2	0.0625	18.2	12.9	114
	08/24/01 12:10	1769 1258 1258 930	SW corner SW corner E wall SW corner	ground S1(V-crack) mid-wall S2	3358	300.5	193.7	502.3	0.0625	0.0625	23.2	5.1	0.045	36.5	29.2	0.0625	18.2	12.9	114
	08/24/01 12:10	1769 1258 1258 930	SW corner SW corner E wall SW corner	ground S1(V-crack) mid-wall S2	3358	300.5	193.7	502.3	0.0625	0.0625	23.2	5.1	0.045	36.5	29.2	0.0625	18.2	12.9	114
	08/24/01 12:10	1769 1258 1258 930	SW corner SW corner E wall SW corner	ground S1(V-crack) mid-wall S2	3358	300.5	193.7	502.3	0.0625	0.0625	23.2	5.1	0.045	36.5	29.2	0.0625	18.2	12.9	114
	08/24/01 12:10	1769 1258 1258 930	SW corner SW corner E wall SW corner	ground S1(V-crack) mid-wall S2	3358	300.5	193.7	502.3	0.0625	0.0625	23.2	5.1	0.045	36.5	29.2	0.0625	18.2	12.9	114
	08/24/01 12:10	1769 1258 1258 930	SW corner SW corner E wall SW corner	ground S1(V-crack) mid-wall S2	3358	300.5	193.7	502.3	0.0625	0.0625	23.2	5.1	0.045	36.5	29.2	0.0625	18.2	12.9	114

W1S-IN

W2S-IN

Kentucky Site 1																				
Structure	Shot Date and Time	Unit	Structure Location	Placement of Transducer(s)	Distance (ft)	Charge Weight/Delay (lb)	Scaled Distance (ft/lb <sup>1/3</sup> )	Scaled Distance (ft/lb <sup>1/2</sup> )	Peak Particle Velocity (in/sec)	T (in/s)	Peak Frequency (Hz)	FFT Frequency (Hz)	V (in/s)	Peak Frequency (Hz)	FFT Frequency (Hz)	R (in/s)	Peak Frequency (Hz)	FFT Frequency (Hz)	Airblast (dB)	
C2S-KY1A	11/13/2000 16:04	1770	NE corner	ground	4800	684	183.5	546.0	0.030	0.020	23.2	21.3	0.015	28.4	21.4	0.030	22.2	18.9	106	
		1010	NE corner	S1						0.015	17.6	3.8	0.040		19.2		0.020	17.6	29.3	
		1010	E wall	mid-wall						0.035	16.5	19.6								
		1050	NE corner	S2						0.015	6.4	3.8	0.020		21.6		0.015	20.4	6.5	
		1050	N wall	mid-wall						0.015							0.045	21.3	19.0	
	11/14/2000	1770	NE corner	ground																
		1770	NE corner	ground																
	11/15/2000 11:48	1770	NE corner	ground	2020	828	70.2	215.6	0.025	0.020	19.6	19.6	3.0	0.020	20.40	2.5	0.025	18.20	12.9	112
		1010	NE corner	S1						0.025	13.4	13.4	3.0	0.040		29.2	0.025	12.80	4.3	
		1010	E wall	mid-wall						0.075	10.2	10.2	10.9							
		1050	NE corner	S2						0.030	8.5	8.5	3.9	0.040		9.8	0.045	5.50	4.4	
		1050	N wall	mid-wall													0.055	8.3	4.4	
	11/16/2000 9:07	1770	NE corner	ground				NOT	TRIGGERED											
		1770	NE corner	ground																
	11/16/2000 16:00	1770	NE corner	ground	2240	414	110.1	301.2	0.025	0.015	24.3	14.8	0.015	0.015	25.6	2.9	0.025	22.2	2.4	110
		1010	NE corner	S1						0.025	15.0	15.0	3.6	0.040		3.6	0.015	18.2	4.4	
		1010	E wall	mid-wall						0.060	14.6	14.6	3.7							
		1050	NE corner	S2						0.025	4.5	4.5	3.7	0.020		14.8	0.025	4.9	4.5	
		1050	N wall	mid-wall													0.040	6.6	4.5	
11/17/2000 signature holes	1770	NE corner	ground				NOT	TRIGGERED												
	12:15																			
	11/17/2000 12:34	1770	NE corner	ground	2020	1044	62.5	132.0	0.045	0.045	23.2	1.8	0.045	22.2	2.9	0.040	19.6	2.0	121	
		1010	NE corner	S1			NOT	TRIGGERED												
		1010	E wall	mid-wall			NOT	TRIGGERED												
		1050	NE corner	S2			NOT	TRIGGERED												
		1050	N wall	mid-wall			NOT	TRIGGERED												
C2S-KY1B																				
	11/13/2000 16:20	1769	SE corner	ground			NOT	TRIGGERED												
		804	SE corner	ground	5000	936	163.4	512.3	0.025	0.025	13.4	6.8	0.015			0.020	8.3	6.5	106	
		1258	SE corner	S1					0.025	0.025	13.1	9.6	0.020			0.020	17	6.4		
		1258	E wall	mid-wall												0.070	13.8	9.4		
		930	SE corner	S2						0.060	9.1	6.0	0.020			0.075	7.3	6.8		
		930	E wall	mid-wall												0.070	8.1	6.8		
	11/15/2000 11:50	1769	SE corner	ground	2020	828	70.2	215.6	0.055	0.025	7.0	6.4	0.025	11.9	2.5	0.055	20.4	6.3	112	
		1258	SE corner	S1					0.030	0.030	14.6	7.8	0.040			0.050	6	6.3		
		1258	E wall	mid-wall						0.090		6.3	0.040			0.170	8.8	6.3		
		930	SE corner	S2							7.0	6.3	0.040		13.3	0.140	7.1	6.3		
		930	E wall	mid-wall												0.125	7.5	6.3		
	11/16/2000 9:07	1769	SE corner	ground	5140	1026	160.5	510.8	0.020	0.010		10.5	0.005			0.020	15	6.5	106	
		1258	SE corner	S1					0.015	0.015	11.6	9.6	0.020		13.0	0.015	13.8	6.5		
		1258	E wall	mid-wall												0.060	13.4	11.0		
		930	SE corner	S2						0.050	8.3	6.1	0.020		13.1	0.050	8	6.8		
		930	E wall	mid-wall												0.050	7.3	6.8		
	11/16/2000 16:00	1769	SE corner	ground	2240	414	110.1	301.2	0.025	0.020	11.9	7.4	0.015		13.1	10.1	0.025	11.9	7.1	110
		1258	SE corner	S1					0.020	0.020	5.0	7.4	0.020			0.025	7.5	7.0		
	1258	E wall	mid-wall												0.080	10.4	10.9			
	930	SE corner	S2						0.045	8.5	7.2	0.020			14.3	0.060	8	7.5		
	930	E wall	mid-wall													0.050	12.4	7.5		
11/17/2000 signature holes	1769	SE corner	ground	1830	936	59.8	187.5	0.020	0.015	11.3	9.8	0.015	16.5	11.0	0.020	14.6	5.8	110		
	1258	SE corner	S1				NOT	TRIGGERED												
	1258	E wall	mid-wall				NOT	TRIGGERED												
	930	SE corner	S2				NOT	TRIGGERED												
	930	E wall	mid-wall				NOT	TRIGGERED												
11/17/2000 12:34	1769	SE corner	ground	2020	1044	62.5	199.6	0.065	0.035	11.6	6.2	0.025		11.3	2.4	0.065	9.1	6.3	120	
	1258	SE corner	S1						0.035	10.8	6.3	0.040				0.060	5.6	6.3		
	1258	E wall	mid-wall													0.130	7.5	6.4		
	930	SE corner	S2						0.090	6.6	6.3	0.040			6.4	0.230	6.5	6.4		
	930	E wall	mid-wall													0.205	6.3	6.4		

## Kentucky Site 2

Structure	Shot Date and Time	Unit	Structure Location	Placement of Transducer(s)	Distance (ft)	Charge Weight/Delay	Scaled Distance (ft/lb <sup>1/3</sup> )	Scaled Distance (ft/lb <sup>1/3</sup> )	Peak Particle Velocity (in/sec)	T (ms)	Peak Frequency (Hz)	FFT Frequency (Hz)	V (in/s)	Peak Frequency (Hz)	FFT Frequency (Hz)	R (in/s)	Peak Frequency (Hz)	FFT Frequency (Hz)	Airblast (dB)
TS-KY2	11/20/2000 9:20a	1770 NW corner	NE corner	ground	2370	183	190.2	453.9	0.025	0.010	21.3	15.4	0.010	21.3	15.4	0.025	30.1	15.38	106
	1050 NE corner	S1							0.025	0.020	21.3	15.4	0.020	21.3	15.4	0.025	24.3	15.3	
	1050 N wall	mid-wall								0.020	25.6	18.1	0.020	25.6	18.1	0.025	16.3	14	
	1010 NE corner	S2								0.045	28.4	31	0.045	28.4	31	0.045	24.4	14	
	11/20/2000 16:09p	1770 NW corner	NE corner	ground	1510	495	67.9	191.3	0.090	0.080	17.6	4.8	0.055	18.2	4.88	0.060	9.1	3.38	118
	1050 NE corner	S1							0.085	0.085	7.3	7	0.080	8.2	7.9	0.140	19.6	26.8	
	1050 N wall	mid-wall							0.145	0.145	7.2	7	0.100	7.6	7.9	0.085	8	7	
	1010 NE corner	S2							0.155	0.155	6	7	0.100	7.6	7.9	0.085	8	7	
	1010 W wall	mid-wall							0.040	0.040	25.6	23.3	0.035	16	18	0.055	18.2	4.31	118
	11/21/2000 14:40	1770 NW corner	NE corner	ground	1670	274	100.9	257.6	0.055	0.055	8.2	7.44	0.060	27	7.63	0.040	12.8	3.94	
	1050 NE corner	S1							0.120	0.120	7.8	7.7	0.080	13.8	8.7	0.055	12.8	18.13	
	1010 NE corner	S2							0.135	0.135	7.8	7.7	0.080	13.8	8.7	0.055	12.8	18.13	
	1010 W wall	mid-wall							0.035	0.035	28.90	5.50	0.030	13.40	6.75	0.035	16.00	8.00	117
	11/21/2000 15:35	1770 NW corner	NE corner	ground	1810	211	124.6	304.6	0.035	0.035	7.8	7.7	0.030	13.40	6.75	0.035	16.00	8.00	117
	1050 NE corner	S1							0.030	0.030	26.90	5.50	0.030	13.40	6.75	0.035	16.00	8.00	117
	1010 NE corner	S2							0.070	0.070	12.10	7.44	0.040	13.40	6.75	0.035	16.00	8.00	117
	1010 W wall	mid-wall							0.050	0.050	12.10	7.44	0.040	13.40	6.75	0.035	16.00	8.00	117
	11/21/2000 16:43	1770 NW corner	NE corner	ground	3710	807	130.6	399.4	0.035	0.035	14.3	2.6	0.030	14.2	2.6	0.035	20.4	2.88	110
	1050 NE corner	S1							0.020	0.020	15	2.6	0.020	14.2	2.6	0.020	20.4	2.88	110
1050 N wall	mid-wall							0.025	0.025	13.1	2.6	0.040	22.2	2.6	0.055	18.9	17.7		
1010 NE corner	S2							0.035	0.035	20.4	2.56	0.040	22.2	2.56	0.040	25.6	15	112	
11/21/2000 16:46	1770 NW corner	NE corner	ground	2520	209	174.3	425.4	0.040	0.040	21.3	21.4	0.025	22.2	4.13	0.040	25.6	15	112	
1050 NE corner	S1							0.030	0.030	25.6	14.8	0.020	24.3	15.1	0.025	25.6	15		
1050 N wall	mid-wall							0.040	0.040	20.4	15.1	0.040	24.3	15.1	0.035	17.6	15		
1010 NE corner	S2							0.070	0.070	25.6	13.1	0.020	16.5	3.5	0.025	9.6	14.1	114	
11/22/2000 10:14	1770 NW corner	NE corner	ground	2300	678	88.3	262.4	0.030	0.030	18.2	15.13	0.020	16.5	15.63	0.015	13.1	6.75		
1050 NE corner	S1							0.015	0.015	22.2	15	0.020	16.5	15.63	0.015	13.1	6.75		
1050 N wall	mid-wall							0.020	0.020	22.2	9.13	0.040	14.2	9.25	0.030	14.2	19.3		
1010 NE corner	S2							0.050	0.050	11.1	9.31	0.050	11.1	9.31	0.050	14.2	19.3		
1010 W wall	mid-wall							0.040	0.040	20.4	18.5	0.010	21.3	14.8	0.040	21.3	18.63	100	
11/20/2000 9:19	1769 NE corner	NE corner	ground	2410	183	178.2	425.2	0.040	0.030	20.4	18.5	0.010	21.3	14.8	0.040	21.3	18.63	100	
1258 NE corner	S1							0.020	0.020	4.4	4.38	0.020	4.4	4.38	0.035	14.2	12.4		
1258 N wall	mid-wall							0.020	0.020	5.3	4.4	0.020	5.3	4.4	0.010	14.2	6.25		
930 NE corner	S2							0.020	0.020	5.3	4.4	0.020	5.3	4.4	0.010	14.2	6.25		
11/20/2000 10:33	1769 NE corner	NE corner	ground	4800	183	340.0	811.6	0.050	0.040	18.200	17.5	0.010	18.2	16.7	0.050	18.2	17.8	100	
1258 NE corner	S1							0.025	0.025	15.000	4.5	0.050	14.2	13.13	0.020	17.6	6.44		
1258 N wall	mid-wall							0.020	0.020	6.2	4.5	0.040	14.2	16.6	0.015	17.6	6.44		
930 NE corner	S2							0.020	0.020	6.2	4.5	0.040	14.2	16.6	0.015	17.6	6.44		
11/20/2000 12:25	1769 NE corner	NE corner	ground	3100	234	202.7	504.0	0.020	0.015	21.3	20.9	0.010	18.2	3.2	0.020	18.2	16.5	110	
1258 NE corner	S1							0.025	0.025	4.600	4.25	0.020	16.5	16	0.015	13.1	4.13		
1258 N wall	mid-wall							0.025	0.025	4.6	4.25	0.020	16.5	16	0.030	13.8	12		
930 NE corner	S2							0.025	0.025	4.6	4.25	0.020	16.5	16	0.015	13.1	4.13		
11/20/2000 13:05	1769 NE corner	NE corner	ground	2180	274	131.7	336.3	0.025	0.025	13.8	12	0.015	9.6	4.5	0.015	19.6	16.13	119	
1258 NE corner	S1							0.025	0.025	21.3	18	0.040	4.38	4.38	0.020	4.8	4.4		
1258 N wall	mid-wall							0.050	0.050	3.8	4.38	0.040	4.38	4.38	0.150	7.4	10.63		
930 NE corner	S2							0.075	0.075	3.7	4.38	0.020	4.38	4.5	0.020	7.5	5.88		
11/20/2000 16:10	1769 NE corner	NE corner	ground	1770	495	79.6	224.2	0.080	0.080	23.2	17	0.030	21.3	7.75	0.080	19.6	18.9	122	
1258 NE corner	S1							0.155	0.155	5.2	4.9	0.040	7.7	7.7	0.065	8.2	6.6		
1258 N wall	mid-wall							0.205	0.205	5	4.94	0.040	8.2	7.75	0.050	6.3	6.63		
930 NE corner	S2							0.020	0.020	5	4.94	0.040	8.2	7.75	0.050	6.3	6.63		
11/20/2000 16:47	1769 NE corner	NE corner	ground	2500	211	172.1	420.7	0.040	0.030	20.4	22.75	0.010	20.4	14.8	0.040	24.3	17.13	106	
1258 NE corner	S1							0.025	0.025	12.4	4.600	0.020	20.4	14.8	0.015	19.6	4.6		
1258 N wall	mid-wall							0.035	0.035	5.2	4.44	0.020	20.4	14.8	0.010	14.2	6.25		
930 NE corner	S2							0.055	0.055	17.6	4.44	0.030	17.6	17.8	0.050	22.2	17.8	118	
11/21/2000 14:39	1769 NE corner	NE corner	ground	1920	274	116.0	296.2	0.080	0.080	20.4	17.8	0.030	17.6	4.2	0.025	22.2	17.8	118	
1258 NE corner	S1							0.105	0.105	4.6	4.31	0.040	17.6	4.2	0.025	7.7	4.38		
1258 N wall	mid-wall							0.150	0.150	4.7	4.31	0.020	17.6	4.2	0.130	10.2	8.56		
930 NE corner	S2							0.070	0.070	22.2	18.25	0.030	21.3	7.75	0.080	19.6	18.9	122	
11/21/2000 15:36	1769 NE corner	NE corner	ground	1700	211	117.0	286.1	0.070	0.070	22.2	18.25	0.030	21.3	7.75	0.080	19.6	18.9	122	
1258 NE corner	S1							0.130	0.130	4.6	4.44	0.060	18.9	4.44	0.055	6.8	4.5		
1258 N wall	mid-wall							0.180	0.180	4.6	4.44	0.040	18.9	4.44	0.065	7.5	5.94		
930 NE corner	S2							0.050	0.050	22.2	17.7	0.010	18.9	4.44	0.050	16	4.44		
11/21/2000 16:42	1769 NE corner	NE corner	ground	3770	808	132.6	405.7	0.050	0.050	4.9	4.3	0.040	17.6	2.56	0.050	17.6	16.9	110	
1258 NE corner	S1							0.065	0.065	4.1	4.31	0.020	17.6	2.56	0.050	17.6	16.9	110	
1258 N wall	mid-wall							0.065	0.065	4.1	4.31	0.020	17.6	2.56	0.050	17.6	16.9	110	
930 NE corner	S2																		

New Mexico

Structure	Shot Date and Time	Unit	Structure Location	Placement of Transducer(s)	Distance (ft)	Charge Weight/Delay (lb)	Scaled Distance (ft/lb <sup>1/3</sup> )	Scaled Distance (ft/lb <sup>1/3</sup> )	Peak Particle Velocity (in/sec)	T (in/s)	Peak Frequency (Hz)	FFT Frequency (Hz)	V (in/s)	Peak Frequency (Hz)	FFT Frequency (Hz)	R (in/s)	Peak Frequency (Hz)	FFT Frequency (Hz)	Airblast (dB)
E1S-NMB	06/22/01 14:20	1769	SE corner	ground	5333	13047	46.7	227.3	0.1625	0.1125	4.7	3.9	0.0875	5.8	6.56	0.163	6.2	3.9	128
		1050	SE corner	S1						0.11	4.8	3.9	0.09	3.94	6.5	0.13	5.5	3.9	
		1050	E wall	mid-wall												0.245	4.6	3.9	
		1906	SE corner	S2						0.135	4.8	3.9	0.09	9.4	3.94	0.19	5.9	3.9	
		1906	S wall	mid-wall						0.185	9.4	3.9							
	6/26/2001 3:57	1769	SE corner	ground	5186	1708	125.5	434.9	0.0125	0.0125	12.1	3.8	0.01	18.2	7.44	0.013	8.8	3.8	112
		1050	SE corner	S1					0.01			3.8	0.01		7.5	0.01	3.7	16.7	
		1050	E wall	mid-wall												0.025	16		
		1906	SE corner	S2					0.02	0.02	6.5	3.8	0.01		7.44	0.015	9.8	3.8	
	6/28/2001 3:03	1769	SE corner	ground	4816	300	278.1	720.8	0.045	0.045	18.2	11.2	0.025	3.1	3.38	0.043	4	4.6	100
		1050	SE corner	S1					0.05	0.05	3.6	3.6	0.05	4.5	4.38	0.05	4.1	4.1	
		1050	E wall	mid-wall					0.06		4.4	4.2	0.06			0.08	5.3	4.1	
		1906	SE corner	S2					0.075	0.075	4.3	4.2	0.05	4.8	3.63	0.06	4.8	4.1	
		1906	S wall	mid-wall					0.075	0.075	4.4	4.1							
	7/3/2001 1:48	1769	SE corner	ground	4478	300	258.5	670.2	0.05	0.05	3.6	3.6	0.05	3.1	3.38	0.085	4	4.6	100
		1050	SE corner	S1					0.055	0.055	3.8	3.5	0.02		3.13	0.045	4.4	4.3	
		1050	E wall	mid-wall												0.055	4.4	4.3	
		1906	SE corner	S2					0.06	0.06	4	3.6	0.02		3.25	0.055	4.3	4.0	
		1906	S wall	mid-wall					0.06	0.06	4	3.5							
	07/05/01 3:04	1769	SE corner	ground	4941	9591	50.5	233.3	0.135	0.135	5.2	3.9	0.103	6	5.2	0.133	10.6	3.8	117
		1050	SE corner	S1					0.11	0.11	5	3.9	0.09	6.5	8.3	0.105	5.3	3.8	
		1050	E wall	mid-wall												0.255	10.6	8.1	
		1906	SE corner	S2					0.17	0.17	6.2	3.9	0.11	7.1	8.3	0.165	7.1	3.8	
		1906	S wall	mid-wall					0.2	0.2	8.8	3.9							
	07/17/01 12:51	1769	SE corner	ground	4806	11183	43.6	206.6	0.1425	0.1425	8.2	4.0	0.1	6.4	7.25	0.123	4.4	3.8	116
		1050	SE corner	S1					0.105	0.105	5.9	4.0	0.11	10.6	7.25	0.115	3.9	3.8	
		1050	E wall	mid-wall												0.275	7.3	3.8	
		1906	SE corner	S2					0.22	0.22	7.7	7.3	0.14	9.8	7.25	0.15	5	3.8	
		1906	S wall	mid-wall					0.305	0.305	8.2	7.3							
	07/23/01 11:22	1769	SE corner	ground	4621	300	268.8	691.6	0.0725	0.0725	4.8	4.6	0.0475	4.7	4.56	0.073	4.1	4.4	110
		1050	SE corner	S1					0.065	0.065	4.1	4.6	0.06	5.3	3.13	0.07	3.8	3.6	
		1050	E wall	mid-wall												0.125	5.1	3.6	
		1906	SE corner	S2					0.08	0.08	5	4.6	0.06	5.6	4.75	0.085	4.3	3.6	
		1906	S wall	mid-wall					0.08	0.08	7.3	4.6							
	07/26/01 2:55	1769	SE corner	ground	5565	600	227.2	661.2	0.105	0.105	3.8	3.7	0.035	5.4	4	0.105	4	3.8	106
		1050	SE corner	S1					0.075	0.075	3.69	4.0	0.03	6.5	3.7	0.105	4	3.8	
		1050	E wall	mid-wall												0.165	5.2	3.9	
		1906	SE corner	S2					0.09	0.09	4.1	3.7	0.04	6.9	4.1	0.13	4.1	3.8	
		1906	S wall	mid-wall					0.09	0.09	4.1	3.7							
	07/26/01 2:55	1769	SE corner	ground	4593	7455	53.2	235.8	0.105	0.105	5.2	8.1	0.070	19.6	8	0.073	8.5	4.4	120
		1050	SE corner	S1					0.09	0.09	5.6	8.2	0.08	8.2	8	0.055	5.8	4.5	
		1050	E wall	mid-wall												0.19	11.1	8.2	
		1906	SE corner	S2					0.165	0.165	6.7	8.3	0.1	9.8	8	0.075	5.1	4.5	
		1906	S wall	mid-wall					0.165	0.165	7.3	8.3							
E2S-NM	06/22/01 14:20	1770	SE corner	ground	3978	13047	34.8	169.5	0.1875	0.1875	7.1	3.9	0.1725	8	7.4	0.258	5.5	4.1	131
		1258	SE corner	S1(V-ceiling)					0.19	0.19	4.5	4.0	0.47	11.1	9.2	0.22	5.1	4.1	
		1258	E wall	mid-wall					0.39	0.39	19.6	12.9				0.41	8.2	4.1	
		930	SE corner	S2					0.61	0.61	4.4	4.0	0.25	8	4.13	0.72	5.9	4.1	
		930	S wall	mid-wall					1.36	1.36	4.3	4.0							
	07/05/01 3:04	1770	SE corner	ground	3458	9591	35.3	163.3	0.31	0.3	8.2	3.7	0.1375	10.2	6.94	0.31	12.1	3.9	117
		1258	SE corner	S1(V-ceiling)					0.24	0.24	4.5	3.7	0.46	15	17.6	0.26	11.1	3.9	
		1258	E wall	mid-wall												0.45	11.6	3.9	
		930	SE corner	S2					0.57	0.57	4.6	3.7	0.22	9.1	17.9	0.59	5	3.9	
		930	S wall	mid-wall					1.09	1.09	4.9	3.9							
	07/17/01 12:51	1770	SE corner	ground	2991	11183	28.3	134.2	0.46	0.33	6.5	3.9	0.225	7.7	3.94	0.46	3.9	3.9	119
		1258	SE corner	S1(V-ceiling)					0.35	0.35	5.3	3.9	0.5	9.4	3.9	0.38	4.1	3.9	
		1258	E wall	mid-wall												0.63	4.5	3.9	
		930	SE corner	S2					1.24	1.24	4.2	3.9	0.31	12.1	3.94	1.52	4.8	3.9	
		930	S wall	mid-wall					2.64	2.64	4.1	3.9							
	07/23/01 11:22	1770	SE corner	ground	2943	300	169.9	440.5	0.23	0.15	3.3	3.8	0.1725	5.2	4	0.23	4.3	4.0	110
		1258	SE corner	S1(V-ceiling)					0.19	0.19	3.5	3.8	0.21	6.2	4	0.26	3.7	4.0	
		1258	E wall	mid-wall												0.44	4.4	4.0	
		930	SE corner	S2					0.48	0.48	4.5	3.8	0.24	5.8	7.13	1.03	4.3	4.0	
		930	S wall	mid-wall					1.09	1.09	4.4	3.8							
	06/26/01 11:04	1770	SE corner	ground	3975	300	229.5	594.9	0.2525	0.2525	5.8	3.9	0.1425	5.8	7.2	0.183	4	3.9	106
		1258	SE corner	S1(V-ceiling)					0.26	0.26	3.8	3.9	0.23	6.9	3.94	0.21	4.4	4.0	
		1258	E wall	mid-wall												0.35	5	4.0	
		930	SE corner	S2					0.97	0.97	4.5	3.9	0.16	7.1	7.2	0.71	4.4	4.0	
		930	S wall	mid-wall					1.64	1.64	3.9	3.9							
	06/26/01 2:55	1770	SE corner	ground	2876	7455	33.3	147.7	0.21	0.21	5.8	8.4	0.1075	11.1	8.1	0.188	7.5	4.1	122
		1258	SE corner	S1(V-ceiling)					0.23	0.23	5.3	4.1	0.24	7.3	8.44	0.16	7.5	4.1	
		1258	E wall	mid-wall												0.32	6.7	4.2	
		930	SE corner	S2					0.59	0.59	4.6	4.3	0.18	13.4	8.4	0.82	6.2	4.2	
		930	S wall	mid-wall					1.28	1.28	4.5	4.3							

New Mexico (cont.)																			
EIS-NMA	06/22/01 14:20	1100 784	NE corner SE corner	ground S1	3675	13047	32.2	156.6	0.3	0.23	9.1	3.9	NR	8.8	11.8	0.3	5.5	4.1	132
		787	SE corner E wall	S2 mid-wall						0.145 0.175	4.2 9.1	4.0 3.9	0.135 NR			0.215 NR	4.6	4.1	
		705								0.34	7.1	9.9	0.155	11.6	9	0.21	4.5	4.1	
	07/05/01 3:04	1100 784	NE corner SE corner	ground S1	2900	13047	25.4	123.6	0.37	0.365	15	18.0	0.16	13.4	18	0.37	5.9	4.1	112
		787	SE corner E wall	S2 mid-wall						0.31 0.435	12.8 13.4	3.8 3.8	0.19 NR	14.2	17.9	0.31	5.3	4.1	
		705								0.54	12.8	18.1	0.22	12.1	17.81	0.285	5.3	4.1	
	07/17/01	1100	NE corner	ground	2423	11183	22.9	108.7	0.74	0.43	11.6	12.6	0.265	13.4	18.13	0.74	15	4.0	118
	12:51	784	SE corner	S1						0.28	10.2	3.8	0.375	14.2	18	0.175	5.1	4.0	
		787	SE corner E wall	S2 mid-wall						0.32	15	3.8	0.395	14.2	18	0.535	3.5	4.0	
		705								1.02	13.4	18.0	0.335	15	12.5	0.495	13.4	4.0	
	07/23/01	1100	NE corner	ground	2095	300	121.0	313.5	0.305	0.23	8	4.4	0.1	4.7	4.44	0.305	4	4.3	112
	11:22	784	SE corner	S1						0.205	4.1	4.1	0.13	8	8.6	0.33	4	4.3	
		787	SE corner	S2						0.235	4.2	4.1	0.135	8	8.6	0.385	4.1	4.3	
		705	E wall	mid-wall						0.37	7.3	4.1	0.135	7.3	4.3	0.33	4.1	4.3	
	06/26/01	1100	NE corner	ground	3144	300	181.5	470.5	0.6	0.3	4.1	3.8	0.14	9.1	4.94	0.6	4	3.8	106
	11:04	784	SE corner	S1						0.285	4.6	4.1	0.145	8.8	8.75	0.575	4	3.8	
		787	SE corner	S2						0.31	5.3	4.1	0.155	7.7	8.75	0.66	4	3.8	
		705	E wall	mid-wall						0.435	3.7	4.1	0.215	7.3	8.2	0.565	4	3.8	
	06/26/01	1100	NE corner	ground	2095	7455	24.3	107.6	0.52	0.33	16	4.1	0.31	17	18.4	0.52	18.2	123	
	2:55	784	SE corner	S1						0.275	12.8	4.1	0.345	17	18	0.335	6	4.0	
		787	SE corner	S2						0.385	12.8	4.1	0.38	16	18	0.395	11.6	4.0	
		705	E wall	mid-wall						0.78	15	18.3	0.19	14.2	8.4	0.31	5.9	4.0	

Structure	Shot Date and Time	Unit	Structure Location	Placement of Transducer(s)	Distance (ft)	Charge Weight/Delay (lb)	Scaled Distance (ft/lb <sup>1/3</sup> )	Peak Particle Velocity (in/sec)	Ohio									
									T (in/s)	Peak Frequency (Hz)	FFT Frequency (Hz)	V (in/s)	Peak Frequency (Hz)	FFT Frequency (Hz)	R (in/s)	Peak Frequency (Hz)	FFT Frequency (Hz)	Airblast (dB)
	03/15/01 12:32	914	NW corner	ground	5120	748	187.2	565.3	0.0375	17	16.9	0.0125	8.3	1.9	0.03	15.5	15.8	112
		919	NW base	living room					0.015	15.5	17.0	0.0175	11.3	8.5	0.015	17.6	15.5	
	03/16/01 14:42	1906	NW top	living room					0.02	12.8	8.5	0.035	13.4	8.5	0.02	13.4	8.1	
		914	NW corner	ground	570	539	24.6	70.2	1.17	22.2	12.8	0.56	24.3	25.3	1.06	17	12.8	129
		919	NW base	living room					0.51	23.2	12.8	0.41	30.1	25.5	0.57	30.1	24.9	
	03/19/01 11:53	1906	NW top	living room					0.455	21.3	8.5	0.68	36.5	25.8	0.455	7	7.3	
		914	NW corner	ground	580	306	33.2	86.2	1.25	18.9	11.5	0.38	26.9	25.1	0.88	18.2	13.5	126
		919	NW base	living room					0.54	18.2	11.0	0.41	22.2	12.5	0.48	14.2	12.0	
	03/19/01 15:42	1906	NW top	living room	600	286	35.5	91.2	0.73	8.9	7.8	0.565	30.1	12.5	0.385	8.6	8.3	
		914	NW corner	ground					0.485	23.2	18.3	0.26	21.3	14.8	0.49	16.5	14.5	120
		919	NW base	living room					0.225	25.6	7.8	0.175	18.9	18.8	0.2425	17.6	14.0	
	03/20/01 13:03	1906	NW top	living room	610	294	35.6	91.9	1.13	7.6	8.0	0.225	34.1	25.5	0.32	7.7	8.3	
		914	NW corner	ground					0.45	24.3	18.3	0.32	28.4	17.8	0.72	20.4	14.3	124
		919	NW base	living room					0.41	24.3	26.8	0.2675	18.9	27.0	0.36	25.4	26.8	
	03/20/01 15:45	1906	NW top	living room	640	304	36.7	95.4	0.88	8	8.3	0.385	18.2	13.3	0.31	17.6	8.5	
		914	NW corner	ground					0.505	23.2	17.8	0.245	25.6	17.8	0.68	18.9	10.4	119
		919	NW base	living room					0.263	23.2	23.0	0.175	22.2	17.8	0.38	22.2	10.0	
	03/21/01 16:02	1906	NW top	living room	4900	2694	94.4	353.1	0.36	9.4	6.9	0.275	17.6	27.5	0.17	8.6	8.4	
		914	NW corner	ground					0.078	16.5	13.8	0.0375	17.6	12.9	0.055	14.2	11.0	112
		919	NW base	living room					0.0375	11.3	13.6	0.035	12.4	12.6	0.04	11.3	6.9	
	03/22/01 16:16	1906	NW top	living room	4900	3254	85.9	331.6	0.06	8.6	8.4	0.06	14.2	14.0	0.06	9.4	8.0	
		914	NW corner	ground					0.0225	14.2	4.9	0.025	12.8	8.4	0.0525	14.6	4.8	116
		919	NW base	living room					0.04	11.1	8.1	0.04	10.8	8.5	0.06	7.1	8.1	
	03/23/01 16:06	1906	NW top	living room	4300	504	191.5	541.5	0.0375	16.5	16.8	0.0075	18.2	10.5	0.0175	14.6	15.4	112
		914	NW corner	ground					0.015	15	17.0	0.0175	12.1	11.0	0.015	14.6	15.0	
		919	NW base	living room					0.015	14.6	8.4	0.035	15.4	14.2	0.02	10.4	8.4	
	03/23/01 16:23	1906	NW top	living room	5000	3408	85.6	333.2	0.095	15.5	14.1	0.0325	9.3	5.5	0.075	13.8	4.8	122
		914	NW corner	ground					0.05	12.4	3.1	0.06	11.1	8.8	0.0475	8.5	4.8	
		919	NW base	living room					0.055	8.6	8.3	0.095	12.8	8.3	0.095	7.5	8.1	
	03/24/01 14:02	1906	NW top	living room	5100	2026	113.3	404.1	0.0375	13.4	12.5	0.03	12.8	4.0	0.0625	12.1	1.3	122
		914	NW corner	ground					0.055	12.8	12.6	0.0475	10.8	12.4	0.0375	11.9	3.4	
		919	NW base	living room					0.06	10.2	8.5	0.1	12.8	12.6	0.07	7.6	9.1	
	03/26/01 14:41	1906	NW top	living room		NO	TRIGGER											
		914	NW corner	ground														
	03/26/01 16:10	1906	NW top	living room		NO	TRIGGER											
		914	NW corner	ground														
	03/27/01 14:36	1906	NW top	living room	4020	832	139.4	428.4	0.05	19.6	20.6	0.0225	23.2	20.1	0.0425	17.6	13.8	114
		914	NW corner	ground					0.05	17.6	13.5	0.0275	10.6	11.3	0.0175	13.4	11.4	
		919	NW base	living room					0.05	10.2	8.3	0.04	10.6	8.3	0.045	9.8	8.3	
	03/27/01 16:02	1906	NW top	living room	5160	4130	80.3	322.5	0.1	0.015	13.4	0.0325	11.1	10.0	0.065	13.1	16.3	114
		914	NW corner	ground					0.065	12.4	9.3	0.0475	10.4	9.9	0.035	4.7	3.3	
		919	NW base	living room					0.1	8.9	8.5	0.095	12.8	8.3	0.075	8.8	8.3	
	03/28/01 14:32	1906	NW top	living room	3970	546	169.9	486.7	0.0425	0.025	16.5	0.025	19.6	7.8	0.0225	13.8	15.4	112
		914	NW corner	ground					0.065	17	11.5	0.0275	11.9	8.1	0.015	20.4	14.8	
		919	NW base	living room					0.0425	bad data								
	03/28/01 16:23	1906	NW top	living room	5300	2056	116.9	417.9	0.055	10	9.3	0.03	8	8.6	0.055	5.1	14.8	112
		914	NW corner	ground					0.0175	10.2	9.3	0.04	8.2	9.0	0.035	5.5	4.8	
		919	NW base	living room					0.0475	bad data								
	03/29/01 14:32	1906	NW top	living room	3900	696	147.8	441.0	0.03	0.035	16.5	0.0075	21.3	2.0	0.015	17.6	15.9	110
		914	NW corner	ground					0.03	15.5	11.5	0.01	15	8.3	0.0075	32	16.0	
		919	NW base	living room					0.03	12.1	8.0	0.02	16.5	16.0	0.015	13.8	9.3	
	03/29/01 16:08	1906	NW top	living room	5540	2056	122.2	436.8	0.075	0.0125	13.4	0.02	14.2	8.6	0.045	11.1	8.3	110
		914	NW corner	ground					0.02	13.1	9.3	0.0325	11.2	9.3	0.04	10.8	8.3	
		919	NW base	living room					0.075	8.2	8.0	0.06	11.9	8.5	0.09	8.6	8.3	
	03/30/01 14:38	1906	NW top	living room		NO	TRIGGER		0.0425									
		914	NW corner	ground					0.15									
	3/31/2001 14:38	1906	NW top	living room		NO	TRIGGER											
		914	NW corner	ground														
	4/2/2001 13:40	1906	NW top	living room	5420	2618	105.9	394.3	0.0425	14.6	15.8	0.0175	9.4	4.0	0.0425	10	15.3	122
		914	NW corner	ground						11.9	7.8	0.0175	12.1	7.8	0.03	5.6	3.9	
		919	NW base	living room					0.025	cannot read								
	04/02/01 15:54	1906	NW top	living room	4790	1030	149.3	475.4	0.0625	0.02	16.5	0.02	28.4	17.8	0.0575	13.8	15.3	106
		914	NW corner	ground					read	14.8	12.0	0.03	15	14.5	0.03	13.4	15.0	
		919	NW base	living room					0.0825	12.4	10.3	0.055	15.5	14.5	0.045	10.4	8.3	
	04/03/01 13:36	1906	NW top	living room	3650	848	125.3	386.5	0.04	0.0325	19.6	0.0225	28.4	19.8	0.0275	18.2	17.3	114
		914	NW corner	ground					0.035	14.2	17.4	0.0225	25.6	19.8	0.0175	24.3	19.0	
		919	NW base	living room					0.04	12.4	8.3	0.025	26.9	19.8	0.02	13.8	8.3	
	04/03/01 15:04	1906	NW top	living room	4790	1161	140.6	456.8	0.0775	17	18.3	0.035	25.6	10.4	0.0775	12.1	10.4	114
		914	NW corner	ground					0.02									
		919	NW base	living room					0.0775	10.8	10.4	0.075	12.1	10.8	0.065	9.3	8.0	
		1906	NW top	living room														

LIS-OH

[illegible]



Ohio (cont.)														
03/16/01	1769	NW corner	ground	1560	539	67.2	192.1	0.1825	0.1825	8.2	6.5	0.1775	39.3	5.5
14:43	930	NW corner	R. A(V). T					0.14		5.3	4.1	0.3	8.8	9.1
	1258	SE corner	V											
	1258	SE corner	R. A(V). T					0.27		5.6	5.1	0.16	12.8	5.3
	1258	SE corner	V											
03/19/01	1769	NW corner	ground	1550	306	88.6	230.5	0.1675	0.1675	10.4	10.8	0.14	30.1	28.0
11:53	930	NW corner	R. A(V). T					0.28		4.3	3.7	0.33	10.4	9.3
	1258	SE corner	V											
	1258	SE corner	R. A(V). T					0.21		4.1	5.0	0.17	11.6	14.3
	1258	SE corner	V											
03/19/01	1769	NW corner	ground	1570	286	92.8	238.7	0.155	0.155	9.1	6.6	0.055	25.6	5.9
15:42	930	NW corner	R. A(V). T					0.145		6.7	4.0	0.32	9.3	9.3
	1258	SE corner	V											
	1258	SE corner	R. A(V). T					0.2		6.3	5.3	0.28	8.5	6.8
	1258	SE corner	V											
03/20/01	1769	NW corner	ground	1550	294	90.4	233.5	0.2	0.2	8.3	9.6	0.1125	42.6	8.9
13:03	930	NW corner	R. A(V). T					0.175		7.1	4.0	0.45	8.8	9.5
	1258	SE corner	V											
	1258	SE corner	R. A(V). T					0.235		6.3	5.1	0.26	8.1	7.9
	1258	SE corner	V											
03/20/01	1769	NW corner	ground	1560	304	90.6	235.4	0.165	0.165	10.4	10.4	0.065	51.2	6.5
15:45	930	NW corner	R. A(V). T					0.135		4.5	3.7	0.26	9.3	10.0
	1258	SE corner	V											
	1258	SE corner	R. A(V). T					0.16		5.9	5.1	0.17	8.1	6.4
	1258	SE corner	V											
03/21/01	1769	NW corner	ground	5630	2694	108.5	405.7	0.05	0.05	10.4	7.0	0.025	12.4	6.5
16:02	930	NW corner	R. A(V). T					0.075		5.8	4.0	0.14	11.3	6.5
	1258	SE corner	V											
	1258	SE corner	R. A(V). T					0.085		5.8	5.4	0.07	7.8	6.4
	1258	SE corner	V											
03/22/01	1769	NW corner	ground	NO	TRIGGER									
16:16	930	NW corner	R. A(V). T											
	1258	SE corner	V											
03/23/01	1769	NW corner	ground	NO	TRIGGER									
16:06	930	NW corner	R. A(V). T											
03/23/01	1769	NW corner	ground	5730	3408	98.2	381.8	0.0475	0.0475	7.8	3.3	0.025	12.4	4.1
16:23	930	NW corner	R. A(V). T					0.135		3.5	3.6	0.07	11.3	6.6
	1258	SE corner	V											
	1258	SE corner	R. A(V). T					0.135		5.8	5.3	0.09	10.2	5.3
	1258	SE corner	V											
03/24/01	1769	NW corner	ground	5840	2026	129.7	462.7	0.04	0.04	11.3	10.0	0.02	4.1	3.8
14:02	930	NW corner	R. A(V). T					0.11		3.8	3.8	0.12	11.6	10.1
	1258	SE corner	V											
	1258	SE corner	R. A(V). T					0.155		8.6	5.4	0.08	10.4	8.8
	1258	SE corner	V											
03/26/01	1769	NW corner	ground	NO	TRIGGER									
14:41	930	NW corner	R. A(V). T											
03/26/01	1769	NW corner	ground	NO	TRIGGER									
03/27/01	1769	NW corner	ground	NO	TRIGGER									
14:36	930	NW corner	R. A(V). T											
03/27/01	1769	NW corner	ground	5900	4130	91.8	368.8	0.0775	0.0775	8.2	10.0	0.02	11.6	9.1
16:02	930	NW corner	R. A(V). T					0.175		4.3	3.6	0.09	11.1	10.0
	1258	SE corner	V											
	1258	SE corner	R. A(V). T					0.075		5.6	3.3	0.07	10.8	9.1
	1258	SE corner	V											
03/28/01	1769	NW corner	ground	NO	TRIGGER									
14:32	930	NW corner	R. A(V). T											
03/28/01	1769	NW corner	ground	6040	2056	133.2	476.2	0.085	0.085	8.3	8.9	0.0175	12.1	8.9
16:23	930	NW corner	R. A(V). T					0.155		4	3.8	0.08	10.8	9.9
	1258	SE corner	V											
	1258	SE corner	R. A(V). T					0.075		5.2	5.4	0.1	8.9	9.1
	1258	SE corner	V											
03/29/01	1769	NW corner	ground	NO	TRIGGER									
14:32	930	NW corner	R. A(V). T											
03/29/01	1769	NW corner	ground	6280	2056	138.5	495.1	0.103	0.103	8.8	8.9	0.018	16	9.0
16:08	930	NW corner	R. A(V). T					0.110		4.5	3.8	0.090	9.8	9.5
	1258	SE corner	V											
	1258	SE corner	R. A(V). T					0.035		3.7	3.3	0.090	10.2	9.0
	1258	SE corner	V											
03/30/01	1769	NW corner	ground	NO	TRIGGER									
14:38	930	NW corner	R. A(V). T											
03/30/01	1769	NW corner	ground	6040	2394	123.4	452.7	0.030	0.030	8.5	3.9	0.008	6.8	4.0
14:38	930	NW corner	R. A(V). T					0.08		3.7	3.8	0.03	13.4	11.4
	1258	SE corner	V											
	1258	SE corner	R. A(V). T					0.06		5.4	5.6	0.04	14.2	6.6
	1258	SE corner	V											
04/02/01	1769	NW corner	ground	6170	2618	120.6	448.9	0.055	0.055	5.3	3.5	0.0125	14.6	3.9
13:40	930	NW corner	R. A(V). T					0.155		3.9	3.9	0.08	8.6	7.7
	1258	SE corner	V											
	1258	SE corner	R. A(V). T					0.22		7.7	5.3	0.13	10	7.6
	1258	SE corner	V											
04/02/01	1769	NW corner	ground	5510	1030	171.7	546.9	0.035	0.035	12.1	12.5	0.015	18.9	12.4
15:54	930	NW corner	R. A(V). T					0.035		9.6	4.1	0.09	12.1	10.1
	1258	SE corner	V											
	1258	SE corner	R. A(V). T					0.04		11.3	5.6	0.08	12.4	14.9
	1258	SE corner	V											
04/03/01	1769	NW corner	ground	NO	TRIGGER									
13:36	930	NW corner	R. A(V). T											
04/03/01	1769	NW corner	ground	5500	1161	161.4	524.5	0.0475	0.0475	11.6	10.0	0.0175	12.8	12.5
15:04	930	NW corner	R. A(V). T					0.06		9.3	3.9	0.16	10.8	10.1
	1258	SE corner	V											
	1258	SE corner	R. A(V). T					0.06		11.1	5.5	0.09	12.4	12.7
	1258	SE corner	V											
	1258	SE corner	R. A(V). T											
	1258	SE corner	V											
	1258	SE corner	R. A(V). T											
	1258	SE corner	V											
	1258	SE corner	R. A(V). T											
	1258	SE corner	V											
	1258	SE corner	R. A(V). T											
	1258	SE corner	V											
	1258	SE corner	R. A(V). T											
	1258	SE corner	V											
	1258	SE corner	R. A(V). T											
	1258	SE corner	V											
	1258	SE corner	R. A(V). T											
	1258	SE corner	V											
	1258	SE corner	R. A(V). T											
	1258	SE corner	V											
	1258	SE corner	R. A(V). T											
	1258	SE corner	V											
	1258	SE corner	R. A(V). T											
	1258	SE corner	V											
	1258	SE corner	R. A(V). T											
	1258	SE corner	V											
	1258	SE corner	R. A(V). T											
	1258	SE corner	V											
	1258	SE corner	R. A(V). T											
	1258	SE corner	V											
	1258	SE corner	R. A(V). T											
	1258	SE corner	V											
	1258	SE corner	R. A(V). T											
	1258	SE corner	V											
	1258	SE corner	R. A(V). T											
	1258	SE corner	V											
	1258	SE corner	R. A(V). T											
	1258	SE corner	V											
	1258	SE corner	R. A(V). T											
	1258	SE corner	V											
	1258	SE corner	R. A(V). T											
	1258	SE corner	V											
	1258	SE corner	R. A(V											

Pennsylvania																				
Structure	Shot Date and Time	Unit	Structure Location	Placement of Transducer(s)	Distance	Charge Weight/Delay	Scaled Distance (ft/lb <sup>1/3</sup> )	Scaled Distance (ft/lb <sup>1/3</sup> )	Peak Particle Velocity (in/sec)	T (in/s)	Peak Frequency (Hz)	FFT Frequency (Hz)	V (in/s)	Peak Frequency (Hz)	FFT Frequency (Hz)	R (in/s)	Peak Frequency (Hz)	FFT Frequency (Hz)	Airblast (dB)	
TD-PA	05/22/01 10:37	1769	SW corner	ground	1437	612	58.1	169.6	0.24	0.14	11.6	7.4	0.065	11.6	7.5	0.24	16.5	7	117	
		930	SW corner	S1					0.105	7	7.0	7.5	0.34	15.5	7.5	0.31	12.4	7		
		930	S wall	mid-wall					0.265	21.3	8.6	7.5								
		1258	SW corner	S2					0.2			7.5	0.34	15	7.5	0.415	15	7.1		
		1258	W wall	mid-wall												0.98	9.4	13.13		
	05/22/01 12:16	1769	SW corner	ground	1458	488	66.1	185.8	0.235	0.235	11.6	8.0	0.095	14.2	7.5	0.185	12.8	7	119	
		930	SW corner	S1					0.125	6.7	7.1	7.1	0.46	14.2	7.38	0.215	14.2	7.13		
		930	S wall	mid-wall					0.445	7.3	7.3	7.3	0.46	13.8	7.4	0.3	8	7.25		
		1258	SW corner	S2					0.3	8.8		7.3	0.46	13.8	7.4	0.3	8	7.25		
		1258	W wall	mid-wall										0.9	10.4	13				
	05/23/01 2:15	1769	SW corner	ground	1483	612	59.9	175.0	0.32	0.165	16.5	7.3	0.07	11.2	6.5	0.32	16.5	17.6	119	
		930	SW corner	S1						0.135	6.2	7.3	0.34	15	16.5 & 7.4	0.33	13.8	17.25 & 6.3		
		930	S wall	mid-wall						0.355	18.9	7.3								
		1258	SW corner	S2						0.21	5.8	7.4	0.35	14.6	16.5 & 7.4	0.27	8.5	7.3		
		1258	W wall	mid-wall						0.165	18.9	20.5	0.115	46.5	20.13	0.195	22.2	19.9	122	
05/24/01 10:41	1769	SW corner	ground	1390	504	61.9	175.0	0.195	0.09	11.6	6.8	0.32	14.2	8.25	0.215	16.5	19.8			
	930	SW corner	S1						0.535	19.6	19.8									
	930	S wall	mid-wall						0.195	9.4	7.0	0.32	13.8	8.25	0.185	9.3	9.25			
	1258	SW corner	S2													1.08	14.6	13		
	1258	W wall	mid-wall										0.0725	9.8	7.5	0.29	8.3	7.13	116	
W1S-PA	05/22/01 10:37	1050	SW corner	ground	1472	612	59.5	173.7	0.29	NR			0.0725	9.8	7.5	0.29	8.3	7.13	116	
		1770	SW corner	S1(V-ceiling)					0.14	17.6			0.53	18.9	17.5	0.24	7.7	7.4		
		1770	S wall	mid-wall					0.39	19.6	12.9									
		1906	SW corner	S2					0.165	6.4	7.1	7.1	0.14	11.1	7.13	0.505	7.6	6.6		
		1906	W wall	mid-wall												0.495	7.2	6.63 & 22.3		
	05/22/01 12:16	1050	SW corner	ground	1507	486	68.4	192.1	0.32	0.32	10.6	7.6	0.0875	19.6	7.4	0.268	7.7	7.13	119	
		1770	SW corner	S1(V-ceiling)					0.23	10			0.42	18.9	20.3	0.17	4.9	7.13		
		1770	S wall	mid-wall					0.51	17.6			26.8 (12.8 & 7.5)							
		1906	SW corner	S2					0.3	7.8			0.11	19.6	7.9	0.39	7.4	6.4		
		1906	W wall	mid-wall												0.49	13.8	6.13 & 24.9		
	05/23/01 2:15	1050	SW corner	ground	1507	612	60.9	177.9	0.2775	0.1375	7	8.4	0.0875	1.9	6.5	0.278	10.2	7.8	118	
		1770	SW corner	S1(V-ceiling)						0.12	7.4	7.0	0.54	21.3	18.5	0.23	6.4	7.63		
		1770	S wall	mid-wall						0.59	16.5	26.1 & 10.8								
		1906	SW corner	S2						0.165	6.7	7.1	0.08	5.8	6.4	0.315	8.2	6.3		
		1906	W wall	mid-wall												0.48	23.2	6.3		
05/24/01 10:41	1050	SW corner	ground	1510	504	67.3	190.1	0.203	0.1675	7.7	8.1	0.095	30.1	20	0.203	17	20.6	125		
	1770	SW corner	S1(V-ceiling)						0.13	8.5	6.5	0.56	18.2	20.3	0.16	14.6	20.9			
	1770	S wall	mid-wall						1.2	17	12.8									
	1906	SW corner	S2						0.19	10.4			0.09	7.2	14.3	0.255	7.2	6.5		
	1906	W wall	mid-wall													0.74	19.6	20.3		

values by 2  
values by 2

Tennessee																				
Structure	Shot Date and Time	Unit	Structure Location	Placement of Transducer(s)	Distance (ft)	Charge Weight/Delay (lb)	Scaled Distance (ft/lb <sup>1/3</sup> )	Scaled Distance (ft/lb <sup>1/3</sup> )	Peak Particle Velocity (in/sec)	T (in/s)	Peak Frequency (Hz)	FFT Frequency (Hz)	V (in/s)	Peak Frequency (Hz)	FFT Frequency (Hz)	R (in/s)	Peak Frequency (Hz)	FFT Frequency (Hz)	Airblast (dB)	
TD-TN	12/12/2000 12:21	1770	E side	ground	1910	1676	46.7	161.2	0.085	0.085	9.6	12.1	0.085	11.9	11.25	0.07	18.2	12.6	124	
		1010	east side center	see note																
		1010	center wall- east	mid-wall						0.92	6.7	13.3								
		1050	west side center	see notes																
		1050	center wall- radial	mid-wall						0.12	11.9	6.6								
	12/12/2000 1770	1770	E side	ground	1225	885	41.2	127.9	0.04	0.04	16	17.5	0.035	11.1	10.88	0.02	18.9	7.8		
	17:00	1010	east side center	see note						0.06	17	17.5	0.06	12.8	12.81	0.05	18.9	6.9		
	3-holes	1010	center wall- east	mid-wall						0.245	15.5	14.4								
		1050	west side center	see notes						0.055	16	17.6								
		1050	center wall- radial	mid-wall																
	12/15/2000 12:05	1770	E side	ground	1820	2809	34.3	129.3	0.24	0.24	24.3	18.8	0.135	15.5	12.88	0.18	11.1	3.8	128	
		1010	east side center	see note						0.195	18.9	6.5	0.28	15	12	0.28	8.2	6.6		
		1010	center wall- east	mid-wall						2.56	13.8	14.1								
		1050	west side center	see notes						0.205	16.5	6.6	0.28	16	12	0.21	14.2	6.6		
		1050	center wall- radial	mid-wall												0.325	17.6	5.8		
L2S-TN	12/12/2000 12:19	1769	NE corner	ground	6110	1676	149.2	515.7	0.055	0.055	32	35.4	0.02	22.2	17.25	0.025	34.1	17.1	106	
		1258	NE corner	first floor corner						0.04	18.2	23.0	0.04		17.38	0.035	24.3	6.9		
		1258	midwall	first floor north wall												0.07	22.2	7.2		
		930	N wall peak	second floor near roof peak						0.05	7.8	7.2	0.04		17.25	0.55	7.3	7.2		
		930	midwall	north wall						mid-wall	not	measured								
	12/12/2000 17:00	1769	NW corner	ground			NOT	TRIGGERED												
	12/15/2000 12:05	1769	NE corner	ground	5230	2809	98.7	371.6	0.195	0.195	32	33.3	0.105	23.2	11.1	0.125	26.9	14.6	120	
		1258	NE corner	first floor corner						0.105	18.2	20.8	0.14	21.3	24.5	0.145	18.9	19.3		
		1258	midwall	first floor north wall													0.26	17.6	7.1	
		930	N wall peak	second floor near roof peak						0.105	18.2	7.1	0.18	21.3	24.75	0.145	8.5	7.1		
		930	midwall	north wall													0.72	21.3	19.8	

## Virginia

Structure	Shot Date and Time	Unit	Structure Location	Placement of Transducer(s)	Distance (ft)	Charge Weight/Delay (lb)	Scaled Distance (ft/lb <sup>1/2</sup> )	Scaled Distance (ft/lb <sup>1/3</sup> )	Peak Particle Velocity (in/sec)	T (in/s)	Peak Frequency (Hz)	FFT Frequency (Hz)	V (in/s)	Peak Frequency (Hz)	R (in/s)	Peak Frequency (Hz)	Airblast (dB)	
TSA-VA	11/06/00 15:58	1769	NE corner	ground	1213	337	66.1	174.6	0.050	0.050	11.9	4.88	0.050	11.6	0.035	12.1	8.25	119
		1050	NE corner	S1					0.040	0.040	7.2	6.75	0.080	12.8	0.040	8.3	8	
			1050	N wall	mid-wall										0.145	18.2	20.13	
			1010	NE corner	S2				0.070	0.070	8.3	6.75	0.080	10.8	0.070	10.8	9.25	
			950	NW corner	S2				0.080	0.080	8.9	6.75	0.060	13.4	0.080	10.6	9.25	
	11/07/00 15:41	1769	NE corner	ground	1300	361	68.4	182.9	0.030	0.030	9.8	9.13	0.015	8.6	0.020	9.6	8	117
		1050	NE corner	S1					0.030	0.030	7.40	7.50	0.040		0.025	9.40	8.13	
		1050	N wall	mid-wall											0.125	18.90	9.25	
		1010	NE corner	S2					0.080	0.080	7.50	7.50	0.040		0.045	8.80	9.25	
		950	NW corner	S2					0.085	0.085	7.80	7.50	0.040	8.60	0.070	8.90	9.25	
	11/08/00 15:46	1769	NE corner	ground	1213	361	63.8	170.7	0.050	0.045	9.10	9.63	0.050	14.60	0.045	10.80	8.88	119
		1050	NE corner	S1					0.045	0.045	7.20	7.00	0.080	12.40	0.050	11.10	8.88	
		1050	N wall	mid-wall											0.135	18.90	21.63	
		1010	NE corner	S2					0.110	0.110	8.10	7.00	0.100	11.30	0.065	9.30	9.00	
		950	NW corner	S2					0.135	0.135	8.5	6.94	0.060	12.8	0.065	8.9	8.94	
	11/09/00 11:56	1769	NE corner	ground	1300	313	73.5	191.8	0.050	0.045	6.8	9.13	0.045	6.8	0.050	10.8	8.25	119
		1050	NE corner	S1					0.050	0.050	6.1	7.13	0.080	8.2	0.045	15.5	8.13	
		1050	N wall	mid-wall											0.245	18.2	8.25	
		1010	NE corner	S2					0.080	0.080	6.8	7.5	0.080	7.2	0.085	8.3	8.13	
		950	NW corner	S2 (3-component)					0.105	0.105	6.4	7.5	0.075	8	0.100	8.3	8.19	
11/10/00 12:21	1769	NE corner	ground	1273	361	67.0	179.1	0.050	0.050	9.4	9.75	0.050	11.1	0.030	13.1	7.75	119	
	1050	NE corner	S1					0.040	0.040	8.3	7	0.080	15.5	0.050	14.2	7.13		
	1050	N wall	mid-wall											0.190	17	21.13		
	1010	NE corner	S2					0.120	0.120	9.8	7.13	0.100	11.1	0.075	8.2	9.63		
	950	NW corner	S2 (3-component)					0.130	0.130	7.3	7.13	0.075	10.6	0.090	9.1	9.63		
11/11/00 13:49	1769	NE corner	ground	1212	361	63.8	170.6	0.060	0.060	12.8	5.88	0.060	9.8	0.045	9.4	6.25	128	
	1050	NE corner	S1					0.060	0.060	8.1	6	0.080	11.6	0.055	8.5	6.13		
	1050	N wall	mid-wall											0.375	7.7	21.25		
	1010	NE corner	S2					0.090	0.090	7.7	7.38	0.080	10	0.090	7.8	6.13		
	950	NW corner	S2 (3-component)					0.100	0.100	6.8	7.38	0.075	9.8	0.105	7.8	6.38		
11/06/00 15:58	1770	NE corner	ground	1390	337	75.7	200.1	0.045	0.045	23.2	9.75	0.035	14.2	0.035	23.2	10.31	118	
	930	NE corner	S1						nm	nm			nm	nm	nm	nm		
	1513	NE corner	S1 (3-component)						0.040	0.040	14.6	4.75	0.045	19.6	0.035	10.6	10.25	
	1258	NE corner	S2						0.070	0.070	10.8	10.31	0.060	24.3	0.190	9.8	10.31	
	1258	N wall	mid-wall												0.060	9.1	10.25	
11/07/00 11:56	1514	NE corner	S2 (3-component)				NOT	TRIGGERED		0.060	8.6	10.25	0.050	24.3	0.060	9.1	10.25	
11/08/00 15:46	1770	NE corner	ground	1360	361	71.6	191.4	0.045	0.045	8.6	11.75	0.035	16.5	0.040	17.6	5.63	116	
	930	NE corner	S1					0.040	0.040	8.000	5.63	0.060	22.2	0.045	17	4.88		
	1513	NE corner	S1 (3-component)					0.040	0.040	7.4	5.25	0.055	14.2	0.040	8.2	5.63		
	1258	NE corner	S2					0.060	0.060	7.7	5.69	0.060	17.6	0.060	8.6	7.06		
	1258	N wall	mid-wall											0.195	9.6	7.13		
	1514	NE corner	S2 (3-component)						0.060	0.060	7.8	7.13	0.055	13.8	0.055	8.2	5.63	
11/09/00 11:56	1770	NE corner	ground	1370	313	77.4	202.2	0.060	0.060	19.6	19.88	0.045	14.6	0.035	19.6	2	116	
	930	NE corner	S1					0.025	0.025	15.5	2	0.040		0.055	22.2	22.38		
	1513	NE corner	S1 (3-component)					0.035	0.035	5.8	7.63	0.050	12.4	0.035	18.2	10.38		
	1258	NE corner	S2					0.035	0.035	16.5	7	0.060	14.2	0.070	8.3	7.63		
	1258	N wall	mid-wall											0.275	11.1	12.63		
	1514	NE corner	S2 (3-component)					0.065	0.065	15.5	7.63	0.050	13.4	0.040	14.6	7		
11/10/00 12:21	1770	NE corner	ground	1375	361	72.4	193.5	0.060	0.060	19.6	11.5	0.035	21.3	0.040	22.2	9.63	119	
	930	NE corner	S1					0.035	0.035	10.6	10.38	0.040		0.050	15.5	5.5		
	1513	NE corner	S1 (3-component)					0.045	0.045	16	5.5	0.040	20.4	0.040	9.3	10.5		
	1258	NE corner	S2					0.060	0.060	10	10.5	0.060	21.3	0.065	7.7	10.38		
	1258	N wall	mid-wall											0.310	7.8	10.5		
	1514	NE corner	S2 (3-component)					0.060	0.060	7.8	10.38	0.045	22.2	0.065	9.6	10.5		
11/11/00 13:49	1770	NE corner	ground					0.045	0.045	18.2	5.88	0.045	7.1	0.045	9.6	5.75	126	
	930	NE corner	S1					0.055	0.055	9.1	5.880	0.060	19.6	0.070	14.6	5.88		
	1258	NE corner	S2					0.090	0.090	8.5	5.88	0.060	8.8	0.090	7.2	6.13		
	1258	N wall	mid-wall											0.450	9.6	10.63		
	1514	NE corner	S2 (3-component)					0.080	0.080	7.5	6	0.060	9.3	0.085	7.6	5.88		

West Virginia Site 1																			
Structure	Shot Date and Time	Unit	Structure Location	Placement of Transducer(s)	Distance (ft)	Charge Weight/Delay (lb)	Scaled Distance (ft/lb <sup>1/3</sup> )	Scaled Distance (ft/lb <sup>1/3</sup> )	Peak Particle Velocity (in/sec)	T (in/s)	Peak Frequency (Hz)	FFT Frequency (Hz)	V (in/s)	Peak Frequency (Hz)	R (in/s)	Peak Frequency (Hz)	FFT Frequency (Hz)	Airblast (dB)	
W3S-VW1	11/27/2000 1659	1769	NE corner	ground	2500	1037	77.6	247.6	0.07	0.045	11.9	15.2	0.045	11.3	0.07	11.1	11.8	12.1	117
		1258	NE corner	S1						0.04	10.6	15.4	0.06	15	0.06	12.1	11.9	12.1	
		1268	N wall	mid-wall											0.11	15.5	12.1		
		900	NE corner	S2						0.065	4.5	4.4	0.18	14.2	0.095	10.4	13.0	7.3	
		900	E wall	mid-wall											0.085	4.6	4.4		
	11/29/2000 1702	1769	NE corner	ground		NOT	TRIGGERED												
		1769	NE corner	ground	4300	2076	94.4	337.9	0.04	0.04	17.6	13.2	0.01		0.04	16.5	13.3	106	
	11/29/2000 956	1258	NE corner	S1						0.03	20.4	13.2	0.02		0.045	13.8	13.0	13.1	
		1268	N wall	mid-wall											0.09	16.5	15.4		
		900	NE corner	S2						0.04	6.7	4.2	0.12	16.5	0.05	16.5	13.3	7.1	
		900	E wall	mid-wall											0.05	8.9	4.2		
	11/29/2000 1700	1769	NE corner	ground		NOT	TRIGGERED												
		1769	NE corner	ground	3880	2076	85.2	304.9	0.06	0.06	13.8	13.5	0.04	21.3	0.05	15.5	13.6	12.7	110
		1258	NE corner	S1						0.055	11.9	13.6	0.06	19.6	0.05	12.1	13.6	12.1	12.6
		1268	N wall	mid-wall											0.14	16	12.7	12.4	16
L1S-WV1		900	NE corner	S2						0.05	7.1	4.3	0.16	15	0.065	13.1	13.4	12.6	12.6
		900	E wall	mid-wall											0.07	8.3	4.3	4.3	
	11/27/2000 1658	1770	SE corner	ground	3400	1037	105.6	336.7	0.09	0.065	13.1	11.6	0.055	17	0.09	13.4	18.5	13.1	114
		1010	SE corner	S1						0.095	13.1	13.1	0.1	22.2	0.08	11.9	18.4	10.8	11.7
		1010	E wall	mid-wall						0.29	16	15.7							
		1050	SE corner	S2						0.08	14.6	13.1	0.1	23.2	0.11	10.8	18.4	7.6	
		1050	S wall	mid-wall											0.24	16.5	16.5	13.1	
	11/28/2000 1702	1770	SE corner	ground	2410	126	214.7	481.5	0.025	0.02	18.2	12.0	0.01		0.025	16.5	2.7	12.4	106
		1010	SE corner	S1						0.025	15.5	12.8	0.045	11.6	0.025	10.4	5.9	12.3	12.3
		1010	E wall	mid-wall							11.6	11.6							
		1050	SE corner	S2						0.03	17	7.8	0.02		0.03	9.4	12.8	9.4	7.9
		1050	S wall	mid-wall											0.06	17		15.6	
	11/29/2000 956	1770	SE corner	ground	4640	2076	101.8	364.7	0.075	0.075	15	11.4	0.035	18.2	0.04	20.4	2.1	14.8	106
		1010	SE corner	S1						0.045	18.2	14.8	0.08	19.6	0.09	17.6	14.8	11.5	
		1010	E wall	mid-wall						0.195	17	19.0							
		1050	SE corner	S2						0.07	18.2	19.2	0.06	23.2	0.075	8.1	14.6	7.8	
	1050	S wall	mid-wall											0.21	18.2	19.1	19.1		
11/29/2000 1702	1770	SE corner	ground	2240	234	146.4	364.2	0.03	0.025	16	12.3	0.02	11.9	0.03	14.2	2.6	12.6	116	
	1010	SE corner	S1						0.035	13.4	12.6	0.040		0.03	14.6	7.9	12.3		
	1010	E wall	mid-wall						0.085	16.5	13.3								
	1050	SE corner	S2						0.045	10.6	7.8	0.02		0.05	8.5	7.9	7.6		
	1050	S wall	mid-wall											0.075	17		13.2		
11/30/2000 1155	1770	SE corner	ground	4420	2076	97.0	347.4	0.07	0.07	13.1	11.9	0.05	18.2	0.05	13.1	18.3	12.4	110	
	1010	SE corner	S1						0.06	17	12.4	0.1	20.4	0.075	17.6	18.3	11.9		
	1010	E wall	mid-wall						0.23	14.2	14.7								
	1050	SE corner	S2						0.065	17	12.6	0.08	24.3	0.08	10.4	18.3	8.1		
	1050	S wall	mid-wall											0.24	17.6	19.5	19.5		
12/1/2000 1706	1770	SE corner	ground	2400	144		200.0	458.6	0.025	0.02	15.5	11.8	0.1		0.025	14.2	3.8	12.5	110
	1010	SE corner	S1						0.025	15.5	12.6	0.02		0.025	16	8.1	8.1	7.7	
	1010	E wall	mid-wall						0.06	17	13.6								
	1050	SE corner	S2						0.025	18.2	8.1	0.065	17.6	0.03	9.6	19.4	7.8		
	1050	S wall	mid-wall											0.065	17.6	19.4	19.4	19.4	

Structure	West Virginia Site 2																		
	Shot Date and Time	Unit	Structure Location	Placement of Transducer(s)	Distance (ft)	Charge Weight/Delay (lb)	Scaled Distance (ft/lb <sup>1/3</sup> )	Scaled Distance (ft/lb <sup>1/3</sup> )	Peak Particle Velocity (in/sec)	T (in/s)	Peak Frequency (Hz)	FFT Frequency (Hz)	V (in/s)	Peak Frequency (Hz)	FFT Frequency (Hz)	R (in/s)	Peak Frequency (Hz)	FFT Frequency (Hz)	Airblast (dB)
TD-WV2	12/4/2000 12:23	1769	NW corner	ground	1870	481	85.3	239.2	0.095	0.095	10.6	7.3	0.085	13.1	7.25	0.09	12.4	7.3	112
		930	N end-middle	S1					0.305	8.9	7.3	7.3	0.12	16.5	7.19	0.085	7.6	7.3	
		930	W wall	mid-wall					0.49	8.6	7.3		0.14	15					
		1258	N end-middle	S2					0.39	7.5	7.3		0.14	15	7.25	0.135	9.1	7.2	
		1258	N wall	mid-wall										0.285	21.3	25.0	21.3	25.0	
	12/4/2000 5:01	1769	NW corner	ground	2410	415	118.3	323.7	0.06	0.055	23.2	6.9	0.05	25.6	14.4	0.06	16.5	6.4	112
		930	N end-middle	S1					0.075	16.5	16.5	7.1	0.08	20.4	14.3	0.04	16	6.4	
		930	W wall	mid-wall					0.115	15	15	7.1	7.1						
		1258	N end-middle	S2					0.065	6	6	7.1	7.1	0.08	23.2	15.9	0.08	11.9	11.2
		1258	N wall	mid-wall										0.175	24.3	24.4	24.3	24.4	
	12/5/2000 12:05	1769	NW corner	ground	2600	973	83.4	263.0	0.05	0.04	14.6	8.9	0.035	15.5	8.5	0.05	6.8	6.3	117
		930	N end-middle	S1					0.08	11.9	11.9	6.8	0.06	22.2	14.1	0.045	9.4	6.3	
		930	W wall	mid-wall					0.11	13.8	13.8	6.8	0.08	18.9	14.1	0.045	9.4	6.3	
		1258	N end-middle	S2					0.085	8.9	8.9	6.8	0.08	18.9	14.25	0.085	7.4	6.3	
		1258	N wall	mid-wall										0.085	14.25	14.25	0.085	7.4	6.3
	12/5/2000 16:55	1769	NW corner	ground	2670	901	89.0	277.1	0.03	0.025	20.4	7.1	0.015	21.3	15.06	0.03	7.2	6.4	112
	930	N end-middle	S1					0.06	7.3	7.3	7.4	0.02	7.4	14.7	0.025	8.1	6.3		
	930	W wall	mid-wall					0.085	7	7	7.4	7.4	0.085	7	15.1	0.03	5.8	6.4	
	1258	N end-middle	S2					0.085	6.9	6.9	7.4	7.4	0.04		15.1	0.03	5.8	6.4	
	1258	N wall	mid-wall										0.015	15	15	0.025	22.2	6.5	
12/6/2000 12:22	1769	NW corner	ground	2630	901	87.6	272.9	0.025	0.025	15.5	15.1	0.015	17	15	14.8	0.025	10.8	9.5	112
	930	N end-middle	S1					0.04	12.8	12.8	7.3	0.04	10.4	13.2	0.04	10.4	5.7	106	
	930	W wall	mid-wall					0.065	11.9	11.9	7.3	0.065	11.9	15.7	0.06	11.3	6.8	116	
	1258	N end-middle	S2					0.05	12.1	12.1	7.3	0.04		15.2	0.045	11.6	11.3		
	1258	N wall	mid-wall										0.065	23.2	0.065	23.2	11.3		
12/6/2000 16:52	1769	NW corner	ground	1730	452	81.4	225.9	0.085	0.085	11.6	7.1	0.065	18.2	14.9	0.075	7.4	7.2	117	
	930	N end-middle	S1					0.175	7.4	7.4	7.2	0.12	16	15	0.08	13.4	7.1		
	930	W wall	mid-wall					0.255	8.8	8.8	7.2	7.2	0.175	16	15	0.08	13.4	7.1	
	1258	N end-middle	S2					0.215	7.4	7.4	7.2	7.2	0.14	15	15	0.1	8.1	7.2	
	1258	N wall	mid-wall										0.025	22.2	22.2	0.025	24.3	7.2	
12/7/2000 12:13	1769	NW corner	ground	2600	793	92.3	281.5	0.04	0.02	21.3	7.1	0.02	14.6	13.2	0.04	10.4	5.7	106	
	930	N end-middle	S1					0.04	12.4	12.4	7.1	7.1	0.04	13	13	0.035	11.1	11.4	
	930	W wall	mid-wall					0.06	13.1	13.1	7.1	7.1	0.06	13.4	11.8	0.055	10.8	11.5	
	1258	N end-middle	S2					0.05	8.9	8.9	7.1	7.1	0.06	13.4	11.8	0.055	10.8	11.5	
	1258	N wall	mid-wall										0.09	21.3	21.3	0.09	21.3	11.5	
12/4/2000 12:23	1770	NW corner	ground	1720	481		78.4	220.0	0.115	0.11	10.6	7.7	0.085	17.6	14.8	0.115	12.8	8.1	112
	1010	all horizontal	upper corner/beam						0.115	13.1	8.9	7.4	0.115	13.1	8.13	0.19	11.9	7.5	
	1010	air channel	vertical on rafter										0.14	17.6	18.63				
	1050	all horizontal	west wall/first floor						0.23	19.6	7.4	7.4	0.145	7.2	7.44	0.08	16.5	11.6	
	1050	air channel	vertical on post										0.145	7.2	7.44				
12/4/2000 5:01	1770	NW corner	ground	2310	415		113.4	310.3	0.035	0.03	13.1	7.4	0.035	18.9	15.63	0.035	15.5	8.1	114
	1010	all horizontal	upper corner/beam						0.055	20.4	20.4	6.4	0.04	22.2	6.06	0.035	19.6	6.4	
	1010	air channel	vertical on rafter										0.06	25.6	19.6				
	1050	all horizontal	west wall/first floor						0.08	24.3	6.5	6.5	0.05	12.4	6.5	0.035	24.3	21.4	
	1050	air channel	vertical on post										0.04		19.56				
12/5/2000 12:05	1770	NW corner	ground	2500	973		80.1	252.9	0.04	0.03	12.1	8.3	0.04	14.2	11.2	0.035	11.6	8.1	117
	1010	all horizontal	upper corner/beam						0.055	13.1	13.1	5.2	0.055	5.8	6.63	0.07	16.5	6.5	
	1010	air channel	vertical on rafter						0.04	9.6	6.3	6.3	0.045	7.2	6.5	0.045	13.4	7.0	
	1050	all horizontal	west wall/first floor						0.075	15	15	6.6	0.065	10.8	10.84	0.045	17	10.8	
12/5/2000 4:54	1770	NW corner	ground	2110	625		84.4	247.3	0.05	0.025	14.2	6.9	0.05	14.6	15.6	0.045	15	8.3	119
	1010	all horizontal	upper corner/beam						0.06	6.8	6.8	6.3	0.065	6.6	6.75	0.065	6.4	6.3	
	1010	air channel	vertical on rafter										0.04		6.75				
	1050	all horizontal	west wall/first floor						0.085	6.4	6.4	6.3	0.065	8	6.25	0.04	22.2	13.1	
12/5/2000 12:05	1770	NW corner	ground	2500	973		80.1	252.9	0.04	0.03	12.1	8.3	0.04	14.2	11.2	0.035	11.6	8.1	117
	1010	all horizontal	upper corner/beam						0.055	13.1	13.1	5.2	0.055	5.8	6.63	0.07	16.5	6.5	
	1010	air channel	vertical on rafter						0.04	9.6	6.3	6.3	0.045	7.2	6.5	0.045	13.4	7.0	
12/5/2000 4:55	1770	NW corner	ground	2550	901		85.0	264.6	0.025	0.015	30.1	8.3	0.025	18.9	14.7	0.02	18.9	8.4	117
	1010	all horizontal	upper corner/beam						0.04	9.6	6.3	6.3	0.045	7.2	6.5	0.045	13.4	7.0	
	1010	air channel	vertical on rafter						0.055	19.6	7.1	7.1	0.03	23.2	7.06	0.02	22.2	11.9	
	1050	all horizontal	west wall/first floor						0.025	13.1	13.4	13.4	0.025	18.2	15.1	0.025	14.6	8.2	114
12/6/2000 12:22	1770	NW corner	ground	2510	901		83.6	260.5	0.025	0.04	11.6	6.3	0.04	6.6	6.5	0.035	11.9	6.3	
	1010	all horizontal	upper corner/beam										0.04		14				
	1010	air channel	vertical on rafter						0.045	10.6	6.3	6.3	0.04	11.6	6.25	0.025	19.6	12.3	
	1050	all horizontal	west wall/first floor										0.02		14				
12/6/2000 4:52	1770	NW corner	ground	1610	452		75.7	210.2	0.09	0.09	10.6	7.3	0.075	15.5	15.31	0.065	15.5	8.6	120
	1010	all horizontal	upper corner/beam						0.11	11.3	11.3	7.2	0.09	8	6.44	0.115	12.1	7.3	
	1010	air channel	vertical on rafter										0.08	20.4	8.2				
	1050	all horizontal	west wall/first floor						0.135	18.2	7.2	7.2	0.115	12.4	7.2	0.06	24.3	12.5	
	1050	air channel	vertical on post						0.02	25.6	3.8	3.8	0.06	32	8.3	0.03	14.2	8.1	106
12/7/2000 12:13	1770	NW corner	ground	2480	793		88.1	268.5	0.03	0.02	26.6	3.8	0.025	14.6	13	0.03	14.2	8.1	106
	1010	all horizontal	upper corner/beam						0.035	4.3	3.8	3.8	0.045	6	5.7	0.035	4	3.8	
	1050	all horizontal	west wall/first floor						0.045	28.4	3.8	3.8	0.035	5.8	10.94	0.025	5.3	12.8	
	1050	air channel	vertical on post						0.02				0.02		11				

## APPENDIX IV

### Typical Waveform Time Histories

Appendix IV contains typical ground motion, airblast, and time-correlated structure response time histories. Data for specific shots were selected based on the largest airblast and significant ground motion amplitudes resulting the in highest structures responses. These are considered to be representative “worst case” shot records in this study.

Peak velocities are provided for each waveform. In the case of superimposed waveforms, the range in velocities provided refers to the peak velocity for each waveform. For clarification, the reader is directed to Appendix III.

The following table summarized the structure designation, shot data and time for selected time histories:

Structure Design	Designation	Shot date	Shot time
Trailer	TS-KY2	11/21/00	15:35
	TS-IN	8/20/01	12:30
	TD-WV2	12/06/00	16:52
	TSA-KY	11/21/00	14:39
	TS-OH	3/28/00	16:23
Log	L2S-WV2	12/06/00	16:52
	L2S-TN	12/15/00	12:05
	L2S-OH	3/16/01	14:43
	L1S-WV1	11/29/00	17:02
	L1S-OH	3/16/01	14:42
Earth and masonry	E1S-NMA	7/26/01	14:55
	E1S-NMB	7/26/01	14:55
	E2S-NM	7/26/01	14:55
Camp	C1S-VA	11/11/00	13:49
	C2S-KYIA	11/15/00	11:48



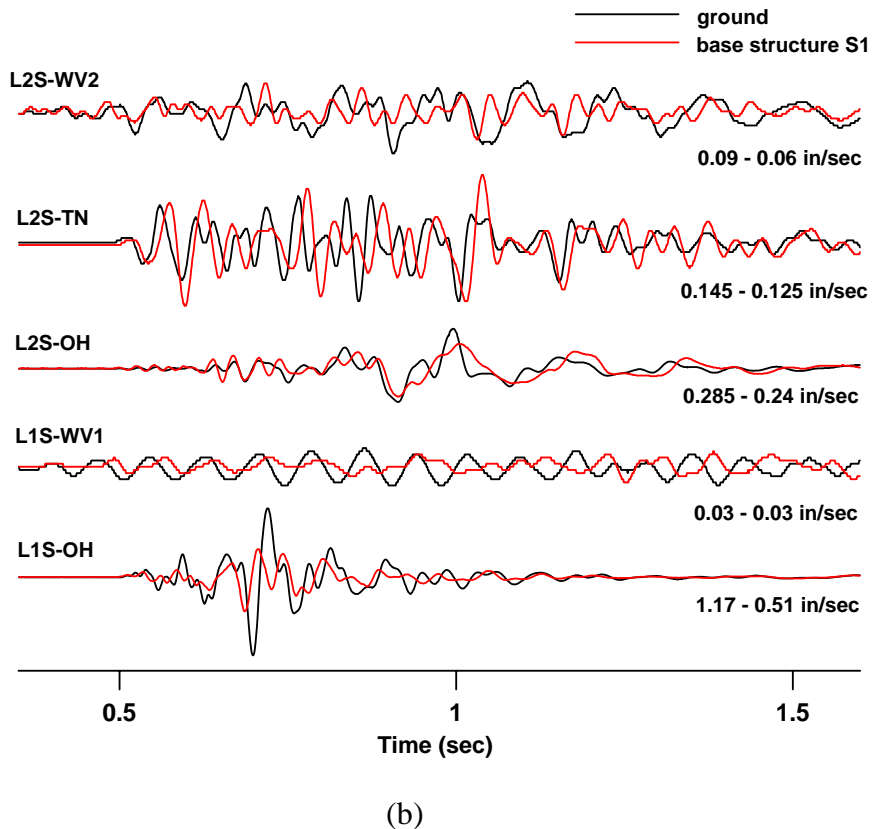
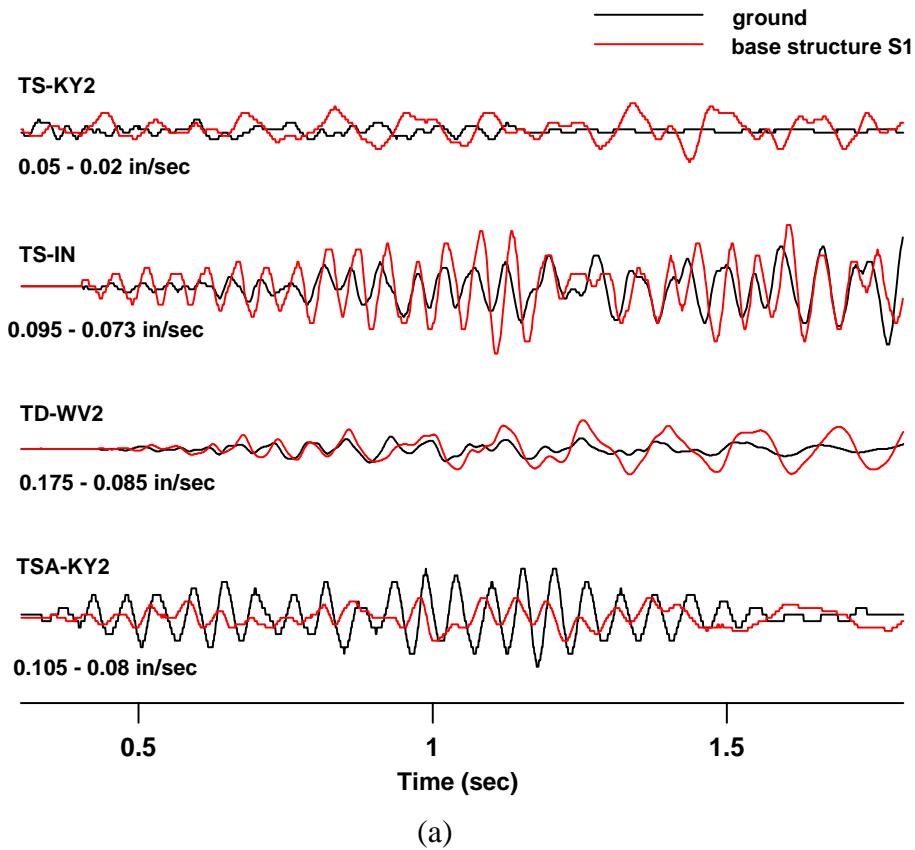
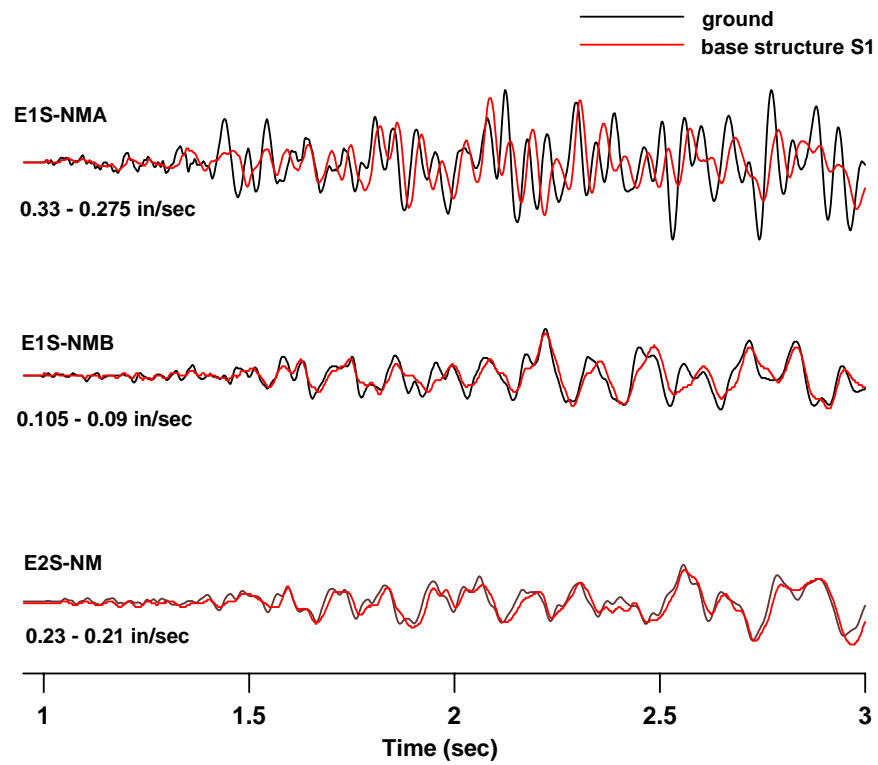
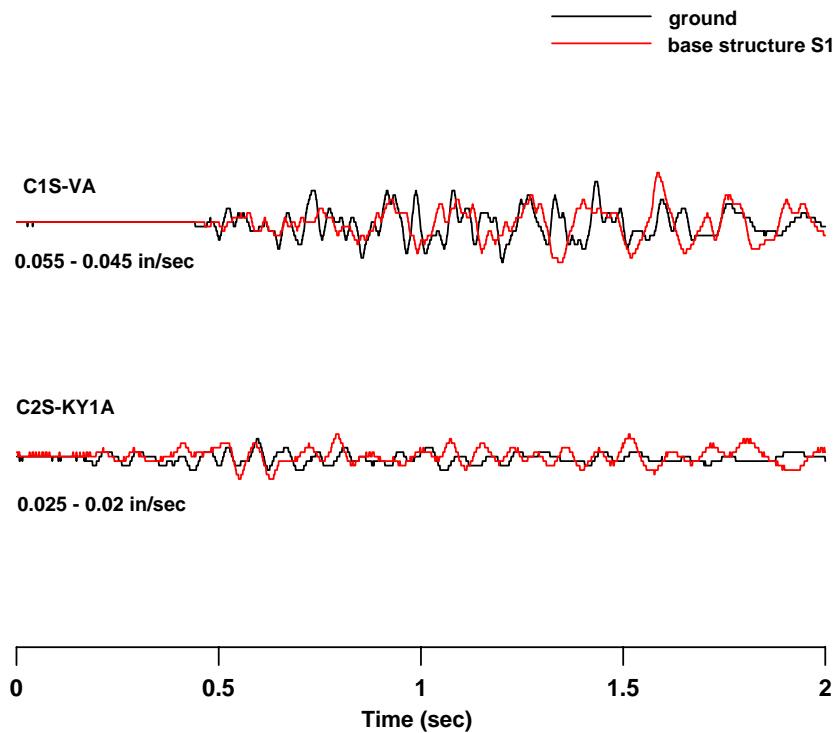


Figure IV-1 Horizontal components of ground motion and lower structure for (a) manufactured and (b) log structures

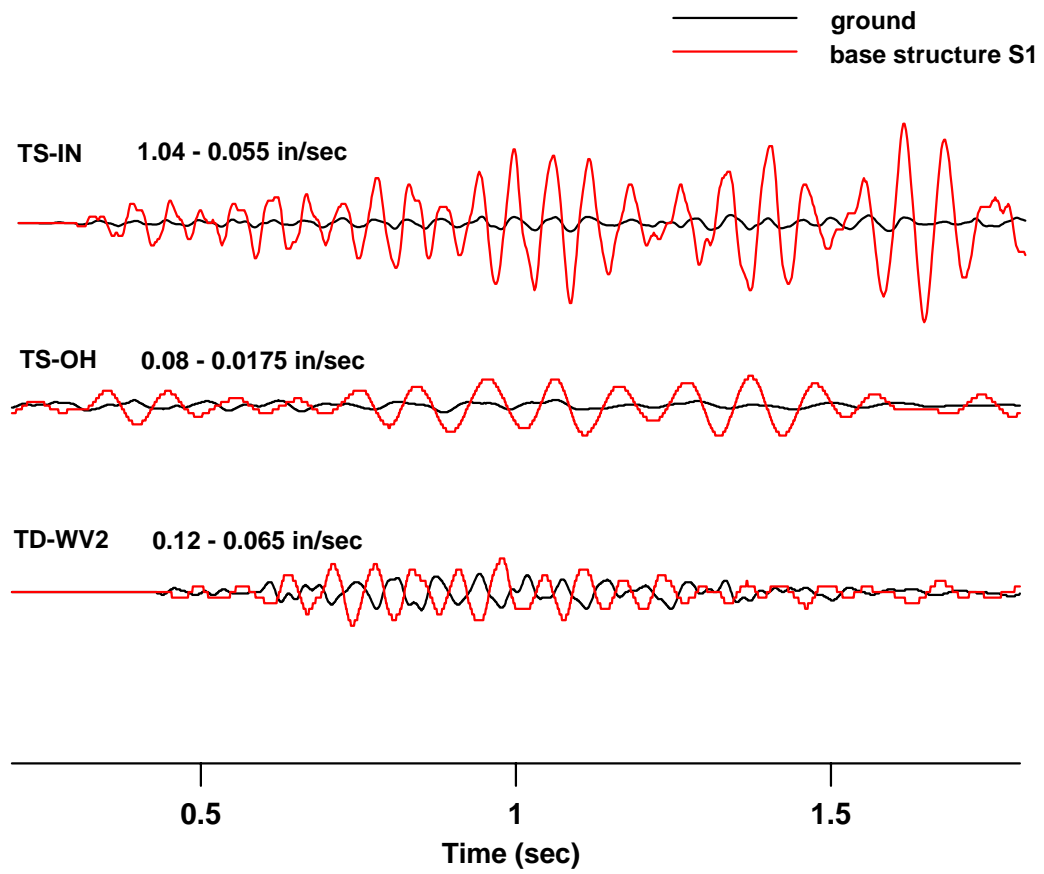


(c)



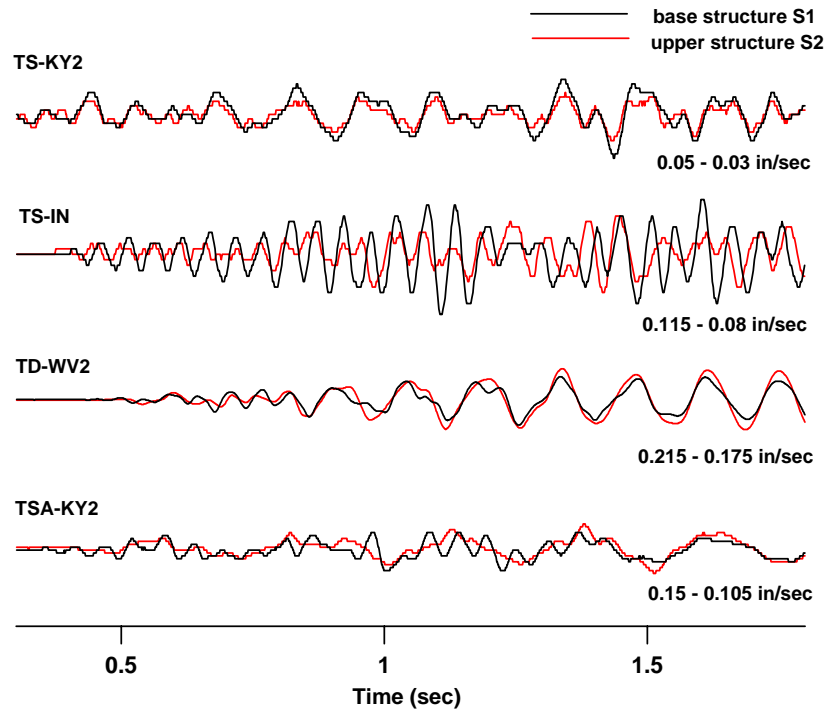
(d)

Figure IV-1 (cont.) Horizontal components of ground motion and lower structure for (c) earth and masonry and (d) camp structures

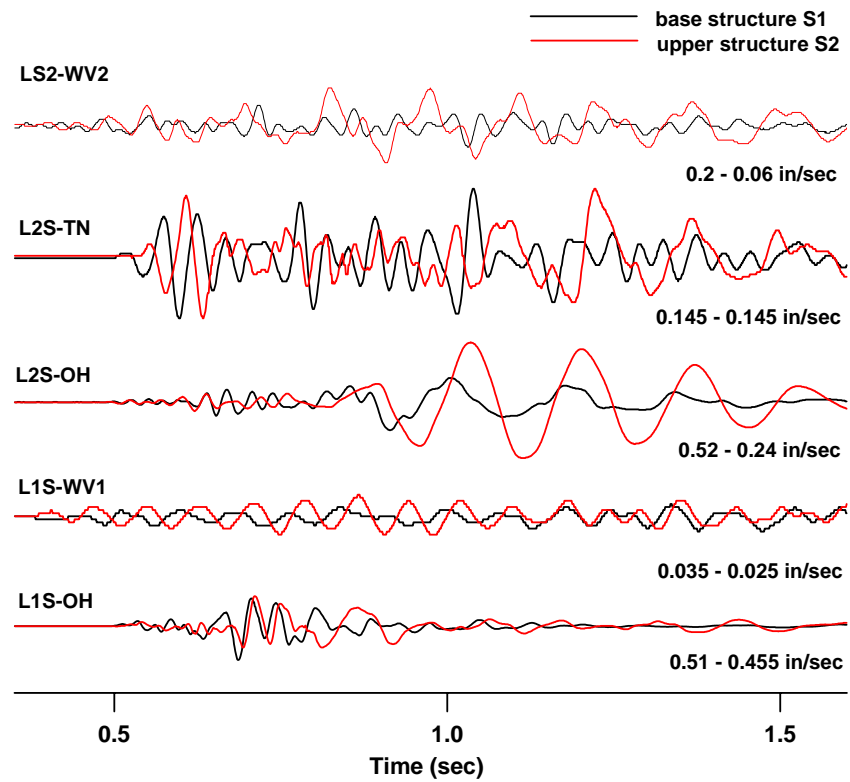


(e)

Figure IV-1 (cont.) Vertical components of ground motion and lower structure for (e) single and double wide trailers

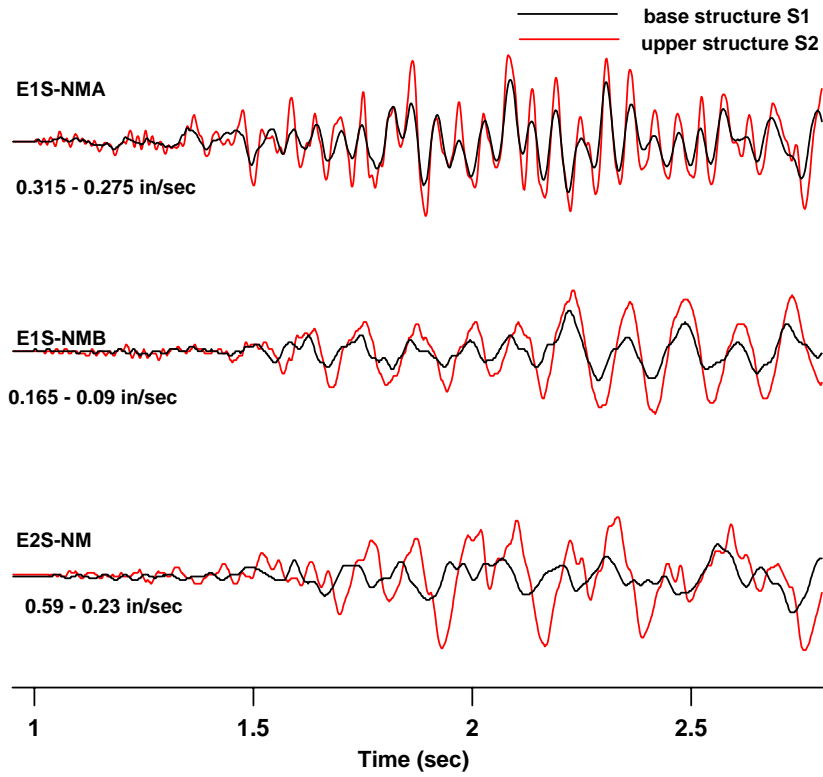


(a)

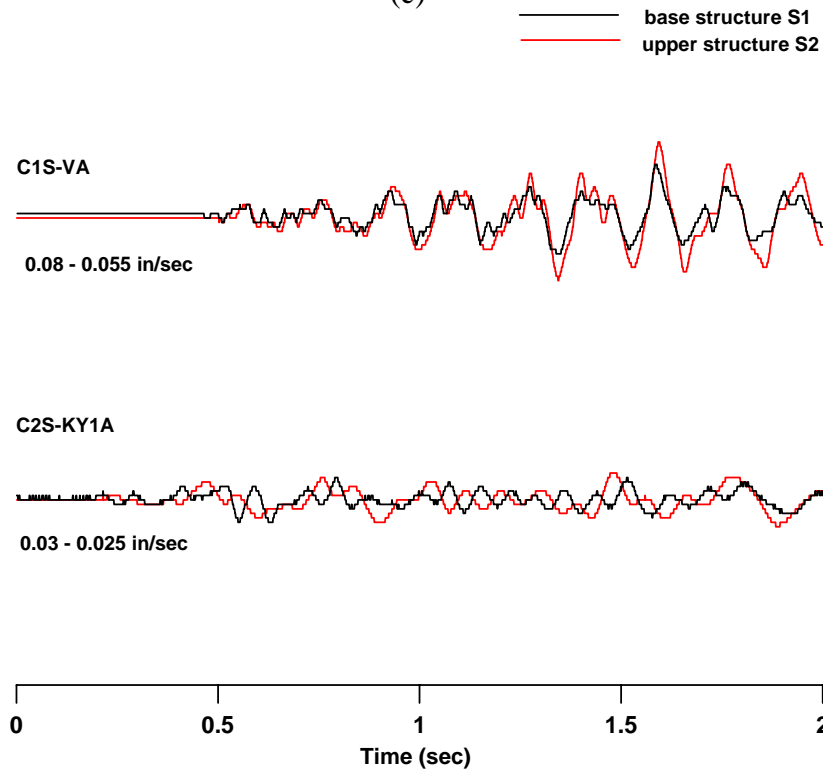


(b)

Figure IV-2 Horizontal components of lower and upper structure response for (a) manufactured and (b) log structures



(c)



(d)

Figure IV-2 Horizontal components of lower and upper structure response for (c) ) earth and masonry and (d) camp structures

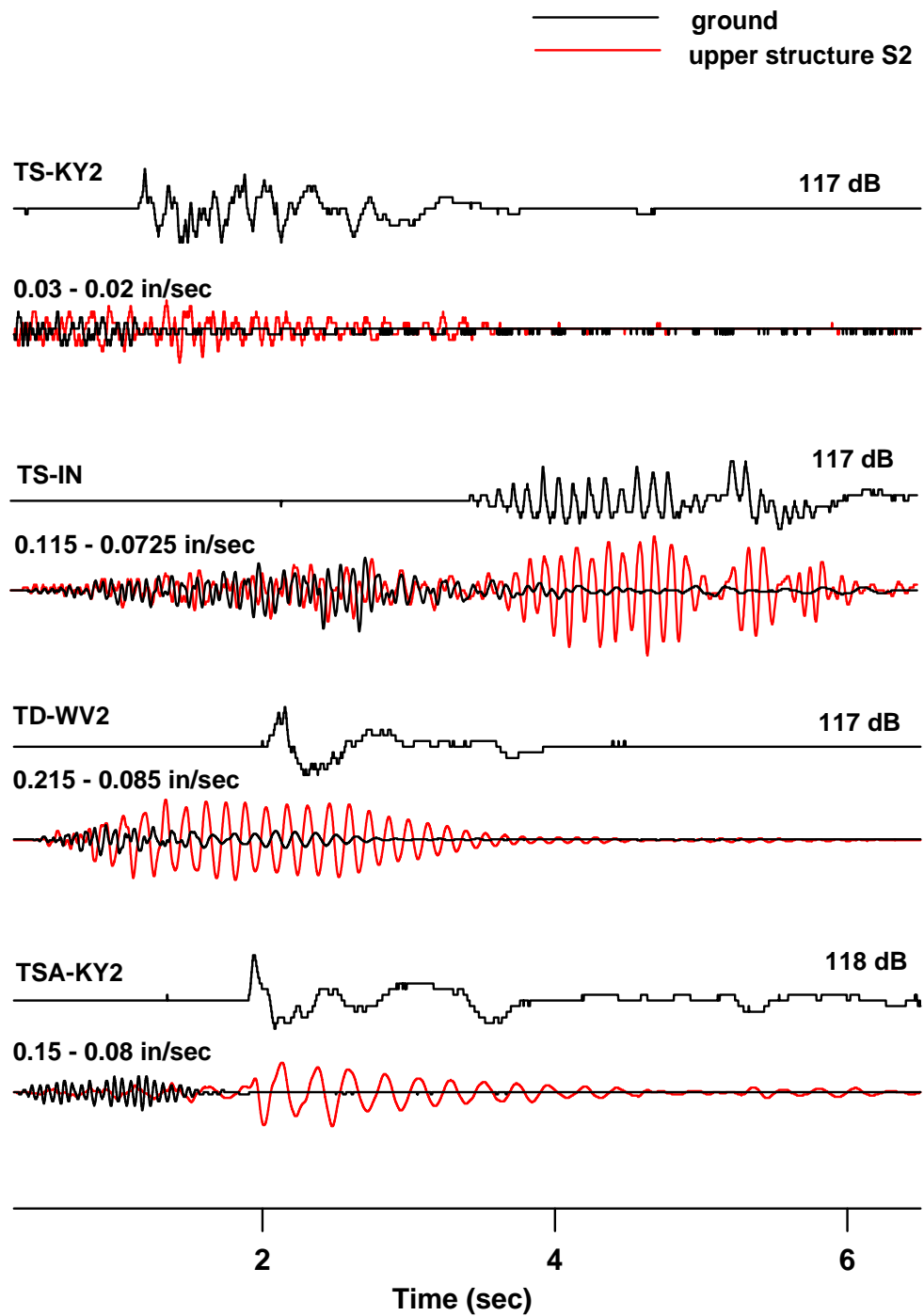


Figure IV-3 Horizontal components of ground motions and upper structure response and air overpressures for manufactured structures

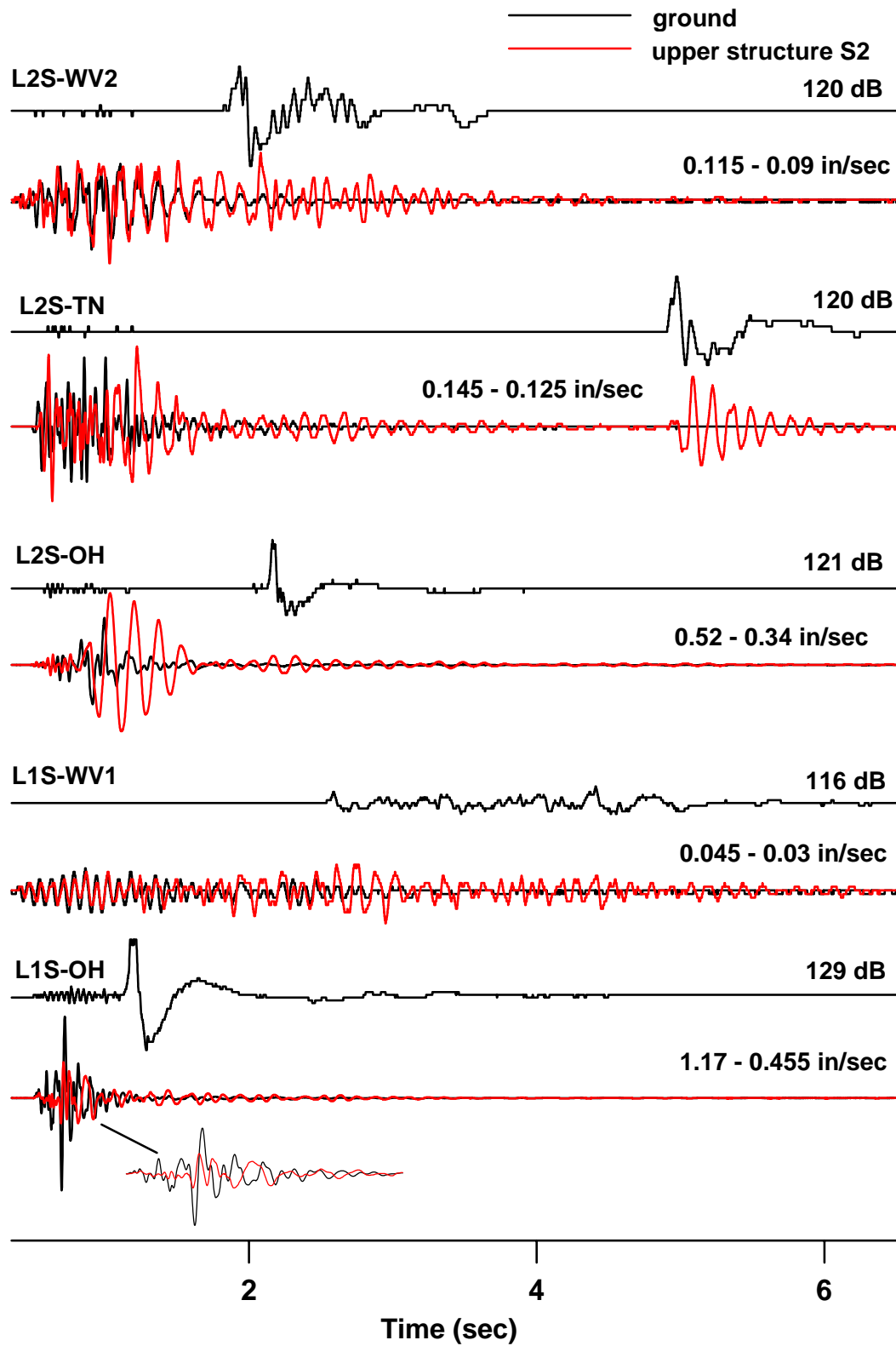


Figure IV-4 Horizontal components of ground motions and upper structure response and air overpressures for log structures

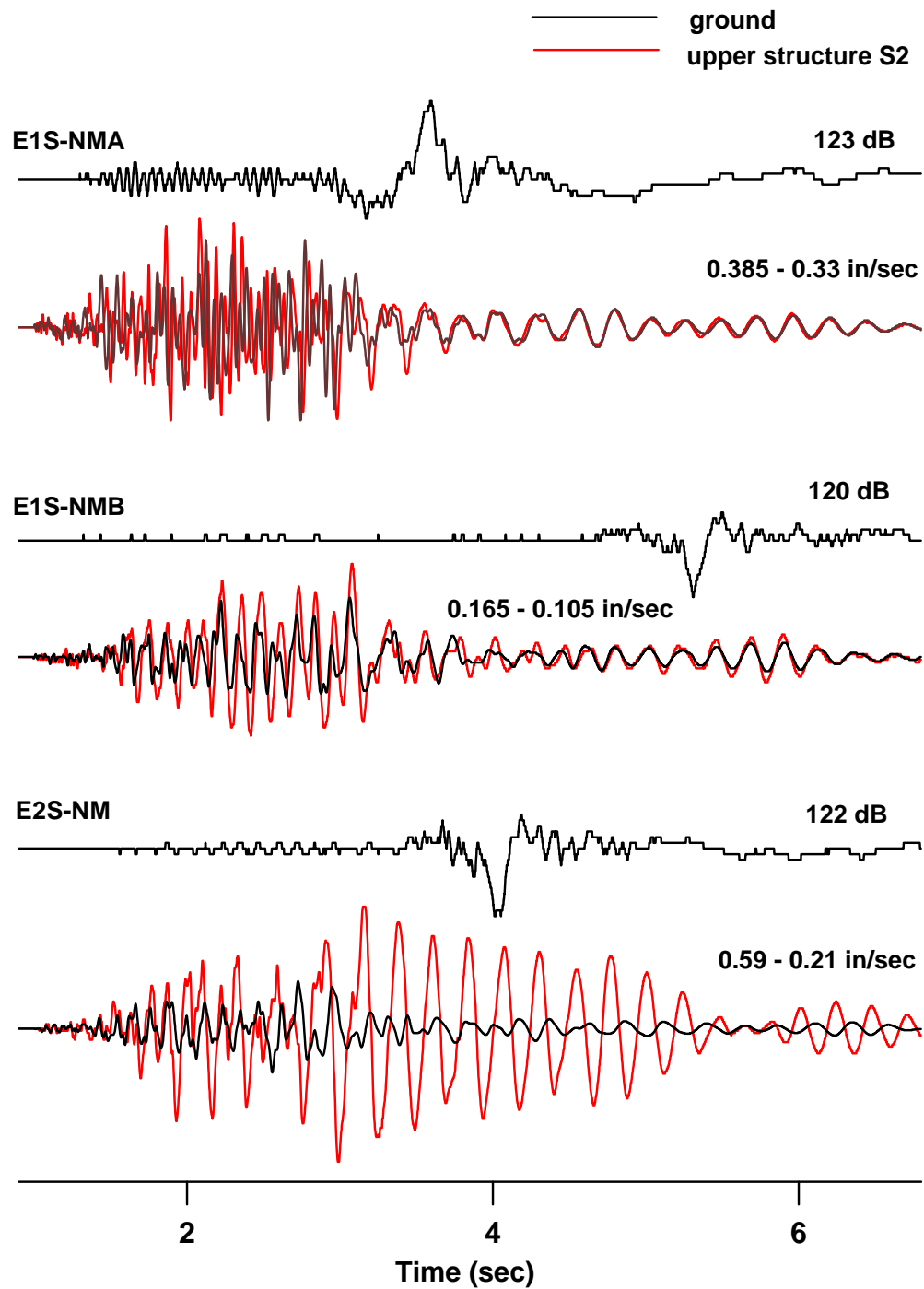


Figure IV-5 Horizontal components of ground motions and upper structure response and air overpressures for earth, masonry, and stone structures



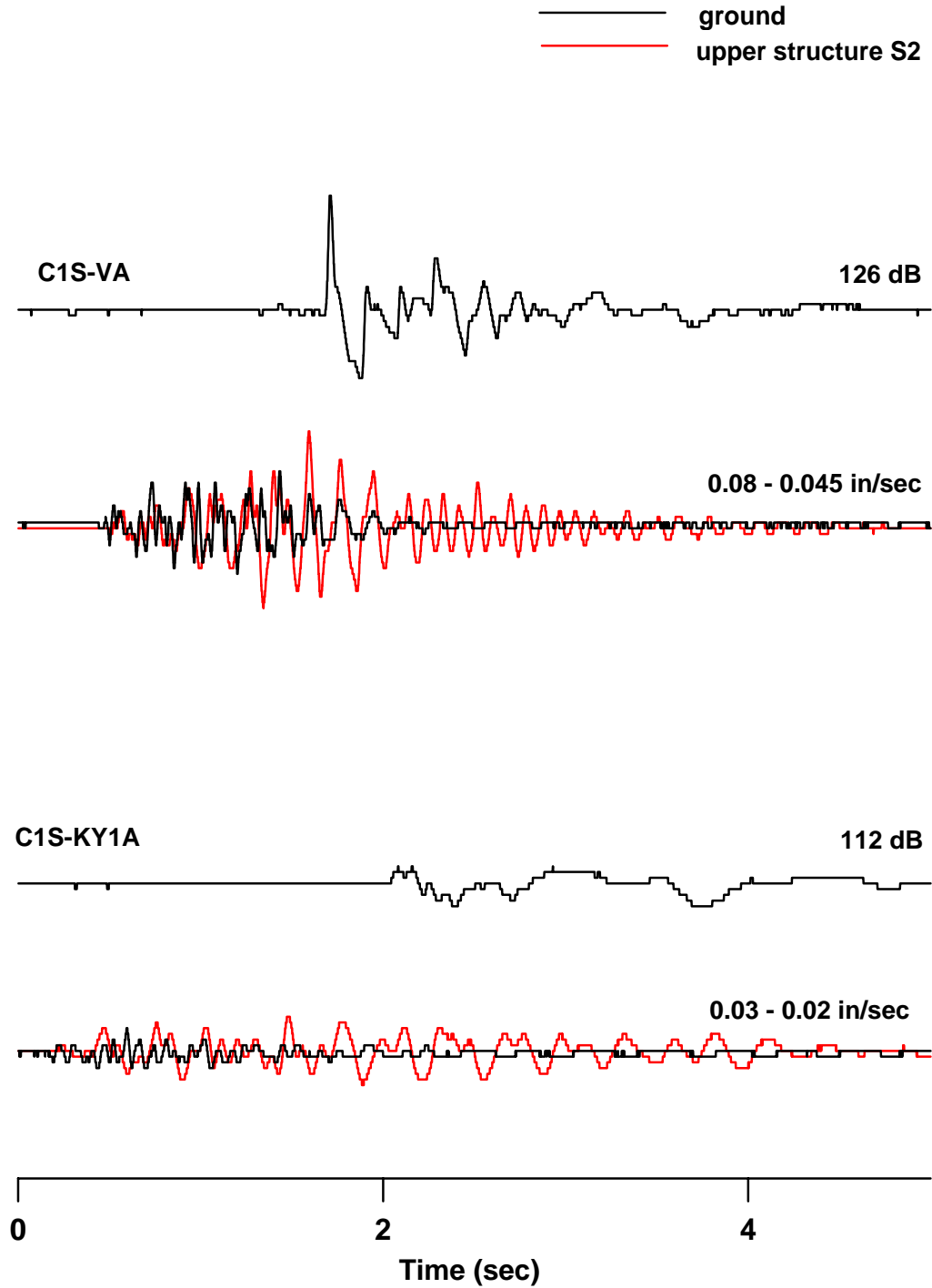


Figure IV-6 Horizontal components of ground motions and upper structure response and air overpressures for camp structures

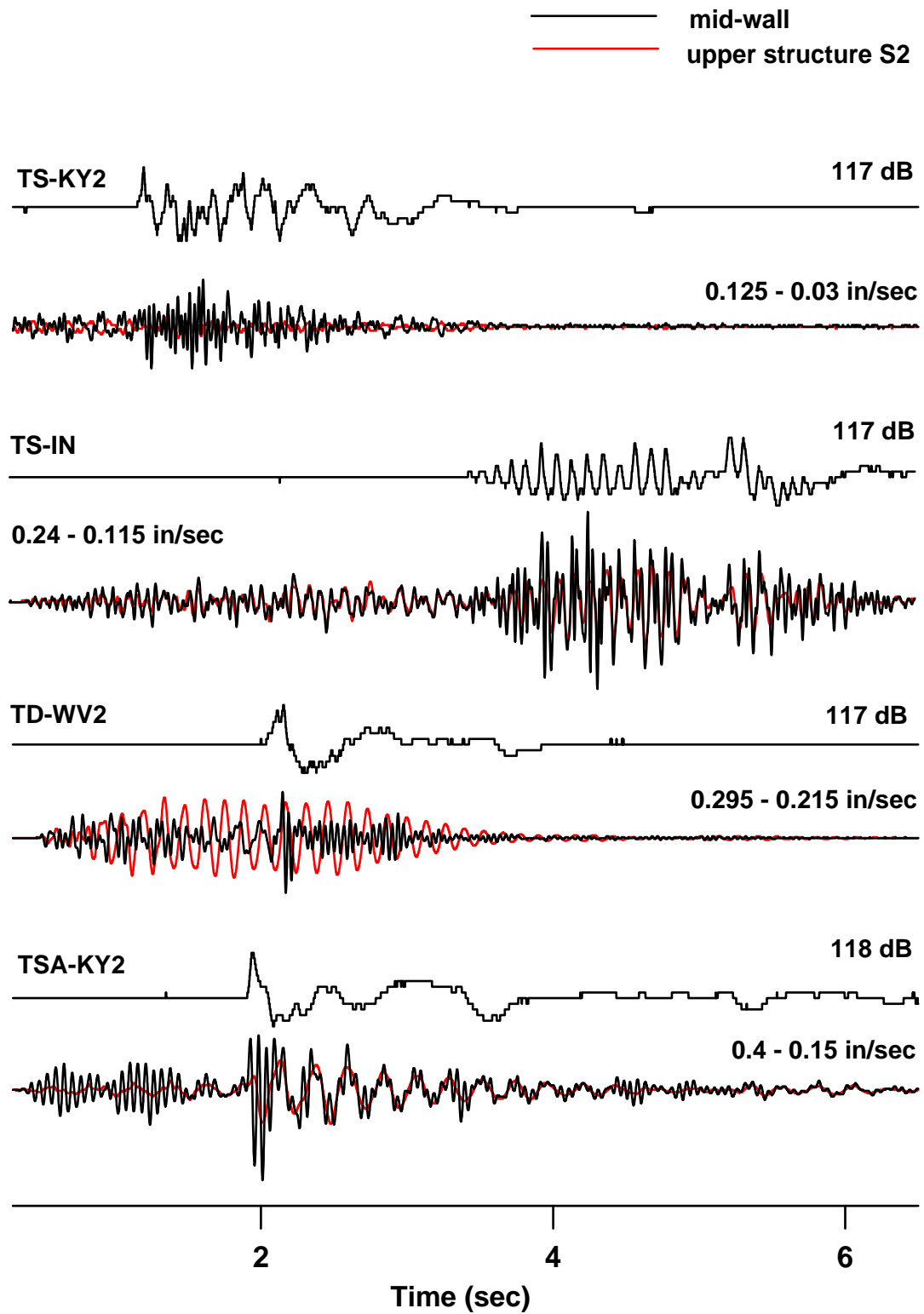


Figure IV-7 Horizontal components of upper structure and mid-wall responses and air overpressures for manufactured structures

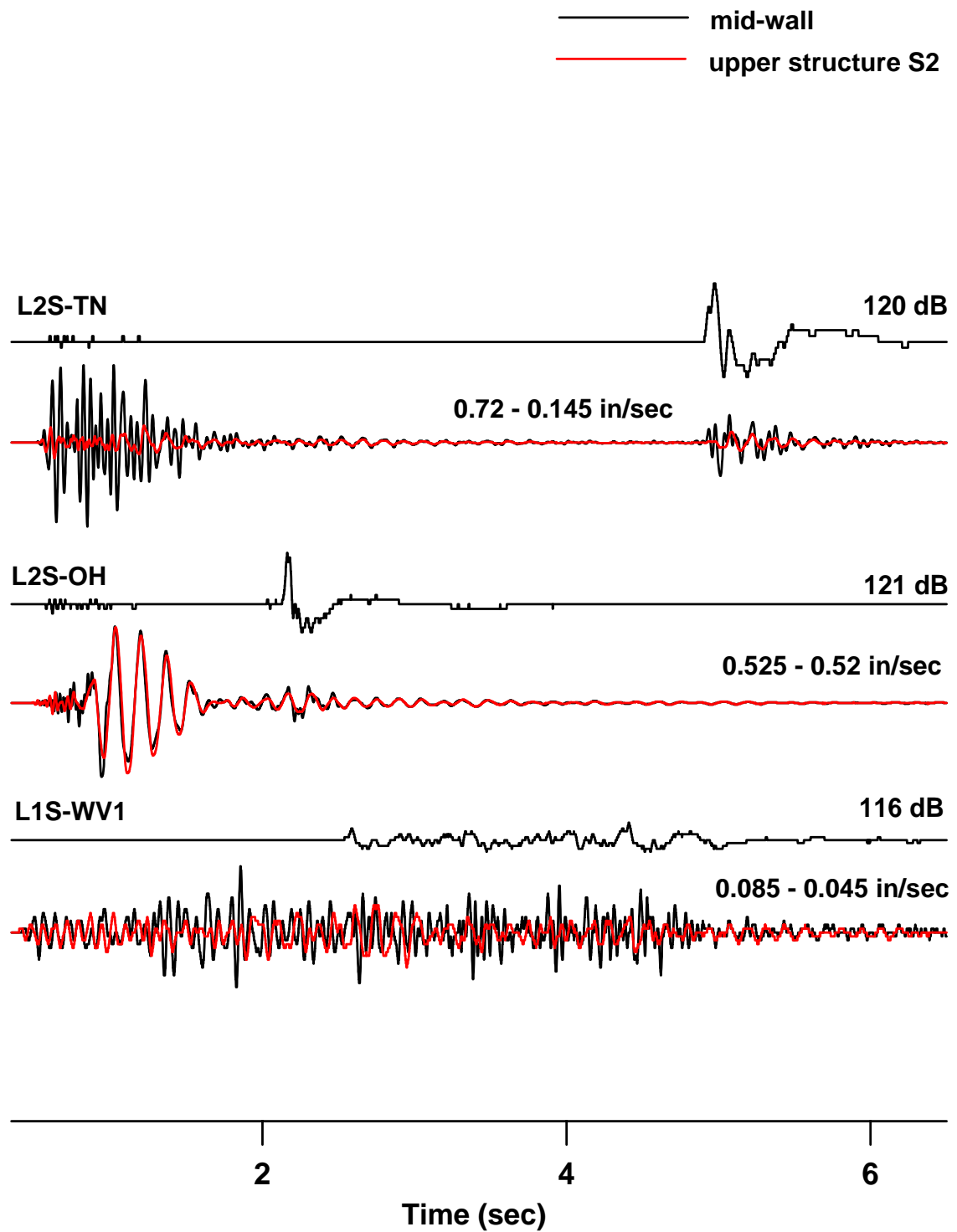


Figure IV-8 Horizontal components of upper structure and mid-wall responses and air overpressures for log structures

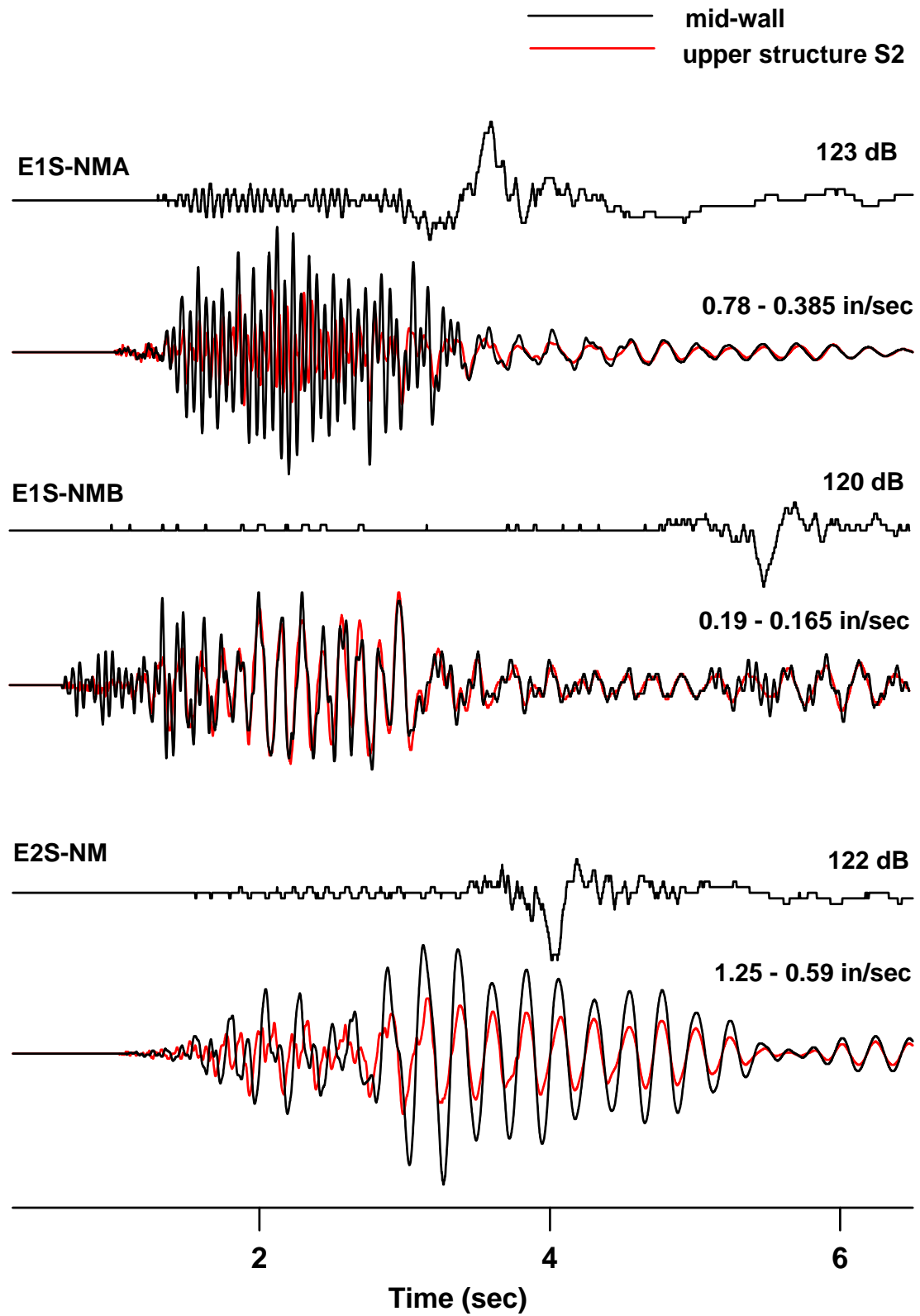


Figure IV-9 Horizontal components of upper structure and mid-wall responses and air overpressures for earth and masonry structures

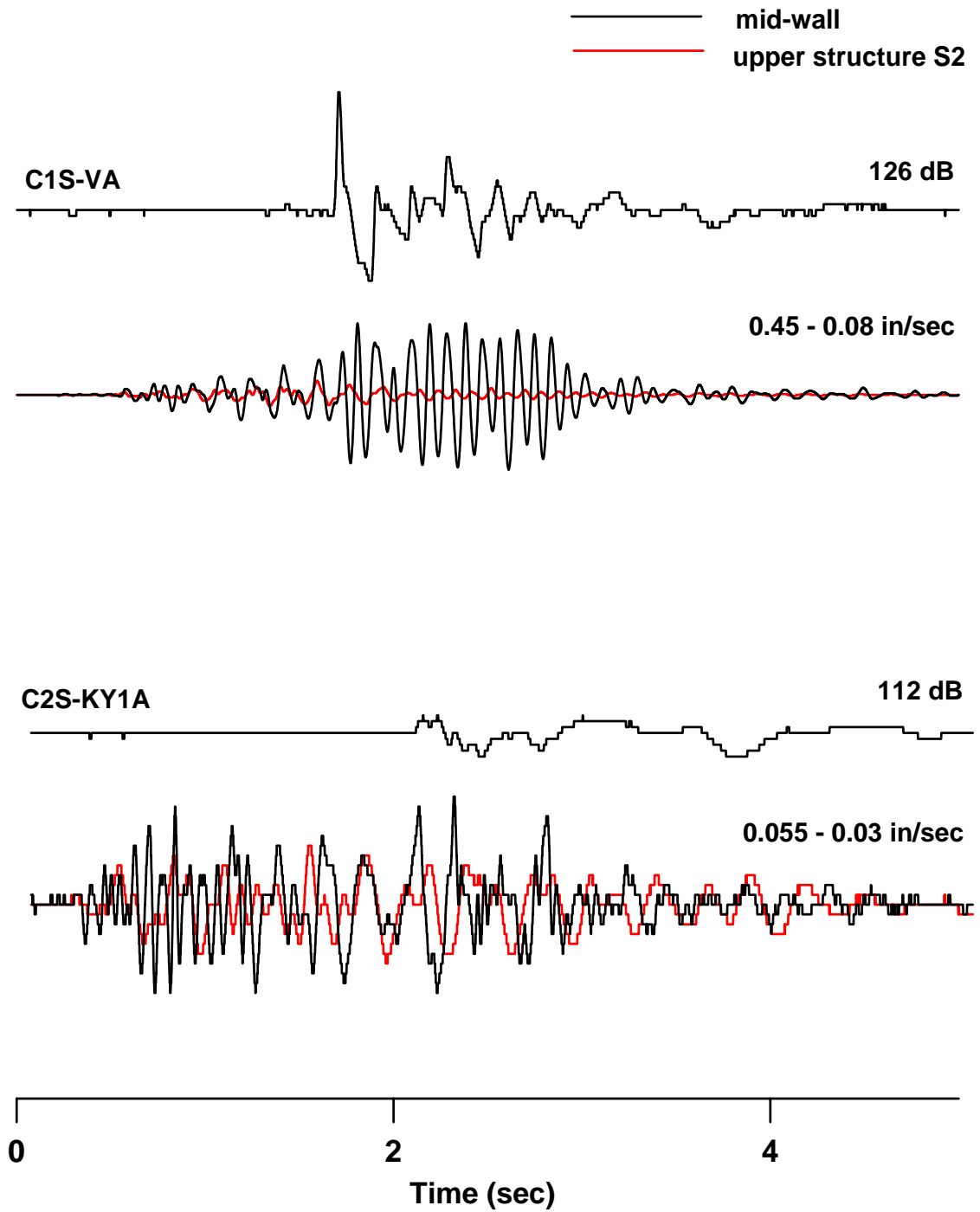
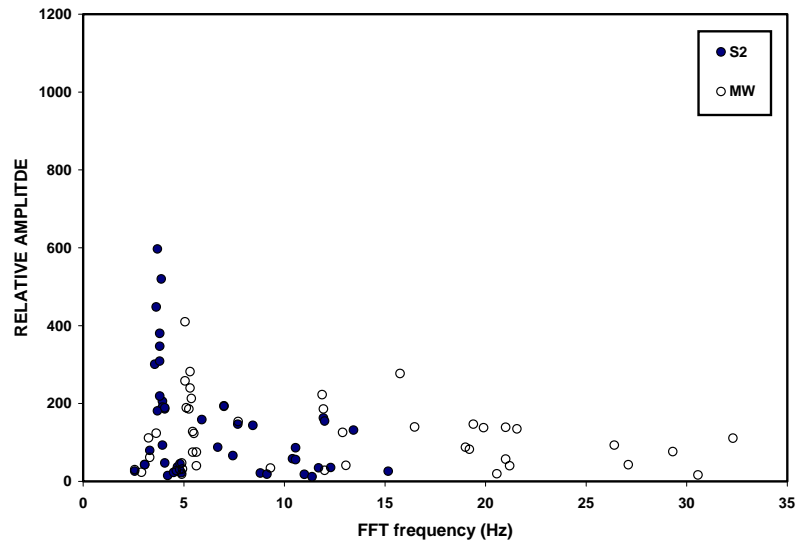


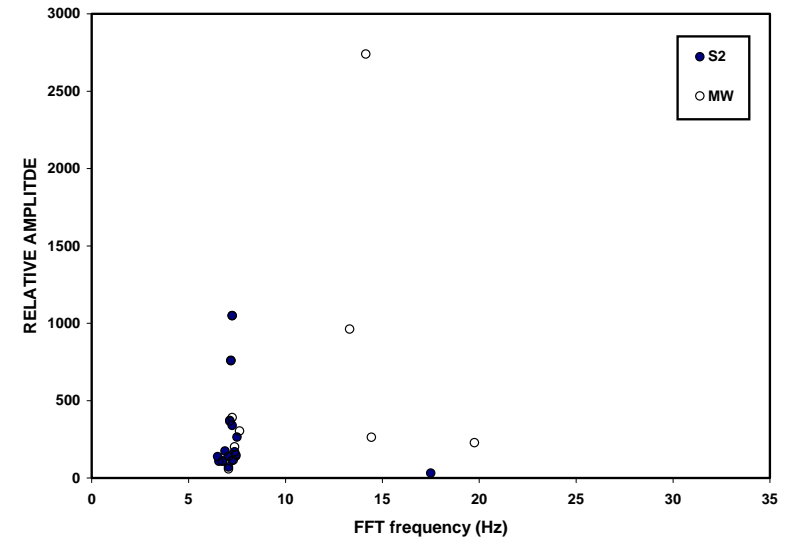
Figure IV-10 Horizontal components of upper structure and mid-wall responses and air overpressures for camp structures

## APPENDIX V

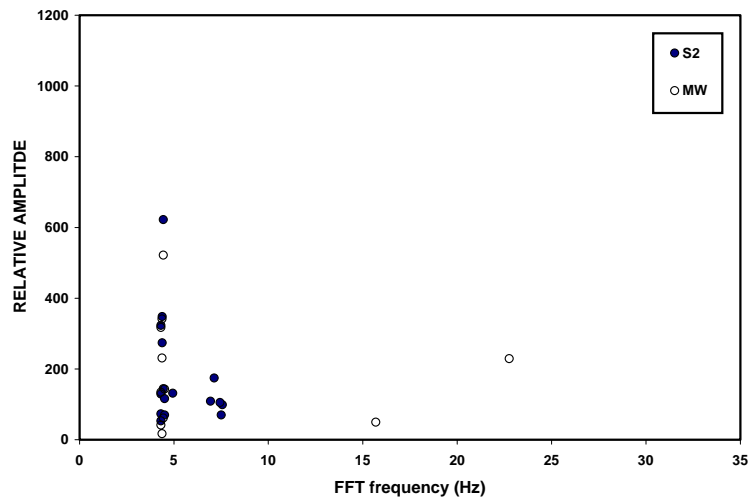
### FFT Frequency Correlation Plots



(a)

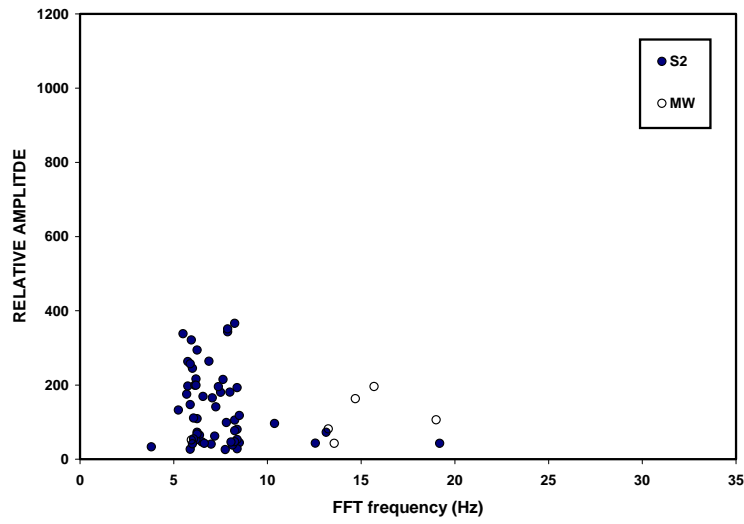


(b)

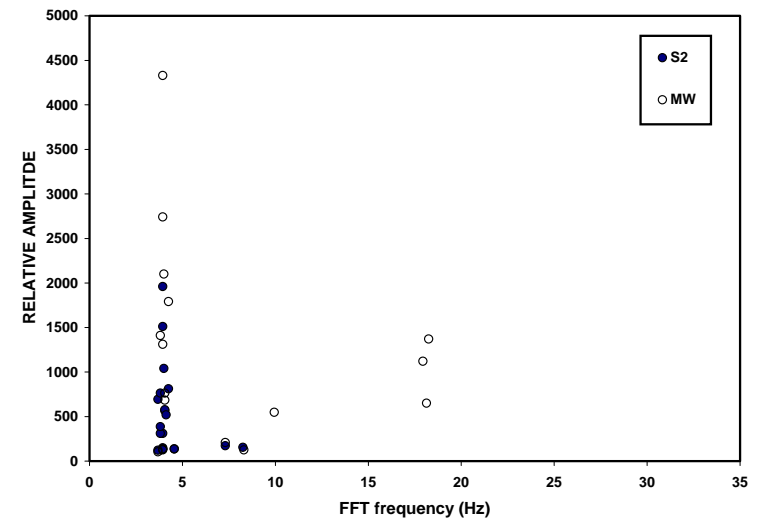


(c)

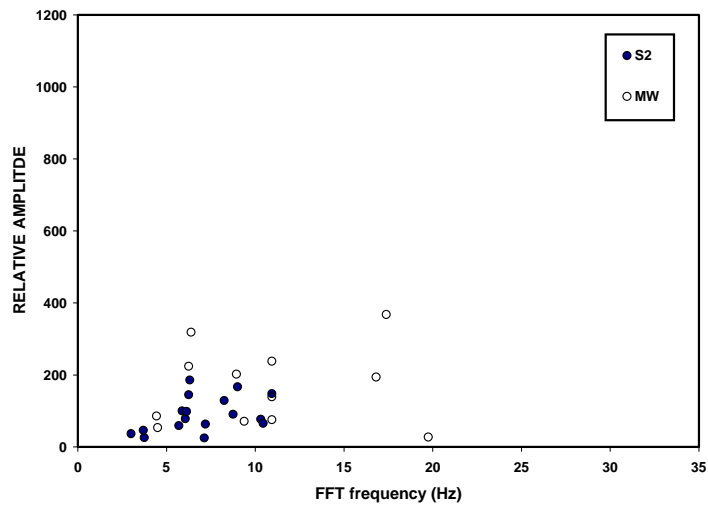
Figure V-1 Trailer responses for (a) single-wide, (b) double-wide and (c) wood frame add-on structures in the transverse direction



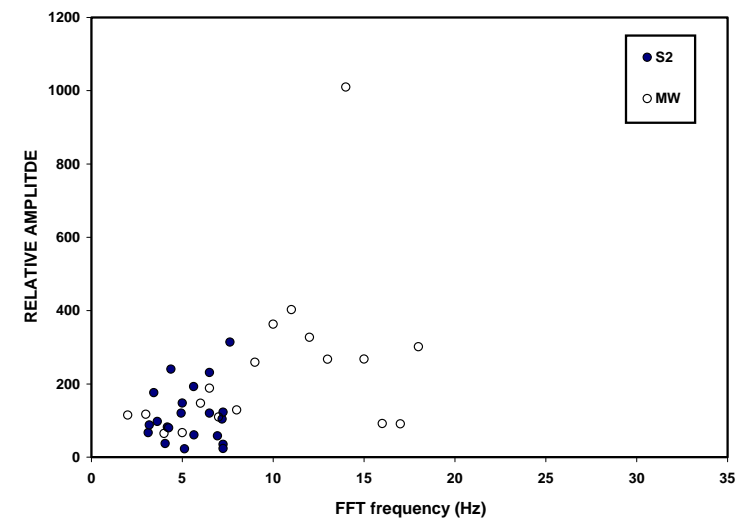
(a)



(b)



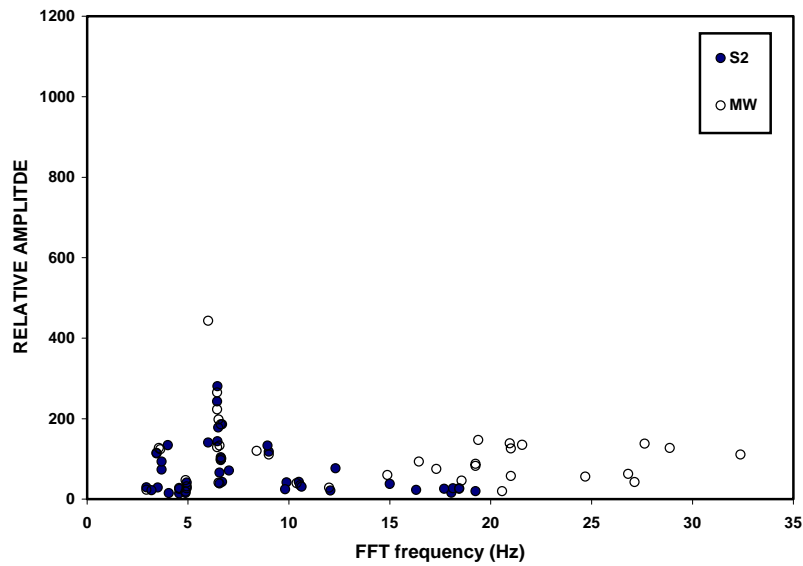
(c)



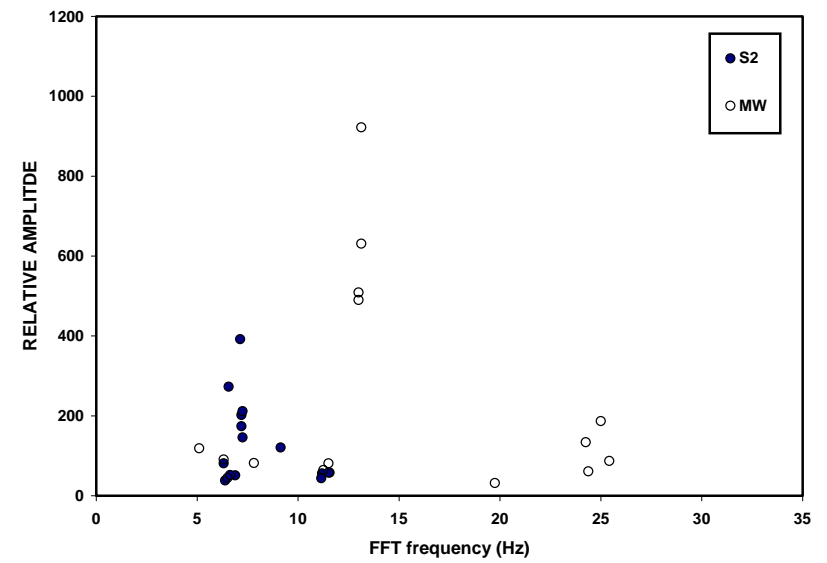
(d)

Figure V-2 Transverse structure response for (a) log (b) earth and masonry, (c) camp, and (d) wood-frame structures

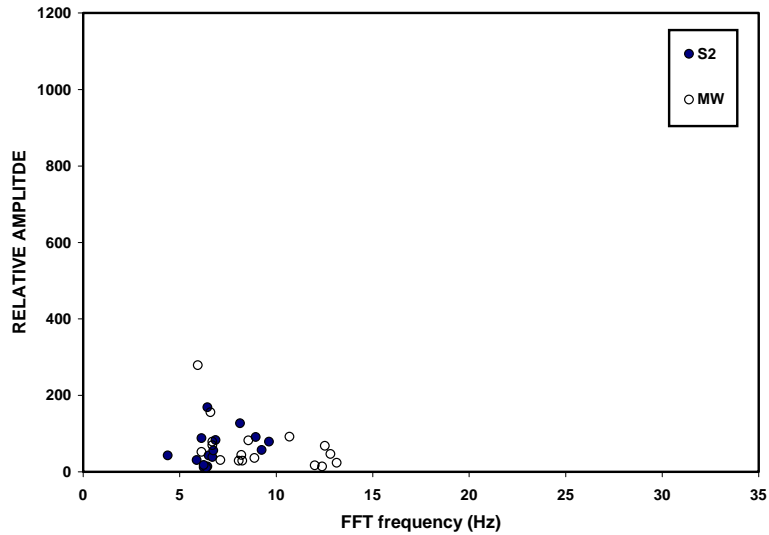




(a)

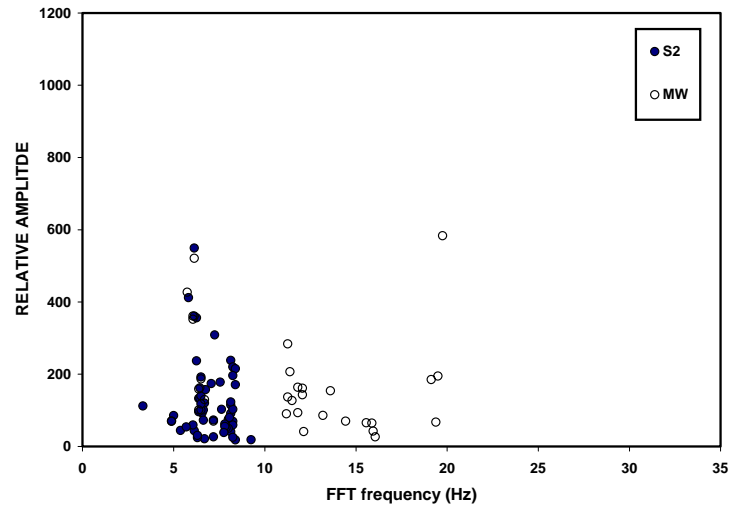


(b)

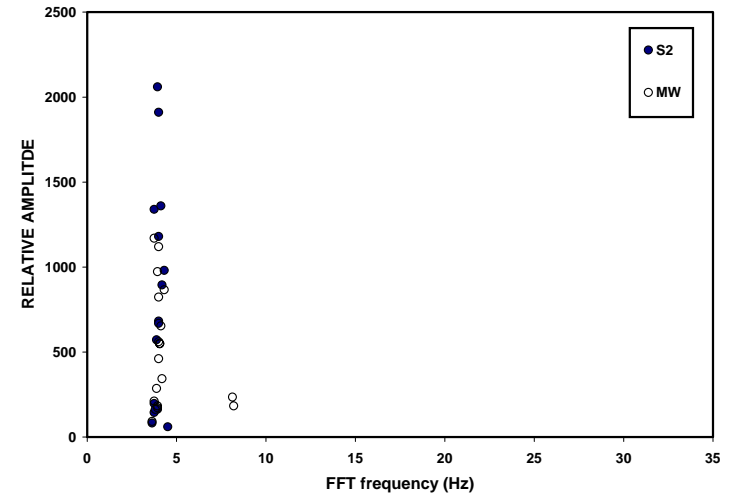


(c)

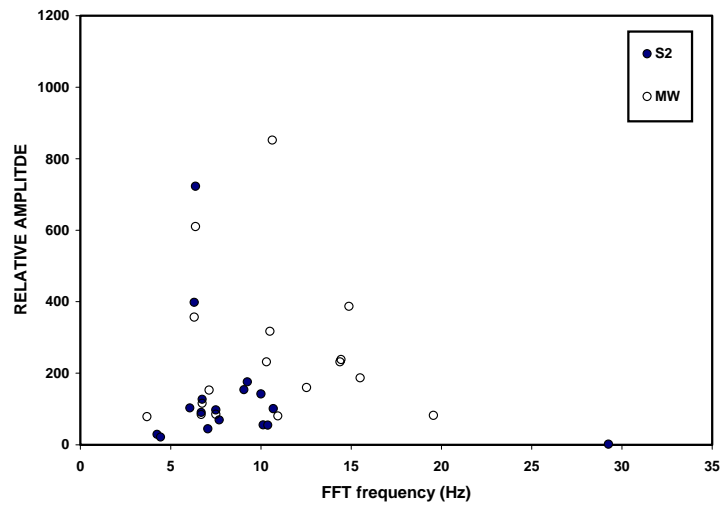
Figure V-3 Trailer responses for (a) single-wide, (b) double-wide and (c) wood frame add-on structures in the radial direction



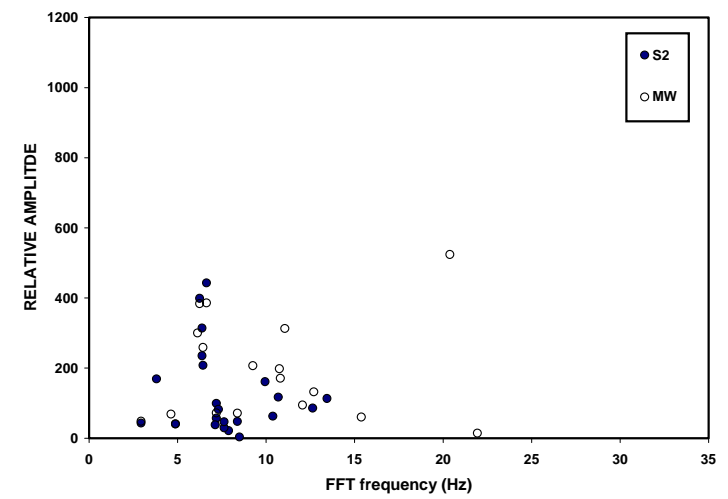
(a)



(b)

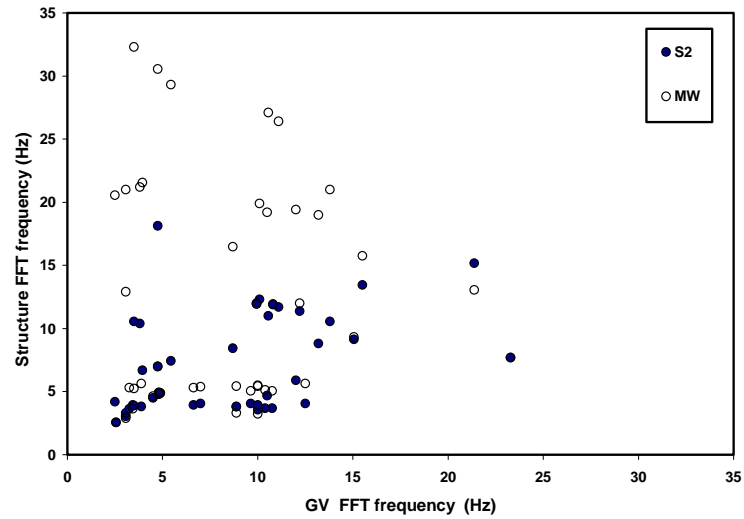


(c)

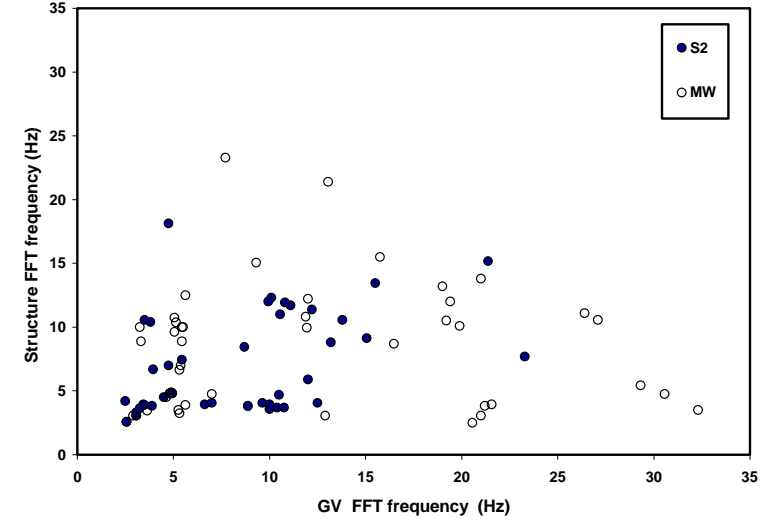


(d)

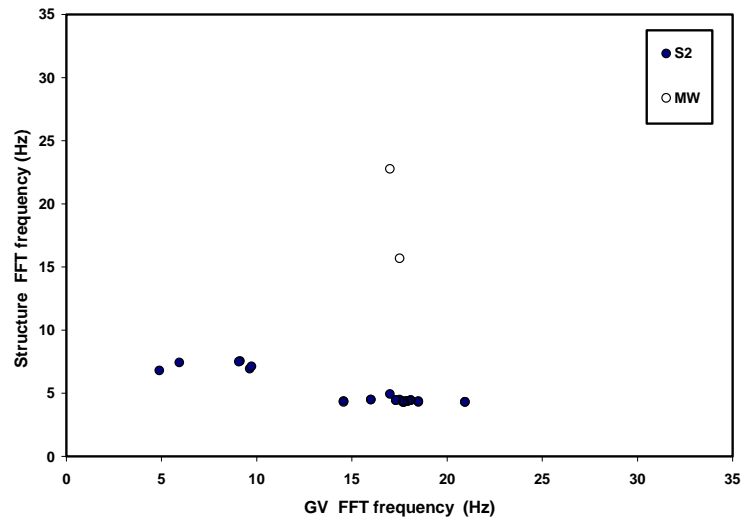
Figure V-4 Radial structure response for (a) log (b) earth and masonry, (c) camp, and (d) wood-frame structures



(a)

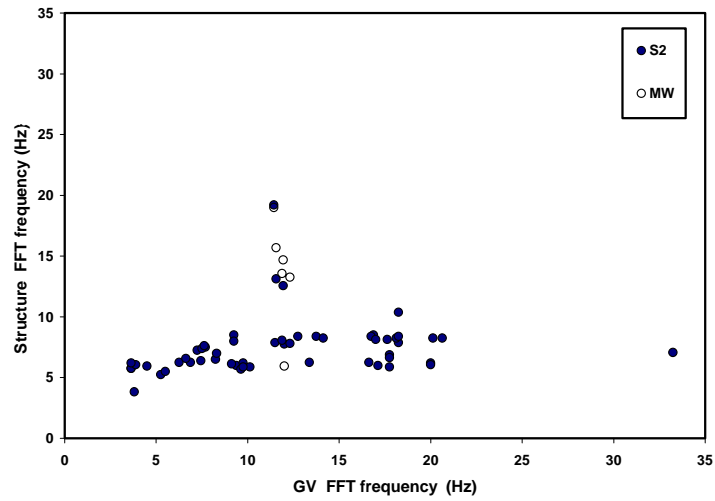


(b)

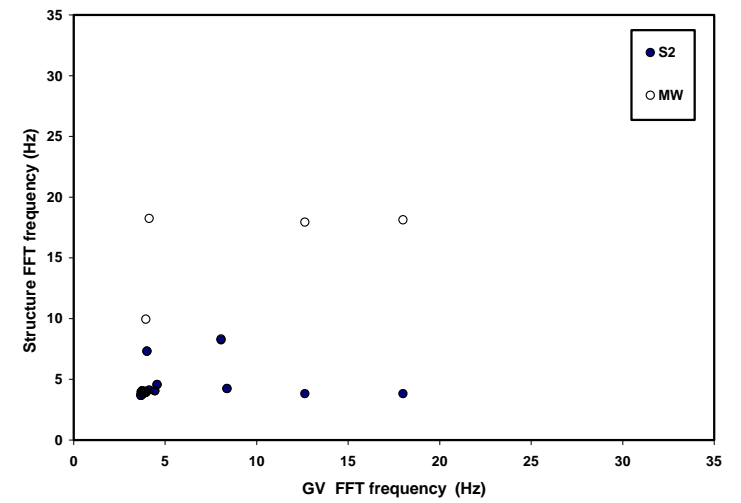


(c)

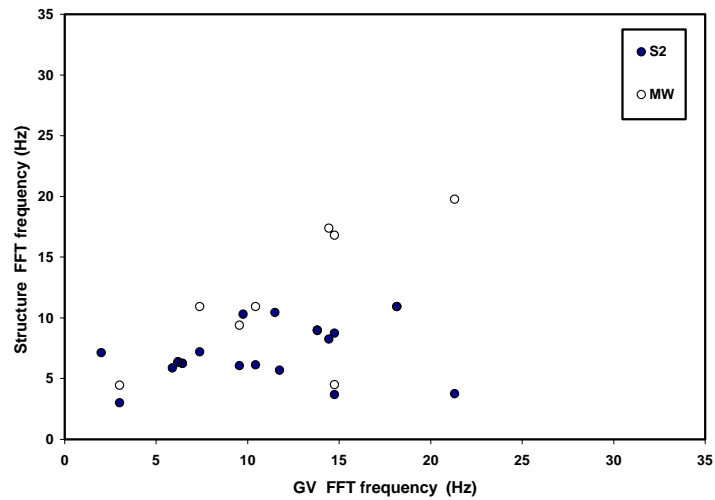
Figure V-5 Trailer responses for (a) single-wide, (b) double-wide and (c) wood frame add-on structures for the transverse component



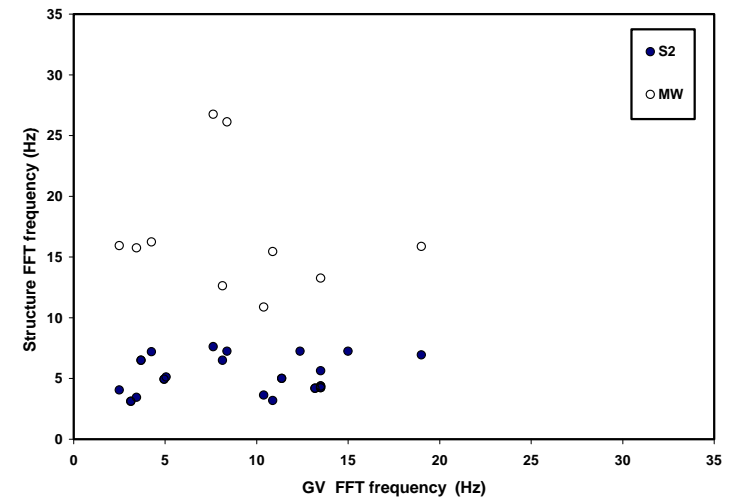
(a)



(b)

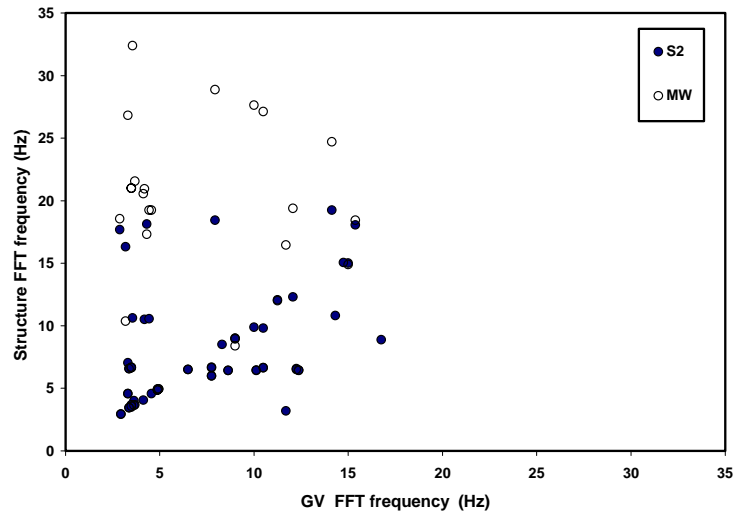


(c)

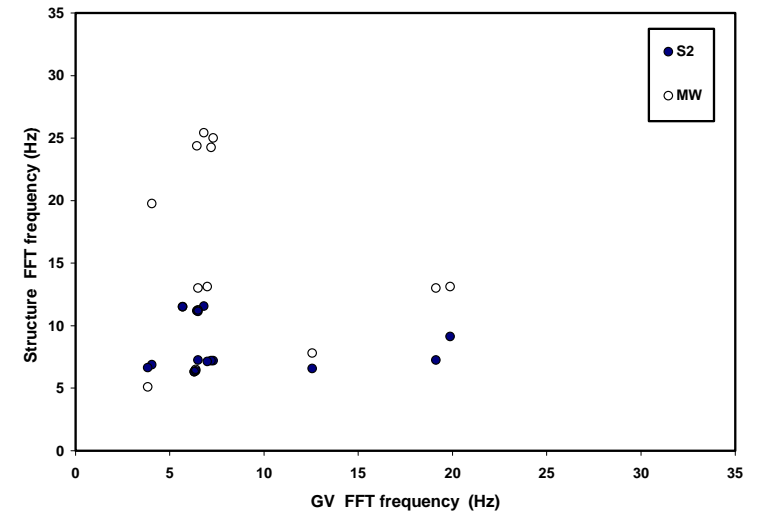


(d)

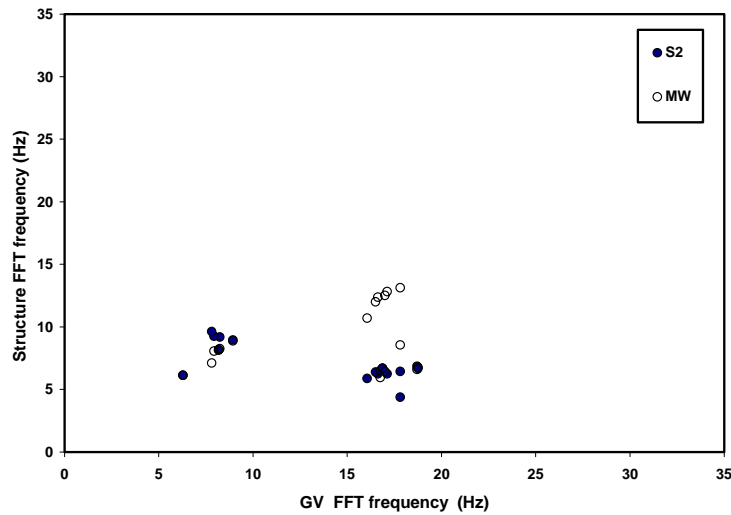
Figure V-6 Transverse structure response for (a) log (b) earth and masonry, (c) camp, and (d) wood-frame structures



(a)

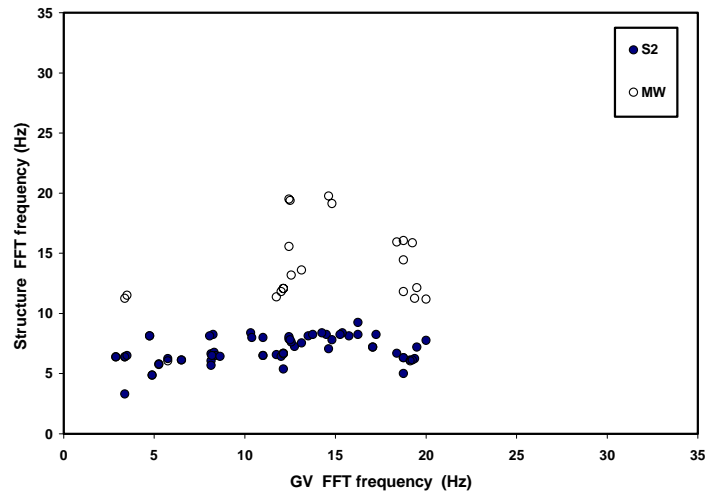


(b)

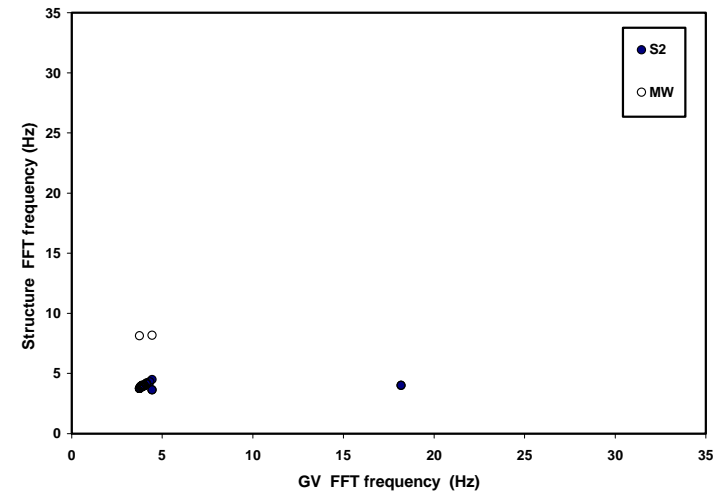


(c)

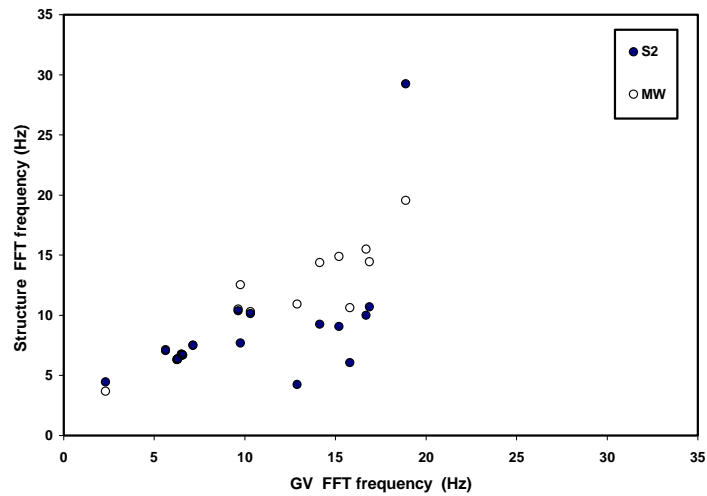
Figure V-7 Trailer responses for (a) single-wide, (b) double-wide and (c) wood frame add-on structures for the radial component



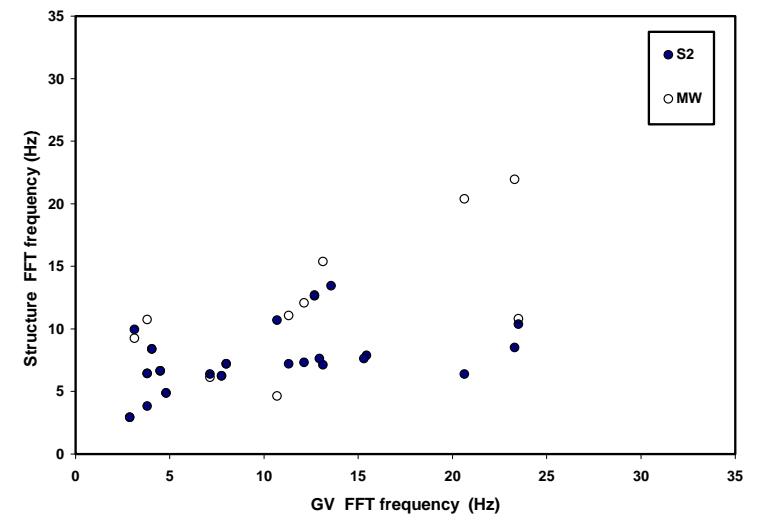
(a)



(b)



(c)



(d)

Figure V-8 Radial structure response for (a) log (b) earth and masonry, (c) camp, and (d) wood-frame structures

## ADDENDUM I

# **DIRECT MEASUREMENT OF CRACK RESPONSE AT FOUR OSM STUDY STRUCTURES**

Professor Charles H. Dowding  
Northwestern University, Evanston, Ill.

Laureen M. McKenna  
Northwestern University, Evanston, Ill.



## **Introduction**

This addendum synthesizes micrometer changes in crack width in response to both long term (environmental) and transient (blast vibration) of four of the structures in the main body. The addendum begins with a description of the genesis of the study and instruments employed. Response of the distressed wood-framed structure in Indiana is then employed to describe a typical suite of measurements. Long term crack response over periods of days to weeks is compared with changes in the temperature and humidity. Transient crack response to blast and occupant induced motions is then compared with peak velocity ground motions and structural response (the traditional approaches to investigation of cracking potential). Finally, the transient and long term changes in crack width are compared.

## **Direct Measurement of the Change in Crack Width**

Currently, complaints are addressed by measuring peak ground motions outside the structure with a blasting or vibration seismograph. These measured peak ground motions are then compared with standards developed by federal or state government agencies. Augmenting the measurement of ground motions, with which the average person may be unfamiliar, with direct measurement of crack response provides another means to discuss what is often of greatest concern, cracking.

Advances in sensor technology and computerized data acquisition now make it possible to simultaneously measure crack response to both long term and vibratory effects. Relatively inexpensive systems that combine measurement of both crack response and ground motion have been developed that involve the manual downloading of data on a periodic basis. They have been employed in this study to investigate their feasibility. These systems can be combined with telecommunications for near real-time display on the internet to allow access to a wide variety of interested parties.

A special dual-purpose sensor like that shown in Figure 1 can be placed across a crack to simultaneously measure long-term and vibratory response in terms of changes in crack width. This direct measurement, termed "crack displacement" is simple to understand and requires no reliance upon empirical guidelines. As shown by the insert in Figure 1, these sensors do not measure total crack width, but rather the change in crack width. Total crack widths could be calculated from the change by adding the change to the initial total crack width. For the remainder of this addendum change in crack width will be referred to as change in crack width or crack displacement.

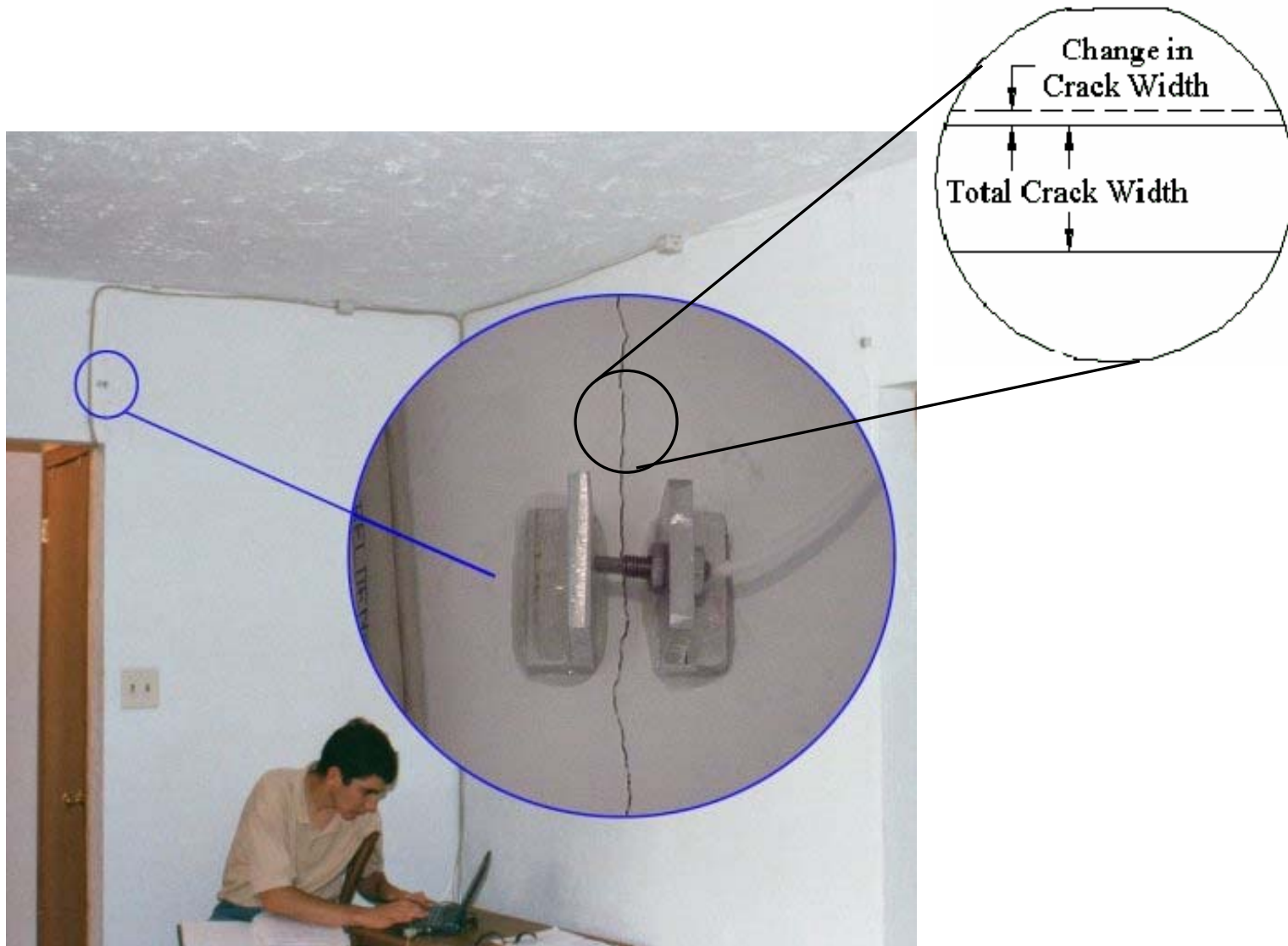


Figure 1 Typical threshold crack in a one-story concrete block house

Maximum total crack width is an index of potential extension of a crack. In other words, the greater the increase in total crack width (displacement plus initial crack width) the greater the potential for crack extension. Figure 2 shows the results of special tests (Miller, 1995) to determine the change in crack length with the change in the crack mouth opening. The change in crack mouth opening is analogous to total crack width, as defined above. In the test summarized by Figure 2, a specimen of cement paste like that shown in the insert, was subjected to increasing force,  $F$ , at the mouth of a crack of length “ $a$ ”. As  $F$  was increased, the crack mouth opening, or crack opening displacement (COD), increased, as did the crack length,  $a$ . The main graph portrays the change in COD with the extension of the crack. For instance, as COD increased from 3.5 micrometers (+ 7 to - 7 =  $14 \times 10^{-5}$  inches =  $140 \times 10^{-6}$  inches = 140 micro-inches) to 7.5 micrometers (+ 15 to -15) the crack extended from 1.4 to 1.6 inches (35.5 to 40.6 mm). Measurements summarized in Figure 2 show the crack extending only when it experiences a displacement that surpasses the maximum total crack width experienced. Thus, if the crack width remains less than its maximum historic value, it will not extend. However by logical extension, it can be said that the greater the crack displacement, the larger is the potential for cracking.

### **Crack Displacement Sensors**

While the authors have employed both eddy current proximity sensor and linear variable differential transformers, LVDT's in other studies, only the eddy current sensors were employed in this study. The principle of employing the same sensor to simultaneously measure crack displacements produced by both long-term and transient effects is not dependent on the type of sensor. Therefore, any number of sensor types can be employed. Details pertaining to the performance of a variety of different displacement sensors used in crack monitoring can be found in (Siebert, 2000) and (Louis, 2000).

Eddy current proximity devices sense the changes in a magnetic eddy current produced by changes in the distance between the sensor and the target. As shown in Figure 1, two aluminum brackets are epoxyed on either side of the crack, at a distance of 0.25 in (6 mm) apart. The eddy current device employed in this study, the Kaman 9000 2U, has a displacement range of 508 micrometers (20 mils) with resolution of 3.9 micro-inches (0.1 micrometers). While the 9000 2U is the more expensive of the Kaman devices, it has the least long- term drift (Siebert, 2000).

A second crack displacement sensor was also affixed to a non-cracked section of the wall in structures W1S-IN and W2S-IN to null out any possible long-term drift and temperature response. The difference in the response of the two sensors (crack minus null) is thus attributed solely to the crack, as described in (Siebert, 2000) and (Dowding and Siebert, 2000). Data presented later will show that null sensor response is typically small and null sensors are often not needed.

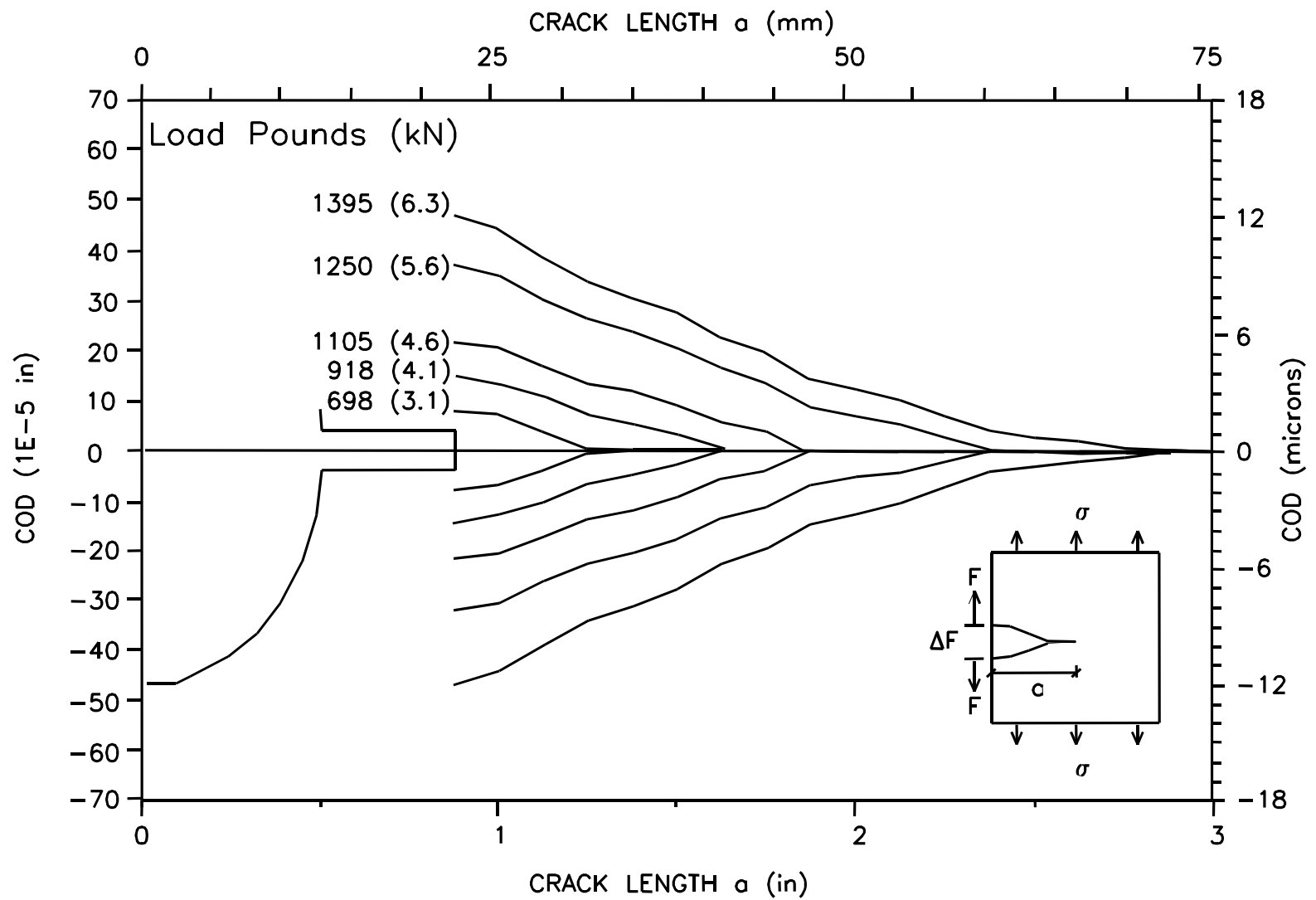


Figure 2 Experimental verification of proportionality of crack width and length

The data acquisition system (DAS), used to collect crack response was a Somat 2000/2100 field computer system (Somat, 1999 and 2001). For transient crack response, the sampling rate of the system was 1000 samples per second. System resolution of the DAS was governed by either A/D resolution or sensor resolution. However, in these cases the two were similar: between 0.65 and 0.083 micrometers per A/D division (unit). Long-term crack measurement was accomplished by measuring crack displacement once every hour. The time series of these “hourly” readings provides the long-term crack displacement time history. This “long term sampling” feature is not available on standard vibration monitors at this time, although its development is underway at most manufacturers.

## Homes and Cracks Studied

The four structures wherein crack response was directly measured are photographed in Figure 3, and diagramed in Figure 4. These four structures were instrumented with crack sensors in addition to the motion sensors that were implemented for the study. The houses were located in Pennsylvania, New Mexico, and Southern Indiana. Both structure type and location varied widely, and included a doublewide trailer (TD-PA), an adobe brick ranch house (E1S-NMB), a bungalow with a concrete block basement (W1S-IN), and a highly distressed wood-framed house (W2S-IN). All structures were one story, and all but E1S-NMB were founded on a basement.

All four structures were subjected to ground motions generated by surface coal mining. Maximum peak ground motions (parallel to the walls containing the cracks) ranged from 0.1 to 0.3 in/sec (2.5 mm/s to 8 mm/s), and generated responses that lasted between 1 to 4 seconds. Occupant induced crack response was recorded in TD-PA and W2S-IN. The blast vibration environment for all 4 structures is summarized in Table 1. See the “velocity transducer” section for details of the location of the velocity transducers. As shown in the table these ground motions generated structural response velocities (upper corner motion, S2 in Table 1) of 0.17 to 0.42 in/sec and S2/S1 structural amplification (where S1 is the lower corner motion) between 1.3 and 1.6 during maximum crack response. Values of S2/G (where G is the ground motion) at the moment of maximum S2 would not be the same as S2/S1.

Long-term response of cracks was monitored at all 4 of the structures for varying lengths of time that were in general shorter than normal. Structures TD-PA, W1S-IN and W2S-IN were observed for one week or less, while E1S-NMB was monitored for approximately 1 month. As will be discussed at the end of the addendum, observation periods of less than a week are too short to observe maximum weather events and thus the long term measurements reported here are in a sense not as long a term as have recorded and reported elsewhere (Dowding, 1996; Louis, 2000; Siebert, 2000; McKenna, 2002).

Even though the cracks monitored were cosmetic in nature, their locations and material types widely varied. These cracks were chosen as the largest and most visible in the structure. As shown at the bottom of Table 2, the crack widths varied from 0.019 to 0.047 in. (19,000 to 47,000 micro-inches or  $\mu$ -in). Their locations in plan view are denoted as “crack sensor” in Figure 4. They were located on 1) interior drywall above an entryway, (TD-PA), 2) interior plaster and lath above a window (W2S-IN), 3) exterior concrete block on the bottom (W1S-IN), and 4) exterior stucco over adobe bricks at the lower corner of a window (E1S-NMB).

Table 1 Summary of maximum crack response to blasting

Structure	Response						Maximum Ground Motion			Blast	
	Maximum peak velocity parallel to cracked wall for shot causing greatest crack response (ips)				Maximum crack response (μin)		Peak Frequency (Hz)	Peak Particle Velocity (ips)	Length of significant excitation (sec)	Distance from crack (ft)	Charge/ Delay (lb)
	g ground	S1 bottom	S2 top	S2/S1	Dynamic	Weather					
<i>Structure Identification</i> <i>Location</i> <i>Wall type</i> <i>Wall thickness (in)</i>											
<b>Trailer, TD-PA</b> Kittanning, PN Drywall 4	0.24	0.31	0.42	1.35	36	945	16.5	0.24	1.2	1440	612
<b>Adobe ranch, E1S-NMB</b> Farmington, NM Adobe 12	0.13	0.11	0.17	1.54	168	984	6.2	0.14	7.1	4940	9590
<b>Bungalow, WIS-IN</b> Francisco, IN Concrete Block 9	0.18	0.13	0.21	1.53	11	472	28.4	0.23	5.8	1500	451
<b>Wood frame house, W2S-IN</b> Francisco, IN Plaster/Lath 6	0.28	0.18	0.25	1.38	535	2047	14	0.3	3.2	2100	1051



Figure 3 Four structures monitored for crack response to long-term and transient effects (clockwise from top left: TD-PA, E1S-NMB, W2S-IN, and W1S-IN)

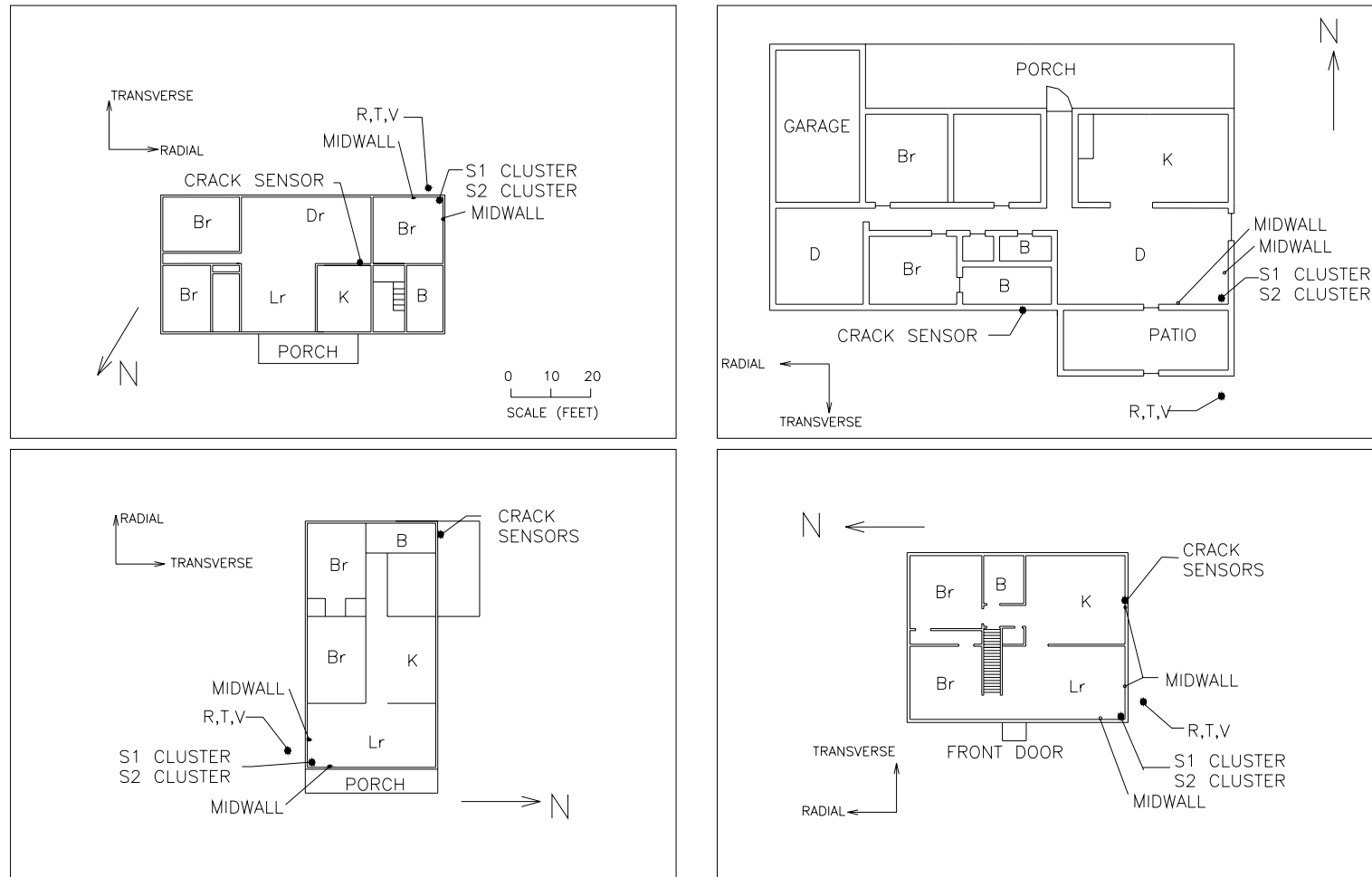


Figure 4 Plan views of four structures monitored for crack response to long-term and transient effects (clockwise from top left: TD-PA, E1S-NMB, W2S-IN, and W1S-IN)



## Velocity Transducers

Placement of velocity transducers has already been described in the main body of the report. Excitation motions were measured with standard seismographs and particle velocity transducers in the horizontally radial (R), horizontally transverse (T), and vertical (V) directions. In this study R is parallel to the long dimension of the structure. These tri-axial geophones were typically located within three to ten feet of the structure and buried approximately 4 to 6 inches in the ground. An air blast (over pressure) transducer, which responded linearly between 2 and 30 Hz was installed on a 3-foot high dowel.

Response motions for the four structures were measured at the interior corner of the house nearest the buried excitation geophone block. As shown in Figure 5, two indoor seismographs, each with four separate, single-axis velocity transducers, were employed. Seismograph, S1, serviced three single-axis velocity transducers (R, T, and V) installed at the bottom corner of the structure, and one on the middle of an adjacent wall. The second interior seismograph, S2, was also connected to four single-axis velocity transducers. The first three were installed in the upper corner, and the fourth on the middle of the remaining adjacent midwall. The indoor seismographs were linked to the outdoor seismograph and thus all three were triggered simultaneously at a ground excitation threshold of 0.02 in/sec at the ground geophones. Data files from each of the three seismographs contained 4 channels of time histories for each triggered event. Each set of time histories was at least 7 seconds long, which was long enough to capture the entire event.

## Measured Response and Example

Figures 6 and 7 compare crack displacement with velocity time histories of excitation ground motions and structure response to two coal mining blasts at the distressed, wood-framed structure, W2S-IN. The first blast consisted of 1051 lbs of ANFO per delay and was initiated 2100 feet from the structure on August 22, 2001 at 17:30. The second blast consisted of 301 lbs of ANFO per delay and was initiated 3730 feet from the structure on 23 august 2001 at 13:00. The two blasts produced peak crack displacements of 535  $\mu$ -in (13.6  $\mu$ -m) and 101  $\mu$ -in (2.6  $\mu$ -m), respectively, with peak ground motions, parallel to the cracked wall (transverse by study convention), of 0.28 in/sec (6.4 mm/sec) and 0.06 in/sec (1.5 mm/sec), respectively. The time histories for the lower corner transverse velocity, S1(t), and the upper corner transverse velocity, S2(t), as well as their difference, S1-S2 (t), are shown. The air blast response is also included in this figure for comparison. While space restrictions prevent inclusion of all 11 time histories, they have been archived electronically and summarized in (McKenna, 2002).

The dominant frequency of each structure was estimated with at least one of two different methods: 1) the zero-point-crossing frequency determination method and 2) Fourier frequency spectra method (Dowding, 1996). The zero-crossing method (calculating the frequency of the structure motion from the inverse of twice the time between two successive zero-crossings) was employed when free response of the upper structure was observed after excitation ground motions. For the distressed wood-framed house, w2s-in, values calculated from free response of the S2 (R and T) motions were averaged, for a dominant frequency of 8 Hz. The Fourier

frequency approach is most useful when there is little or no free response observed. In this method, the ratio of the FFT spectra of the structure response divided by the ground motion provides a means to determine the dominant frequency of the cracked wall. Dominant response frequencies estimated from these ratios of FFT spectra were also approximately 8 Hz.

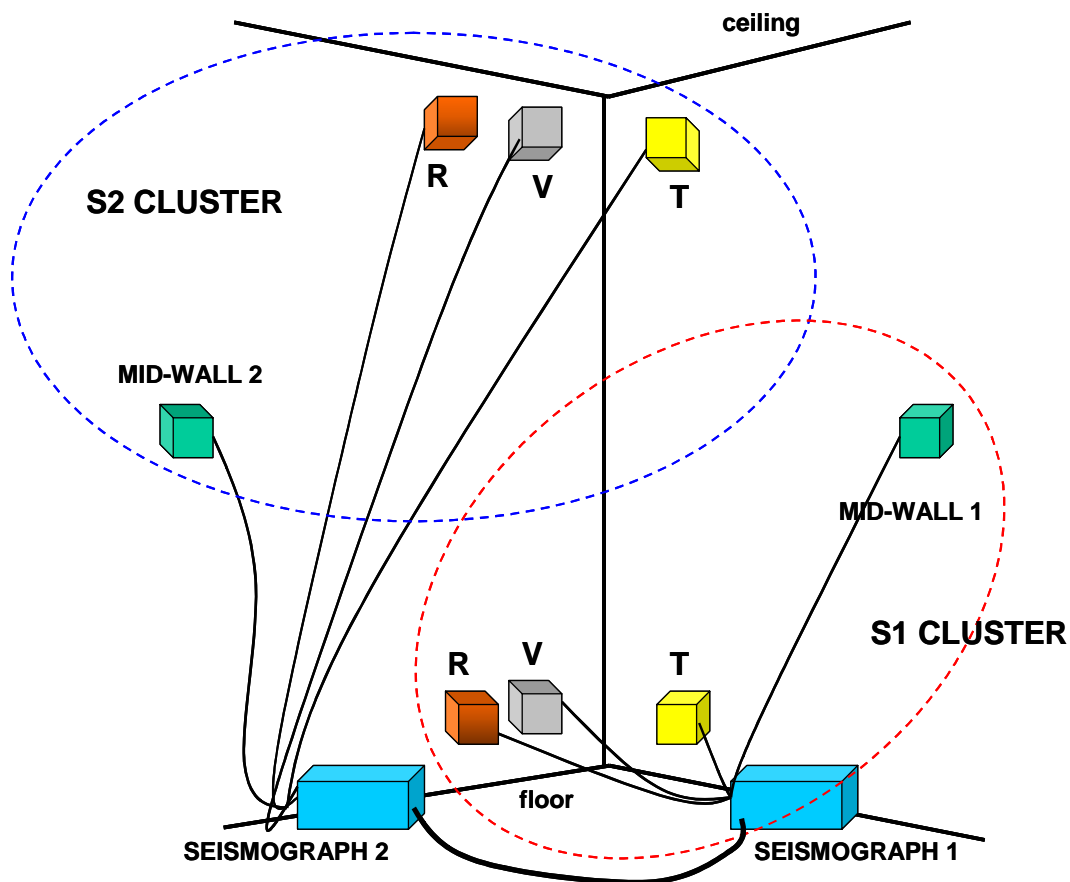


Figure 5 Typical indoor velocity transducer and seismograph set-up (Martell, 2002)

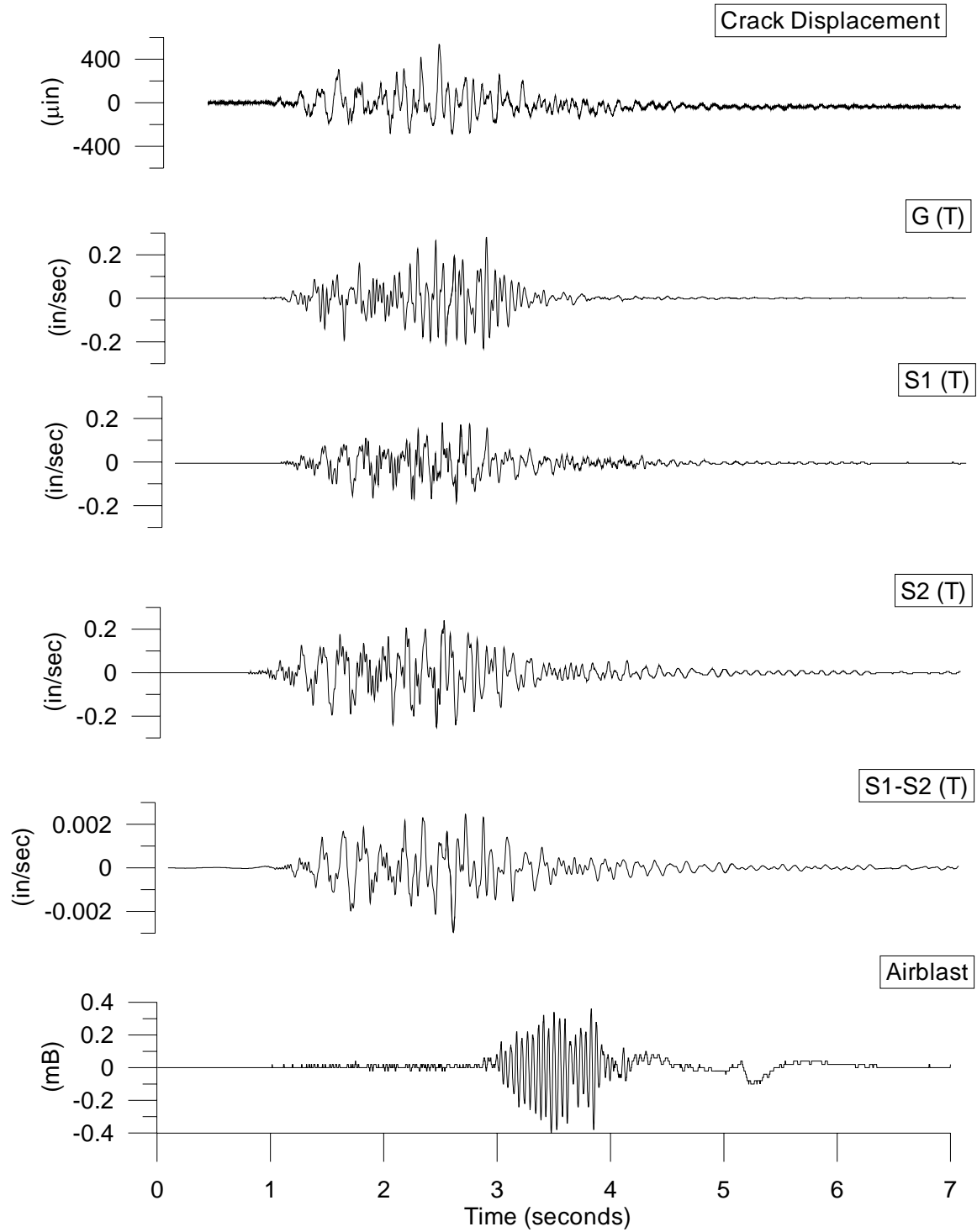


Figure 6 Time histories of crack displacement on August 22, 2001 at 17:30 compared to transverse ground, S1, and S2 structure motions, calculated displacement of the structure S1-S2 (T), and air blast response

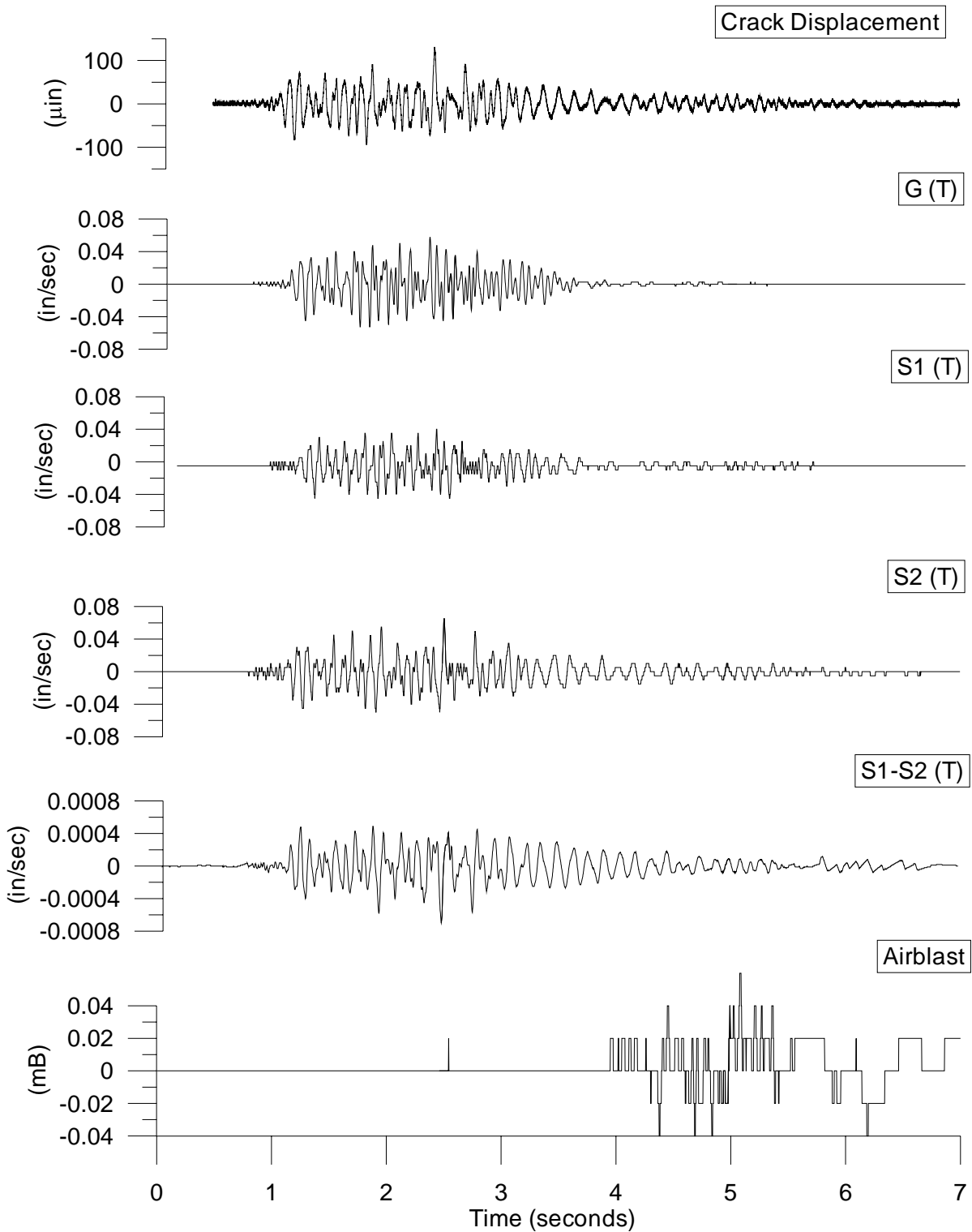


Figure 7 Time histories of crack displacement on August 23, 2001 at 13:00 compared to transverse ground, S1, and S2 structure motions, calculated displacement of the structure S1-S2(T), and air blast response

The response spectra of transverse ground motions, from the August 22 blast, as well as the one on August 23, are displayed in Figure 8. This is a pseudo velocity spectrum (PVRs) wherein the response velocity is estimated as  $2\pi f$  times the relative displacement, which is calculated from the ground vibration time history (Dowding, 1996). The spectrum gives the relative displacements of a family of structures with differing natural frequencies,  $f_n$ , with a common assumed damping of 5%. Since the approximate dominant frequency of W2S-IN was 8 Hz, the estimated displacements of the structure relative to the blast-induced ground motion were 0.0059 in or 5900  $\mu$ -in (150  $\mu$ -m) and 0.0024 or 2400  $\mu$ -in (61  $\mu$ -m), respectively, as shown by the intersection of the vertical 8-Hertz line with the response spectrum. These relative displacements are normally assumed to take place completely within the structure and its walls.

### **Crack Response to Long-Term Environmental Effects**

Crack displacement response for structure W2S-IN, is compared with the variation of weather indicators (temperature and humidity) in Figure 9 to illustrate interrelationships for the house during its three days of observation. Complete sets of these observations, for all structures, are contained in (McKenna, 2002). Long-term crack displacement was measured hourly during the monitoring period, while temperature and humidity were measured every 10 minutes. A Supco data logger was employed to measure temperature and humidity for these structures. This sensor, operated separately from the DAS, recorded readings every 10 minutes and measurements were integrated later with the structure and crack response data.

Average values of crack displacement (and temperature and humidity) were systemically calculated at every hourly measurement taken (and are shown in Figure 9 with diamond-constructed lines). These 24-hour “rolling” averages consisted of the measurements from 12 hours before and 12 hours after each hourly measurement. For example, at 12:00 p.m. on August 22, 2001, a 24-hour average crack displacement was calculated from the 24 measurements recorded between 12:00 a.m. on August 23 to 12:00 on August 24. For the first and last 12 rolling averages computed, the first and last measurement recorded was counted more than once in the respective averages, in order to have 24 measurements included in every average.

Overall averages, shown with the thick solid lines in Figure 9, were computed for crack displacement, temperature, and humidity throughout the whole monitoring period. Hourly measurements from the first to last hour were included in these averages.

Long-term crack response is enlarged in Figure 10 to define the specific long-term trends employed in this study, to facilitate the comparison of long-term response of all structures. Collectively, the actual measurements, 24-hour averages, and overall averages were used to determine crack response to weather effects. Weather effects have three distinct contributors 1) frontal movements that change overall temperature and humidity for periods of several days to several weeks, 2) daily responses to changes in average temperature and solar radiation, and 3) weather fronts that contain extremes of unusual weather or other environmental effects.

(1) Crack displacement of 535  $\mu$ -in on August 22 PPV = 0.28 in/sec

(2) Crack displacement of 130  $\mu$ -in on August 23 PPV = 0.06 in/sec

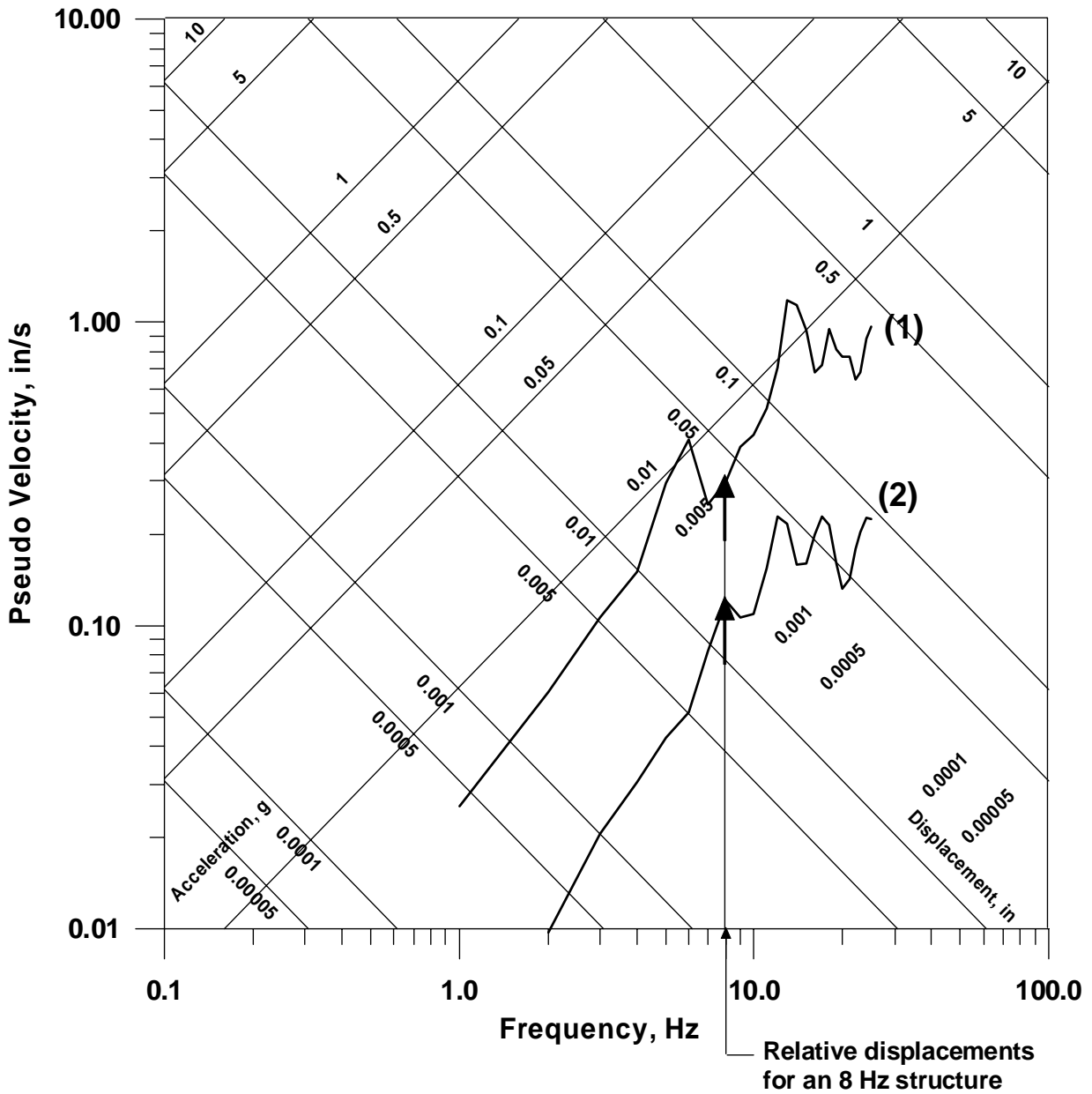


Figure 8 Single degree of freedom response spectra of transverse motions produced by blasts on August 22, 2001 at 17:30 and August 23, 2001 at 13:00, showing estimated relative displacements of an 8 Hz structure

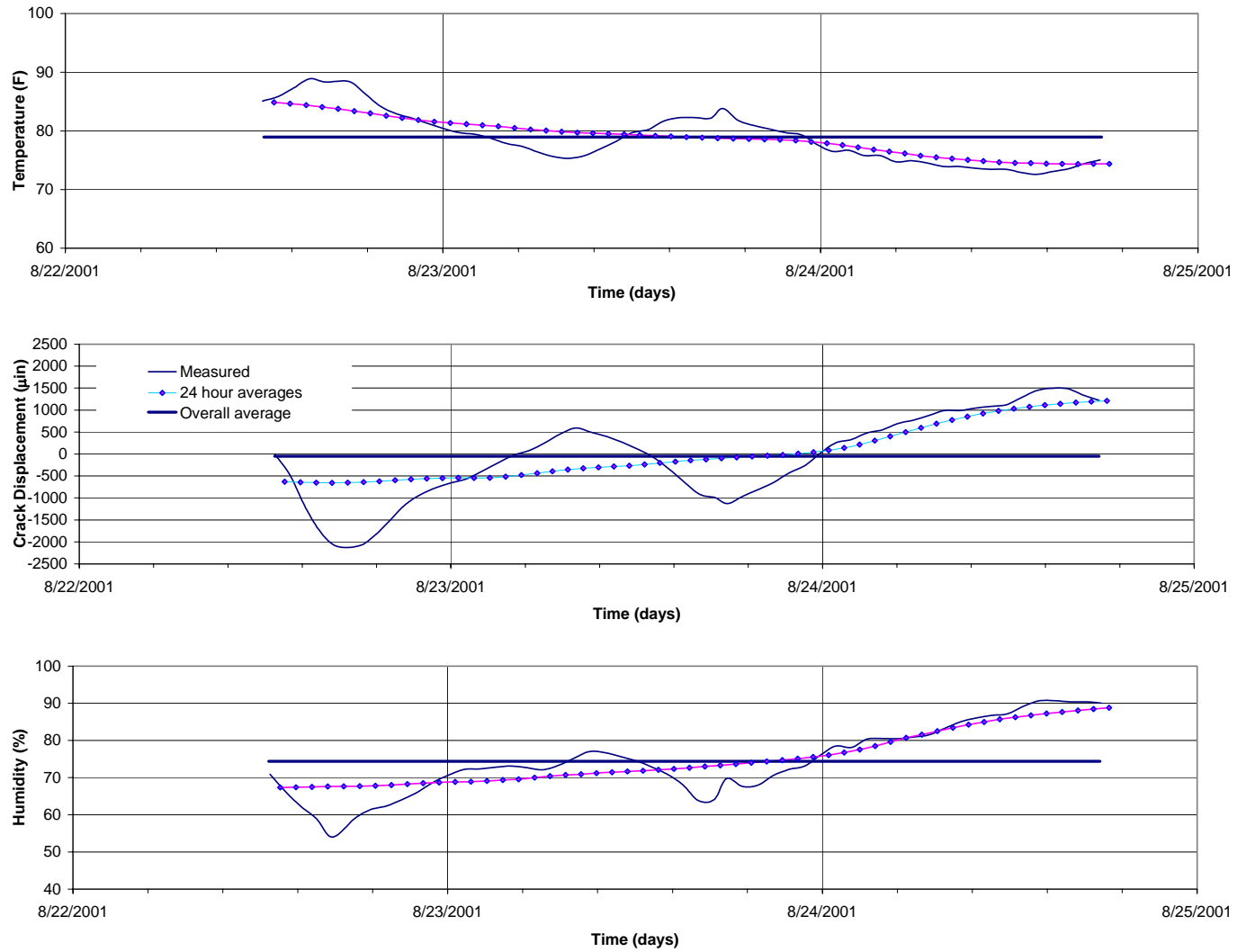


Figure 9 Long-term crack response and weather versus time for structure W2S-IN

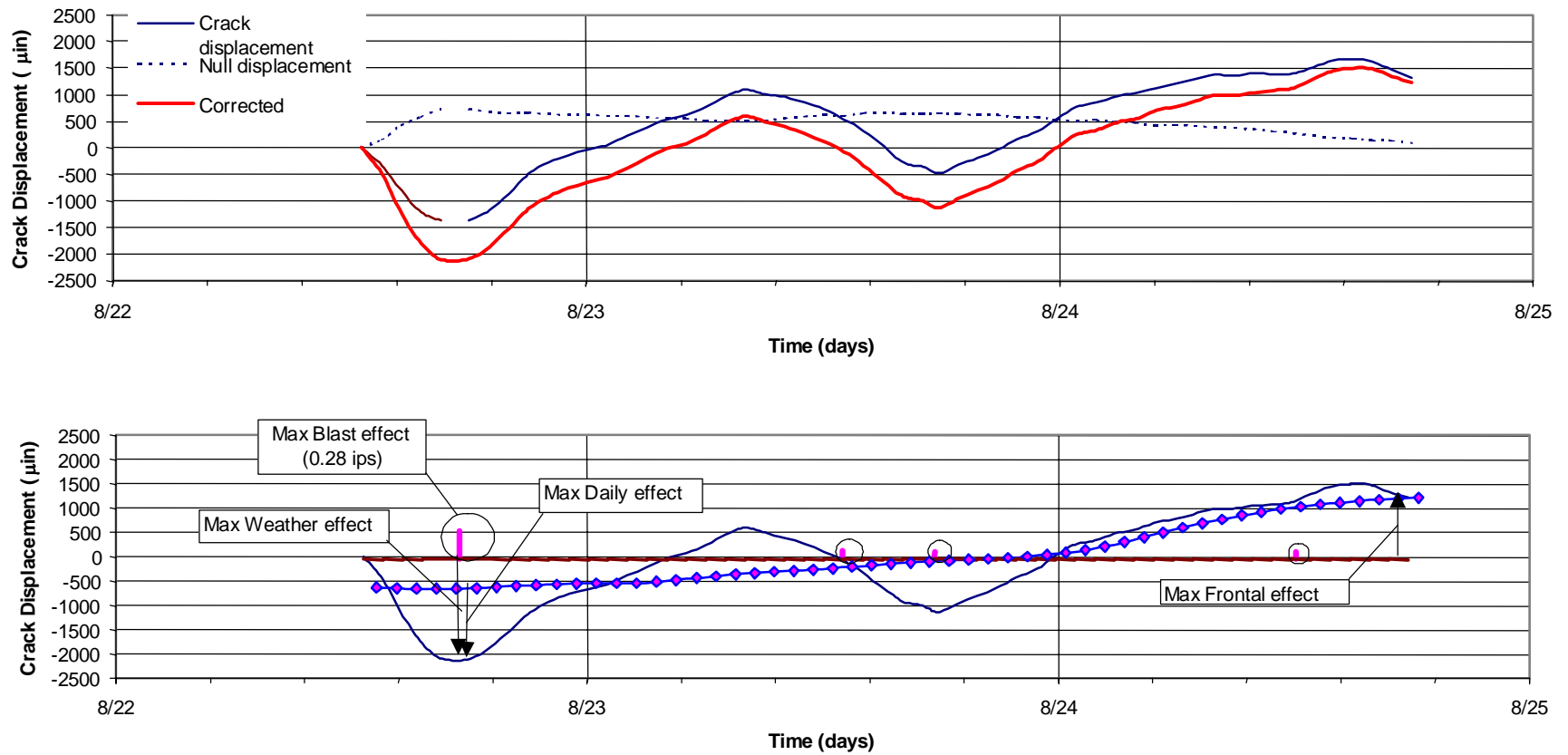


Figure 10 Typical crack response due to long-term phenomena and maximum zero to peak dynamic blast events



As shown on Figure 10, the frontal effect is defined as the deviation of the peak 24-hour average value from the overall computed average. In between each instance when the 24-hour average line crossed the overall average line, the frontal effect was calculated at the peak 24-hour average value and taken as an absolute value. The maximum frontal effect on crack displacement during the three-day monitoring period of structure W2S-IN occurred at the end and was some 1300  $\mu$ -in (32  $\mu$ -m). The daily effect is defined as the difference between the peak actual measurement and the 24-hour average. In between each instance when the actual measurement line crossed the overall average line, the daily effect was calculated (actual minus 24-hour average) and taken as an absolute value. The maximum daily effect on crack displacement during the three-day monitoring period occurred at the beginning and is some 1500  $\mu$ -in (38  $\mu$ -m). The weather effect is defined as the difference between the peak actual measurement and the overall computed average. In between each instance when the actual measurement crossed the overall average line, the weather effect was calculated (actual minus overall average) and taken as an absolute value. The maximum weather effect on crack displacement during the three-day monitoring period also occurred at the beginning and was 2024  $\mu$ -in (52  $\mu$ -m).

### **Comparison of Long-term, and Vibratory Crack Displacement**

These specific observations at the distressed house, shown in Figure 10, illustrate how small blast-induced responses are compared to those produced by weather. Furthermore, the weather response of the crack was small compared with the actual width of the crack, determined to be 47,400  $\mu$ -in (1200  $\mu$ -m). As discussed earlier, it was observed that cracks extended when the maximum total crack width is exceeded. In order to display the relatively small responses associated with the blasts, the four resulting peak displacements are encircled. The maximum dynamic crack displacement response of 535  $\mu$ -in or 13.6  $\mu$ -m (0.28 in/sec at 15 Hz) is approximately 1/4 of the 2024  $\mu$ -in maximum weather effect response during only 3 days of observation. The dynamic crack response for the August 23 blast (in Figure 6) of 101  $\mu$ -in (2.6  $\mu$ -m) (0.06 in/sec at 14 Hz) was less than 1/20<sup>th</sup> of the maximum weather displacement. Had this structure been monitored for a longer period, the maximum weather response would have been larger.

Both dynamic and long-term crack displacements are small compared to the width of the crack, 47,200  $\mu$ -in. The magnitude of each dynamic measurement corresponds to the absolute, maximum zero-to-peak displacement of the crack during the significant portion of vibratory motion. This zero to peak measure is similar to the peak particle velocity measure employed in past research. Figure 11 shows long-term weather and blast-induced responses from a previous structure studied during a much longer monitoring period some 9 months (Dowding, 1996). Blast-induced responses depicted in this figure result from blasting vibration levels reaching as high as 0.75 in/sec. This case history (Dowding, 1996) involved large distances from large coal mining blasts where the dominant frequency of the surface wave induced ground motions was similar to the natural frequency of the structure, some 7 Hz. Structural amplification, defined by the velocity response ratio  $S_2/G$ , the traditional approach, was as high as 2.8.

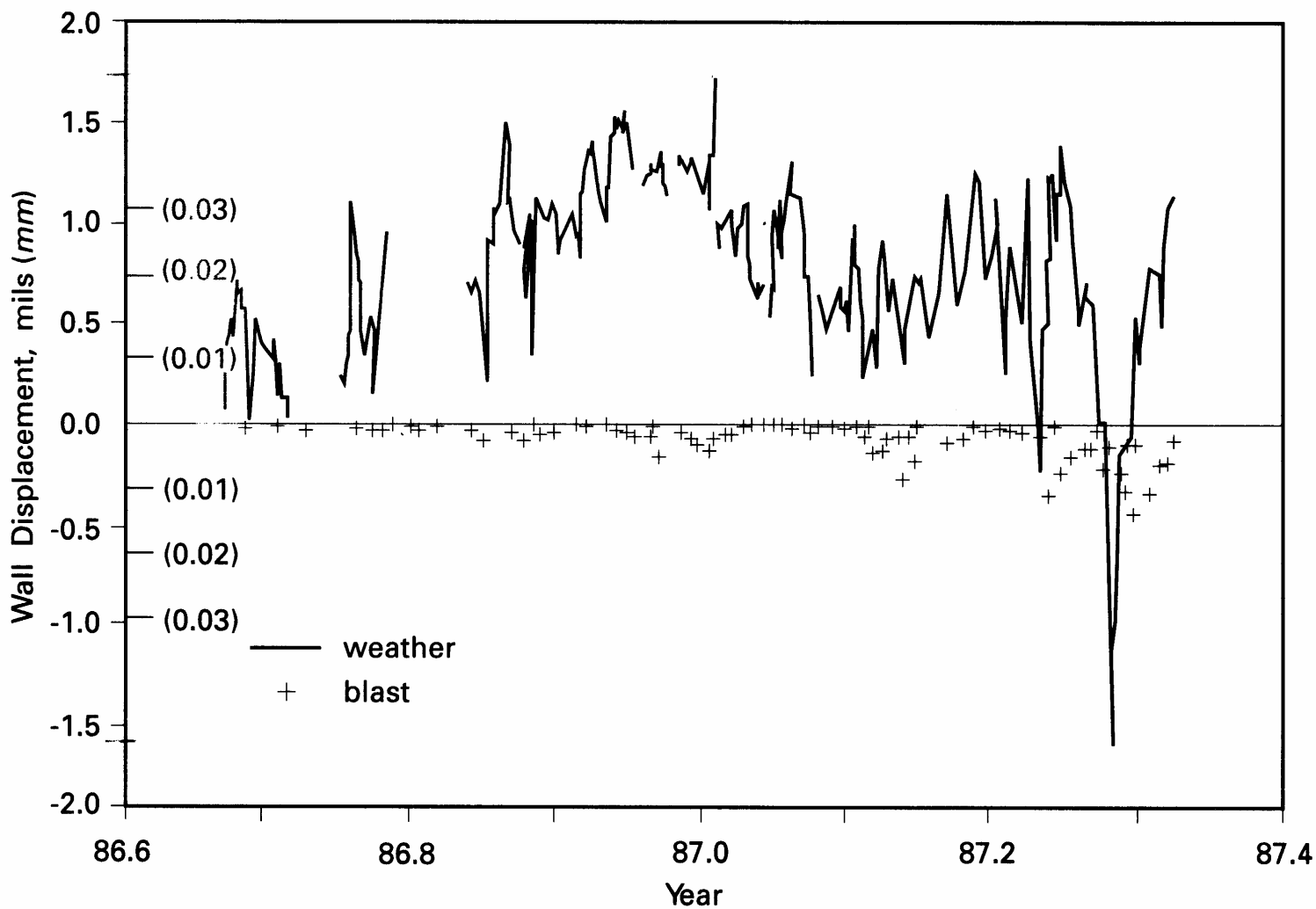


Figure 11 Comparison of weather and blast-induced crack displacements from a previous study (Dowding, 1996)

This figure further emphasizes the large difference in magnitude between weather response and blast-induced response of cracks when large weather events and seasonal effects are included in the observations.

Table 2 Comparison of crack displacement response from environmental and vibration effects

	(TD-PA) Trailer Interior Drywall	(E1S-NMB) Ranch Exterior Adobe	(W1S-IN) Bugalow Exterior Concrete Block	(W2S-IN) Distressed Frame Interior Plaster/Lath
Event	Displacement (micro-inches)			
Max Frontal Effect	451	354	118	630
Max Daily effect	639	984	354	984
Max Weather effect	962	984	472	2,042
Max Blast event (ppv in ips)	35 (0.32)	165 (0.13)	12(0.23)	535 (0.30)
Blast event at 0.10 ips	12	79	8	197
Slamming door	98 (6) <sup>1</sup>	-	-	63 (14) <sup>1</sup>
Jumping	59 (10) <sup>1</sup>	-	-	75 (16) <sup>1</sup>
Hammering	8 (11) <sup>1</sup>	-	-	87 (1) <sup>1</sup>
Shutting window	-	-	-	161 (3) <sup>1</sup>
Walking on Stairs	-	-	-	-
Foundation Response (Permenant)	-	630	-	-
Width of crack (micro-inches)	27,559	31,496	19,685	47,244
Days of observation ( ΔT in deg F)	5 (13)	35 (51)	4 (30)	3 (17)

Notes:

(1) Distance to crack in feet

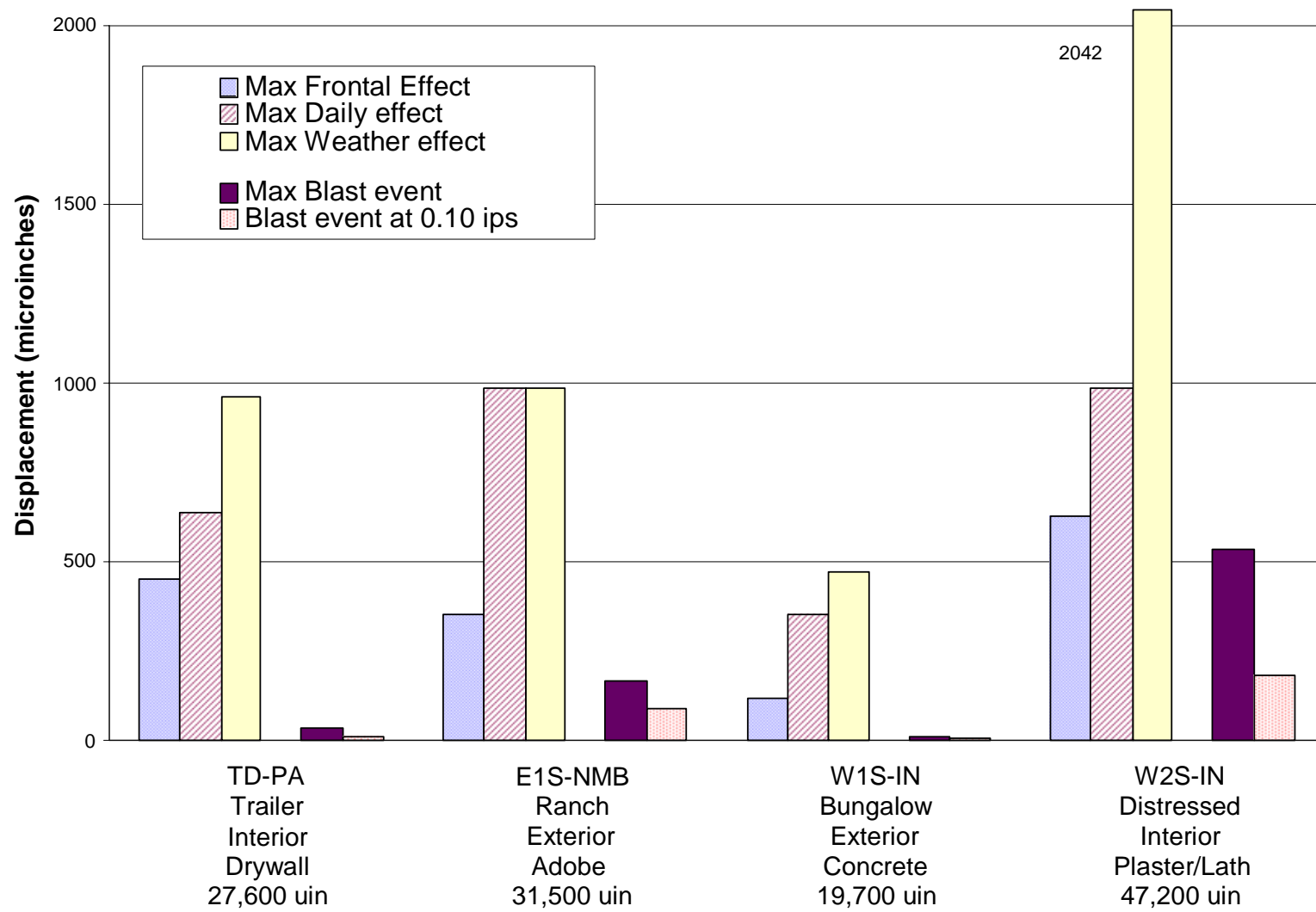


Figure 12 Comparison of measured crack displacements due to static and dynamic events

Environmental and vibratory responses of cracks in all 4 structures are compared in Table 2 and Figure 12. In addition to weather and vibratory crack responses, responses to occupant activities in structures TD-PA and W2S-IN are also included in Table 2. The length of monitoring of each structure (in days) is also included in the table. The implications of these measurements will be discussed further in the end of the addendum.

For all four structures, maximum weather effects are at least 10 times greater than the vibratory effects produced by ground motions of 0.1 in/sec. The 0.1 in/sec level is that at which the vibration is noticeable. As described earlier, the maximum weather effect is defined as the maximum difference in the peak actual measurements from the overall computed averages of crack displacement during the study period. The vibratory response is the maximum, zero to peak crack displacement during the vibratory response. Both long-term, weather, and transient, vibratory, responses are measured by the same sensor, and thus are directly comparable.

As shown in Table 2, response to occupant activity can be as large as that produced by vibratory excitation. Activities presented are a common subset of the tests conducted at two of the four structures. These tests were not undertaken at the other two structures. Distances from the crack to the location of the activity are shown along with the crack responses produced. Those activities closest to the crack produced the greatest response. The greatest response, 161  $\mu$ -in (4.1  $\mu$ -m), was produced by shutting a window three feet away from the crack in structure W2S-IN.

Seasonal events, such as the rainstorm that occurred in New Mexico (during monitoring of structure E1S-NMB), create large and relatively permanent crack responses, as was seen in the measured long-term response of the structure. A half of an inch rainfall at the adobe home, E1S-NMB, which did not have a basement, produced a 630  $\mu$ -in (16  $\mu$ -m) change that remained for the duration of the monitoring period (McKenna, 2002). This permanent deformation is 8 times greater than the response of the crack to 0.1 in/sec blast-induced ground motions. These types of extreme events typically are expected to be observed only within periods of six months or longer. The large magnitude and permanence of the crack response implies that seasonally extreme events produce even larger crack displacement than other events reported for most of the structures in this study.

### **Comparison of Vibratory Crack Displacement with Structural Response from Velocity Measurements**

Measured crack response is compared in Figures 13 and 14 with the more traditional estimates of relative wall displacement or cracking potential in order to determine the similarity of the approaches. This addendum focuses on direct measurement of crack response. Traditionally, ground particle velocity or structural velocity response is measured to deduce or estimate relative wall displacement or gross strain as an index of crack response and/or cracking potential. Structural velocity responses are manipulated to calculate relative displacements (or strain) in the plane of the wall, which are then compared to critical levels. Computed relative displacements can be estimated by a number of methods such as the integration of velocity time histories, the Single Degree of Freedom response spectrum method, and estimation based on sinusoidal approximation. Also included is a comparison with the peak parallel ground motions,

since it is the method by which vibratory activities are regulated. All of these comparisons are presented in Figures 13 and 14. Since crack displacements are measured in the plane of the wall, comparisons with structural and wall responses are made in the plane of the wall. Thus, the important velocities are always in the direction parallel to the wall with the crack.

Relative wall displacements can be most directly calculated from pairs of measured structural velocity responses. These calculations are compared in Figures 13 (a) and (b) with the directly measured crack displacement. Subtraction of perfectly time correlated ( $\pm 0.001$  sec) pairs of integrated velocity time histories to create a relative displacement time history is the most direct method of computing peak relative wall displacement. In these cases the pairs are: 1) upper corner, S2, minus lower corner, S1 (S2-S1), and 2) S2 minus ground (S2-G). From the resulting time history, the peak relative displacement is determined for comparison with the measured crack displacement.

If measured structure response is not available, but ground motions are, a third, less precise index is sometimes calculated from the integrated ground particle velocity alone. Figure 13 (c) shows the comparison between peak measured crack displacements and these peak integrated values of the particle velocity.

Relative wall displacements can be estimated by calculating single degree of freedom (SDOF) relative displacement responses from the ground velocity time histories as described in (Dowding, 1996). Two such comparisons are made with the directly measured crack displacements in Figures 13 (d) and (e). A standard damping ratio of 5% is used for all calculations. Estimated relative displacements are found from either: (d) SDOF relative displacement response at the dominant frequency of the super structure or (e) the average of responses between 10 and 15 Hz. Average values of natural frequencies for typical residential structure walls typically range between 10 and 15 Hz. Since the monitored cracks were located on walls that can respond to both superstructure and wall motions, depending on the design of the walls and the ground motions, both approaches were taken to estimate a relative displacement associated with the ground motion. Figure 13 (d) shows the comparison of measured displacement with the estimated displacement for the dominant frequency of the structure, while Figure 13 (e) shows that with the average of estimated displacements in the 10 to 15 Hz range.

The traditional method of estimating cracking potential is measuring the peak particle velocity (PPV). PPV in the direction parallel to the plane of the wall is compared with measured crack displacements in Figure 13 (f).

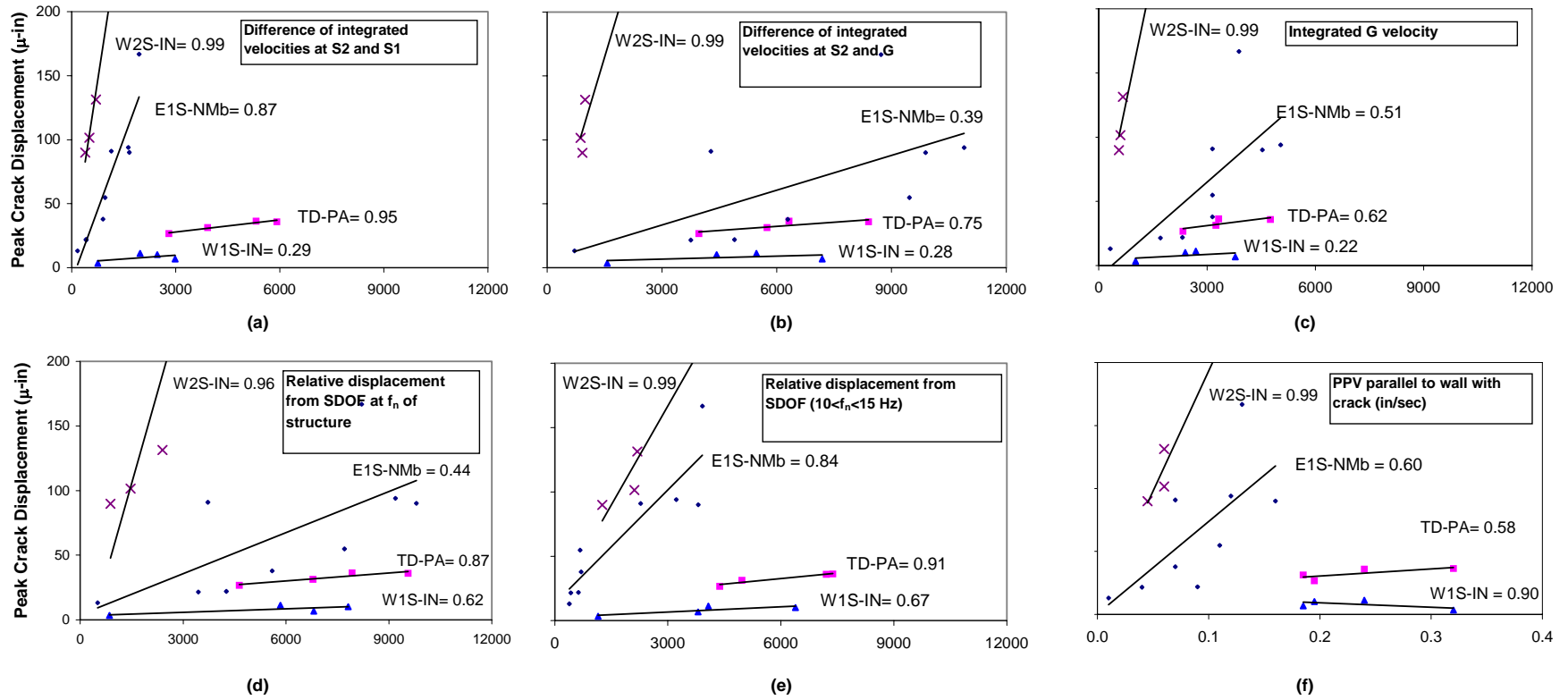


Figure 12 Comparison of  $R^2$  correlations between measured crack displacements and estimated displacements and peak parallel ground motions

Relative wall displacements can be approximated visually from time histories by assuming that velocity time histories approximate sinusoidal waveforms. Wall displacement,  $\delta$ , can be estimated with the following equation:

$$\delta = v/2\pi f$$

Where  $v$  is a given PPV in a time history and  $f$  is the frequency of the velocity at the time it occurs. The frequency is determined by taking the inverse of twice the time between the zero-crossings enclosing the given PPV. Displacements approximated in this manner can be determined for both upper and lower elevations of the wall of a structure and subtracted in order to obtain various measures of relative displacement.

Figure 14 compares directly measured crack displacement with six methods of approximating relative wall displacements. Approximated relative displacements have been produced from the following pairs of velocity time histories: (a) ground motion,  $G$ , and upper corner,  $S2$ , at the time of peak  $G$ , (b)  $G$  and  $S2$  at the time of peak  $S2$ , and (c) peak  $G$  and peak  $S2$ , regardless of the time at which each occurs. For the two time-correlated pairs, (a) and (b), displacement is still computed at the same time, regardless of the magnitude of velocity at that point in time, for either of the time histories. In other words, if the velocity of one of the time histories is 0.0 in/sec and the velocity of the other is 0.3 in/sec, then the displacement of the first time history would be considered zero, and the relative displacement would be equal to that computed from the second time history. The resulting values from  $\delta(S2)-\delta(G_{\max})$ ,  $\delta(S2_{\max})-\delta(G)$ , and  $\delta(S2_{\max})-\delta(G_{\max})$ , were all used as representative values of estimated displacements. Comparisons between measured crack displacements and these approximated displacements are presented graphically as Figure 14 (a), (b), and (c), respectively.

In addition, three more pairs were analyzed, where velocity in the lower corner,  $S1$ , was used in place of ground motion,  $G$ . ( $G$  and  $S1$  at the time of peak  $G$ ,  $G$  and  $S1$  at the time of peak  $S1$ , and peak  $G$  and peak  $S1$ , regardless of the time at which each occurs) these resulting values from  $\delta(S1)-\delta(G_{\max})$ ,  $\delta(S1_{\max})-\delta(G)$ , and  $\delta(S1_{\max})-\delta(G_{\max})$ , were also used as representative values of estimated displacements. Comparisons between measured crack displacements and these computed displacements are presented graphically as Figure 14 (d), (e), and (f), respectively.

The last pair, in both sets of three is not as precise as the others, as it fails to take into account the necessity of simultaneity of the motions. Such values do not depict an estimated displacement at a given time, but rather, a maximum possible displacement. Therefore, it would be expected that the first two pairs of both sets would yield better correlations with the measured displacements than would the last pairs.



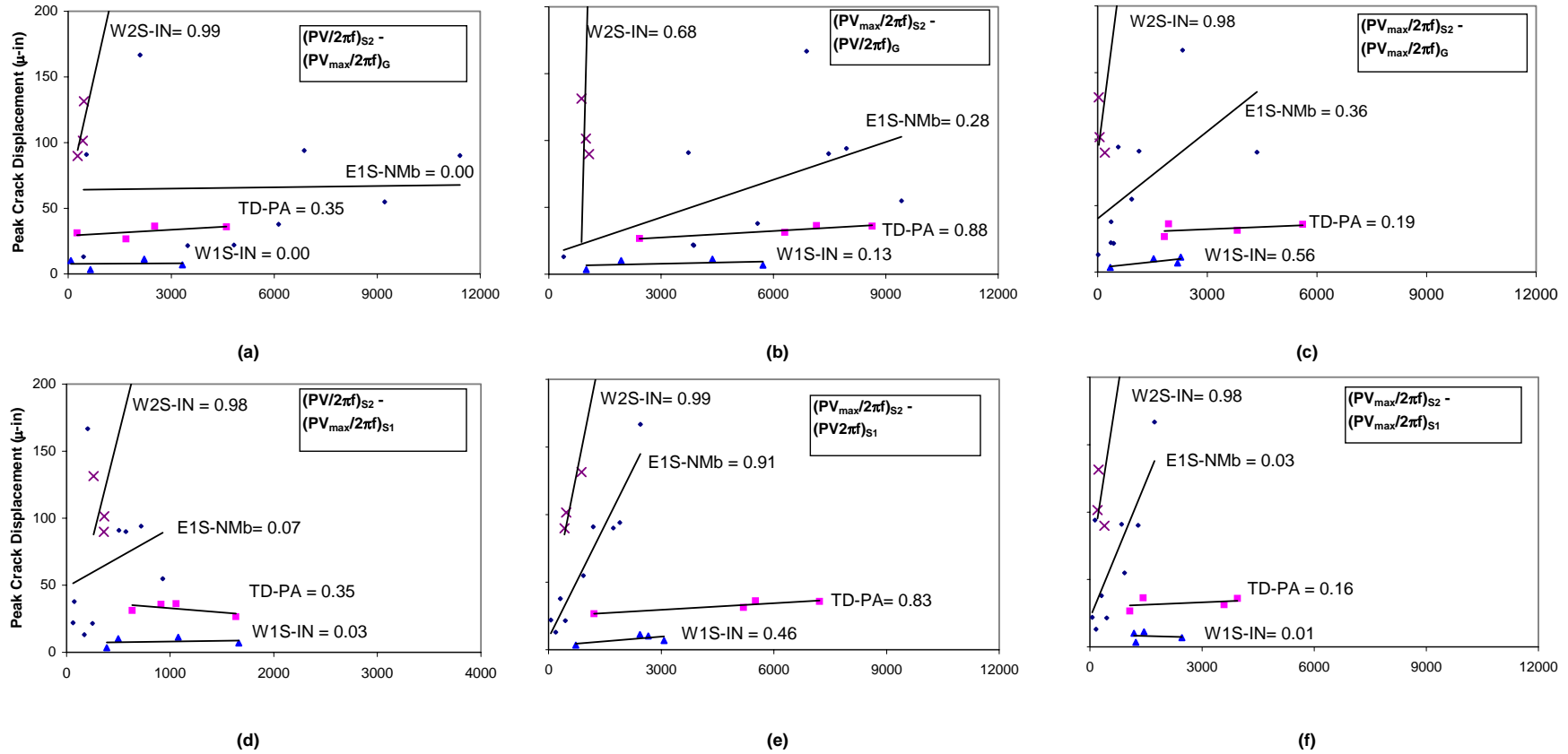


Figure 13 Comparison of  $R^2$  correlations between measured crack displacements and estimated relative displacement

## Discussion

Dual-purpose sensors described herein could be placed across a crack to simultaneously measure long-term and vibratory changes in crack width to augment the traditional approach of measuring particle velocity. This augmentation might be helpful where blasting or construction vibrations occur for sustained periods of time, as many complainants who believe that construction vibrations disturb their homes or buildings tend to focus their discussion on cosmetic cracks like that in Figure 1. Because people interpret the response of buildings through their senses, they tend to believe that if the vibrations can be felt and associated noise heard, there could be a negative effect on the structure. Additional measurement of crack response would allow comparison between the effects of the "silent crackers" – temperature, humidity, long term distortion, material changes, etc - to the phenomena that is felt and heard – blasting.

This addendum presents measured crack responses associated with this study of atypical response in order to 1) introduce the concept of crack measurement and 2) demonstrate that a single transducer and computer system can be employed to detect both long term and vibratory response of cracks. It was and is not meant to set forth an argument for any set of conclusions, except that such measurement could augment the traditional means of assessing the potential for cracking from blasting vibrations. Thus this addendum is not meant to be a definitive treatise on crack measurement and structural response. That discussion would take far more space than possible because of the myriad of considerations that would need to be considered. The detailed discussion of the measurements was included to demonstrate the manner in which this new type of data could be employed.

Data presented in this addendum is limited by the time that was allotted for the measurement of long term response. Because of this short time of observation, long term crack response of the four structures studied does not include significant changes in weather, seasonal weather changes, or other seasonal environmental effects. "long-term" relative to the age and environmental stress history of a structure must of necessity be described in terms of no less than months. Only one of the four structures was monitored for more than 5 days. Observation of only a handful of days is too short to observe the effects of a significant change in the weather.

Thus the reader is cautioned not to extrapolate from these data to draw general conclusions. For instance, one might be tempted to conclude from the detailed example presented that vibratory response is significant compared to long term response. It is for these three days, but these measurements do not include any weather extremes or seasonal effects.

Differences in relations between measured crack and structural response are small compared to the large impact of weather related response, as demonstrated above. Changes in crack width produced by noticeable ground motions of 0.1 in/sec were less than 200  $\mu$ -in; whereas, the maximum weather responses during one week (or less) periods of observation were 500 to 2000  $\mu$ -m. The crack in structure W2S-IN that showed the largest motion response (197  $\mu$ -in) also showed the largest weather response (2045 $\mu$ -in). More measurements are needed to draw general conclusions about the implications of these observations.

Of all of the responses calculated by traditional means, measured crack displacement

correlated best with those resulting from the difference in integrated velocity time histories of the upper and lower corners, (S2-S1). This correlation is shown in Figure 13 (a). This high correlation was expected, as (S2-S1) is the relative displacement of the wall, which is proportional to the gross, in-plane, shear strain in the wall. In a sense, this calculated difference also could be considered as a direct measurement of the wall strain when measured at the upper and lower elevations of a single story wall of constant cross section.

The second best correlation with the measured crack displacement is obtained from the pseudo velocity response spectrum (PVRS), with the average of responses between 10 and 15 Hz. The PVRS is a derivative of calculated relative displacement that accounts for the structural response frequency, as well as, the full excitation time history (Siskind et al 1980, Dowding, 1985, and 1996). These correlations, shown in Figure 13 (e), are almost identical to that between the two direct measures of wall strain. This frequency range lies between the natural frequency of super structures and walls. Correlations are lower with PVRS displacements for the estimated dominant frequency associated with each superstructure.

A number of factors affect the relationship between directly measured crack displacement and structural response (or estimated relative wall displacements), one of which is crack location. The crack in structure W1S-IN was located at the top of the basement wall, only 3 feet from the ground surface. Magnitudes of crack response for this structure were smaller than all other observed crack response in this study, even though it sustained peak parallel ground motions as high as 0.2 in/sec, as shown in Figure 12. However, this low response was expected, as the basement wall moves with the ground and thus is not free to respond, as is the superstructure. Vibratory displacements of this crack would not be expected to correlate well with estimated measures, which presume free response of the structure. Crack displacement of this basement wall best correlates to peak parallel ground motion, because it is most directly related to ground strains. The worst correlation with this crack response occurs with calculated displacement (between S2 and S1), as these responses are for the above ground, freely responding portion of the structure.

Another factor that may affect the relationship between crack displacement and structure response is the actual magnitude of crack width. The most responsive of the cracks in wall covering of the superstructure, also tended to be the widest. Consider the crack in structure W2S-IN, which was uniformly wide, like that in Figure 1, and extended the entire distance between the window top and the ceiling. The correlations for this structure are uniformly the highest. However, these high correlations may have resulted from the large range of measured crack displacements. Graphs in Figures 13 and 14 have been truncated at measured peak crack displacements of 200  $\mu$ -in in order to include the lower ranges of response. The one missing point for W2S-IN is located at 535  $\mu$ -in, which corresponds to a peak particle velocity of 0.28 in/sec (7 mm/s) parallel to the wall containing the crack.

## Conclusions

This addendum presents measurements of the response of cosmetic cracks to long term environmental effects as well as blast-induced ground motions in four structures. Crack sensors employed in this study allowed simultaneous measurement of both long-term (environmental or

weather induced) and vibration (blast induced) changes in crack width in a variety of wall materials. Cosmetic cracks monitored in this study occurred in 1) exterior stucco over adobe bricks as well as concrete masonry units, and 2) interior plaster and lath, as well as dry wall. Structures were framed with wood, concrete masonry units, and adobe, and included a trailer, an adobe ranch house, a concrete block basement, and a wood framed house.

Direct measurements of vibratory cosmetic crack response of the four structures subjected to blast-induced peak particle velocities between 0.1 and 0.3 in/sec were compared with a wide range of estimates of the wall distortion. Twelve of these methods were compared to the measured crack response in order to determine the best correlations. Through these comparisons, it was possible to estimate crack responses at 0.1 in/sec, which is assumed to be noticeable to a wide range of individuals.

Long-term cosmetic crack response to weather induced changes was measured in all four of the structures over periods of 3 to 36 days. Three of the four structures were monitored for 5 days or less and most likely did not capture the effects of significant changes in weather. The long-term response was subdivided into effects caused by 1) daily changes, 2) passage of weather fronts occurring over a period of days, and 3) extremes of unusual weather or other environmental effects.

Synthesis of these measurements and calculations leads to the following conclusions with regard to this set of observations, noting that more work and measurements are needed to generalize these conclusions:

- Long-term response of the monitored cosmetic cracks in these four cases with short observation periods is at least 4 to 5 times larger than the vibratory response of cracks at maximum measured peak particle velocities and more than 7 to 10 times greater at low but noticeable levels.
- Extreme events such as rainstorms in dry climates can cause offsets and or extreme crack displacements that are much larger than those induced by typical weather changes.
- Vibratory crack response induced by household activities can approach or exceed the vibratory response to low but noticeable peak particle velocities. The response varies as a function of distance from the crack in which the activity occurs.
- Crack displacements induced by typical changes in weather and noticeable vibrations are far smaller than the width of the cracks.
- Measured crack displacements correlate best with the difference in calculated displacement of the top and bottom corners of the structure. These displacements are calculated by integrating time correlated velocity time histories of structure motion measured in the plane of the wall containing the crack.
- Measured crack displacements also correlated well with estimates made from ground motions that take into account the time history of the excitation and response characteristics of the structure using the single degree of freedom response method.

- Responses of the same type of sensor, one across the crack and the other on adjacent, uncracked material (a null sensor), show crack displacements to be large compared to the combination wall material and sensor response measured by the null sensor. Therefore, a null sensor may not be necessary in many cases.

## **Acknowledgements**

Support of a large number of individuals and organizations were necessary for this project. Their cooperation is deeply appreciated and gratefully acknowledged. The infrastructure technology institute at northwestern university, directed by David Schulz, has supported autonomous crack monitoring technology through a grant from the Federal Highway Administration. Two members of the ITI instrumentation staff, Daniel Marron and David Kosnik, played key roles in the development of the ACM hardware and software. Results not presented herein are chronicled in three Northwestern University M.S. theses by Damien Siebert, Michael Louis, and Laureen McKenna.

Intensive instrumentation of the four structures summarized herein was made possible through the cooperation of the Department of the Interior's Office of Surface Mining program to measure response of atypical structures. Kenneth Eltschlager, Dennis Clark, and Mike Rosenthal, as well as a number of representatives from supporting state agencies, provided field support for the OSM program. Finally, without the fieldwork, instrumentation, and sharing of data by Professor Cathy Aimone-Martin and Mary Alena Martell of the New Mexico Institute of Mining and Technology, data presented herein would not exist.

## **Reference**

- Aimone-Martin, C.T., M. A. Martell, L. M. McKenna, D. E. Siskind, and C. H. Dowding, 2003, "Comparative Study of Structure Response to Coal Mine Blasting", Office of Surface Mining Reclamation and Enforcement Appalachian Regional Coordinating Center, Pittsburgh, Pennsylvania.
- Dowding, C. H., 1996, Construction Vibrations, Prentice Hall, Upper Saddle River, New Jersey, Chapter 13, "Comparison of Environmental and Vibration-Induced Crack Movement".
- Louis, M., 2000, Autonomous Crack Comparometer Phase II , M.S. Thesis, Department of Civil and Environmental Engineering, Northwestern University, Evanston, IL.
- Martell, M.A., 2002, Log Structure Response to Coal Mine Blasting, M.S. Thesis, New Mexico Institute of Mining and Technology, Socorro, NM.
- McKenna, L., 2002, Comparison of Crack Response in Diverse Structures to Dynamic Events and Weather Phenomena, M.S. Thesis, Department of Civil and Environmental Engineering, Northwestern University, Evanston, IL.

Miller, R., 1989, Analysis of the Fracture Process Zone in Mortar Using Laser Holographic Interferometry, PhD Thesis, Department of Civil and Environmental Engineering, Northwestern University, Evanston, IL.

Siebert, D., 2000, Autonomous Crack Comparometer, M.S. Thesis, Department of Civil and Environmental Engineering, Northwestern University, Evanston, IL.

Somat TCS for Windows, version 2.0, 1999, Somat Corporation, Champaign, IL.

White Seismographs Data Analysis, Version 5.0.4, 1998, White Industrial Seismology, Inc., Joplin, Mo.

## ADDENDUM II

# **GUIDELINES FOR MEASURING RESIDENTIAL STRUCTURE RESPONSE**

**Prepared by:**        **C. T. Aimone-Martin**  
                             **Aimone-Martin Associates, LLC**  
                             **Socorro, New Mexico**

**Kenneth K. Eltschlager**  
**Office of Surface Mining**  
**Reclamation and Enforcement**  
**Pittsburgh, Pennsylvania**

**February 2003**



## 1.0 INTRODUCTION

Occasionally, structures near mines may be instrumented to determine their response to incoming ground vibrations and airblast. These guidelines will assist with instrumentation and analyses to measure and evaluate structure response from blasting. The methodologies described in these guidelines are intended to ensure consistent measurement of structural response and evaluation of structure characteristics. The field techniques employ traditional vibration instrumentation with exact time correlations.

The methods detailed herein allow for the proper:

- comparison of velocity vibration time histories within structures relative to ground vibrations,
- evaluation of the influence of ground vibrations and airblast on the structure,
- evaluation of structure response to determine the natural frequency,
- determination of structure response amplification of ground vibrations,
- computation of differential displacements of construction components and corner motions to estimate global and in-plane tensile wall strains, and
- comparison of results with historical vibration observations.

## 2.0 STRUCTURE RESPONSE

### 2.1 Background

Current regulations to control blasting vibrations are based upon measurements of ground vibrations. There may be occasions to directly measure structure motions. In such cases the most exact procedure will involve measurements of motion that allow back calculation of wall strains. These wall strains are most exactly calculated from displacements measured near the top and bottom corners of walls of uniform construction.

The below ground portion of a structure or basement to which the superstructure is attached is normally well coupled to and vibrates with the ground for most dwelling. Often the lower first floor wall corner motions are similar to those of the ground. When this is the case, ground motions may be used to estimate lower wall corner motions. *However, trailers may be an exception.* Trailers and many manufactured homes normally rest on uncemented concrete masonry unit (CMU) pillars without perimeter wall support and are not tied to interior piers. This results in poor coupling to the ground because each block is free to move independently and ground velocities are not effectively transmitted into the structure.

The above ground portion of a structure shakes or responds to ground vibrations and/or airblast with three degrees of freedom: front to back, side to side, and torsionally. However, trailers tend to “bounce” and are free to readily vibrate in the vertical direction at amplitudes that may be greater than ground vibrations. When the frequency of the incoming vibrations matches the natural frequencies of the house, the whole (or gross) structure horizontal response may be

amplified and sustain velocities greater than the horizontal velocities measured in the ground. The greater the difference in frequencies between the vibration of the ground and the house, the less the house responds in amplitude. The natural frequency of typical homes is between 4-12 Hertz (Hz).

Figure 1 shows simplified diagrams of whole (gross or corner) structure and mid-wall responses. Figure 1(a) is a plan view of a typical structure showing the convention used for velocity sensor orientation with respect to the long axis of the structure. Vertical wall diagrams are shown of wall 1 (Figure 1b) and wall 2 (Figure 1c). Whole structure deformations are represented by upper corner (labeled as S2) displacements minus those at the lower corner (S1). Wall bending response (mid-wall, MW, motions normal to the wall surface) is approximated in the wall section view Figure 1(d) and applies to both walls 1 and 2.

A sensor placed in the ground with the proper orientation to compare with structure response is shown in Figure 1. Normally the longitudinal or radial component is directed parallel to the longest axis of the structure. *Note that this sensor orientation may be contrary to the convention that is traditionally used when the radial or longitudinal velocity transducer is pointed toward the blast.*

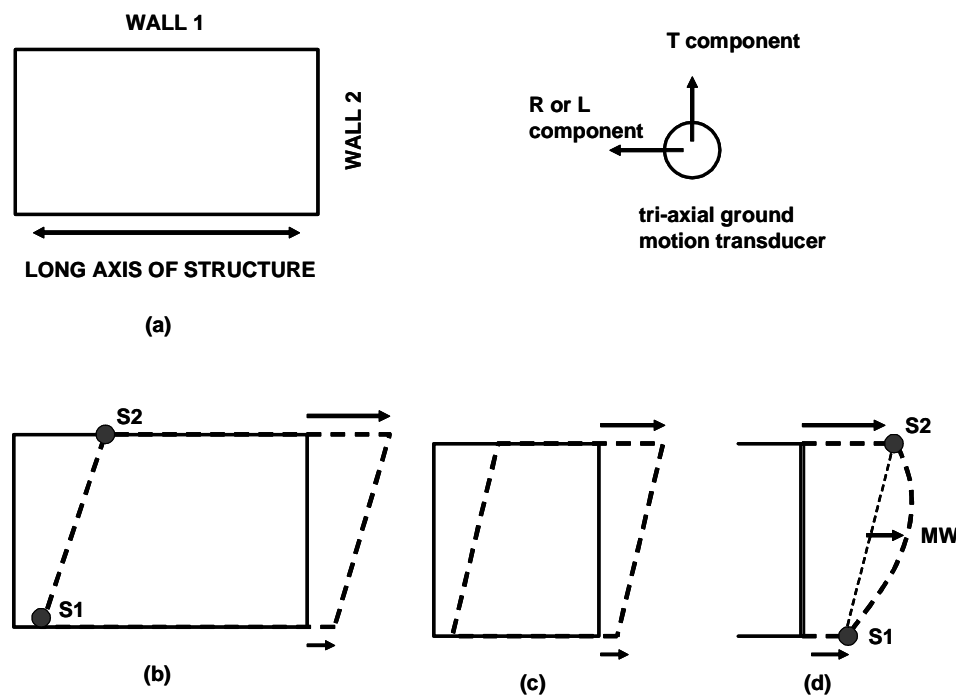


Figure 1 (a) Plan view of structure showing nomenclature for walls, (b) wall 1 and (c) wall 2 whole structure shearing, and (d) typical mid-wall bending

## 2.2 Natural Frequency

The natural frequency of a structure is most easily determined as it comes to rest once ground motions have stopped as discussed later. Full waveform records allow visual interpretation of the natural frequency by simply counting the number of cycles per second during these free vibrations. When no free response of the structure is obvious because of continued ground motion or airblast, Fast Fourier Transform (FFT) spectral analysis may be necessary to approximate the natural structure frequency.

## 2.3 Amplification

The above ground portion of each structure will respond more than the ground when excited at its natural frequency. Amplification is a comparative measure of the maximum structure response to ground velocity (GV) at the same point in time. Amplification occurs when the motion at S2 becomes larger than that at GV. Amplification varies for typical and atypical structures. When the ground vibration frequency is significantly higher than that of the structure the motion is equal to that of the ground

## 2.4 Strains

Strains determine the likelihood of cosmetic cracking. Global (whole) structure strains may be estimated from the measurements of differential structure motions calculated in terms of displacements. The process of calculating displacements involves integrating the velocity time histories at S1 and S2 to obtain displacement time histories and finding the largest time-correlated difference between corner responses (S2 minus S1) over the recorded time history.

Lower corner motions (S1) near the structure foundations often have the same response relative to ground vibrations (GV). If this is the case, GV approximates S1 and may be used for strain calculations. For structures that are not well-coupled to the foundation and the ground (e.g. trailers), the lower corner may move in a different manner than the ground vibrations (GV). If this is the case, S1 monitoring is necessary. Measurements of existing crack motions correlate best with the difference in integrated velocity time histories from the upper and lower corners (S2-S1) as shown in Addendum I of “Comparative Study of Structure Response to Coal Mine Blasting” (Aimone-Martin, et al., 2003).

## 3.0 INSTRUMENTATION

### 3.1 Blasting Seismographs

Methodology in this Addendum assumes that commonly-available blasting seismographs are used and that they adhere to the “ISEE Performance Specifications for Blasting Seismographs”. *It is recommended that the seismograph manufacturer be contacted to ensure that the necessary hardware and software are available.*

While the results presented by Aimone-Martin, et al., (2003) were obtained using small single axis transducers, small tri-axial transducers (less than 2.0 inches square or diameter) may be employed if installed properly. The disadvantages of using tri-axial sensors are the mounting requirements needed to support the large sensor mass on walls, and the large number of seismographs required to measure both whole structure and mid-wall responses. In addition, only three of the four seismograph channels are utilized with interior units

At a minimum the instrumentation system includes two blasting seismographs to measure whole structure response. If differential response between GV and S1 is possible, then three seismographs are necessary. If mid-wall motions are required, one to two additional blasting seismographs will be needed.

### **3.2 Time-Related Motions**

All records should be time correlated. This can be accomplished by physically connecting the seismographs in series. A common time base is produced by physically connecting the units. The exterior (master) seismograph, once triggered, must in turn produce a signal to trigger the interior seismographs. A single cable can be used to connect the two (or more) seismographs in series via the serial download port using “Y” cable connectors.

In addition, the resolution (or gain) designed for the airblast and vibration channels must be checked for consistency. Otherwise, modifications may be made to the connector (interface) box to vary the gain for some or all of the channels.

### **3.3 Polarity Testing of Tri-axial Sensors**

When comparing time correlated motions it is important to document the polarity of the sensors for any given direction of motion. Prior to deploying equipment in the field, polarity testing should be conducted on all sensors to ensure common transducer wiring for consistent voltage output (positive or negative). For example, the vertical component should show positive velocity amplitude for vertical ground motion in an upward direction. This is *normally* the case for the first arrival of ground vibration. The radial or longitudinal component should show positive amplitude when motion is in the direction of the arrow traditionally placed on the sensor housing to indicate the R (or L) direction. The transverse horizontal component can be mounted with any convention and it is difficult to predict polarity direction. However, each manufacturer will generally use a consistent convention for attaching wire leads to the transducer and transverse time history outputs among each sensor should be similar for any given motion direction.

Polarity becomes critical when measuring and comparing relative motions between the ground or lower structure corner with the upper corner of structures, particularly in the horizontal components. This directionality is important because differential displacements must be calculated in order to estimate gross structure strains and in-plane wall strains. If polarities are not matched, differential displacements may be over two times greater than displacements for a common polarity.

Polarity tests can be easily performed by taping all sensors mounted with identical orientations to a sturdy but movable object such as a cardboard box. Move the box in each of three directions parallel to each sensor component (for instance, against the radial or longitudinal “arrow” and in a vertical direction), recording each motion using the smallest record length practical. Using the seismograph software, plot and compare the time histories near the time history arrival to observe consistent first motion arrival pulses (positive or negative).

## 4.0 INSTRUMENT INSTALLATION

### 4.1 Instrument Locations

At a minimum the instrumentation system includes two blasting seismographs to measure whole structure response as shown in Figure 2, one inside the house (S2) and one outside (GV, not shown). If GV cannot approximate S1 a third seismograph is necessary. If mid-wall motions are required, one or two additional sensors can be mounted as shown in Figure 3.

For two story structures, it is important to place the upper and lower corner transducers on one floor at a time. This is particularly important when the construction materials are different among the different stories. Wall strains computed from differential displacements measured at

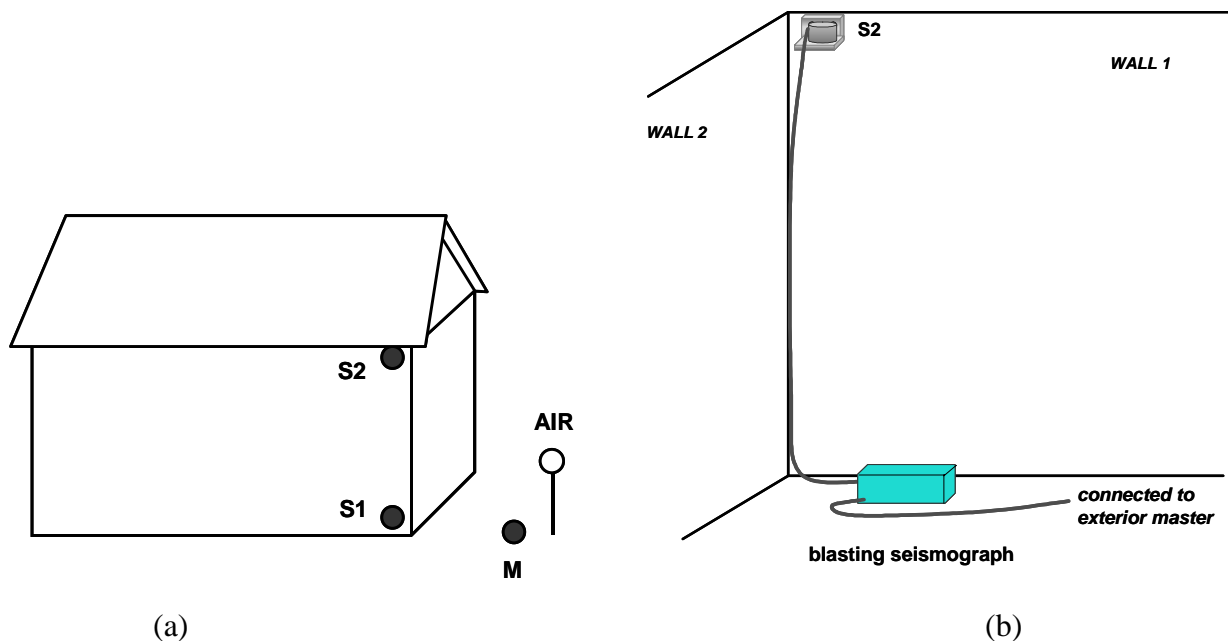


Figure 2 Positions of velocity transducers to measure whole structure response and excitations  
 (a) showing the interior units relative to the exterior master (M) triggering unit  
 (b) showing a cut-away section of the interior corner sensor locations

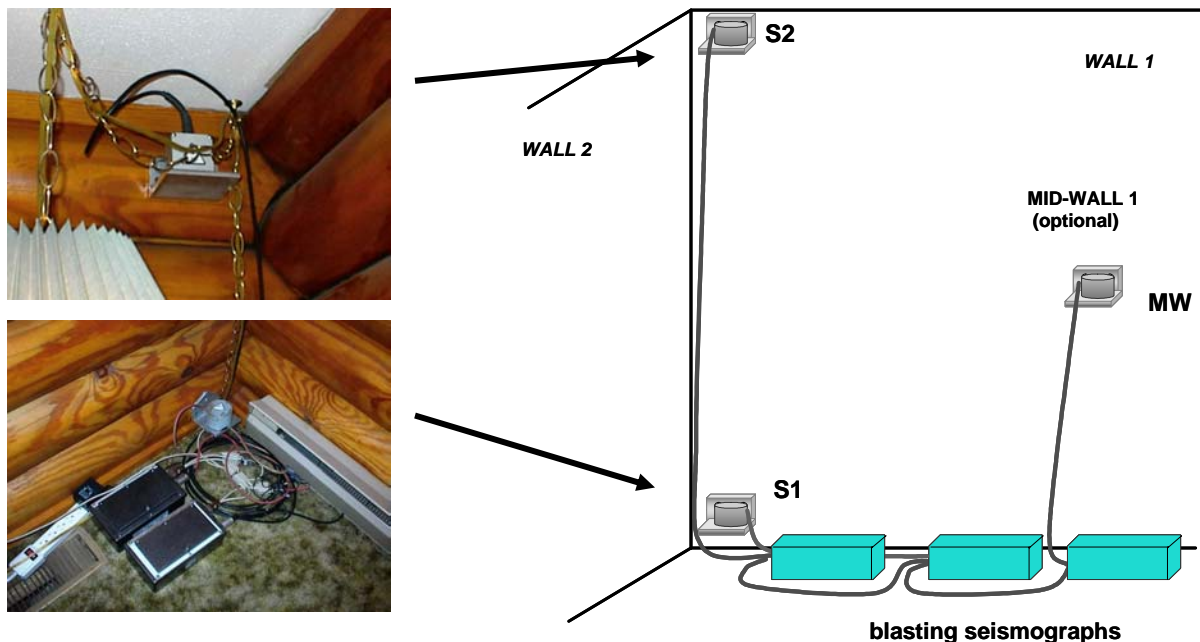


Figure 3 Transducer positions to measure whole structure and mid-wall (one wall only) bending response

wall corners can only represent one wall or material and should not be extended to two stories unless the structure can be assumed to respond uniformly as shown in Figure 1.

#### 4.2 Ground Vibration Measurements

A blasting seismograph should be set outside the house at the same corner of the intended structure monitoring. Installation should be consistent with the “ISEE Field Practice Guidelines for Blasting Seismographs.” The only exception is the orientation of the ground tri-axial sensor where the radial channel must be aligned with the long axis of the house as shown in Figure 1.

#### 4.3 Mounting Sensors Inside the Structure

Methods to attach single-axis sensors that disturb walls the least include drywall screws or gluing. Tri-axial sensors, because of their large weight in size, must be screwed to the wall. Care must be taken to minimize the damage to residential walls. Owners of structures may be willing to allow minor wall surface damage from screws or gluing. However, it is always prudent practice to explain to the owner that surface cosmetic wall damage may occur and be prepared to provide minor wall repairs.

While single axis sensors are preferred, tri-axial sensors may be employed if properly installed. Tri-axial sensors require “L”-shaped brackets for interior mounting as shown in Figures 2 and 3. Because of the weight of these sensors, drywall screws must be used to attach to walls. Standard aluminum 6061 T6 structural angles, 1/4 to 3/8 in. in thickness, are suitable

for bracket material. The horizontal base should be sufficiently wide to accommodate the sensor. A small amount of hot glue using a glue gun is adequate for affixing the transducer to the bracket. Holes may be machined on the back (vertical) plate for use with screws.

Some sensors may be mounted on the structure exterior. Depending on the component being evaluated, such as a brick veneer, outside mounting may be essential. It is important to ensure that the brick veneer is attached to the load bearing walls with masonry tabs.

### **4.3 Mounting at Other Structures**

Other structures such as water towers, silos, electric towers, barns, etc., may be monitored by carefully mounting seismographs in the appropriate locations on a case-by-case basis.

## **5.0 RESPONSE MONITORING**

### **5.1 Waveform record**

Full waveform records of each event are necessary to evaluate the structure response characteristics. Be sure that the data is recorded digitally for subsequent analysis.

### **5.2 Seismograph Settings**

All seismographs in series must have the same settings for sample rate and record length. Sample rates of 1024 or 512 per second are sufficient to measure structure response. Total record length should be long enough to ensure the recording of any free response well after the arrival of the airblast pulse and well after the ground motions have ceased. Depending on the structure distance from the blast, set the record time for a total time equal to at least five to seven seconds *plus* one second for every 1000 ft. of distance to the blast. For example, if the structure is 3000 ft. from the blast, a minimum record length of 8 to 10 seconds is required.

The exterior master unit must be set on the trigger mode while the remaining seismographs measuring structure response should be placed on manual or slave mode. Again, this setting depends on the manufacturer. Ground motion and airblast trigger levels of 0.03 inches per second (in/sec) and 125 decibels (dB) are recommended.

The upper range for the interior seismograph units should be set to at least 5.0 in/sec to capture the higher velocity motions that may be reached in the upper structure and mid-walls. However, if the distance to the blast is beyond 2000 to 3000 ft. and expected peak ground velocities are less than 0.3 in/sec, an upper range of 2.5 in/sec will allow good resolution of structure time history motions at low amplitudes. It is critical that time histories show amplitudes well above the lowest resolution of the seismograph in order to accurately integrate velocity time-based motions for analysis. It is best to check with the manufacturer to assist with setting the amplitude range to maximize the data quality.

## **6.0 STRUCTURE RESPONSE ANALYSIS**

Structure response analyses are outlined in the U.S. Bureau of Mines and reported in RI 8507 and by Aimone-Martin, et al., (2003). Basic analyses should include estimation of natural frequency and amplification of the structure. Advanced analyses include strain estimation.

### **6.1 Time correlated waveforms**

Velocity time histories of the ground, lower, and upper structure must be correlated in time in order to calculate strains. Two examples of time correlated motions are given in Figure 4. Other approximate approaches may involve errors in calculating displacements.

### **6.2 Estimating Whole Structure Natural Frequency**

Whole structure natural frequency is estimated during free response of the structure, i.e. after the ground vibrations have stopped as shown in Figure 5 or after the airblast induced motion. The normal range of structure natural frequency is reported to be 4 to 12 Hz. Visual estimation, zero-crossing, or FFT methods can be used to determine the structure frequency.

If the waveform is uniform, visual estimation is possible by identifying a one second window during free response and counting the number of cycles. In Figure 5, between seconds 4 and 5 there are 4 cycles for a frequency of 4 Hz.

If only a few cycles of free response exist, the “zero” crossing method of calculating frequency can be employed. In Figure 5 near second 4, the wave crosses the zero line 0.125 second apart as determined from the software. Since that is a half of a wave, the period of a full wave is 0.25s. Taking the inverse of the period yields natural frequency of 4 Hz.

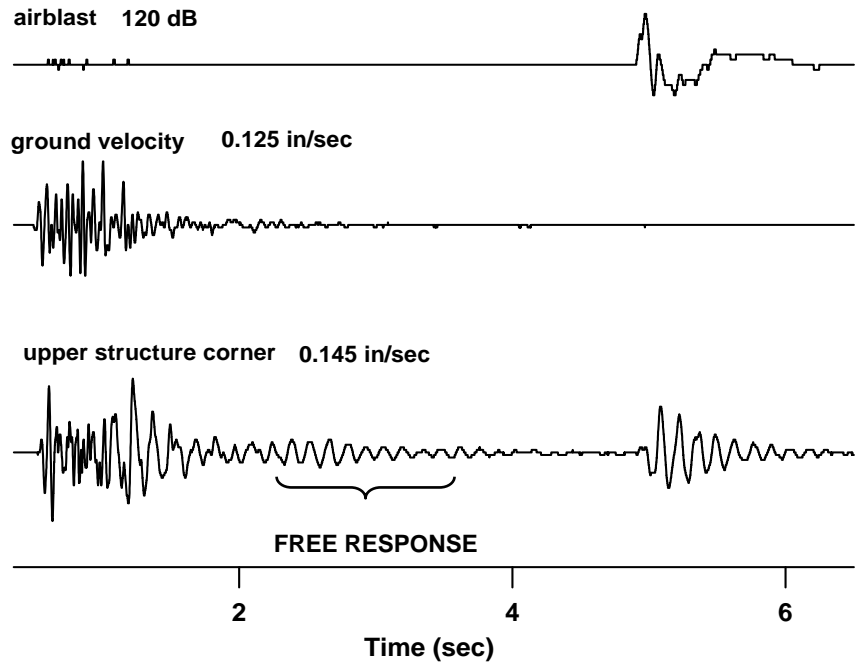
One alternative to calculating natural frequency from free response is to calculate the Fast Fourier Transform (FFT) of the response motion. While this may not always yield satisfactory results, it may be useful. Most seismograph software has an option to display the FFT graph to observe the distribution of frequency content.

Figure 6 is an FFT plot of the S2 time history in Figure 5. The 3.9 Hz peak value compares well with the 4 Hz computed using the “zero” crossing method over that portion of the time history during free response. Hence, FFT analysis provides a good measure of structure free response. This agreement is good because the record involves free response. When there is no free response, the approach is more complicated as described in Dowding (1996).

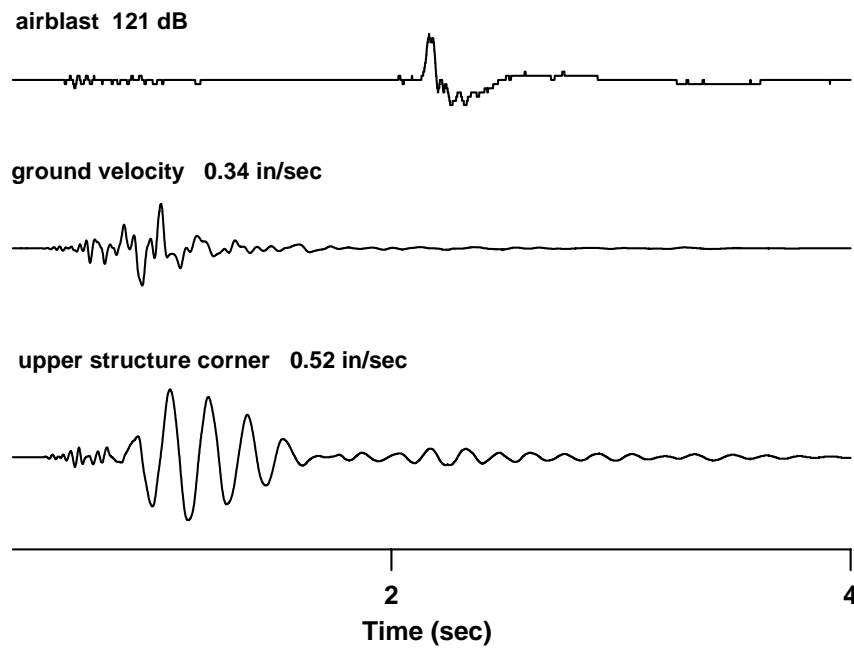
### **6.3 Whole Structure Amplification of Ground Vibrations**

Amplification is a comparative measure of the maximum structure response to ground vibration at the same point in time. Amplification occurs when motion at S2 becomes larger than that at S1.





(a)



(b)

Figure 4 Airblast, ground velocity, and upper structure corner response time histories showing strong structure response within (a) the airblast phase and (b) the ground motion phase

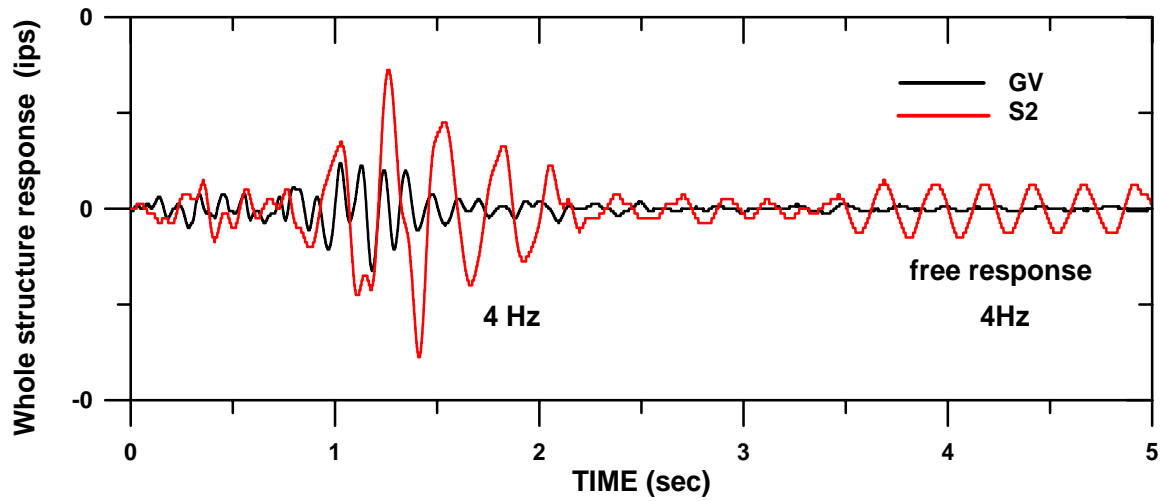


Figure 5 Whole structure response (S2) and ground vibrations (GV) showing structure free response for a single wide trailer at 4 Hz when ground motions have arrested

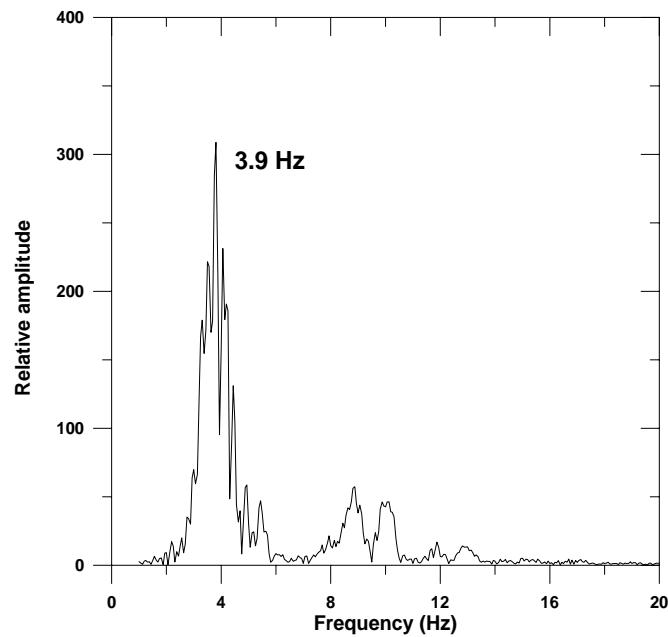


Figure 6 FFT plot of relative amplitude versus frequency for S2 given in Figure 5, showing a strong predominance at 3.9 Hz

In the 1980 study, Siskind, et al., describes amplification in terms of velocity. This method involved finding the peak upper structures velocity response and dividing this by the nearest preceding ground velocity that most likely drove the structure. This approximate approach is described as equation (1),

$$AF = \frac{S2_{peak}}{GV} \quad (1)$$

where  $S2_{peak}$  is the peak velocity of the upper structure and GV is the velocity of the ground motion for the same direction component at the corresponding moment of time or immediately preceding the time of the peak S2 motion.

Waveform analysis necessary to calculate AF values can be carried out in one of two ways depending on available seismograph software. One way is to display the time histories of the vibration component of interest recorded in the ground (GV) and at the upper structure corner (S2) in the same display window shown in Figure 7. Find the peak velocity at S2 then establish the peak GV for the same phase (the negative pulse in this case) at a time just prior to S2 peak as indicated in Figure 7. The vertical line represents a common time mark to locate peaks. AF for this example is

$$AF = \frac{0.30}{0.135} = 2.22$$

If the seismograph software does not have this windowing feature comparing different recorded events, then the time histories can be converted to ASCII format and saved. Using a convenient plotting software package, the time histories can be plotted together with a common time base and the peaks selected in the same manner described above. A third way is to graphically print the waveforms on the same scale and overlay the waveforms to observe which ground vibration amplitude is driving the peak response.

The range of amplification factors for trailers reported by Aimone-Martin, et al. (2003) are shown in Figure 8. The data can be compared to Figure 39 in U.S. Bureau of Mines RI 8507 where the U.S. Bureau of Mines found the highest AF to be 4 and an average value for all structures of 1.5. The average AF in the 2003 study was 1.9 for all 25 atypical structures with a maximum of 5 at one structure.

To compare and project structure response to ground vibrations, the peak upper corner (S2) velocity value of either the R or T component (whichever is the larger), termed peak upper corner horizontal component, is plotted against the corresponding peak horizontal value of ground vibration (GV). An example of this plot is shown in Figure 9. The line shown envelopes of all U.S. Bureau of Mines data reported in RI 8507 Figure 35. In this example, all data in Figure 9 fall within the data range reported by the U.S. Bureau of Mines.

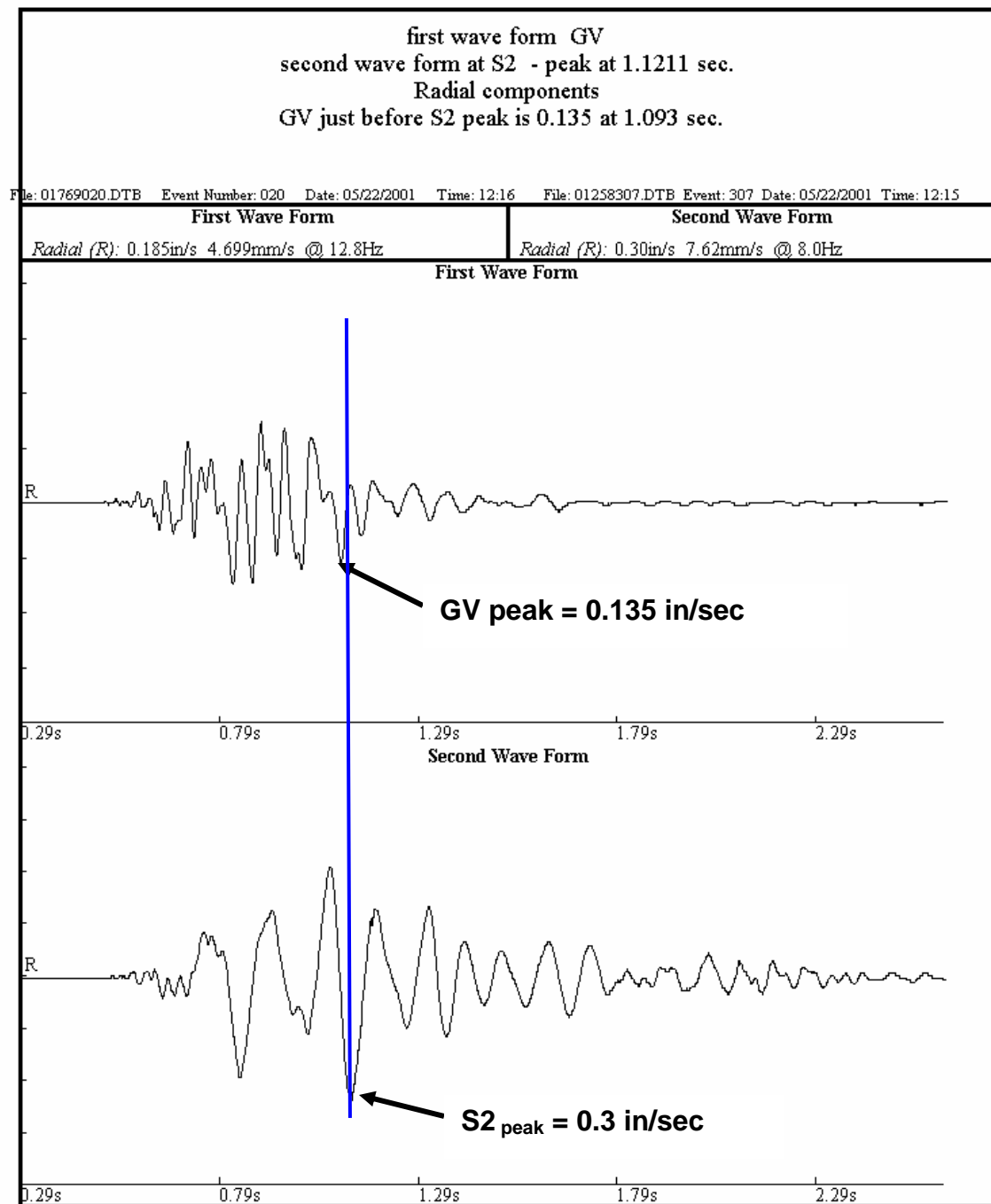


Figure 7 Comparing radial vibration time histories recorded at the upper structure (S2, top) and in the ground (GV, bottom)

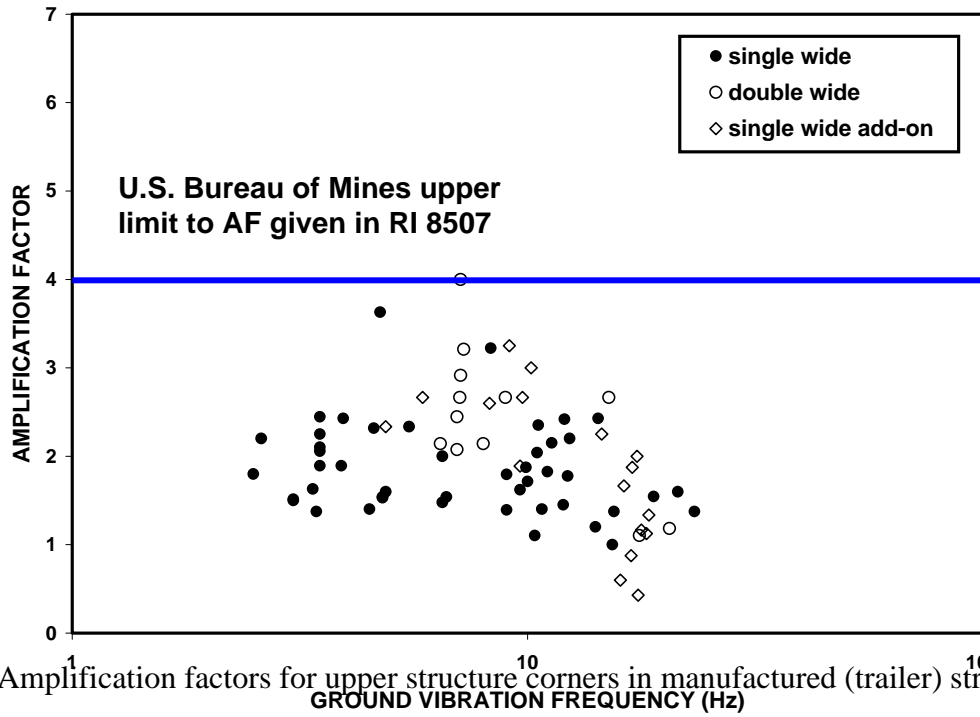


Figure 8 Amplification factors for upper structure corners in manufactured (trailer) structures

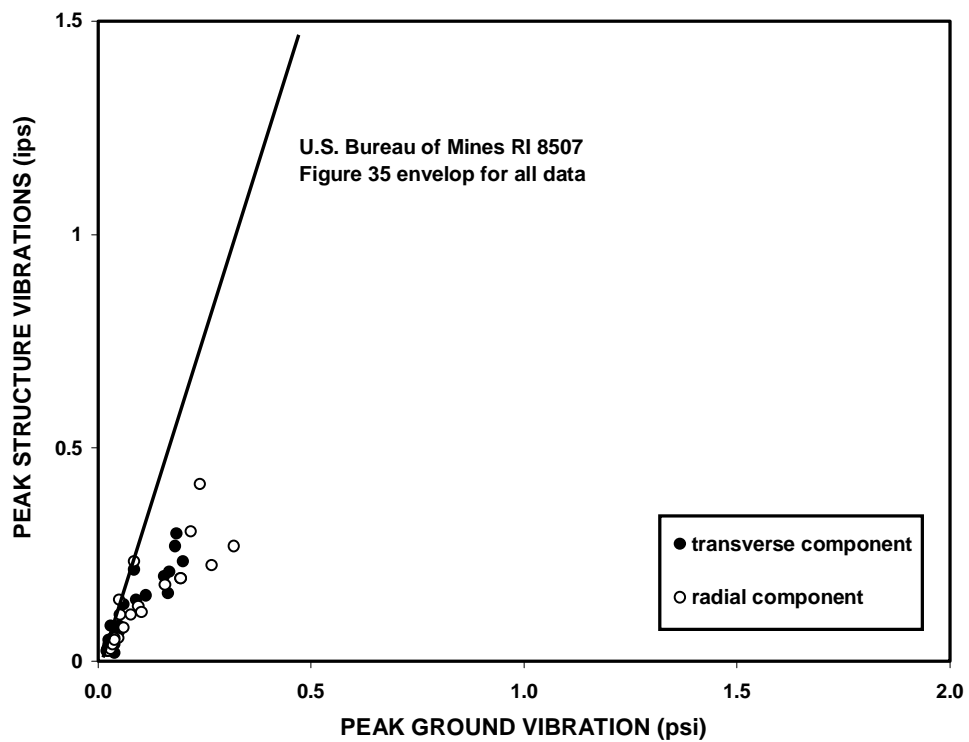


Figure 9 Structure upper corner response from peak ground vibrations for horizontal components, the slope of the line represents an amplification factor of 3

## 6.4 Airblast Induced Structure Response

Unlike ground vibrations, airblast impacts the house through the roof and walls of the structure. Airblast analyses include evaluating the upper corner response (S2) and mid-wall (MW) response to air over pressure (in terms of pounds per square inch, psi) as an indication of structure sensitivity to airblast. If the seismograph software does not report airblast in terms of pressure, the following relationship can be used to convert airblast pressure in psi to sound pressure level, SPL, in decibels (dB):

$$\text{SPL (dB)} = 20 \log \text{AP (psi)} + 170.8 \quad (2)$$

The natural frequency can be estimated during airblast excitations if free response of the upper structure is observed within the structure time history as discussed in Section 6.2. However, if strains are to be estimated from airblast, seismographs must be located at S1 and S2. Then in-plane tensile wall strains can be estimated from differential displacement time histories between the upper and lower structure corners.

The maximum horizontal structure response at S2 (the larger of wall 1 or wall 2) and the peak mid-wall responses (MW) are plotted against airblast overpressure, in pounds per square inch (psi) in Figures 10 and 11 taken from Aimone-Martin, et al., (2003) and compared with historical data provided by Siskind (2002). Whole structure response sensitivity to airblast in Figure 10 was found by Aimone-Martin to be 77 in/sec/psi, for well-confined blasts, and 155 in/sec/psi, for unusually high frequency airblasts. In comparison, historical U.S. Bureau of Mines structure response data and values provided by Siskind (2002) for equivalent type airblasts were 42 and 135 in/sec/psi, respectively.

In contrast to whole structure response, the envelope for trailer mid-wall responses to airblast shown in Figure 11 was 442 in/sec/psi. For other structure types, exclusive of trailers, the upper envelope was 266 in/sec/psi. Siskind (2002) reported an upper envelope of 319 in/sec/psi that did not include trailers.

## 6.5 Strain Analysis

Lower structure horizontal responses (S1) are generally equal to or lower in amplitude than the same component of ground motion for all structure design with the exception of trailers and other structures that are not well-coupled to the ground. By comparing the peak amplitude of the lower corner with the ground motion, a determination can be made whether or not a lower corner sensor is necessary for structure response measurements. However, if strains are to be estimated from airblast impacts, measurement at S1 is essential.

The time histories of wall 1 for three trailers taken from Aimone-Martin, et al., (2003) are shown in Figure 12 to illustrate this point. Trailer dimensions are long (wall 1) compared with the width (wall 2) and they tend to exhibit higher response in a direction perpendicular to the long axis. The lower corner response (S1) of the single wide is higher in amplitude than the ground motions, whereas the double wide and single wide add-on designs do not show this lower corner amplification of ground vibrations. Therefore, in the later two cases, a lower sensor may

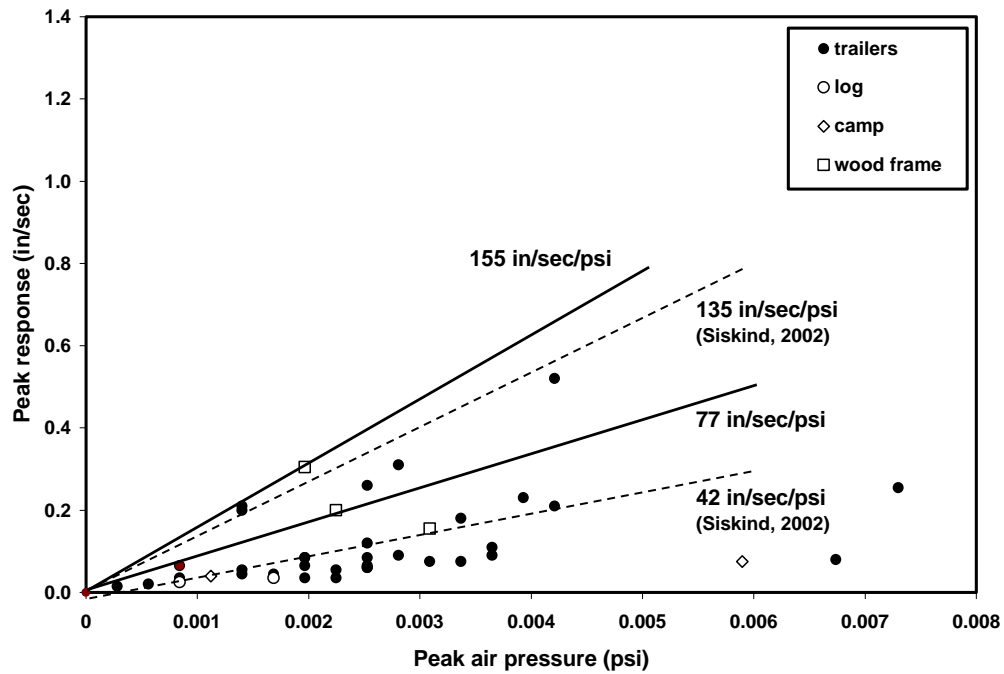


Figure 10 Airblast-induced whole structure response measured at S2

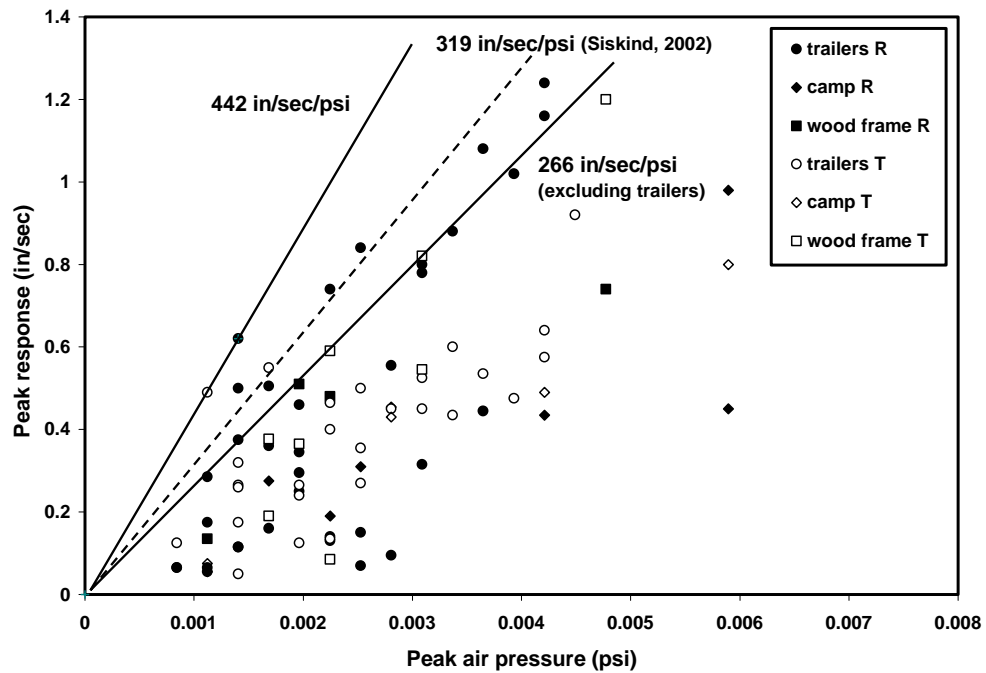


Figure 11 Airblast-induced mid-wall response (wall 1 = T and wall 2 = R in this case)

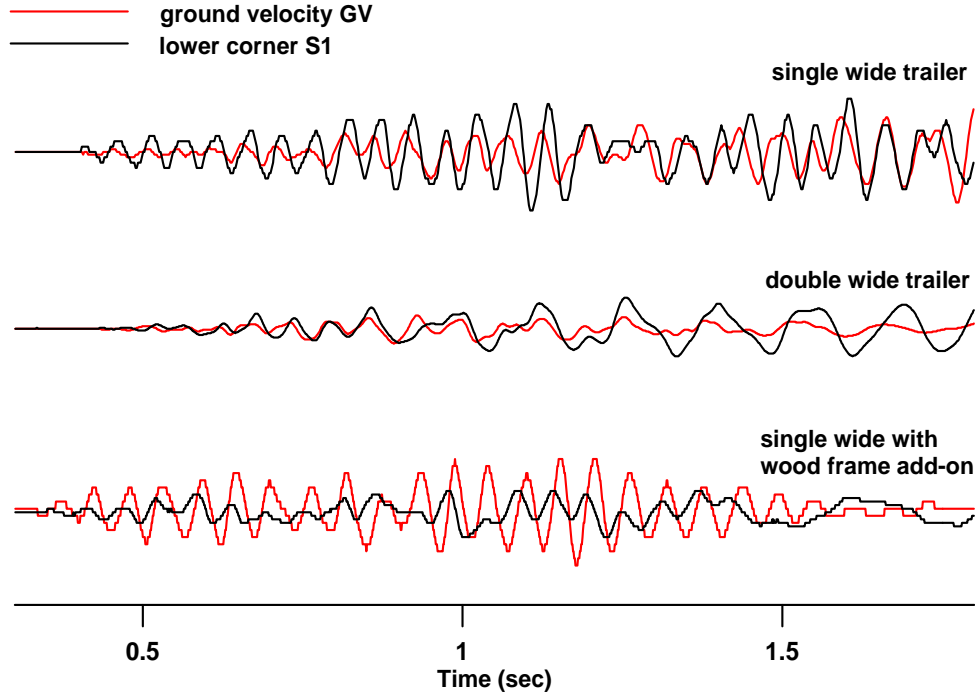


Figure 12 Comparison of velocity time histories for the ground (GV) and lower structure corner (S1)

not be necessary and lower corners may be estimated using the ground motions. However, for single wide trailers, a lower sensor is necessary for structure response analysis.

Estimating wall strains from calculated gross structure shear strains requires the calculation of differential structure displacement time histories, or S2 minus S1 over time. The ASCII format of velocity time histories for the upper (S2) and lower (S1) structure corners are first converted to displacement time histories by mathematical integration using seismograph software (if this feature is available) or using software such as NUVIB developed at Northwestern University, MATHCAD®, or similar software. By computing S2-S1 over time, the peak or maximum whole structure differential displacement,  $\Delta\delta_{\max}$ , between the upper and lower structure corner can be determined.

The maximum global structure shear strain of the wall,  $\gamma$ , is computed knowing the wall height (or measured distance between the transducers placed at S2 and S1) as follows:

$$\gamma = \frac{\Delta\delta_{\max}}{L} \quad (3)$$



where  $L$  is the wall height in inches and  $\Delta\delta_{\max}$  is in inches. Therefore  $\gamma$  is given as  $\mu\text{-in./in.}$  or  $\mu\text{-strains}$ .

The maximum in-plane tensile wall strain,  $\epsilon_L$ , for a square wall is then computed as

$$\epsilon_{L(\max)} = (0.5) \gamma_{\max} \quad (4)$$

In-plane tensile strains are critical to threshold wall cracking potential. Refer to Siskind (2000) for crack threshold strain levels in various materials.

## 7.0 Structure Response Evaluation

The goal of structure response measurements is to recognize when responses exceed values that may indicate unusual vibration characteristics. The primary indicator of damage potential is strain, which is related to frequency matching, structure amplification and gross structure differential motions. If structure vibrations approach or exceed historical observations, blasting may need to be modified to keep damage probabilities within acceptable ranges.

Ground vibration limits are typically between 0.5 and 1.0 in/sec while airblast limits are typically 133 dB or 0.01288 psi. When ground vibration frequencies match the structure's natural frequency (4 – 12 Hz), structure response amplitude to either the ground velocity or airblast may be as high as 1.5 in/sec measured in the upper corner (Aimone-Martin, et al., 2003). If responses are measured in excess of 1.5 in/sec, strain estimates should be made and compared to the threshold tensile strains for the appropriate building material.

## References

Aimone-Martin, C.T., M. A. Martell, L. M. McKenna, D. E. Siskind, and C. H. Dowding, 2003, Comparative Study of Structure Response to Coal Mine Blasting, Office of Surface Mining Reclamation and Enforcement Appalachian Regional Coordinating Center, Pittsburgh, Pennsylvania.

Dowding, C.H., 1996, *Construction Vibrations*, Prentice Hall.

Siskind, D.E., M. S. Stagg, J. W. Kopp, and C. H. Dowding, 1980, Structure Response and Damage Produced by Ground Vibration From Surface Mine Blasting, U.S. Bureau of Mines RI 8507.

Siskind, D.E., 2000, *Vibrations from Blasting*, International Society of Explosives Engineers.

Siskind, D.E., 2002, personal communication.